Molecular detection, genetic diversity and prevalence of major porcine viral pathogens

by

Yin Wang

B.V.M., Yangzhou University, 2010
M.S., Yangzhou University, 2013
M.S., Kansas State University, 2015

AN ABSTRACT OF A DISSERTATION

submitted in partial fulfillment of the requirements for the degree

DOCTOR OF PHILOSOPHY

Department of Diagnostic Medicine/Pathobiology
College of Veterinary Medicine

KANSAS STATE UNIVERSITY
Manhattan, Kansas

2020

Abstract

Infectious diseases of food animals have major impacts on economic returns and public health. Effective surveillance and control of animal diseases are very important, in which rapid and accurate detection of etiological agents play a critical role. Molecular diagnostics have been developed and used extensively. Because of its high sensitivity, high specificity, high-throughput and short turnaround time, molecular diagnostics is considered a powerful tool for detection and identification of infectious agents.

Several molecular assays have been developed and validated for major swine virus detections in this dissertation. In Chapter 2.1, a multiplex quantitative real-time PCR assay (mqPCR) was developed to detect and differentiate two porcine circoviruses (PCV) associated with the diseases of similar clinical signs: the novel PCV type 3 (PCV3) and the well-known economically important PCV type 2 (PCV2). In Chapter 2.2, a mqPCR assay was developed and validated for detection and differentiation of three PCV2 genotypes, PCV2a, PCV2b and PCV2d, the most frequently circulating genotypes in the US. In Chapter 2.3, a real-time RT-PCR (RT-qPCR) assay of Seneca Valley virus 1 (SVV-1) was developed and multiplexed with the published foot-and-mouth virus (FMDV) assays to differentiate the two viruses, which cause clinically similar vesicular diseases in swine. In Chapter 2.4, a real-time PCR assay was developed for rapid detection of African swine fever virus (ASFV). Its current spread in Asia and Europe resulted in significant economic losses on the global swine industry. In Chapter 2.5, the Luminex xTAG assay was developed to detect type 2 porcine reproductive and respiratory syndrome virus (PRRSV-2), one of most economically significant viruses in the US. The multiplexing assay allowed to differentiation of the field strains from the vaccine strains. In the design of the molecular assays described above, the most recent sequence databases were built to obtain high strain coverages.

The analytical and diagnostic analyses showed high sensitivities and specificities. Subsequent evaluation of clinical samples of different sample types indicated good diagnostic applicability. Finally, addition of the internal controls helped to monitor extractions and amplification efficiencies and to avoid false negative results.

Genetic diversity and prevalence of PCV3 and PCV2 were investigated (Chapter 3.1). It showed high prevalence of PCV3 and PCV2 in the swine herds of the Midwestern region of the US in 2016-2018. The phylogenetic analysis indicated low genetic diversity of PCV3, but high genetic diversity of PCV2. A new genotype, PCV2i, was proposed and the genotypes, PCV2a, PCV2b and PCV2d, were indicated as those circulating in the region. Finally, genetic diversity analysis of Rotavirus C (RVC) was conducted (Chapter 3.2). Thirty-one complete genomes were sequenced with next generation sequencing technology and analyzed with all available published reference sequences. Based on the phylogenetic analysis, several new genotypes were defined here, G18-G31 for VP7, P[22]-P[26] for VP4, R5 for VP1, A9-A12 for NSP1, N9-N10 for NSP2, T7-T9 for NSP3 and E6-E8 for NSP4. Genotyping of the 31 complete genomes indicated reassortment existed in 7 segments, VP7, VP4, VP6, VP2, NSP1, NSP2 and NSP3. The study updated the genotypes of RVC strains to help understand its diversity and evolution.

Molecular detection, genetic diversity and prevalence of major porcine viral pathogens

by

Yin Wang

B.V.M., Yangzhou University, 2010
M.S., Yangzhou University, 2013
M.S., Kansas State University, 2015

A DISSERTATION

submitted in partial fulfillment of the requirements for the degree

DOCTOR OF PHILOSOPHY

Department of Diagnostic Medicine/Pathobiology
College of Veterinary Medicine

KANSAS STATE UNIVERSITY
Manhattan, Kansas

2020

Approved by:

Major Professor
Jianfa Bai

Copyright

Abstract

Infectious diseases of food animals have major impacts on economic returns and public health. Effective surveillance and control of animal diseases are very important, in which rapid and accurate detection of etiological agents play a critical role. Molecular diagnostics have been developed and used extensively. Because of its high sensitivity, high specificity, high-throughput and short turnaround time, molecular diagnostics is considered a powerful tool for detection and identification of infectious agents.

Several molecular assays have been developed and validated for major swine virus detections in this dissertation. In Chapter 2.1, a multiplex quantitative real-time PCR assay (mqPCR) was developed to detect and differentiate two porcine circoviruses (PCV) associated with the diseases of similar clinical signs: the novel PCV type 3 (PCV3) and the well-known economically important PCV type 2 (PCV2). In Chapter 2.2, a mqPCR assay was developed and validated for detection and differentiation of three PCV2 genotypes, PCV2a, PCV2b and PCV2d, the most frequently circulating genotypes in the US. In Chapter 2.3, a real-time RT-PCR (RT-qPCR) assay of Seneca Valley virus 1 (SVV-1) was developed and multiplexed with the published foot-and-mouth virus (FMDV) assays to differentiate the two viruses, which cause clinically similar vesicular diseases in swine. In Chapter 2.4, a real-time PCR assay was developed for rapid detection of African swine fever virus (ASFV). Its current spread in Asia and Europe resulted in significant economic losses on the global swine industry. In Chapter 2.5, the Luminex xTAG assay was developed to detect type 2 porcine reproductive and respiratory syndrome virus (PRRSV-2), one of most economically significant viruses in the US. The multiplexing assay allowed to differentiation of the field strains from the vaccine strains. In the design of the molecular assays described above, the most recent sequence databases were built to obtain high strain coverages.

The analytical and diagnostic analyses showed high sensitivities and specificities. Subsequent evaluation of clinical samples of different sample types indicated good diagnostic applicability. Finally, addition of the internal controls helped to monitor extractions and amplification efficiencies and to avoid false negative results.

Genetic diversity and prevalence of PCV3 and PCV2 were investigated (Chapter 3.1). It showed high prevalence of PCV3 and PCV2 in the swine herds of the Midwestern region of the US in 2016-2018. The phylogenetic analysis indicated low genetic diversity of PCV3, but high genetic diversity of PCV2. A new genotype, PCV2i, was proposed and the genotypes, PCV2a, PCV2b and PCV2d, were indicated as those circulating in the region. Finally, genetic diversity analysis of Rotavirus C (RVC) was conducted (Chapter 3.2). Thirty-one complete genomes were sequenced with next generation sequencing technology and analyzed with all available published reference sequences. Based on the phylogenetic analysis, several new genotypes were defined here, G18-G31 for VP7, P[22]-P[26] for VP4, R5 for VP1, A9-A12 for NSP1, N9-N10 for NSP2, T7-T9 for NSP3 and E6-E8 for NSP4. Genotyping of the 31 complete genomes indicated reassortment existed in 7 segments, VP7, VP4, VP6, VP2, NSP1, NSP2 and NSP3. The study updated the genotypes of RVC strains to help understand its diversity and evolution.

Table of Contents

List of Figures

List of Tables

Acknowledgements

First and foremost, I would like to thank my major advisor, Dr. Jianfa Bai, for his support and encouragement during my study. Learned from him, I totally understand the power of persistence and inspiration. With his mentor, I finished several projects, presented my data in various professional conferences, published in peer-reviewed journals and earned awards from conferences and the college. I really appreciated that he gave me tremendous freedom and trust in conducting the projects.

Secondly, I would like to thank my committee members, Drs. T. G. Nagaraja, Megan Niederwerder and Jason Woodworth. I'm so lucky that they generously gave me precious suggestions from different perspectives and tremendously support to my career.

Thirdly, I would like to thank Swine Health Information Center and National Pork Board, funded 4 projects in my study. Also, I'd like to thank Kansas State Veterinary Diagnostic Laboratory (KSVDL) for supporting my research during the past 4 years.

I'd like to thank our collaborators, Dr. Ying Fang in University of Illinois at Urbana-Champaign, Dr. Jianqiang Zhang of Iowa State University and Drs. Wei Jia, Amaresh Das, Lizhe Xu and Kimberly Dodd of Foreign Animal Disease Diagnostic Laboratory, APHIS, Plum Island Animal Disease Center. Also, I'd like to thank our collaborators in KSVDL, Dr. Lalitha Peddirreddi, Yuan Feng and Dr. Jinping Fu of KSVDL Molecular Service Laboratory and Dr. Roman Pogranichniy and Joe Anderson in KSVDL Virology Laboratory. This work would not be possible without the support from you!

Next, I'd like to thank my colleagues and also friends in KSVDL Molecular R&D Laboratory, Elizabeth Porter, Nanyan Lu, Dr. Lance Noll, Colin Stoy, Dr. Xuming Liu, Dr. Junsheng Dong, Cong Zhu, Hao Shi, Dr. Xue Leng, Dr. Wanglong Zheng and Dr. Hewei Zhang.

Finally, I’d like to deeply thank my parents, Peizhen Wang and Laizhong Wang, who always stand by me. I’d like to thank my aunts, uncles and cousins in China, whose care let me feel warm here. Also, I want to thank my parents in law, Jufang Qin and Jianming Guo, for your help during the years. At the end, I’d like to thank my husband, Rui Guo, and my daughter, Gwen Guo for keeping me busy and being a better researcher, mom, and wife.

Chapter 1 Literature Review

1.1 Molecular diagnostic technologies to identify pathogens for animal infectious diseases

Infectious diseases caused by viruses in animals have a tremendous impact on public health and economy. Early accurate diagnostics is critical to control the diseases efficiently. Traditional or conventional diagnostics include direct observation of the presence of the microorganism by optical microscopy, hunt for the etiological components by histopathological examination, and detection of the presence of the antibodies produced in the immune responses by different immunological assays, such as the enzyme-linked immunosorbent assay (ELISA) and agglutination tests. Differently, the advanced molecular diagnostics is designed to detect nucleic acids, DNA or RNA, which display several advantages. Firstly, sequence specificity of DNA or RNA makes molecular detection highly specific. Secondly, nucleic acid amplification technology allows molecular detection to be highly sensitive. Genes can be amplified by millions of folds with the polymerase chain reaction (PCR). Thirdly, molecular diagnostic tests have short turnaround time. Generally, the sample preparation is very simple without long incubation time or culture step. Furthermore, molecular diagnostics has the capacity to multiplex, like the fluorescence-based multiplex PCR. Multiplexing helps to lower the cost for each pathogen detection. Recently, a lot of molecular diagnostic technologies have been developed to identify pathogens, three of which would be introduced below for their application in the dissertation.

1.1.1 TaqMan real-time PCR assay

The PCR technique was invented in the 1980s (Mullis et al., 1986). It has become the gold standard molecular assay in biomedical science. In the reaction, the thermostable Thermus aquaticus (Taq) DNA polymerase adds deoxynucleotides (dNTPs) sequentially following the primers to form the complementary strand. After 30 to 40 times of amplification cycles, the target gene regions are copied for millions of folds resulting in easily detectable DNA fragments. However, the classic endpoint PCR can't quantify the initial target molecules. Therefore, the TaqMan real-time PCR was invented (Gibson, Heid, & Williams, 1996; Heid, Stevens, Livak, & Williams, 1996). Besides the primers, a hydrolysis probe is included to emit fluorescent signal upon cleavage owing to the 5' to 3' exonuclease activity of polymerase (Holland, Abramson, Watson, & Gelfand, 1991). As shown in Figure 1.1.1, there's a quencher fluorochrome at the non-extendable 3' end, which can absorb the fluorescent signal of the reporter fluorescence in close proximity due to fluorescence resonance energy transfer (FRET). When the probe is replaced with the extended complementary strand, it's cleaved by the polymerase to release the reporter fluorescence from the quencher. The fluorescent emission is measured in each amplification cycle. The number of cycles required to reach the threshold to detect the fluorescent signal is CT value, correlated to the copy number of initial target molecules.

Besides its high sensitivity and specificity (Holland et al., 1991), the real time PCR has great capability to multiplex. Use of different reporter and quencher dyes makes it possible to detect different target molecules in a single reaction (Wittwer, Herrmann, Gundry, & Elenitoba-Johnson, 2001). Multiplexing helps the assay to be more efficient and saves both time and costs.

Another advantage is convenient but powerful data analysis, such as standard curve analysis and high-resolution melt analysis. Also, the technology has high flexibility. Firstly, addition of reverse transcriptase makes it suitable to RNA viruses (Bustin, 2000). Secondly, the range of probe length can be wide. For example, attachment of a minor groove binding (MGB) molecule allows for shorter probe design with increased melting temperature (Tm) (Kutyavin et al., 2000). Therefore, TaqMan real time PCR has been wildly applied in virus detection of major animal diseases, including swine or avian influenza viruses (W. Chen et al., 2007; Richt et al., 2004), bluetongue virus (Vanbinst, Vandenbussche, Dernelle, & De Clercq, 2010) and Rift valley fever virus (Garcia et al., 2001).

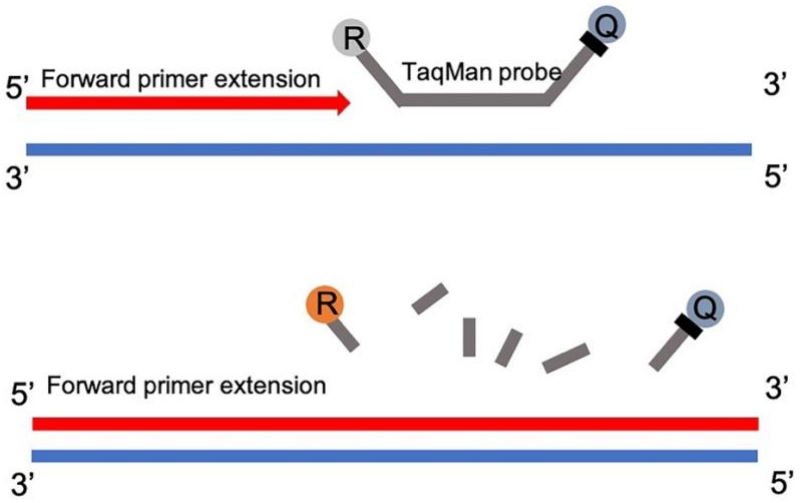

Figure 1.1.1 Schematic of TaqMan real time PCR

The fluorescent emission is measured when the reporter fluorescence is released from the quencher of the Taqman probe during primer extension in each amplification cycle (Holland et al., 1991).

1.1.2 Luminex xMAP® technology

Luminex xMAP® technology is a bead-based technology with major advancement in multiplexing. Each bead can be distinguished from another for its unique spectral address. Coated with proteins or nucleic acids on the beads, the assay can work similar to ELISA or nucleic acid hybridization procedure (https://www.luminexcorp.com/xmap-technology/). To detect target DNA or RNA extracted from the samples, the beads are coupled with nucleic acid probe tags, complementary to the forward primers. Therefore, the amplified target molecules can hybridize with the probe tags in the beads. The reverse primers with biotinylated oligos can bind to streptavidin with high affinity. Besides the internal dyes to identify each bead particle, fluorescence signal from streptavidin-R-Phycoerythrin (SAPE) is to identify the target molecules. (Figure 1.1.2) The median fluorescent intensity (MFI) is measured to determine whether the sample is positive of the target molecule. Like real time PCR, standard curve analysis can be performed to evaluate its sensitivity.

Luminex xMAP Technology allows multiplexing of up to 500 targets within a single reaction. It lowers the costs and save time compared to other multiplex assays, like real-time PCR. For human disease diagnostics, some commercial or non-commercial assays are developed for detecting viruses, such as respiratory viruses (Brunstein, Cline, McKinney, & Thomas, 2008; Krunic, Merante, Yaghoubian, Himsworth, & Janeczko, 2011) and enteric viruses (Ohrmalm et al., 2012). In animal disease diagnostics, most of Luminex assays are for antibody detection, including the porcine viruses, porcine respiratory and respiratory syndrome virus (PRRSV) (Langenhorst et al., 2012) and porcine circovirus type 2 (PCV2) (Lin, Wang, Murtaugh, &

Ramamoorthy, 2011). However, some nucleic acid detection assays were developed recently, like identification of the five common canine viruses (M. L. Wu et al., 2018) and the four avian respiratory viruses (Cong et al., 2018).

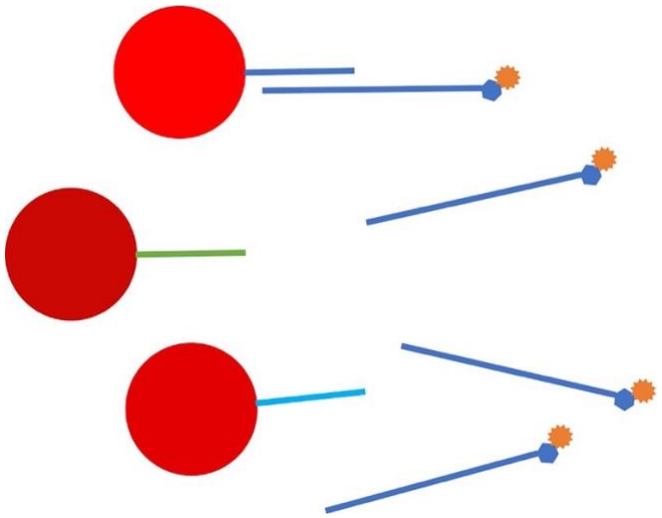

Figure 1.1.2 Schematic of nucleic acid assay analysis on Luminex xMAP® beads

Each bead with unique color dye has a unique probe tag complementary to the target sequence. The fluorescence signal can be only detected on beads when the hybridization succeeds. (http://cdn2.hubspot.net/hub/128032/file-213083097-pdf/ Luninex-xMapCook book.pdf)

1.1.3 Next generation sequencing (NGS) technologies

Compared to Sanger sequencing, NGS technologies are high throughput sequencing methods characterized by massively paralleling of sequencing and data generation. The commercial platforms are based on the concept of sequencing by synthesis (SBS) or single molecular sequencing (SMS) (McCombie, McPherson, & Mardis, 2019). Due to the difficulty in data collection from single molecule in SMS (Amarasinghe et al., 2020), SBS is selected by most

of the commercial platforms, one of which is Illumina. The procedure includes library preparation, amplification on the flow cell, sequence by synthesis and data analysis (Bentley et al., 2008; Dohm, Lottaz, Borodina, & Himmelbauer, 2008; J. Guo et al., 2008). Briefly, the genomic DNA molecules are cleaved by transposons and added with sequencing primers at each end. Then, the sequences complementary to those on flow cells and indexes are added by PCR result in sequencing ready fragments. After attachment on the flow cells, the complementary strands are amplified, named bridge amplification, which followed by repeat runs of amplification to create double stranded fragments, named clonal amplification. Washed off the reverse strands, forward strands are the templates to hybridize with fluorescently tagged dNTP. Each base of the fluorescent signal is recorded by the machine, named sequence by synthesis. Finally, the genomic DNA sequences are achieved through the process of data analysis, generally including quality control, assembly and alignment (Figure 1.1.3).

Within the past decade, NGS technologies have experienced extraordinary progress, which brought fast, low cost and whole genome wide sequencing. In public health, it has been wildly used in virus studies to discover novel viruses, like severe acute respiratory syndrome coronavirus-2 (SARS-CoV-2) (Zhu et al., 2020), investigate variability of viral genomes, like Pandemic 2009 Influenza A virus (Kuroda et al., 2010), and trace their evolution, like human immunodeficiency virus (HIV) (Tebit & Arts, 2011). In veterinary medicine, NGS technologies are increasingly applied to study animal infectious diseases, such as genetic diversity of foot-and-mouth disease

virus (FMDV) (Wright et al., 2011), discovery of porcine circovirus type 3 (PCV3) (Palinski et al., 2017) and transmission of influenza viruses in ferrets (Wilker et al., 2013).

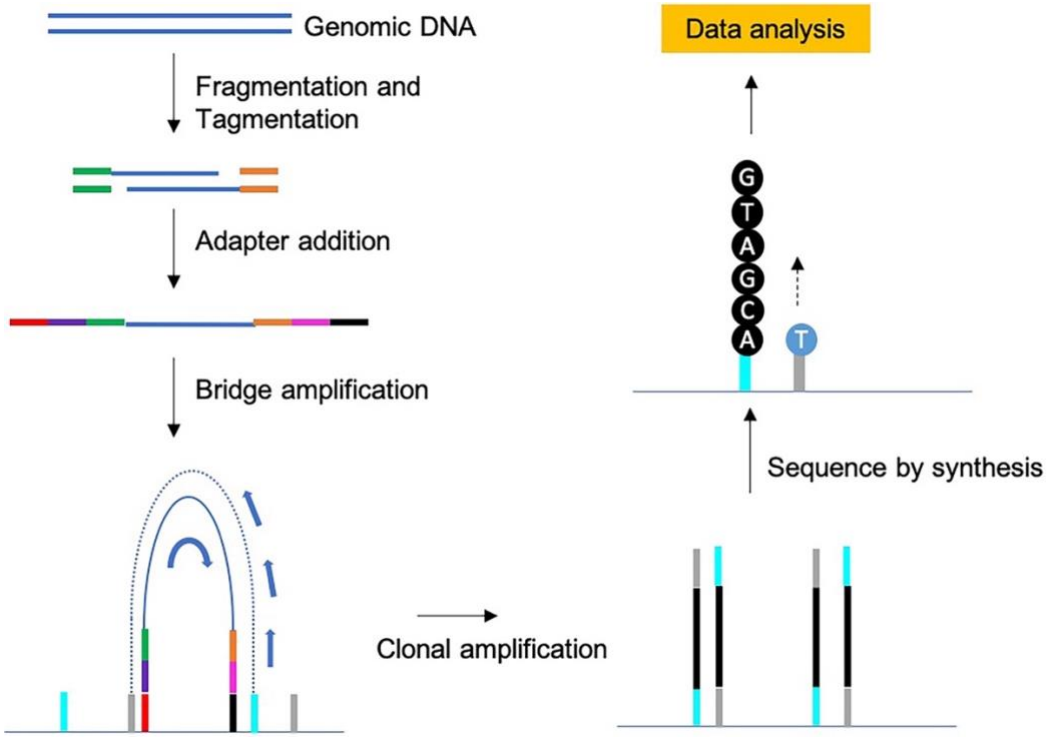

Figure 1.1.3 Schematic of Illumina next generation sequencing technology based on Sequencing by synthesis

The genomic DNA molecules are cleaved by transposons and added with sequencing primers at each end. Then, the sequences complementary to those on flow cells and indexes are added by PCR resulted in sequencing ready fragments. After attachment on the flow cells, the complementary strands are amplified, named bridge amplification, which followed by repeat runs of amplification creating double stranded fragments, named clonal amplification. When washed off the reverse strands, forward strands are the templates to hybridize with fluorescently tagged

dNTP. Each base of the fluorescent signal is recorded by the machine, named sequence by synthesis (SBS). Finally, the genomic DNA sequences are achieved through the process of data analysis (Bentley et al., 2008).

1.2 Viruses of animal infectious diseases

1.2.1 Porcine circovirus type 2 (PCV2)

1.2.1.1 Impact of the disease

Porcine circovirus associated disease (PCVAD) is one of the most important swine diseases, which has caused immense economic losses in the global swine industry (Allan et al., 1998; Firth, Charleston, Duffy, Shapiro, & Holmes, 2009). PCVAD is comprised of several clinical conditions, including post-weaning multi-systemic wasting syndrome (PMWS), porcine dermatitis and nephropathy syndrome (PDNS), reproductive disorders and respiratory disease. PMWS is characterized by wasting with or without symptoms such as dyspnea, pallor of the skin, diarrhea and icterus in young pigs (Chae, 2004). The clinical signs of PDNS include multifocal erythematous skin lesions associated with dermal necrotizing vasculitis and renal enlargement with cortical petechiae in growing and finishing pigs (Thomson, Higgins, Smith, & Done, 2002). Reproductive disorders appear as high rates of abortion, stillbirth and fetal mummification in herds (West et al., 1999). Respiratory disease is characterized by slow growth, poor weight gain, lethargy, fever, cough, and dyspnea in growing and finishing pigs (J. Kim, Chung, & Chae, 2003).

1.2.1.2 PCV2 classification and genome characterization

PCV2 plays the major role in PCVAD, which belongs to family *Circoviridae*, genus *Cirovirus*. The small non-enveloped virus has a circular single-stranded DNA genome of about 1,760 bp (Ren, Chen, & Ouyang, 2016). There're two major ambisense open reading frames (ORFs) in the viral genome, ORF1 and ORF2. (Figure 1.2.1) ORF1 codes for the replicase (Rep) protein and ORF2 for the capsid (Cap) protein. The Rep protein is a non-structural protein and functions for the viral replication, while the structural Cap protein dominates immunogenicity (Mankertz et al., 2004; Nawagitgul et al., 2002).

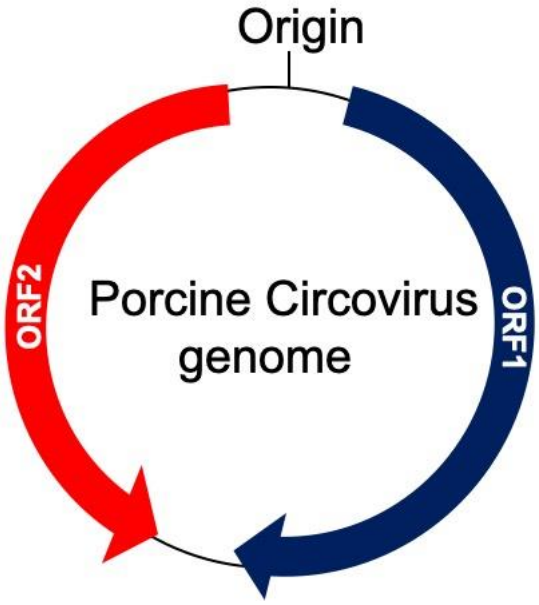

Figure 1.2.1 Schematic of genome structure of porcine circoviruses

They have two major ambisense open reading frames (ORFs) in the viral genome, ORF1 and ORF2. ORF1 codes for the replicase (Rep) protein and ORF2 for the capsid (Cap) protein. (Rosario et al., 2017)

1.2.1.3 Global distribution and diversity

PCV2 infection has been reported in swine herds worldwide (C. T. Xiao, Halbur, & Opriessnig, 2015). As a DNA virus, PCV2 has high evolutionary mutation rate of 1.2×10^{-3} substitutions/ site/year and has been constantly evolving (Firth et al., 2009). With the emerging viral strains, PCV2 has been mainly divided into 5 genotypes, namely PCV2a–2e strains, according to the diversity level of the ORF2 nucleotide sequences (Franzo, Tucciarone, Cecchinato, & Drigo, 2016; C. T. Xiao et al., 2015).

In the past 20 years, two major shifts in the predominant genotype were observed globally: PCV2a towards PCV2b around 2003 and PCV2b towards PCV2d around 2012. Although the genotype shift in 2003 was associated with increased pathogenic virulence, the PCV2a-based vaccines were still effective against the emerged PCV2b strains (Afolabi, Iweriebor, Obi, & Okoh, 2019; Beach & Meng, 2012). The genotype shift to the PCV2d strains appears to be associated with both the increased pathogen virulence and vaccine failure (Beach & Meng, 2012; L. J. Guo et al., 2012; C. T. Xiao et al., 2015).

1.2.1.4 Diagnostics

PCV2 infection is ubiquitous in healthy and sick pigs (Allan & Ellis, 2000). Therefore, the first step is to assess the clinical signs of PCVAD described above. Based on the results, DNA or antibody can be detected by several techniques. For DNA detection, PCR is widely used, including regular PCR (Huang, Hung, Wu, & Chien, 2004; J. Kim, Choi, Han, & Chae, 2001), nested PCR (J. Kim, Han, Choi, & Chae, 2003; Larochelle, Bielanski, Muller, & Magar, 2000) and real time

PCR assays (Q. Liu, Wang, Willson, & Babiuk, 2000; Olvera, Sibila, Calsamiglia, Segales, & Domingo, 2004). In addition, labeled DNA probes are applied to hybridize with the specific portion of PCV2 genomes in *in situ* hybridization (ISH) assays (McNeilly et al., 1999; Sirinarumitr et al., 2000). For antibody detection, several serological assays are developed, including indirect fluorescent antibody (IFA) assays (Allan et al., 1998; Pogranichnyy et al., 2000), ELISA (S. Q. Sun et al., 2010; Walker et al., 2000) and neutralization assays (Meerts, Van Gucht, Cox, Vandebosch, & Nauwynck, 2005; Pogranichnyy et al., 2000). Besides the rapid detection methods, the viral particles are sometimes detected by immunohistochemistry (IHC) assays (McNeilly et al., 1999; Sorden, Harms, Nawagitgul, Cavanaugh, & Paul, 1999) and electron microscopy observation (X. Liu et al., 2019; Yan, Zhu, & Yang, 2014).

1.2.2 PCV3

1.2.2.1 Impact of the disease

PCV3 was found in pigs with clinical disease similar to PCVAD in the US (Palinski et al., 2017). Thenceforth, its association with PCVAD-like clinical manifestations has been demonstrated in many studies, including PDNS (Arruda et al., 2019; Palinski et al., 2017; Zhai et al., 2017), reproductive failure (Arruda et al., 2019; Bera et al., 2020; G. H. Chen et al., 2017; Deim et al., 2019; Faccini et al., 2017; S. H. Kim et al., 2018; Palinski et al., 2017; Zou et al., 2018) and respiratory disease (Bera et al., 2020; Kedkovid et al., 2018; S. H. Kim et al., 2018). PCV3 is also related with other clinical symptoms, such as central nervous system signs (Arruda

et al., 2019; G. H. Chen et al., 2017) and systemic inflammatory disease (Arruda et al., 2019; Phan et al., 2016).

The pathogenesis and the impact of PCV3 on animal health are still unclear. However, one study illustrated that PDNS-like disease can be reproduced in pigs with the PCV3 infectious clone (Jiang et al., 2019) and recently PCV3 was isolated using primary porcine kidney cells (Oh & Chae, 2020).

1.2.2.2 PCV3 classification and genome characterization

Clustered together with PCV2, PCV3 belongs to family *Circoviridae*, genus *Cirovirus*. It's a small non-enveloped virus with a circular single-stranded DNA genome of about 2,000 bp. Like PCV2, it has two major ambisense ORFs, ORF1 coded for the replicase (Rep) protein and ORF2 for the capsid (Cap) protein. (Figure 1.2.1) (Palinski et al., 2017)

1.2.2.3 Global distribution and diversity

Since its discovery in 2015 in the US, PCV3 has been reported in many countries, including South Korea, China, Thailand, Brazil, Italy, Spain, Sweden, Germany and Poland (Faccini et al., 2017; Fux et al., 2018; S. H. Kim et al., 2018; Klaumann et al., 2018; Qi et al., 2019; Stadejek, Wozniak, Milek, & Biernacka, 2017; Sukmak et al., 2019; Tochetto et al., 2018; Ye, Berg, Fossum, Wallgren, & Blomstrom, 2018).

Based on limited PCV3 sequences, two major genotypes, PCV3a and PCV3b, were suggested by phylogenetic analysis in a previous study, which indicated a fast evolution rate like PCV2 (Li et al., 2018). However, analyzed with more sequences, recent studies indicated a far

slower evolution rate, approximately 10^{-5} substitution/site/year and only one genotype was proposed (Franzo et al., 2020; Franzo et al., 2019).

1.2.2.4 Diagnostics

Different from PCV2, PCV3 is discovered with NGS technology (Palinski et al., 2017). For rapid detection of its DNA genome, numerous molecular assays were developed, including real time PCR assays (G. H. Chen et al., 2017; J. Wang, Zhang, et al., 2017), loop-mediated isothermal amplification (LAMP) assays (Y. R. Park et al., 2018; Zheng et al., 2018) and digital PCR assays (Y. Liu, Meng, Shi, & Li, 2019; Y. Zhang et al., 2019). Additionally, ISH and IHC assays were developed to study its distribution in the tissues (Arruda et al., 2019; Jiang et al., 2019; S. H. Kim et al., 2018). For antibody detection, ELISA assays were established with bacteria or baculovirus expressed capsid proteins as the coating antigens (Deng et al., 2018; S. Zhang et al., 2019)

1.2.3 Type 2 porcine reproductive and respiratory syndrome virus (PRRSV-2)

1.2.3.1 Impact of the porcine reproductive and respiratory syndrome (PRRS)

PRRS is one of the most economically significant viral disease to the pork industry in the US. It was estimated that PRRS could results in annual losses of $664 million losses in the national breeding and growing-pig herds (Holtkamp et al., 2013). The clinical presentations in pregnant sows include reproductive failure, such as abortion and stillborn fetuses, fever, pneumonia, red/blue discoloration of the ears and vulva and death (Albina, Madec, Cariolet, & Torrison, 1994; Done & Paton, 1995; Hopper, White, & Twiddy, 1992). In neonatal pigs, the animals can develop

severe dyspnea and tachypnea. Also, they may exhibit edema, blue discoloration of the ears, central nervous system signs and death (Albina et al., 1994; Hopper et al., 1992; Paton, Brown, Scott, Done, & Edwards, 1992; Rossow et al., 1995).

1.2.3.2 PRRSV-2 classification and genome characterization

PRRSV, the causative agent is an enveloped, positive single-stranded RNA virus, belonging to family *Arteriviridae* and order *Nidovirales* (Cavanagh, 1997). Due to clear genome divergence, PRRSV was divided into two different species, PRRSV-1 and PRRSV-2 by the International Committee on Taxonomy of Viruses (ICTV) in 2016 (Kappes & Faaberg, 2015; Kuhn et al., 2016). Although a few circulating PRRSV-1 strains circulated have been reported recently (A. P. Wang et al., 2019), PRRSV-2 is the main species affecting the swine industry in the US. PRRSV-2 has the genome of about 15.5 kb in length, which contains more than 10 open reading frames (ORFs). From 5' untranslated region (UTR) to 3' UTR, ORF1a and ORF1b encode non-structural proteins (nsps), nsp1α, nsp1β, nsp2-nsp6, nsp7α, nsp7β and nsp8-nsp12, and ORFs, 2-7, encode structural proteins, GP2, E, GP3, GP4, GP5a, GP5, M and N, respectively. (Figure 1.2.2) (Kappes & Faaberg, 2015)

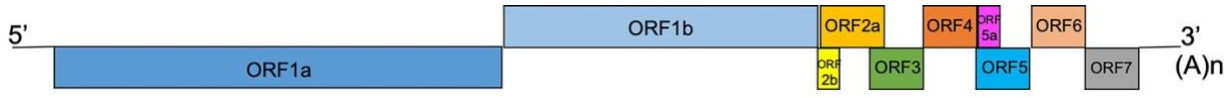

Figure 1.2.2 Schematic of genome structure of PRRSV-2

PRRSV-2 genome contains more than10 ORFs, ORF1a and ORF1b encoded non-structural proteins and ORF2-ORF7 encoded structural proteins, respectively. (Snijder, Kikkert, & Fang, 2013)

1.2.3.3 Global distribution and diversity

PRRSV-2 has worldwide distribution, including Asian (Z. Guo, Chen, Li, Qiao, & Zhang, 2018), North American (Shi et al., 2013) and European countries or areas (Stadejek, Stankevicius, Murtaugh, & Oleksiewicz, 2013).

Because of lacking proofreading mechanism during RNA replication, PRRSV-2 has a high evolution rate of approximate 10^{-2} substitution/site/year (Hanada, Suzuki, Nakane, Hirose, & Gojobori, 2005). Among the genes, nsp2 is well known as the most variable region with mutations and deletions (Allende et al., 2000; Tian et al., 2007), and ORF5 encoded the major envelope protein is highly variable (N. Chen, Trible, Kerrigan, Tian, & Rowland, 2016; Meng, Paul, Halbur, & Morozov, 1995).

1.2.3.4 Diagnostics

A lot of molecular technologies have been applied for PRRSV-2 RNA detection, including the conventional multiplex reverse transcription PCR (RT-PCR) (Hu et al., 2016; Li et al., 2017; X. L. Wu et al., 2017; K. Yang et al., 2017; Zhao et al., 2019), RT-Real time PCR assay (N. Chen et al., 2019; J. Y. Park et al., 2019), ORF5 sequence based restriction fragment length polymorphism (RFLP) (Ramirez et al., 2019), LAMP (J. Y. Park et al., 2016), melting curve analysis (J. Y. Sun et al., 2018), microarray (Erickson et al., 2018), Luminex xTAG (L. Xiao et al., 2018), droplet digital PCR (Q. Yang et al., 2017) and NGS (J. Zhang et al., 2017). For its antibody detection, various serological tests have been developed, such as ELISA (Dea, Wilson, Therrien, & Cornaglia, 2000; Seuberlich, Tratschin, Thur, & Hofmann, 2002; Takikawa et al.,

1996), IFA assays (Cho, Freese, Yoon, Trigo, & Joo, 1993; I. J. Yoon et al., 1992), immunoperoxidase monolayer antibody (IPMA) assays (Decorte et al., 2014; K. J. Yoon et al., 1995) and neutralization assays (Ouyang et al., 2013; I. J. Yoon, Joo, Goyal, & Molitor, 1994).

1.2.4 Seneca Valley virus 1 (SVV-1)

1.2.4.1 Impact of the disease

The SVV-1 causes vesicular disease in pigs. The clinical manifestations include vesicles on the snouts and coronary bands, lameness, anorexia, lethargy, fever and diarrhea (Hause, Myers, Duff, & Hesse, 2016; Segales, Barcellos, Alfieri, Burrough, & Marthaler, 2017). Therefore, it's clinically indistinguishable from other vesicular diseases, such as Foot-and-mouth disease (FMD), swine vesicular disease (SVD) and vesicular stomatitis (VS). Due to severe negative economic implications of FMD, SVD and VS, every swine vesicular disease outbreak is investigated, incuding those caused by SVV-1. In a recent outbreak, the etiology was also confirmed to lead to neonatal mortality (Gimenez-Lirola, Rademacher, et al., 2016).

1.2.4.2 SVV-1 classification and genome characterization

The SVV-1 is a non-enveloped, single-stranded positive-sense RNA virus. It's the only member in genus *Senecavirus*, family *Picornaviridae* (Adams et al., 2015). SVV-1 has the genome of approximately 7.3 kb in length (Venkataraman et al., 2008), comprised of each UTR at 3' and 5' end and a large single ORF. The 5'UTR has a covalently linked protein, named VPg, that probably acts during replication, and internal ribosome entry site (IRES) (Tuthill, Groppelli, Hogle, & Rowlands, 2010; Willcocks et al., 2011).The large open reading frame encodes a

polyprotein, including a leader (L) and three major proteins, P1, P2 and P3. P1 is further cleaved into 4 structural capsid proteins, VP1-4. P2 and P3 are cleaved into non-structural proteins 2A-C and 3A-D respectively, related to virus replication. (Figure 1.2.3) (Hales et al., 2008; Tuthill et al., 2010)

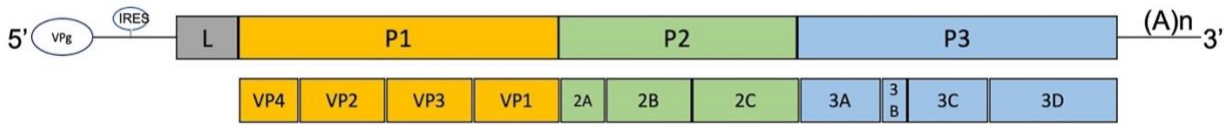

Figure 1.2.3 Schematic of SVV-1 genome

The 5'UTR has a covalently linked protein, named VPg, that probably acts during replication and internal ribosome entry site (IRES). The large open reading frame encodes a polyprotein, including a leader (L) and three major proteins, P1, P2 and P3. P1 is further cleaved into 4 structural capsid proteins, VP1-4. P2 and P3 are cleaved into non-structural proteins 2A-C and 3A-D. (Segales et al., 2017)

1.2.4.3 Global distribution and diversity

Since its recrudescence in 2015, several countries have reported increased SVV-1 cases. Thus, the virus presents in swine population globally, including the US, Canada, Brazil, Colombia, Thailand and China (Armson et al., 2019; Fowler et al., 2017; Leme et al., 2015; Pasma, Davidson, & Shaw, 2008; Saeng-chuto et al., 2018; D. Sun, Vannucci, Knutson, Corzo, & Marthaler, 2017; Q. Wu et al., 2016).

Like most single-stranded RNA viruses, SVV-1 has high nucleotide substitution rate. The previous phylogenetic analyses indicated strains evolved into different clusters (B. Guo et al.,

2016; Saeng-chuto et al., 2018; Xu et al., 2017). Compared to the similarity of the genome sequences, the VP1 protein has the highest degree of divergence in P1 structure protein region. In P2 and P3 protein region, 3A and 3D are more diverse than other non-structural proteins 2A, 2B, 2C, 3B, and 3C. (Saeng-chuto et al., 2018)

1.2.4.4 Diagnostics

Although virus isolation is considered as the 'gold standard' (Hales et al., 2008), several molecular assays have been established for rapid antigen diagnosis, including conventional PCR assays, RT-qPCR assays, RT-LAMP assays and reverse transcription droplet digital PCR assay. In these assays, the 3D region, VP1 coding region and 5' UTR are the selected detection targets (Agnol, Otonel, Leme, Alfieri, & Alfieri, 2017; Bracht, O'Hearn, Fabian, Barrette, & Sayed, 2016; Feronato et al., 2018; Fowler et al., 2017; Gimenez-Lirola, Rademacher, et al., 2016; Z. Zhang, Zhang, Lin, Chen, & Wu, 2019). In addition, ISH and IHC are applied to detect the virus in the tissues (Leme et al., 2016; Resende, Marthaler, & Vannucci, 2017). For antibody detection, ELISA, IFA and neutralizing assays have been established (Dvorak et al., 2017; Gimenez-Lirola, Rademacher, et al., 2016; Goolia et al., 2017; Yang, van Bruggen, & Xu, 2012).

1.2.5 Foot-and-mouth disease virus (FMDV)

1.2.5.1 Impact of the disease

Foot-and-mouth disease (FMD) is a highly contagious disease of cloven-hoofed animals including pigs, cattle, sheep and goats (Alexandersen, Zhang, Donaldson, & Garland, 2003). It's one of the most economically important animal diseases globally (Jamal & Belsham, 2013). It's

estimated that FMD leads to losses of $10-20 billion each year in the endemic areas (Knight-Jones & Rushton, 2013). Although the United States eradicated FMD and has not seen the disease since 1929, the disease is still a major concern and listed as one of the Tier-1 select agents by the US Department of Agriculture (USDA) because of its ability to spread very quickly and significant economic impact. The clinical manifestations include fever, lameness and vesicular lesions on the mouth and feet (Alexandersen et al., 2003). Although the mortality rate is low in adults, it dramatically affects animal production with lost weight and reduced milk yield for long perids of time due to persistent infection in a high portion of sick animals (Alexandersen, Zhang, & Donaldson, 2002).

1.2.5.2 FMDV classification and genome characterization

FMD is caused by FMDV, a single-stranded positive-sense RNA virus, which belongs to the genus *Aphthovirus* in family *Picornaviridae* (Jamal & Belsham, 2013). FMDV has the genome of 8.4 kb in length, comprised of a large ORF and UTR at each 5' and 3' end. The ORF encodes a single polyprotein, which cleaves into L, P1-2A, P2 and P3. P1-2A is further processed into mature proteins, structural proteins (VP1-4) and non-structural protein 2A; P2 is processed into non-structural proteins, 2B and 2C ; and P3 is processed into non-structural proteins, 3A, 3B1-3, 3C and 3D. The 5'UTR has a covalently linked protein VPg and distinct replication related elemtents, including a poly C tract (Cn), pseudoknots (PK) and IRES. (Jamal & Belsham, 2013; Kristensen & Belsham, 2019) (Figure 1.2.4)

Figure 1.2.4 Schematic of FMDV genome

The large ORF encodes a single polyprotein, which cleaved into L, P1-2A, P2 and P3. P1-2A is further processed into structural proteins (VP1-4) and non-structural protein 2A; P2 is processed into non-structural proteins, 2B and 2C ; and P3 is processed into non-structural proteins, 3A, 3B1-3, 3C and 3D. The 5'UTR has a covalently linked protein VPg and distinct replication related elemtents, poly C tract (Cn), pseudoknots (PK) and IRES. (Jamal & Belsham, 2013)

1.2.5.3 Global distribution and diversity

FMDV has global distribution and two-thirds of the continents are considered FMDV endemic, including Europe, Africa, Asia and South America. (Arzt et al., 2019; Poonsuk, Gimenez-Lirola, & Zimmerman, 2018)

Lack of proofreading mechanisms has resulted in a high mutation rate during FMDV replication, in both structural-coding and nonstructural protein-coding regions. Combined with the recombination events that can occur in the protein-coding regions, the high level of FMDV genetic diversity has been observed (Garcia-Arriaza, Ojosnegros, Davila, Domingo, & Escarmis, 2006). For their extensive variation in capsid protein, there's no cross-reaction among the seven serotypes, O, A, C, SAT1, SAT2, SAT3 and Asia-1, and limited cross-reaction among different strains within the same serotype (Asfor et al., 2020; Paton, Reeve, Capozzo, & Ludi, 2019).

1.2.5.4 Diagnostics

Assays are well established to detect either the virus or antibody that induced during infection. For virus detection, the most used and validated tests are real time PCR assays (Ferris, King, Reid, Shaw, & Hutchings, 2006; Shaw et al., 2007). Several standardized assays are applied following the recommendation from the World Organization for Animal Health (OIE) or USDA (Callahan et al., 2002; Reid et al., 2001; Reid, Grierson, Ferris, Hutchings, & Alexandersen, 2003; Shaw et al., 2007). In addition, several other virus detection assays are established, including direct complement fixation tests (Ferris & Dawson, 1988; Rice & Brooksby, 1953), antigen-capture ELISA (Morioka, Fukai, Sakamoto, Yoshida, & Kanno, 2014; Roeder & Le Blanc Smith, 1987) and lateral-flow assays (Ferris et al., 2010; Oem et al., 2009). For antibody detection, indirect complement fixation tests, neutralization assays and ELISA are developed and generally used in clinic (Biswal, Jena, Mohapatra, Bisht, & Pattnaik, 2014; Pacheco, Arzt, & Rodriguez, 2010; Sakaki, Suphavilai, & Chandarkeo, 1978; Senthilkumaran et al., 2017).

1.2.6 African swine fever virus (ASFV)

1.2.6.1 Impact of the disease

African swine fever (ASF) is a highly contagious swine viral disease, characterized by a wide range of clinical signs ranging from subclinical signs to sudden death that often occurs within 7 − 10 days but can be as early as 4 days after infection (Bellini, Rutili, & Guberti, 2016). When infected with the virulent stains, it usually displays acute viral haemorrhagic disease in domestic pigs, characterized with clinical signs including high fever, reddened skin and cyanosis, severe depression, vomiting, diarrhea, difficult breathing, abortion and death. The mortality can approach

100%. Thus, ASF is one of the most serious swine infectious diseases (Blome, Gabriel, & Beer, 2013). It has attracted worldwide attention since its spread through Western Europe and Asia in 2017, and particularly to China, the largest pork producer in the world (Ge et al., 2018). The outbreak has caused severe economic losses in the global swine industry. Previous studies demonstrated that the worldwide epidemic situation may dramatically increase the risk of introduction to ASF-free countries, such as the USA and Japan (Ito, Jurado, Sanchez-Vizcaino, & Isoda, 2020; Jurado et al., 2019).

1.2.6.2 ASFV classification and genome characterization

ASFV is the causative agent of ASF, the only member of the family *Asfarviridae* (Alonso et al., 2018). It's a large double-stranded DNA virus, with a linear genome of 173–193 kb long, encoding 151–167 ORFs (Salas & Andres, 2013). The differences in genome length between strains are from the multigene families (MGF) and the short tandem repeats (Dixon, Bristow, Wilkinson, & Sumption, 1990; Lubisi, Bastos, Dwarka, & Vosloo, 2007). The genes encoded on both DNA strands across the complete genome, including the genes related to replication, repair and transcription, structural protein genes, the gene involved in immune evasion, multigene families and some genes of unknown functions. (Figure 1.2.5)

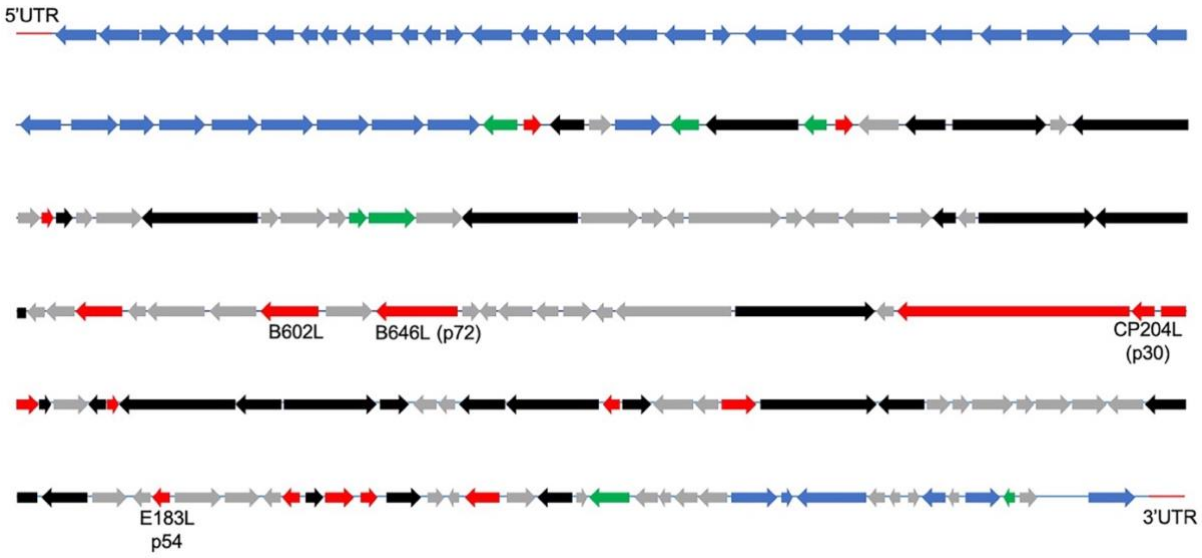

Figure 1.2.5 Schematic of ASFV genome

The ASFV genome encodes more than 150 genes flanking with 5'UTR and 3'UTR. In the genes, some are multigene families (in blue) with different functions, some are related to evasion from immune system (in green), some are transcribed and translated into structural proteins (in red), some are related to genome replication, repair and transcription (in black) and others with unknown functions (in gray). The arrows indicate the direction they are encoded. Four genes used for genotyping are labelled with their gene names and familiar protein names. (Dixon, Chapman, Netherton, & Upton, 2013)

1.2.6.3 Global distribution and diversity

ASFV was firstly identified in domestic and wild pigs in British East Africa (Kenya Colony) in the early 1900s. The disease gained the first access trans-continentally to Portugal in 1957. In 1960, it spread to Spain and then to other European countries (Plowright, Parker, & Peirce,

1969). In 2007, the second transcontinental spread to Georgia in the Caucasus occurred from a ship at a Black Sea port (Costard et al., 2009). Subsequent outbreaks were reported in the adjacent countries including Armenia, Azerbaijan and Russian Federation, and then the Eastern European countries of Estonia and Poland (Gogin, Gerasimov, Malogolovkin, & Kolbasov, 2013). In 2018, the disease was first reported in China (Ge et al., 2018). Since then, the virus has spread continuously into other Asian countries, including Thailand, South Korea, Mongolia, Vietnam, the Philippines, Indonesia and Cambodia (Gaudreault, Madden, Wilson, Trujillo, & Richt, 2020). Although there's no ASF reported in America or Oceania, it has posed high risk of worldwide dissemination.

Twenty-two genotypes have been identified based on the major capsid protein (p72) gene (B646L) (Bastos et al., 2003; Lubisi, Bastos, Dwarka, & Vosloo, 2005; Lubisi et al., 2007) Although it doesn't always provide adequate typing resolution to discriminate between viruses of different biological phenotypes, the easy genotyping system is wildly used as a fast method to identity new ASFV strains (Malogolovkin et al., 2015). Recently, other genes were added for genotyping, such as p54 (E183L), p30 (CP205L) and B602L genes (Bastos, Penrith, Macome, Pinto, & Thomson, 2004; Gallardo et al., 2009; Lubisi et al., 2005, 2007; Nix, Gallardo, Hutchings, Blanco, & Dixon, 2006). In addition, MGFs are the most diverse genetic components, which can greatly affect ASFV genome structure and replication (Dixon et al., 2013).

1.2.6.4 Diagnostics

With a lack of specific treatment or effective vaccine, diagnosis plays a critical role in the disease control. Thus, an array of assays have been developed for the virus or antibody detection. To detect the virus, hemadsorption, IFA, ELISA or lateral flow assays were established (de Leon, Bustos, & Carrascosa, 2013; Gallardo et al., 2015; Oura, Edwards, & Batten, 2013). Due to lower sensitivity and specificity, molecular detection is more popular in clinic, such as real time PCR (Haines, Hofmann, King, Drew, & Crooke, 2013; A. Wang et al., 2020), LAMP (D. Wang et al., 2020), recombinase polymerase amplification (RPA) (J. Wang, Wang, Geng, & Yuan, 2017), bead-based multiplex PCR (L. Xiao et al., 2018) and whole genome sequencing (O'Donnell et al., 2019). Among the assays, real-time PCR is considered more reliable, sensitive and cost effective. For antibody detection, several technologies are used for assay development, including ELISA (Gimenez-Lirola, Mur, et al., 2016; Pastor, Arias, & Escribano, 1990), indirect immunoperoxidase assays (IPA) (Pan, Huang, & Hess, 1982) and lateral flow tests (Sastre et al., 2016).

1.2.7 Rotavirus C (RVC)

1.2.7.1 Impact of the disease

Rotaviruses are the major etiologies of gastroenteritis in humans and animals, especially in children and young animals (Bernstein, 2009; Dhama, Chauhan, Mahendran, & Malik, 2009). Recently, RVC is detected more frequently in both humans and pigs (Campanha et al., 2020; Chepngeno, Diaz, Paim, Saif, & Vlasova, 2019). Several studies have demonstrated RVC was associated with diarrheal disease, causing significant economic losses (Martella et al., 2007; Marthaler et al., 2013).

1.2.7.2 RVC classification and genome characterization

RVC belongs to the family *Reoviridae*, genus *Rotavirus*. It's a non-enveloped double-stranded RNA virus with a genome consisting of 11 segments, coded for six structural proteins, VP1, VP2, VP3, VP4, VP6 and VP7, and five non-structural proteins, NSP1, NSP2, NSP3, NSP4 and NSP5 (Sadiq, Bostan, Yinda, Naseem, & Sattar, 2018) Each segment includes the ORF in the middle and untranslated sequences at 5' and 3' ends (Desselberger, 2014). (Figure 1.2.6)

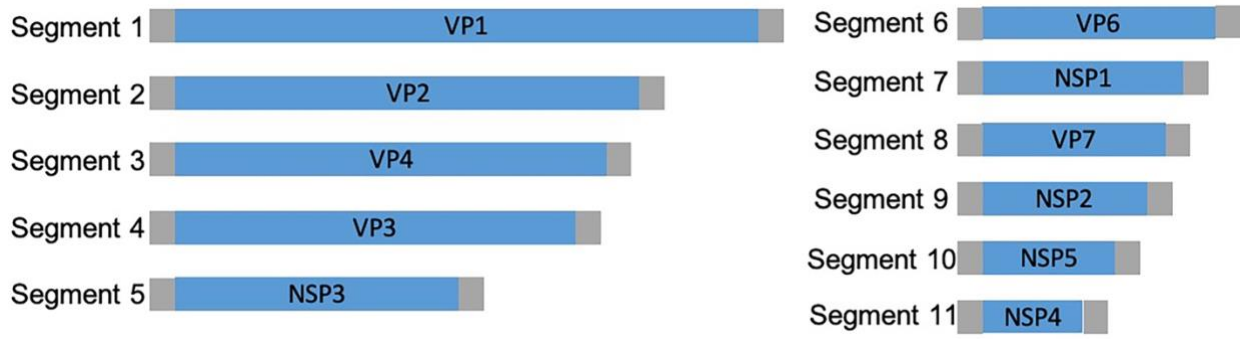

Figure 1.2.6 Schematic of RVC genome

The RVC genome consists of 11 RNA segments, coded for six structural proteins, VP1- VP4, VP6 and VP7, and five non-structural proteins, NSP1- NSP5. Each segment includes the ORF in the middle and untranslated sequences at two ends. The 11 segments are placed according to lengths of the ORFs based on the reference strain RVC/Pig/United States/Cowden/1980.

1.2.7.3 Global distribution and diversity

RVC has a global distribution in human and pigs, including North America (Chepngeno et al., 2019), South America (Costa, Flores, Amorim, Mendes, & Santos, 2020), Asia (Joshi, Walimbe, Dilpak, Cherian, & Gopalkrishna, 2019) and Europe (Theuns et al., 2016). Rotaviruses

have high diversity because of high mutation rates and frequent reassortment (Donker & Kirkwood, 2012; Matthijnssens et al., 2010; McDonald, Nelson, Turner, & Patton, 2016). Due to the difficulty of culturing the virus *in vitro*, serological typing of RVC is limited. Therefore, genotyping of RVC is based on genome sequence data. Since 2008, a full genome-based classification system has been established for RVA genotyping (Matthijnssens et al., 2008). Similarly, RVC strains have been classified based on the complete genomes, included 18G, 21P, 13I, 4R, 6C, 6M, 9A, 8N, 6T, 5E and 4H for genes VP7, VP4, VP6, VP1, VP2, VP3, NSP1, NSP2, NSP3, NSP4 and NSP5, respectively (Suzuki & Hasebe, 2017).

1.2.7.4 Diagnostics

Limited in virus culture, molecular detection is widely used to detect RVC segments, VP4, VP6 and VP7, in which, RT-PCR (Kattoor et al., 2017; Tuanthap et al., 2018) and real time PCR (Mori et al., 2013; Rahman et al., 2005) are the major methods. For virus classification, both Sanger sequencing and NGS technology are applied (Suzuki & Hasebe, 2017; Theuns et al., 2016).

1.3 Reference

Adams, M. J., Lefkowitz, E. J., King, A. M., Bamford, D. H., Breitbart, M., Davison, A. J., . . . Carstens, E. B. (2015). Ratification vote on taxonomic proposals to the International Committee on Taxonomy of Viruses (2015). Arch Virol, 160(7), 1837-1850. doi:10.1007/s00705-015-2425-z

Afolabi, K. O., Iweriebor, B. C., Obi, C. L., & Okoh, A. I. (2019). Genetic characterization and diversity of porcine circovirus type 2 in non-vaccinated South African swine herds. Transbound Emerg Dis, 66(1), 412-421. doi:10.1111/tbed.13036

Agnol, A. M. D., Otonel, R. A. A., Leme, R. A., Alfieri, A. A., & Alfieri, A. F. (2017). A TaqMan-based qRT-PCR assay for Senecavirus A detection in tissue samples of neonatal piglets. Molecular and Cellular Probes, 33, 28-31. doi:10.1016/j.mcp.2017.03.002

Albina, E., Madec, F., Cariolet, R., & Torrison, J. (1994). Immune response and persistence of the porcine reproductive and respiratory syndrome virus in infected pigs and farm units. Vet Rec, 134(22), 567-573. doi:10.1136/vr.134.22.567

Alexandersen, S., Zhang, Z., & Donaldson, A. I. (2002). Aspects of the persistence of foot-and-mouth disease virus in animals--the carrier problem. Microbes Infect, 4(10), 1099-1110. doi:10.1016/s1286-4579(02)01634-9

Alexandersen, S., Zhang, Z., Donaldson, A. I., & Garland, A. J. (2003). The pathogenesis and diagnosis of foot-and-mouth disease. J Comp Pathol, 129(1), 1-36. doi:10.1016/s0021-9975(03)00041-0

Allan, G. M., & Ellis, J. A. (2000). Porcine circoviruses: a review. J Vet Diagn Invest, 12(1), 3-14. doi:10.1177/104063870001200102

Allan, G. M., McNeilly, F., Kennedy, S., Daft, B., Clarke, E. G., Ellis, J. A., . . . Adair, B. M. (1998). Isolation of porcine circovirus-like viruses from pigs with a wasting disease in the USA and Europe. J Vet Diagn Invest, 10(1), 3-10. doi:10.1177/104063879801000102

Allende, R., Kutish, G. F., Laegreid, W., Lu, Z., Lewis, T. L., Rock, D. L., . . . Osorio, F. A. (2000). Mutations in the genome of porcine reproductive and respiratory syndrome virus responsible for the attenuation phenotype. Arch Virol, 145(6), 1149-1161. doi:10.1007/s007050070115

Alonso, C., Borca, M., Dixon, L., Revilla, Y., Rodriguez, F., Escribano, J. M., & Ictv Report, C. (2018). ICTV Virus Taxonomy Profile: Asfarviridae. J Gen Virol, 99(5), 613-614. doi:10.1099/jgv.0.001049

Amarasinghe, S. L., Su, S., Dong, X. Y., Zappia, L., Ritchie, M. E., & Gouil, Q. (2020). Opportunities and challenges in long-read sequencing data analysis. Genome Biology, 21(1). doi:ARTN 3010.1186/s13059-020-1935-5

Armson, B., Walsh, C., Morant, N., Fowler, V. L., Knowles, N. J., & Clark, D. (2019). The development of two field-ready reverse transcription loop-mediated isothermal amplification assays for the rapid detection of Seneca Valley virus 1. Transbound Emerg Dis, 66(1), 497-504. doi:10.1111/tbed.13051

Arruda, B., Pineyro, P., Derscheid, R., Hause, B., Byers, E., Dion, K., . . . Schwartz, K. (2019). PCV3-associated disease in the United States swine herd. Emerg Microbes Infect, 8(1), 684-698. doi:10.1080/22221751.2019.1613176

Arzt, J., Fish, I., Pauszek, S. J., Johnson, S. L., Chain, P. S., Rai, D. K., . . . Stenfeldt, C. (2019). The evolution of a super-swarm of foot-and-mouth disease virus in cattle. Plos One, 14(4), e0210847. doi:10.1371/journal.pone.0210847

Asfor, A. S., Howe, N., Grazioli, S., Berryman, S., Parekh, K., Wilsden, G., . . . Tuthill, T. J. (2020). Detection of Bovine Antibodies against a Conserved Capsid Epitope as the Basis of a Novel Universal Serological Test for Foot-and-Mouth Disease. J Clin Microbiol, 58(6). doi:10.1128/JCM.01527-19

Bastos, A. D., Penrith, M. L., Cruciere, C., Edrich, J. L., Hutchings, G., Roger, F., . . . G, R. T. (2003). Genotyping field strains of African swine fever virus by partial p72 gene characterisation. Arch Virol, 148(4), 693-706. doi:10.1007/s00705-002-0946-8

Bastos, A. D., Penrith, M. L., Macome, F., Pinto, F., & Thomson, G. R. (2004). Co-circulation of two genetically distinct viruses in an outbreak of African swine fever in Mozambique: no evidence for individual co-infection. Vet Microbiol, 103(3-4), 169-182. doi:10.1016/j.vetmic.2004.09.003

Beach, N. M., & Meng, X. J. (2012). Efficacy and future prospects of commercially available and experimental vaccines against porcine circovirus type 2 (PCV2). Virus Res, 164(1-2), 33-42. doi:10.1016/j.virusres.2011.09.041

Bellini, S., Rutili, D., & Guberti, V. (2016). Preventive measures aimed at minimizing the risk of African swine fever virus spread in pig farming systems. Acta Veterinaria Scandinavica, 58. doi:ARTN 8210.1186/s13028-016-0264-x

Bentley, D. R., Balasubramanian, S., Swerdlow, H. P., Smith, G. P., Milton, J., Brown, C. G., . . . Smith, A. J. (2008). Accurate whole human genome sequencing using reversible terminator chemistry. Nature, 456(7218), 53-59. doi:10.1038/nature07517

Bera, B. C., Choudhary, M., Anand, T., Virmani, N., Sundaram, K., Choudhary, B., & Tripathi, B. N. (2020). Detection and genetic characterization of porcine circovirus 3 (PCV3) in pigs in India. Transbound Emerg Dis, 67(3), 1062-1067. doi:10.1111/tbed.1346

Bernstein, D. I. (2009). The changing epidemiology of rotavirus gastroenteritis. Introduction. Pediatr Infect Dis J, 28(3 Suppl), S49. doi:10.1097/INF.0b013e3181967bda

Biswal, J. K., Jena, S., Mohapatra, J. K., Bisht, P., & Pattnaik, B. (2014). Detection of antibodies specific for foot-and-mouth disease virus infection using indirect ELISA based on recombinant nonstructural protein 2B. Arch Virol, 159(7), 1641-1650. doi:10.1007/s00705-013-1973-3

Blome, S., Gabriel, C., & Beer, M. (2013). Pathogenesis of African swine fever in domestic pigs and European wild boar. Virus Res, 173(1), 122-130. doi:10.1016/j.virusres.2012.10.026

Bracht, A. J., O'Hearn, E. S., Fabian, A. W., Barrette, R. W., & Sayed, A. (2016). Real-Time Reverse Transcription PCR Assay for Detection of Senecavirus A in Swine Vesicular Diagnostic Specimens. Plos One, 11(1), e0146211. doi:10.1371/journal.pone.0146211

Brunstein, J. D., Cline, C. L., McKinney, S., & Thomas, E. (2008). Evidence from multiplex molecular assays for complex multipathogen interactions in acute respiratory infections. J Clin Microbiol, 46(1), 97-102. doi:10.1128/JCM.01117-07

Bustin, S. A. (2000). Absolute quantification of mRNA using real-time reverse transcription polymerase chain reaction assays. J Mol Endocrinol, 25(2), 169-193. doi:10.1677/jme.0.0250169

Callahan, J. D., Brown, F., Csorio, F. A., Sur, J. H., Kramer, E., Long, G. W., . . . Nelson, W. M. (2002). Use of a portable real-time reverse transcriptase-polymerase chain reaction assay for rapid detection of foot-and-mouth disease virus. Journal of the American Veterinary Medical Association, 220(11), 1636-1642. doi:DOI 10.2460/javma.2002.220.1636

Campanha, J. E. T., Possatti, F., Lorenzetti, E., de Almeida Moraes, D., Alfieri, A. F., & Alfieri, A. A. (2020). Longitudinal study of rotavirus C VP6 genotype I6 in diarrheic piglets up to 1 week old. Braz J Microbiol. doi:10.1007/s42770-020-00234-z

Cavanagh, D. (1997). Nidovirales: a new order comprising Coronaviridae and Arteriviridae. Arch Virol, 142(3), 629-633. Retrieved from https://www.ncbi.nlm.nih.gov/pubmed/9349308

Chae, C. (2004). Postweaning multisystemic wasting syndrome: a review of aetiology, diagnosis and pathology. Vet J, 168(1), 41-49. doi:10.1016/j.tvjl.2003.09.018

Chen, G. H., Mai, K. J., Zhou, L., Wu, R. T., Tang, X. Y., Wu, J. L., . . . Ma, J. Y. (2017). Detection and genome sequencing of porcine circovirus 3 in neonatal pigs with congenital tremors in South China. Transbound Emerg Dis, 64(6), 1650-1654. doi:10.1111/tbed.12702

Chen, N., Trible, B. R., Kerrigan, M. A., Tian, K., & Rowland, R. R. R. (2016). ORF5 of porcine reproductive and respiratory syndrome virus (PRRSV) is a target of diversifying selection as infection progresses from acute infection to virus rebound. Infect Genet Evol, 40, 167-175. doi:10.1016/j.meegid.2016.03.002

Chen, N., Ye, M., Xiao, Y., Li, S., Huang, Y., Li, X., . . . Zhu, J. (2019). Development of universal and quadruplex real-time RT-PCR assays for simultaneous detection and differentiation of porcine reproductive and respiratory syndrome viruses. Transbound Emerg Dis, 66(6), 2271-2278. doi:10.1111/tbed.13276

Chen, W., He, B., Li, C., Zhang, X., Wu, W., Yin, X., . . . Wang, J. (2007). Real-time RT-PCR for H5N1 avian influenza A virus detection. J Med Microbiol, 56(Pt 5), 603-607. doi:10.1099/jmm.0.47014-0

Chepngeno, J., Diaz, A., Paim, F. C., Saif, L. J., & Vlasova, A. N. (2019). Rotavirus C: prevalence in suckling piglets and development of virus-like particles to assess the influence of maternal immunity on the disease development. Vet Res, 50(1), 84. doi:10.1186/s13567-019-0705-4

Cho, S. H., Freese, W. R., Yoon, I. J., Trigo, A. V., & Joo, H. S. (1993). Seroprevalence of indirect fluorescent antibody to porcine reproductive and respiratory syndrome virus in selected swine herds. J Vet Diagn Invest, 5(2), 259-260. doi:10.1177/104063879300500220

Cong, F., Zhu, Y., Liu, X., Li, X., Chen, M., Huang, R., & Guo, P. (2018). Development of an xTAG-multiplex PCR array for the detection of four avian respiratory viruses. Mol Cell Probes, 37, 1-5. doi:10.1016/j.mcp.2017.10.002

Costa, F. B., Flores, P. S., Amorim, A. R., Mendes, G. D. S., & Santos, N. (2020). Porcine rotavirus C strains carrying human-like NSP4 and NSP5. Zoonoses Public Health. doi:10.1111/zph.12713

Costard, S., Wieland, B., de Glanville, W., Jori, F., Rowlands, R., Vosloo, W., . . . Dixon, L. K. (2009). African swine fever: how can global spread be prevented? Philosophical Transactions of the Royal Society B-Biological Sciences, 364(1530), 2683-2696. doi:10.1098/rstb.2009.0098

de Leon, P., Bustos, M. J., & Carrascosa, A. L. (2013). Laboratory methods to study African swine fever virus. Virus Res, 173(1), 168-179. doi:10.1016/j.virusres.2012.09.013

Dea, S., Wilson, L., Therrien, D., & Cornaglia, E. (2000). Competitive ELISA for detection of antibodies to porcine reproductive and respiratory syndrome virus using recombinant E. coli-expressed nucleocapsid protein as antigen. J Virol Methods, 87(1-2), 109-122. doi:10.1016/s0166-0934(00)00158-0

Decorte, I., Van Breedam, W., Van der Stede, Y., Nauwynck, H. J., De Regge, N., & Cay, A. B. (2014). Detection of total and PRRSV-specific antibodies in oral fluids collected with different rope types from PRRSV-vaccinated and experimentally infected pigs. BMC Vet Res, 10, 134. doi:10.1186/1746-6148-10-134

Deim, Z., Dencso, L., Erdelyi, I., Valappil, S. K., Varga, C., Posa, A., . . . Rakhely, G. (2019). Porcine circovirus type 3 detection in a Hungarian pig farm experiencing reproductive failures. Vet Rec, 185(3), 84. doi:10.1136/vr.104784

Deng, J., Li, X., Zheng, D., Wang, Y., Chen, L., Song, H., . . . Tian, K. (2018). Establishment and application of an indirect ELISA for porcine circovirus 3. Arch Virol, 163(2), 479-482. doi:10.1007/s00705-017-3607-7

Desselberger, U. (2014). Rotaviruses. Virus Res, 190, 75-96. doi:10.1016/j.virusres.2014.06.016

Dhama, K., Chauhan, R. S., Mahendran, M., & Malik, S. V. (2009). Rotavirus diarrhea in bovines and other domestic animals. Vet Res Commun, 33(1), 1-23. doi:10.1007/s11259-008-9070-x

Dixon, L. K., Bristow, C., Wilkinson, P. J., & Sumption, K. J. (1990). Identification of a variable region of the African swine fever virus genome that has undergone separate DNA rearrangements leading to expansion of minisatellite-like sequences. J Mol Biol, 216(3), 677-688. doi:10.1016/0022-2836(90)90391-X

Dixon, L. K., Chapman, D. A., Netherton, C. L., & Upton, C. (2013). African swine fever virus replication and genomics. Virus Res, 173(1), 3-14. doi:10.1016/j.virusres.2012.10.020

Dohm, J. C., Lottaz, C., Borodina, T., & Himmelbauer, H. (2008). Substantial biases in ultra-short read data sets from high-throughput DNA sequencing. Nucleic Acids Research, 36(16), e105. doi:10.1093/nar/gkn425

Done, S. H., & Paton, D. J. (1995). Porcine reproductive and respiratory syndrome: clinical disease, pathology and immunosuppression. Vet Rec, 136(2), 32-35. doi:10.1136/vr.136.2.32

Donker, N. C., & Kirkwood, C. D. (2012). Selection and evolutionary analysis in the nonstructural protein NSP2 of rotavirus A. Infect Genet Evol, 12(7), 1355-1361. doi:10.1016/j.meegid.2012.05.002

Dvorak, C. M., Akkutay-Yoldar, Z., Stone, S. R., Tousignant, S. J., Vannucci, F. A., & Murtaugh, M. P. (2017). An indirect enzyme-linked immunosorbent assay for the identification of antibodies to Senecavirus A in swine. BMC Vet Res, 13(1), 50. doi:10.1186/s12917-017-0967-x

Erickson, A., Fisher, M., Furukawa-Stoffer, T., Ambagala, A., Hodko, D., Pasick, J., . . . Lung, O. (2018). A multiplex reverse transcription PCR and automated electronic microarray assay

for detection and differentiation of seven viruses affecting swine. Transbound Emerg Dis, 65(2), e272-e283. doi:10.1111/tbed.12749

Faccini, S., Barbieri, I., Gilioli, A., Sala, G., Gibelli, L. R., Moreno, A., . . . Nigrelli, A. (2017). Detection and genetic characterization of Porcine circovirus type 3 in Italy. Transbound Emerg Dis, 64(6), 1661-1664. doi:10.1111/tbed.12714

Feronato, C., Leme, R. A., Diniz, J. A., Agnol, A. M. D., Alfieri, A. F., & Alfieri, A. A. (2018). Development and evaluation of a nested-PCR assay for Senecavirus A diagnosis. Trop Anim Health Prod, 50(2), 337-344. doi:10.1007/s11250-017-1436-z

Ferris, N. P., & Dawson, M. (1988). Routine application of enzyme-linked immunosorbent assay in comparison with complement fixation for the diagnosis of foot-and-mouth and swine vesicular diseases. Vet Microbiol, 16(3), 201-209. doi:10.1016/0378-1135(88)90024-7

Ferris, N. P., King, D. P., Reid, S. M., Shaw, A. E., & Hutchings, G. H. (2006). Comparisons of original laboratory results and retrospective analysis by real-time reverse transcriptase-PCR of virological samples collected from confirmed cases of foot-and-mouth disease in the UK in 2001. Vet Rec, 159(12), 373-378. doi:10.1136/vr.159.12.373

Ferris, N. P., Nordengrahn, A., Hutchings, G. H., Paton, D. J., Kristersson, T., Brocchi, E., . . . Merza, M. (2010). Development and laboratory validation of a lateral flow device for the detection of serotype SAT 2 foot-and-mouth disease viruses in clinical samples. J Virol Methods, 163(2), 474-476. doi:10.1016/j.jviromet.2009.09.022

Firth, C., Charleston, M. A., Duffy, S., Shapiro, B., & Holmes, E. C. (2009). Insights into the Evolutionary History of an Emerging Livestock Pathogen: Porcine Circovirus 2. Journal of Virology, 83(24), 12813-12821. doi:10.1128/Jvi.01719-09

Fowler, V. L., Ransburgh, R. H., Poulsen, E. G., Wadsworth, J., King, D. P., Mioulet, V., . . . Bai, J. (2017). Development of a novel real-time RT-PCR assay to detect Seneca Valley virus-1 associated with emerging cases of vesicular disease in pigs. J Virol Methods, 239, 34-37. doi:10.1016/j.jviromet.2016.10.012

Franzo, G., Delwart, E., Fux, R., Hause, B., Su, S., Zhou, J. Y., & Segales, J. (2020). Genotyping Porcine Circovirus 3 (PCV-3) Nowadays: Does It Make Sense? Viruses-Basel, 12(3). doi:ARTN 26510.3390/v12030265

Franzo, G., He, W., Correa-Fiz, F., Li, G., Legnardi, M., Su, S., & Segales, J. (2019). A Shift in Porcine Circovirus 3 (PCV-3) History Paradigm: Phylodynamic Analyses Reveal an Ancient Origin and Prolonged Undetected Circulation in the Worldwide Swine Population. Adv Sci (Weinh), 6(22), 1901004. doi:10.1002/advs.201901004

Franzo, G., Tucciarone, C. M., Cecchinato, M., & Drigo, M. (2016). Porcine circovirus type 2 (PCV2) evolution before and after the vaccination introduction: A large scale epidemiological study. Scientific Reports, 6. doi:ARTN 3945810.1038/srep39458

Fux, R., Sockler, C., Link, E. K., Renken, C., Krejci, R., Sutter, G., . . . Eddicks, M. (2018). Full genome characterization of porcine circovirus type 3 isolates reveals the existence of two distinct groups of virus strains. Virology Journal, 15(1), 25. doi:10.1186/s12985-018-0929-3

Gallardo, C., Mwaengo, D. M., Macharia, J. M., Arias, M., Taracha, E. A., Soler, A., . . . Bishop, R. P. (2009). Enhanced discrimination of African swine fever virus isolates through nucleotide sequencing of the p54, p72, and pB602L (CVR) genes. Virus Genes, 38(1), 85-95. doi:10.1007/s11262-008-0293-2

Gallardo, C., Nieto, R., Soler, A., Pelayo, V., Fernandez-Pinero, J., Markowska-Daniel, I., . . . Arias, M. (2015). Assessment of African Swine Fever Diagnostic Techniques as a Response to the Epidemic Outbreaks in Eastern European Union Countries: How To Improve Surveillance and Control Programs. Journal of Clinical Microbiology, 53(8), 2555-2565. doi:10.1128/Jcm.00857-15

Garcia, S., Crance, J. M., Billecocq, A., Peinnequin, A., Jouan, A., Bouloy, M., & Garin, D. (2001). Quantitative real-time PCR detection of Rift Valley fever virus and its application to evaluation of antiviral compounds. J Clin Microbiol, 39(12), 4456-4461. doi:10.1128/JCM.39.12.4456-4461.2001

Garcia-Arriaza, J., Ojosnegros, S., Davila, M., Domingo, E., & Escarmis, C. (2006). Dynamics of mutation and recombination in a replicating population of complementing, defective viral genomes. J Mol Biol, 360(3), 558-572. doi:10.1016/j.jmb.2006.05.027

Gaudreault, N. N., Madden, D. W., Wilson, W. C., Trujillo, J. D., & Richt, J. A. (2020). African Swine Fever Virus: An Emerging DNA Arbovirus. Frontiers in Veterinary Science, 7. doi:ARTN 21510.3389/fvets.2020.00215

Ge, S., Li, J., Fan, X., Liu, F., Li, L., Wang, Q., . . . Wang, Z. (2018). Molecular Characterization of African Swine Fever Virus, China, 2018. Emerging Infectious Diseases, 24(11), 2131-2133. doi:10.3201/eid2411.181274

Gibson, U. E., Heid, C. A., & Williams, P. M. (1996). A novel method for real time quantitative RT-PCR. Genome Res, 6(10), 995-1001. doi:10.1101/gr.6.10.995

Gimenez-Lirola, L. G., Mur, L., Rivera, B., Mogler, M., Sun, Y. X., Lizano, S., . . . Zimmerman, J. (2016). Detection of African Swine Fever Virus Antibodies in Serum and Oral Fluid Specimens Using a Recombinant Protein 30 (p30) Dual Matrix Indirect ELISA. Plos One, 11(9). doi:ARTN e016123010.1371/journal.pone.0161230

Gimenez-Lirola, L. G., Rademacher, C., Linhares, D., Harmon, K., Rotolo, M., Sun, Y., . . . Pineyro, P. (2016). Serological and Molecular Detection of Senecavirus A Associated with an Outbreak of Swine Idiopathic Vesicular Disease and Neonatal Mortality. J Clin Microbiol, 54(8), 2082-2089. doi:10.1128/JCM.00710-16

Gogin, A., Gerasimov, V., Malogolovkin, A., & Kolbasov, D. (2013). African swine fever in the North Caucasus region and the Russian Federation in years 2007-2012. Virus Res, 173(1), 198-203. doi:10.1016/j.virusres.2012.12.007

Goolia, M., Vannucci, F., Yang, M., Patnayak, D., Babiuk, S., & Nfon, C. K. (2017). Validation of a competitive ELISA and a virus neutralization test for the detection and confirmation of antibodies to Senecavirus A in swine sera. J Vet Diagn Invest, 29(2), 250-253. doi:10.1177/1040638716683214

Guo, B., Pineyro, P. E., Rademacher, C. J., Zheng, Y., Li, G., Yuan, J., . . . Yoon, K. J. (2016). Novel Senecavirus A in Swine with Vesicular Disease, United States, July 2015. Emerging Infectious Diseases, 22(7), 1325-1327. doi:10.3201/eid2207.151758

Guo, J., Xu, N., Li, Z., Zhang, S., Wu, J., Kim, D. H., . . . Ju, J. (2008). Four-color DNA sequencing with 3'-O-modified nucleotide reversible terminators and chemically cleavable fluorescent dideoxynucleotides. Proc Natl Acad Sci U S A, 105(27), 9145-9150. doi:10.1073/pnas.0804023105

Guo, L. J., Fu, Y. J., Wang, Y. P., Lu, Y. H., Wei, Y. W., Tang, Q. H., . . . Liu, C. M. (2012). A Porcine Circovirus Type 2 (PCV2) Mutant with 234 Amino Acids in Capsid Protein Showed More Virulence In Vivo, Compared with Classical PCV2a/b Strain. Plos One, 7(7). doi:ARTN e4146310.1371/journal.pone.0041463

Guo, Z., Chen, X. X., Li, R., Qiao, S., & Zhang, G. (2018). The prevalent status and genetic diversity of porcine reproductive and respiratory syndrome virus in China: a molecular epidemiological perspective. Virology Journal, 15(1), 2. doi:10.1186/s12985-017-0910-6

Haines, F. J., Hofmann, M. A., King, D. P., Drew, T. W., & Crooke, H. R. (2013). Development and validation of a multiplex, real-time RT PCR assay for the simultaneous detection of classical and African swine fever viruses. Plos One, 8(7), e71019. doi:10.1371/journal.pone.0071019

Hales, L. M., Knowles, N. J., Reddy, P. S., Xu, L., Hay, C., & Hallenbeck, P. L. (2008). Complete genome sequence analysis of Seneca Valley virus-001, a novel oncolytic picornavirus. J Gen Virol, 89(Pt 5), 1265-1275. doi:10.1099/vir.0.83570-0

Hanada, K., Suzuki, Y., Nakane, T., Hirose, O., & Gojobori, T. (2005). The origin and evolution of porcine reproductive and respiratory syndrome viruses. Molecular Biology and Evolution, 22(4), 1024-1031. doi:10.1093/molbev/msi089

Hause, B. M., Myers, O., Duff, J., & Hesse, R. A. (2016). Senecavirus A in Pigs, United States, 2015. Emerging Infectious Diseases, 22(7), 1323-1325. doi:10.3201/eid2207.151951

Heid, C. A., Stevens, J., Livak, K. J., & Williams, P. M. (1996). Real time quantitative PCR. Genome Res, 6(10), 986-994. doi:10.1101/gr.6.10.986

Holland, P. M., Abramson, R. D., Watson, R., & Gelfand, D. H. (1991). Detection of specific polymerase chain reaction product by utilizing the 5'----3' exonuclease activity of Thermus aquaticus DNA polymerase. Proc Natl Acad Sci U S A, 88(16), 7276-7280. doi:10.1073/pnas.88.16.7276

Holtkamp, D. J., Kliebenstein, J. B., Neumann, E. J., Zimmerman, J. J., Rotto, H. F., Yoder, T. K., . . . Haley, C. A. (2013). Assessment of the economic impact of porcine reproductive and respiratory syndrome virus on United States pork producers. Journal of Swine Health and Production, 21(2), 72-84. Retrieved from <Go to ISI>://WOS:000315319600005

Hopper, S. A., White, M. E., & Twiddy, N. (1992). An outbreak of blue-eared pig disease (porcine reproductive and respiratory syndrome) in four pig herds in Great Britain. Vet Rec, 131(7), 140-144. doi:10.1136/vr.131.7.140

Hu, L., Lin, X., Nie, F., ZexiaoYang, Yao, X., Li, G., . . . Wang, Y. (2016). Simultaneous typing of seven porcine pathogens by multiplex PCR with a GeXP analyser. J Virol Methods, 232, 21-28. doi:10.1016/j.jviromet.2015.12.004

Huang, C., Hung, J. J., Wu, C. Y., & Chien, M. S. (2004). Multiplex PCR for rapid detection of pseudorabies virus, porcine parvovirus and porcine circoviruses. Vet Microbiol, 101(3), 209-214. doi:10.1016/j.vetmic.2004.04.007

Ito, S., Jurado, C., Sanchez-Vizcaino, J. M., & Isoda, N. (2020). Quantitative risk assessment of African swine fever virus introduction to Japan via pork products brought in air passengers' luggage. Transbound Emerg Dis, 67(2), 894-905. doi:10.1111/tbed.13414

Jamal, S. M., & Belsham, G. J. (2013). Foot-and-mouth disease: past, present and future. Vet Res, 44, 116. doi:10.1186/1297-9716-44-116

Jiang, H. J., Wang, D., Wang, J., Zhu, S. S., She, R. P., Ren, X. X., . . . Liu, J. (2019). Induction of Porcine Dermatitis and Nephropathy Syndrome in Piglets by Infection with Porcine Circovirus Type 3. Journal of Virology, 93(4). doi:ARTN e02045-1810.1128/JVI.02045-18

Joshi, M. S., Walimbe, A. M., Dilpak, S. P., Cherian, S. S., & Gopalkrishna, V. (2019). Whole-genome-based characterization of three human Rotavirus C strains isolated from gastroenteritis outbreaks in Western India and a provisional intra-genotypic lineage classification system. J Gen Virol, 100(7), 1055-1072. doi:10.1099/jgv.0.001284

Jurado, C., Mur, L., Perez Aguirreburualde, M. S., Cadenas-Fernandez, E., Martinez-Lopez, B., Sanchez-Vizcaino, J. M., & Perez, A. (2019). Risk of African swine fever virus introduction into the United States through smuggling of pork in air passenger luggage. Sci Rep, 9(1), 14423. doi:10.1038/s41598-019-50403-w

Kappes, M. A., & Faaberg, K. S. (2015). PRRSV structure, replication and recombination: Origin of phenotype and genotype diversity. Virology, 479-480, 475-486. doi:10.1016/j.virol.2015.02.012

Kattoor, J. J., Saurabh, S., Malik, Y. S., Sircar, S., Dhama, K., Ghosh, S., . . . Singh, R. K. (2017). Unexpected detection of porcine rotavirus C strains carrying human origin VP6 gene. Vet Q, 37(1), 252-261. doi:10.1080/01652176.2017.1346849

Kedkovid, R., Woonwong, Y., Arunorat, J., Sirisereewan, C., Sangpratum, N., Lumyai, M., . . . Thanawongnuwech, R. (2018). Porcine circovirus type 3 (PCV3) infection in grower pigs from a Thai farm suffering from porcine respiratory disease complex (PRDC). Veterinary Microbiology, 215, 71-76. doi:10.1016/j.vetmic.2018.01.004

Kim, J., Choi, C., Han, D. U., & Chae, C. (2001). Simultaneous detection of porcine circovirus type 2 and porcine parvovirus in pigs with PMWS by multiplex PCR. Vet Rec, 149(10), 304-305. doi:10.1136/vr.149.10.304

Kim, J., Chung, H. K., & Chae, C. (2003). Association of porcine circovirus 2 with porcine respiratory disease complex. Vet J, 166(3), 251-256. doi:10.1016/s1090-0233(02)00257-5

Kim, J., Han, D. U., Choi, C., & Chae, C. (2003). Simultaneous detection and differentiation between porcine circovirus and porcine parvovirus in boar semen by multiplex seminested

polymerase chain reaction. Journal of Veterinary Medical Science, 65(6), 741-744. Retrieved from <Go to ISI>://WOS:000184061900015

Kim, S. H., Park, J. Y., Jung, J. Y., Kim, H. Y., Park, Y. R., Lee, K. K., . . . Park, C. K. (2018). Detection and genetic characterization of porcine circovirus 3 from aborted fetuses and pigs with respiratory disease in Korea. J Vet Sci, 19(5), 721-724. doi:10.4142/jvs.2018.19.5.721

Klaumann, F., Franzo, G., Sohrmann, M., Correa-Fiz, F., Drigo, M., Nunez, J. I., . . . Segales, J. (2018). Retrospective detection of Porcine circovirus 3 (PCV-3) in pig serum samples from Spain. Transbound Emerg Dis, 65(5), 1290-1296. doi:10.1111/tbed.12876

Knight-Jones, T. J., & Rushton, J. (2013). The economic impacts of foot and mouth disease - what are they, how big are they and where do they occur? Prev Vet Med, 112(3-4), 161-173. doi:10.1016/j.prevetmed.2013.07.013

Kristensen, T., & Belsham, G. J. (2019). Identification of plasticity and interactions of a highly conserved motif within a picornavirus capsid precursor required for virus infectivity. Sci Rep, 9(1), 11747. doi:10.1038/s41598-019-48170-9

Krunic, N., Merante, F., Yaghoubian, S., Himsworth, D., & Janeczko, R. (2011). Advances in the diagnosis of respiratory tract infections: role of the Luminex xTAG respiratory viral panel. Ann N Y Acad Sci, 1222, 6-13. doi:10.1111/j.1749-6632.2011.05964.x

Kuhn, J. H., Lauck, M., Bailey, A. L., Shchetinin, A. M., Vishnevskaya, T. V., Bao, Y., . . . Goldberg, T. L. (2016). Reorganization and expansion of the nidoviral family Arteriviridae. Arch Virol, 161(3), 755-768. doi:10.1007/s00705-015-2672-z

Kuroda, M., Katano, H., Nakajima, N., Tobiume, M., Ainai, A., Sekizuka, T., . . . Sata, T. (2010). Characterization of Quasispecies of Pandemic 2009 Influenza A Virus (A/H1N1/2009) by De Novo Sequencing Using a Next-Generation DNA Sequencer. Plos One, 5(4). doi:ARTN e1025610.1371/journal.pone.0010256

Kutyavin, I. V., Afonina, I. A., Mills, A., Gorn, V. V., Lukhtanov, E. A., Belousov, E. S., . . . Hedgpeth, J. (2000). 3 '-minor groove binder-DNA probes increase sequence specificity at PCR extension temperatures. Nucleic Acids Research, 28(2), 655-661. doi:DOI 10.1093/nar/28.2.655

Langenhorst, R. J., Lawson, S., Kittawornrat, A., Zimmerman, J. J., Sun, Z., Li, Y., . . . Fang, Y. (2012). Development of a fluorescent microsphere immunoassay for detection of antibodies against porcine reproductive and respiratory syndrome virus using oral fluid samples as an alternative to serum-based assays. Clin Vaccine Immunol, 19(2), 180-189. doi:10.1128/CVI.05372-11

Larochelle, R., Bielanski, A., Muller, P., & Magar, R. (2000). PCR detection and evidence of shedding of porcine circovirus type 2 in boar semen. Journal of Clinical Microbiology, 38(12), 4629-4632. doi:Doi 10.1128/Jcm.38.12.4629-4632.2000

Leme, R. A., Oliveira, T. E., Alcantara, B. K., Headley, S. A., Alfieri, A. F., Yang, M., & Alfieri, A. A. (2016). Clinical Manifestations of Senecavirus A Infection in Neonatal Pigs, Brazil, 2015. Emerging Infectious Diseases, 22(7), 1238-1241. doi:10.3201/eid2207.151583

Leme, R. A., Zotti, E., Alcantara, B. K., Oliveira, M. V., Freitas, L. A., Alfieri, A. F., & Alfieri, A. A. (2015). Senecavirus A: An Emerging Vesicular Infection in Brazilian Pig Herds. Transbound Emerg Dis, 62(6), 603-611. doi:10.1111/tbed.12430

Li, Y., Ji, G., Xu, X., Wang, J., Li, Y., Tan, F., & Li, X. (2017). Development and Application of an RT-PCR to Differentiate the Prevalent NA-PRRSV Strains in China. Open Virol J, 11, 66-72. doi:10.2174/1874357901711010066

Lin, K., Wang, C., Murtaugh, M. P., & Ramamoorthy, S. (2011). Multiplex method for simultaneous serological detection of porcine reproductive and respiratory syndrome virus and porcine circovirus type 2. J Clin Microbiol, 49(9), 3184-3190. doi:10.1128/JCM.00557-11

Liu, Q., Wang, L., Willson, P., & Babiuk, L. A. (2000). Quantitative, competitive PCR analysis of porcine circovirus DNA in serum from pigs with postweaning multisystemic wasting syndrome. J Clin Microbiol, 38(9), 3474-3477. doi:10.1128/JCM.38.9.3474-3477.2000

Liu, X., Ouyang, T., Ouyang, H., Liu, X., Niu, G., Huo, W., . . . Ren, L. (2019). Human cells are permissive for the productive infection of porcine circovirus type 2 in vitro. Sci Rep, 9(1), 5638. doi:10.1038/s41598-019-42210-0

Liu, Y., Meng, H., Shi, L., & Li, L. (2019). Sensitive detection of porcine circovirus 3 by droplet digital PCR. J Vet Diagn Invest, 31(4), 604-607. doi:10.1177/1040638719847686

Lubisi, B. A., Bastos, A. D., Dwarka, R. M., & Vosloo, W. (2005). Molecular epidemiology of African swine fever in East Africa. Arch Virol, 150(12), 2439-2452. doi:10.1007/s00705-005-0602-1

Lubisi, B. A., Bastos, A. D., Dwarka, R. M., & Vosloo, W. (2007). Intra-genotypic resolution of African swine fever viruses from an East African domestic pig cycle: a combined p72-CVR approach. Virus Genes, 35(3), 729-735. doi:10.1007/s11262-007-0148-2

Malogolovkin, A., Burmakina, G., Titov, I., Sereda, A., Gogin, A., Baryshnikova, E., & Kolbasov, D. (2015). Comparative analysis of African swine fever virus genotypes and serogroups. Emerging Infectious Diseases, 21(2), 312-315. doi:10.3201/eid2102.140649

Mankertz, A., Caliskan, R., Hattermann, K., Hillenbrand, B., Kurzendoerfer, P., Mueller, B., . . . Finsterbusch, T. (2004). Molecular biology of Porcine circovirus: analyses of gene expression and viral replication. Vet Microbiol, 98(2), 81-88. doi:10.1016/j.vetmic.2003.10.014

Martella, V., Banyai, K., Lorusso, E., Bellacicco, A. L., Decaro, N., Carnero, M., . . . Buonavoglia, C. (2007). Prevalence of group C rotaviruses in weaning and post-weaning pigs with enteritis. Veterinary Microbiology, 123(1-3), 26-33. doi:10.1016/j.vetmic.2007.03.003

Marthaler, D., Rossow, K., Culhane, M., Collins, J., Goyal, S., Ciarlet, M., & Matthijnssens, J. (2013). Identification, phylogenetic analysis and classification of porcine group C rotavirus VP7 sequences from the United States and Canada. Virology, 446(1-2), 189-198. doi:10.1016/j.virol.2013.08.001

Matthijnssens, J., Ciarlet, M., Heiman, E., Arijs, I., Delbeke, T., McDonald, S. M., . . . Van Ranst, M. (2008). Full genome-based classification of rotaviruses reveals a common origin

between human Wa-Like and porcine rotavirus strains and human DS-1-like and bovine rotavirus strains. J Virol, 82(7), 3204-3219. doi:10.1128/JVI.02257-07

Matthijnssens, J., Heylen, E., Zeller, M., Rahman, M., Lemey, P., & Van Ranst, M. (2010). Phylodynamic analyses of rotavirus genotypes G9 and G12 underscore their potential for swift global spread. Molecular Biology and Evolution, 27(10), 2431-2436. doi:10.1093/molbev/msq137

McCombie, W. R., McPherson, J. D., & Mardis, E. R. (2019). Next-Generation Sequencing Technologies. Cold Spring Harb Perspect Med, 9(11). doi:10.1101/cshperspect.a036798

McDonald, S. M., Nelson, M. I., Turner, P. E., & Patton, J. T. (2016). Reassortment in segmented RNA viruses: mechanisms and outcomes. Nat Rev Microbiol, 14(7), 448-460. doi:10.1038/nrmicro.2016.46

McNeilly, F., Kennedy, S., Moffett, D., Meehan, B. M., Foster, J. C., Clarke, E. G., . . . Allan, G. M. (1999). A comparison of in situ hybridization and immunohistochemistry for the detection of a new porcine circovirus in formalin-fixed tissues from pigs with post-weaning multisystemic wasting syndrome (PMWS). J Virol Methods, 80(2), 123-128. doi:10.1016/s0166-0934(99)00043-9

Meerts, P., Van Gucht, S., Cox, E., Vandebosch, A., & Nauwynck, H. J. (2005). Correlation between type of adaptive immune response against porcine circovirus type 2 and level of virus replication. Viral Immunology, 18(2), 333-341. doi:DOI 10.1089/vim.2005.18.333

Meng, X. J., Paul, P. S., Halbur, P. G., & Morozov, I. (1995). Sequence comparison of open reading frames 2 to 5 of low and high virulence United States isolates of porcine reproductive and respiratory syndrome virus. J Gen Virol, 76 (Pt 12), 3181-3188. doi:10.1099/0022-1317-76-12-3181

Mori, K., Hayashi, Y., Akiba, T., Nagano, M., Tanaka, T., Hosaka, M., . . . Shirasawa, H. (2013). Multiplex real-time PCR assays for the detection of group C rotavirus, astrovirus, and Subgenus F adenovirus in stool specimens. J Virol Methods, 191(2), 141-147. doi:10.1016/j.jviromet.2012.10.019

Morioka, K., Fukai, K., Sakamoto, K., Yoshida, K., & Kanno, T. (2014). Evaluation of monoclonal antibody-based sandwich direct ELISA (MSD-ELISA) for antigen detection of foot-and-mouth disease virus using clinical samples. Plos One, 9(4), e94143. doi:10.1371/journal.pone.0094143

Mullis, K., Faloona, F., Scharf, S., Saiki, R., Horn, G., & Erlich, H. (1986). Specific enzymatic amplification of DNA in vitro: the polymerase chain reaction. Cold Spring Harb Symp Quant Biol, 51 Pt 1, 263-273. doi:10.1101/sqb.1986.051.01.032

Nawagitgul, P., Harms, P. A., Morozov, I., Thacker, B. J., Sorden, S. D., Lekcharoensuk, C., & Paul, P. S. (2002). Modified indirect porcine circovirus (PCV) type 2-based and recombinant capsid protein (ORF2)-based enzyme-linked immunosorbent assays for detection of antibodies to PCV. Clin Diagn Lab Immunol, 9(1), 33-40. doi:10.1128/cdli.9.1.33-40.2002

Nix, R. J., Gallardo, C., Hutchings, G., Blanco, E., & Dixon, L. K. (2006). Molecular epidemiology of African swine fever virus studied by analysis of four variable genome regions. Arch Virol, 151(12), 2475-2494. doi:10.1007/s00705-006-0794-z

O'Donnell, V. K., Grau, F. R., Mayr, G. A., Sturgill Samayoa, T. L., Dodd, K. A., & Barrette, R. W. (2019). Rapid Sequence-Based Characterization of African Swine Fever Virus by Use of the Oxford Nanopore MinION Sequence Sensing Device and a Companion Analysis Software Tool. J Clin Microbiol, 58(1). doi:10.1128/JCM.01104-19

Oem, J. K., Ferris, N. P., Lee, K. N., Joo, Y. S., Hyun, B. H., & Park, J. H. (2009). Simple and rapid lateral-flow assay for the detection of foot-and-mouth disease virus. Clin Vaccine Immunol, 16(11), 1660-1664. doi:10.1128/CVI.00213-09

Oh, T., & Chae, C. (2020). First isolation and genetic characterization of porcine circovirus type 3 using primary porcine kidney cells. Veterinary Microbiology, 241. doi:ARTN 10857610.1016/j.vetmic.2020.108576

Ohrmalm, C., Eriksson, R., Jobs, M., Simonson, M., Stromme, M., Bondeson, K., . . . Blomberg, J. (2012). Variation-tolerant capture and multiplex detection of nucleic acids: application to detection of microbes. J Clin Microbiol, 50(10), 3208-3215. doi:10.1128/JCM.06382-11

Olvera, A., Sibila, M., Calsamiglia, M., Segales, J., & Domingo, M. (2004). Comparison of porcine circovirus type 2 load in serum quantified by a real time PCR in postweaning multisystemic wasting syndrome and porcine dermatitis and nephropathy syndrome naturally affected pigs. J Virol Methods, 117(1), 75-80. doi:10.1016/j.jviromet.2003.12.007

Oura, C. A., Edwards, L., & Batten, C. A. (2013). Virological diagnosis of African swine fever--comparative study of available tests. Virus Res, 173(1), 150-158. doi:10.1016/j.virusres.2012.10.022

Ouyang, K., Binjawadagi, B., Kittawornrat, A., Olsen, C., Hiremath, J., Elkalifa, N., . . . Renukaradhya, G. J. (2013). Development and validation of an assay to detect porcine reproductive and respiratory syndrome virus-specific neutralizing antibody titers in pig oral fluid samples. Clin Vaccine Immunol, 20(8), 1305-1313. doi:10.1128/CVI.00276-13

Pacheco, J. M., Arzt, J., & Rodriguez, L. L. (2010). Early events in the pathogenesis of foot-and-mouth disease in cattle after controlled aerosol exposure. Vet J, 183(1), 46-53. doi:10.1016/j.tvjl.2008.08.023

Palinski, R., Pineyro, P., Shang, P., Yuan, F., Guo, R., Fang, Y., . . . Hause, B. M. (2017). A Novel Porcine Circovirus Distantly Related to Known Circoviruses Is Associated with Porcine Dermatitis and Nephropathy Syndrome and Reproductive Failure. J Virol, 91(1). doi:10.1128/JVI.01879-16

Pan, I. C., Huang, T. S., & Hess, W. R. (1982). New method of antibody detection by indirect immunoperoxidase plaque staining for serodiagnosis of African swine fever. J Clin Microbiol, 16(4), 650-655. doi:10.1128/JCM.16.4.650-655.1982

Park, J. Y., Kim, S. H., Lee, K. K., Kim, Y. H., Moon, B. Y., So, B., & Park, C. K. (2019). Differential detection of porcine reproductive and respiratory syndrome virus genotypes

by a fluorescence melting curve analysis using peptide nucleic acid probe-mediated one-step real-time RT-PCR. J Virol Methods, 267, 29-34. doi:10.1016/j.jviromet.2019.02.008

Park, J. Y., Park, S., Park, Y. R., Kang, D. Y., Kim, E. M., Jeon, H. S., . . . Park, C. K. (2016). Reverse-transcription loop-mediated isothermal amplification (RT-LAMP) assay for the visual detection of European and North American porcine reproductive and respiratory syndrome viruses. J Virol Methods, 237, 10-13. doi:10.1016/j.jviromet.2016.08.008

Park, Y. R., Kim, H. R., Kim, S. H., Lee, K. K., Lyoo, Y. S., Yeo, S. G., & Park, C. K. (2018). Loop-mediated isothermal amplification assay for the rapid and visual detection of novel porcine circovirus 3. J Virol Methods, 253, 26-30. doi:10.1016/j.jviromet.2017.12.006

Pasma, T., Davidson, S., & Shaw, S. L. (2008). Idiopathic vesicular disease in swine in Manitoba. Can Vet J, 49(1), 84-85. Retrieved from https://www.ncbi.nlm.nih.gov/pubmed/18320985

Pastor, M. J., Arias, M., & Escribano, J. M. (1990). Comparison of two antigens for use in an enzyme-linked immunosorbent assay to detect African swine fever antibody. Am J Vet Res, 51(10), 1540-1543. Retrieved from https://www.ncbi.nlm.nih.gov/pubmed/2240773

Paton, D. J., Brown, I. H., Scott, A. C., Done, S. H., & Edwards, S. (1992). Isolation of a Lelystad virus-like agent from British pigs and scanning electron microscopy of infected macrophages. Vet Microbiol, 33(1-4), 195-201. doi:10.1016/0378-1135(92)90047-w

Paton, D. J., Reeve, R., Capozzo, A. V., & Ludi, A. (2019). Estimating the protection afforded by foot-and-mouth disease vaccines in the laboratory. Vaccine, 37(37), 5515-5524. doi:10.1016/j.vaccine.2019.07.102

Phan, T. G., Giannitti, F., Rossow, S., Marthaler, D., Knutson, T. P., Li, L., . . . Delwart, E. (2016). Detection of a novel circovirus PCV3 in pigs with cardiac and multi-systemic inflammation. Virology Journal, 13(1), 184. doi:10.1186/s12985-016-0642-z

Plowright, W., Parker, J., & Peirce, M. A. (1969). African swine fever virus in ticks (Ornithodoros moubata, murray) collected from animal burrows in Tanzania. Nature, 221(5185), 1071-1073. doi:10.1038/2211071a0

Pogranichnyy, R. M., Yoon, K. J., Harms, P. A., Swenson, S. L., Zimmerman, J. J., & Sorden, S. D. (2000). Characterization of immune response of young pigs to porcine circovirus type 2 infection. Viral Immunol, 13(2), 143-153. doi:10.1089/vim.2000.13.143

Poonsuk, K., Gimenez-Lirola, L., & Zimmerman, J. J. (2018). A review of foot-and-mouth disease virus (FMDV) testing in livestock with an emphasis on the use of alternative diagnostic specimens. Anim Health Res Rev, 19(2), 100-112. doi:10.1017/S1466252318000063

Qi, S., Su, M., Guo, D., Li, C., Wei, S., Feng, L., & Sun, D. (2019). Molecular detection and phylogenetic analysis of porcine circovirus type 3 in 21 Provinces of China during 2015-2017. Transbound Emerg Dis, 66(2), 1004-1015. doi:10.1111/tbed.13125

Rahman, M., Banik, S., Faruque, A. S., Taniguchi, K., Sack, D. A., Van Ranst, M., & Azim, T. (2005). Detection and characterization of human group C rotaviruses in Bangladesh. J Clin Microbiol, 43(9), 4460-4465. doi:10.1128/JCM.43.9.4460-4465.2005

Ramirez, M., Bauermann, F. V., Navarro, D., Rojas, M., Manchego, A., Nelson, E. A., . . . Rivera, H. (2019). Detection of porcine reproductive and respiratory syndrome virus (PRRSV) 1-

7-4-type strains in Peru. Transbound Emerg Dis, 66(3), 1107-1113. doi:10.1111/tbed.13134

Reid, S. M., Ferris, N. P., Hutchings, G. H., Zhang, Z., Belsham, G. J., & Alexandersen, S. (2001). Diagnosis of foot-and-mouth disease by real-time fluorogenic PCR assay. Vet Rec, 149(20), 621-623. doi:10.1136/vr.149.20.621

Reid, S. M., Grierson, S. S., Ferris, N. P., Hutchings, G. H., & Alexandersen, S. (2003). Evaluation of automated RT-PCR to accelerate the laboratory diagnosis of foot-and-mouth disease virus. J Virol Methods, 107(2), 129-139. doi:10.1016/s0166-0934(02)00210-0

Ren, L., Chen, X., & Ouyang, H. (2016). Interactions of porcine circovirus 2 with its hosts. Virus Genes, 52(4), 437-444. doi:10.1007/s11262-016-1326-x

Resende, T. P., Marthaler, D. G., & Vannucci, F. A. (2017). A novel RNA-based in situ hybridization to detect Seneca Valley virus in neonatal piglets and sows affected with vesicular disease. Plos One, 12(4), e0173190. doi:10.1371/journal.pone.0173190

Rice, C. E., & Brooksby, J. B. (1953). Studies of the complement-fixation reaction in virus systems. V. In foot and mouth disease using direct and indirect methods. J Immunol, 71(5), 300-310. Retrieved from https://www.ncbi.nlm.nih.gov/pubmed/13118165

Richt, J. A., Lager, K. M., Clouser, D. F., Spackman, E., Suarez, D. L., & Yoon, K. J. (2004). Real-time reverse transcription-polymerase chain reaction assays for the detection and differentiation of North American swine influenza viruses. J Vet Diagn Invest, 16(5), 367-373. doi:10.1177/104063870401600501

Roeder, P. L., & Le Blanc Smith, P. M. (1987). Detection and typing of foot-and-mouth disease virus by enzyme-linked immunosorbent assay: a sensitive, rapid and reliable technique for primary diagnosis. Res Vet Sci, 43(2), 225-232. Retrieved from https://www.ncbi.nlm.nih.gov/pubmed/2825310

Rosario, K., Breitbart, M., Harrach, B., Segales, J., Delwart, E., Biagini, P., & Varsani, A. (2017). Revisiting the taxonomy of the family Circoviridae: establishment of the genus Cyclovirus and removal of the genus Gyrovirus. Arch Virol, 162(5), 1447-1463. doi:10.1007/s00705-017-3247-y

Rossow, K. D., Collins, J. E., Goyal, S. M., Nelson, E. A., Christopher-Hennings, J., & Benfield, D. A. (1995). Pathogenesis of porcine reproductive and respiratory syndrome virus infection in gnotobiotic pigs. Vet Pathol, 32(4), 361-373. doi:10.1177/030098589503200404

Sadiq, A., Bostan, N., Yinda, K. C., Naseem, S., & Sattar, S. (2018). Rotavirus: Genetics, pathogenesis and vaccine advances. Rev Med Virol, 28(6), e2003. doi:10.1002/rmv.2003

Saeng-chuto, K., Stott, C. J., Wegner, M., Kaewprommal, P., Piriyapongsa, J., & Nilubol, D. (2018). The full-length genome characterization, genetic diversity and evolutionary analyses of Senecavirus A isolated in Thailand in 2016. Infection Genetics and Evolution, 64, 32-45. doi:10.1016/j.meegid.2018.06.011

Sakaki, K., Suphavilai, P., & Chandarkeo, T. (1978). Inactivated-concentrated virus antigen for indirect complement fixation test of foot-and-mouth disease. Natl Inst Anim Health Q (Tokyo), 18(3-4), 128-134. Retrieved from https://www.ncbi.nlm.nih.gov/pubmed/216926

Salas, M. L., & Andres, G. (2013). African swine fever virus morphogenesis. Virus Res, 173(1), 29-41. doi:10.1016/j.virusres.2012.09.016

Sastre, P., Perez, T., Costa, S., Yang, X., Raber, A., Blome, S., . . . Rueda, P. (2016). Development of a duplex lateral flow assay for simultaneous detection of antibodies against African and Classical swine fever viruses. J Vet Diagn Invest, 28(5), 543-549. doi:10.1177/1040638716654942

Segales, J., Barcellos, D., Alfieri, A., Burrough, E., & Marthaler, D. (2017). Senecavirus A: An Emerging Pathogen Causing Vesicular Disease and Mortality in Pigs? Veterinary Pathology, 54(1), 11-21. doi:10.1177/0300985816653990

Senthilkumaran, C., Yang, M., Bittner, H., Ambagala, A., Lung, O., Zimmerman, J., . . . Nfon, C. (2017). Detection of genome, antigen, and antibodies in oral fluids from pigs infected with foot-and-mouth disease virus. Can J Vet Res, 81(2), 82-90. Retrieved from https://www.ncbi.nlm.nih.gov/pubmed/28408775

Seuberlich, T., Tratschin, J. D., Thur, B., & Hofmann, M. A. (2002). Nucleocapsid protein-based enzyme-linked immunosorbent assay for detection and differentiation of antibodies against European and North American porcine reproductive and respiratory syndrome virus. Clin Diagn Lab Immunol, 9(6), 1183-1191. doi:10.1128/cdli.9.6.1183-1191.2002

Shaw, A. E., Reid, S. M., Ebert, K., Hutchings, G. H., Ferris, N. P., & King, D. P. (2007). Implementation of a one-step real-time RT-PCR protocol for diagnosis of foot-and-mouth disease. J Virol Methods, 143(1), 81-85. doi:10.1016/j.jviromet.2007.02.009

Shi, M., Lemey, P., Singh Brar, M., Suchard, M. A., Murtaugh, M. P., Carman, S., . . . Chi-Ching Leung, F. (2013). The spread of type 2 Porcine Reproductive and Respiratory Syndrome Virus (PRRSV) in North America: a phylogeographic approach. Virology, 447(1-2), 146-154. doi:10.1016/j.virol.2013.08.028

Sirinarumitr, T., Morozov, I., Nawagitgul, P., Sorden, S. D., Harms, P. A., & Paul, P. S. (2000). Utilization of a rate enhancement hybridization buffer system for rapid in situ hybridization for the detection of porcine circovirus in cell culture and in tissues of pigs with postweaning multisystemic wasting syndrome. J Vet Diagn Invest, 12(6), 562-565. doi:10.1177/104063870001200612

Snijder, E. J., Kikkert, M., & Fang, Y. (2013). Arterivirus molecular biology and pathogenesis. J Gen Virol, 94(Pt 10), 2141-2163. doi:10.1099/vir.0.056341-0

Sorden, S. D., Harms, P. A., Nawagitgul, P., Cavanaugh, D., & Paul, P. S. (1999). Development of a polyclonal-antibody-based immunohistochemical method for the detection of type 2 porcine circovirus in formalin-fixed, paraffin-embedded tissue. J Vet Diagn Invest, 11(6), 528-530. doi:10.1177/104063879901100607

Stadejek, T., Stankevicius, A., Murtaugh, M. P., & Oleksiewicz, M. B. (2013). Molecular evolution of PRRSV in Europe: current state of play. Vet Microbiol, 165(1-2), 21-28. doi:10.1016/j.vetmic.2013.02.029

Stadejek, T., Wozniak, A., Milek, D., & Biernacka, K. (2017). First detection of porcine circovirus type 3 on commercial pig farms in Poland. Transbound Emerg Dis, 64(5), 1350-1353. doi:10.1111/tbed.12672

Sukmak, M., Thanantong, N., Poolperm, P., Boonsoongnern, A., Ratanavanichrojn, N., Jirawattanapong, P., . . . Wajjwalku, W. (2019). The retrospective identification and molecular epidemiology of porcine circovirus type 3 (PCV3) in swine in Thailand from 2006 to 2017. Transbound Emerg Dis, 66(1), 611-616. doi:10.1111/tbed.13057

Sun, D., Vannucci, F., Knutson, T. P., Corzo, C., & Marthaler, D. G. (2017). Emergence and whole-genome sequence of Senecavirus A in Colombia. Transboundary and Emerging Diseases, 64(5), 1346-1349. doi:10.1111/tbed.12669

Sun, J. Y., Bingga, G., Liu, Z. C., Zhang, C. H., Shen, H. Y., Guo, P. J., & Zhang, J. F. (2018). A novel HRM assay for differentiating classical strains and highly pathogenic strains of type 2 porcine reproductive and respiratory syndrome virus. Molecular and Cellular Probes, 39, 25-32. doi:10.1016/j.mcp.2018.03.004

Sun, S. Q., Guo, H. C., Sun, D. H., Yin, S. H., Shang, Y. J., Cai, X. P., & Liu, X. T. (2010). Development and validation of an ELISA using a protein encoded by ORF2 antigenic domain of porcine circovirus type 2. Virology Journal, 7. doi:Artn 27410.1186/1743-422x-7-274

Suzuki, T., & Hasebe, A. (2017). A provisional complete genome-based genotyping system for rotavirus species C from terrestrial mammals. J Gen Virol, 98(11), 2647-2662. doi:10.1099/jgv.0.000953

Takikawa, N., Kobayashi, S., Ide, S., Yamane, Y., Tanaka, Y., & Yamagishi, H. (1996). Detection of antibodies against porcine reproductive and respiratory syndrome (PRRS) virus in swine sera by enzyme-linked immunosorbent assay. Journal of Veterinary Medical Science, 58(4), 355-357. doi:10.1292/jvms.58.355

Tebit, D. M., & Arts, E. J. (2011). Tracking a century of global expansion and evolution of HIV to drive understanding and to combat disease. Lancet Infect Dis, 11(1), 45-56. doi:10.1016/S1473-3099(10)70186-9

Theuns, S., Conceicao-Neto, N., Zeller, M., Heylen, E., Roukaerts, I. D., Desmarets, L. M., . . . Matthijnssens, J. (2016). Characterization of a genetically heterogeneous porcine rotavirus C, and other viruses present in the fecal virome of a non-diarrheic Belgian piglet. Infect Genet Evol, 43, 135-145. doi:10.1016/j.meegid.2016.05.018

Thomson, J. R., Higgins, R. J., Smith, W. J., & Done, S. H. (2002). Porcine dermatitis and nephropathy syndrome. clinical and pathological features of cases in the United Kingdom (1993-1998). J Vet Med A Physiol Pathol Clin Med, 49(8), 430-437. doi:10.1046/j.1439-0442.2002.00475.x

Tian, K., Yu, X., Zhao, T., Feng, Y., Cao, Z., Wang, C., . . . Gao, G. F. (2007). Emergence of fatal PRRSV variants: unparalleled outbreaks of atypical PRRS in China and molecular dissection of the unique hallmark. Plos One, 2(6), e526. doi:10.1371/journal.pone.0000526

Tochetto, C., Lima, D. A., Varela, A. P. M., Loiko, M. R., Paim, W. P., Scheffer, C. M., . . . Roehe, P. M. (2018). Full-Genome Sequence of Porcine Circovirus type 3 recovered from serum of sows with stillbirths in Brazil. Transbound Emerg Dis, 65(1), 5-9. doi:10.1111/tbed.12735

Tuanthap, S., Phupolphan, C., Luengyosluechakul, S., Duang-In, A., Theamboonlers, A., Wattanaphansak, S., . . . Poovorawan, Y. (2018). Porcine rotavirus C in pigs with gastroenteritis on Thai swine farms, 2011-2016. PeerJ, 6, e4724. doi:10.7717/peerj.4724

Tuthill, T. J., Groppelli, E., Hogle, J. M., & Rowlands, D. J. (2010). Picornaviruses. Curr Top Microbiol Immunol, 343, 43-89. doi:10.1007/82_2010_37

Vanbinst, T., Vandenbussche, F., Dernelle, E., & De Clercq, K. (2010). A duplex real-time RT-PCR for the detection of bluetongue virus in bovine semen. J Virol Methods, 169(1), 162-168. doi:10.1016/j.jviromet.2010.07.019

Venkataraman, S., Reddy, S. P., Loo, J., Idamakanti, N., Hallenbeck, P. L., & Reddy, V. S. (2008). Structure of Seneca Valley Virus-001: an oncolytic picornavirus representing a new genus. Structure, 16(10), 1555-1561. doi:10.1016/j.str.2008.07.013

Walker, I. W., Konoby, C. A., Jewhurst, V. A., McNair, I., McNeilly, F., Meehan, B. M., . . . Allan, G. M. (2000). Development and application of a competitive enzyme-linked immunosorbent assay for the detection of serum antibodies to porcine circovirus type 2. J Vet Diagn Invest, 12(5), 400-405. doi:10.1177/104063870001200502

Wang, A., Jia, R., Liu, Y., Zhou, J., Qi, Y., Chen, Y., . . . Zhang, G. (2020). Development of a novel quantitative real-time PCR assay with lyophilized powder reagent to detect African swine fever virus in blood samples of domestic pigs in China. Transbound Emerg Dis, 67(1), 284-297. doi:10.1111/tbed.13350

Wang, A. P., Zhang, J. Q., Shen, H. G., Zheng, Y., Feng, Q., Yim-Im, W., . . . Li, G. W. (2019). Genetic diversity of porcine reproductive and respiratory syndrome virus 1 in the United States of America from 2010 to 2018. Veterinary Microbiology, 239. doi:ARTN 10848610.1016/j.vetmic.2019.108486

Wang, D., Yu, J., Wang, Y., Zhang, M., Li, P., Liu, M., & Liu, Y. (2020). Development of a real-time loop-mediated isothermal amplification (LAMP) assay and visual LAMP assay for detection of African swine fever virus (ASFV). J Virol Methods, 276, 113775. doi:10.1016/j.jviromet.2019.113775

Wang, J., Wang, J., Geng, Y., & Yuan, W. (2017). A recombinase polymerase amplification-based assay for rapid detection of African swine fever virus. Can J Vet Res, 81(4), 308-312. Retrieved from https://www.ncbi.nlm.nih.gov/pubmed/29081590

Wang, J., Zhang, Y., Wang, J., Liu, L., Pang, X., & Yuan, W. (2017). Development of a TaqMan-based real-time PCR assay for the specific detection of porcine circovirus 3. J Virol Methods, 248, 177-180. doi:10.1016/j.jviromet.2017.07.007

West, K. H., Bystrom, J. M., Wojnarowicz, C., Shantz, N., Jacobson, M., Allan, G. M., . . . Ellis, J. A. (1999). Myocarditis and abortion associated with intrauterine infection of sows with porcine circovirus 2. J Vet Diagn Invest, 11(6), 530-532. doi:10.1177/104063879901100608

Wilker, P. R., Dinis, J. M., Starrett, G., Imai, M., Hatta, M., Nelson, C. W., . . . Friedrich, T. C. (2013). Selection on haemagglutinin imposes a bottleneck during mammalian transmission of reassortant H5N1 influenza viruses. Nat Commun, 4, 2636. doi:10.1038/ncomms3636

Willcocks, M. M., Locker, N., Gomwalk, Z., Royall, E., Bakhshesh, M., Belsham, G. J., . . . Roberts, L. O. (2011). Structural features of the Seneca Valley virus internal ribosome entry site (IRES) element: a picornavirus with a pestivirus-like IRES. J Virol, 85(9), 4452-4461. doi:10.1128/JVI.01107-10

Wittwer, C. T., Herrmann, M. G., Gundry, C. N., & Elenitoba-Johnson, K. S. (2001). Real-time multiplex PCR assays. Methods, 25(4), 430-442. doi:10.1006/meth.2001.1265

Wright, C. F., Morelli, M. J., Thebaud, G., Knowles, N. J., Herzyk, P., Paton, D. J., . . . King, D. P. (2011). Beyond the consensus: dissecting within-host viral population diversity of foot-and-mouth disease virus by using next-generation genome sequencing. J Virol, 85(5), 2266-2275. doi:10.1128/JVI.01396-10

Wu, M. L., Cong, F., Zhu, Y. J., Lian, Y. X., Chen, M. L., Huang, R., & Guo, P. J. (2018). Multiplex Detection of Five Canine Viral Pathogens for Dogs as Laboratory Animals by the Luminex xTAG Assay. Frontiers in Microbiology, 9. doi:ARTN 178310.3389/fmicb.2018.01783

Wu, Q., Zhao, X., Chen, Y., He, X., Zhang, G., & Ma, J. (2016). Complete Genome Sequence of Seneca Valley Virus CH-01-2015 Identified in China. Genome Announc, 4(1). doi:10.1128/genomeA.01509-15

Wu, X. L., Xiao, L., Lin, H., Yang, M., Chen, S. J., An, W., . . . Tang, Z. Z. (2017). A Novel Capillary Electrophoresis-Based High-Throughput Multiplex Polymerase Chain Reaction System for the Simultaneous Detection of Nine Pathogens in Swine. Biomed Res Int, 2017, 7243909. doi:10.1155/2017/7243909

Xiao, C. T., Halbur, P. G., & Opriessnig, T. (2015). Global molecular genetic analysis of porcine circovirus type 2 (PCV2) sequences confirms the presence of four main PCV2 genotypes and reveals a rapid increase of PCV2d. J Gen Virol, 96(Pt 7), 1830-1841. doi:10.1099/vir.0.000100

Xiao, L., Wang, Y., Kang, R., Wu, X., Lin, H., Ye, Y., . . . Li, X. (2018). Development and application of a novel Bio-Plex suspension array system for high-throughput multiplexed nucleic acid detection of seven respiratory and reproductive pathogens in swine. J Virol Methods, 261, 104-111. doi:10.1016/j.jviromet.2018.08.017

Xu, W., Hole, K., Goolia, M., Pickering, B., Salo, T., Lung, O., & Nfon, C. (2017). Genome wide analysis of the evolution of Senecavirus A from swine clinical material and assembly yard environmental samples. Plos One, 12(5), e0176964. doi:10.1371/journal.pone.0176964

Yan, M., Zhu, L., & Yang, Q. (2014). Infection of porcine circovirus 2 (PCV2) in intestinal porcine epithelial cell line (IPEC-J2) and interaction between PCV2 and IPEC-J2 microfilaments. Virology Journal, 11, 193. doi:10.1186/s12985-014-0193-0

Yang, K., Tian, Y., Zhou, D., Duan, Z., Guo, R., Liu, Z., . . . Liu, W. (2017). A Multiplex RT-PCR Assay to Detect and Discriminate Porcine Reproductive and Respiratory Syndrome Viruses in Clinical Specimens. Viruses, 9(8). doi:10.3390/v9080205

Yang, M., van Bruggen, R., & Xu, W. (2012). Generation and diagnostic application of monoclonal antibodies against Seneca Valley virus. J Vet Diagn Invest, 24(1), 42-50. doi:10.1177/1040638711426323

Yang, Q., Xi, J., Chen, X., Hu, S., Chen, N., Qiao, S., . . . Bao, D. (2017). The development of a sensitive droplet digital PCR for quantitative detection of porcine reproductive and respiratory syndrome virus. Int J Biol Macromol, 104(Pt A), 1223-1228. doi:10.1016/j.ijbiomac.2017.06.115

Ye, X., Berg, M., Fossum, C., Wallgren, P., & Blomstrom, A. L. (2018). Detection and genetic characterisation of porcine circovirus 3 from pigs in Sweden. Virus Genes, 54(3), 466-469. doi:10.1007/s11262-018-1553-4

Yoon, I. J., Joo, H. S., Christianson, W. T., Kim, H. S., Collins, J. E., Morrison, R. B., & Dial, G. D. (1992). An indirect fluorescent antibody test for the detection of antibody to swine infertility and respiratory syndrome virus in swine sera. J Vet Diagn Invest, 4(2), 144-147. doi:10.1177/104063879200400205

Yoon, I. J., Joo, H. S., Goyal, S. M., & Molitor, T. W. (1994). A modified serum neutralization test for the detection of antibody to porcine reproductive and respiratory syndrome virus in swine sera. J Vet Diagn Invest, 6(3), 289-292. doi:10.1177/104063879400600326

Yoon, K. J., Zimmerman, J. J., Swenson, S. L., McGinley, M. J., Eernisse, K. A., Brevik, A., . . . Platt, K. B. (1995). Characterization of the humoral immune response to porcine reproductive and respiratory syndrome (PRRS) virus infection. J Vet Diagn Invest, 7(3), 305-312. doi:10.1177/104063879500700302

Zhai, S. L., Zhou, X., Zhang, H., Hause, B. M., Lin, T., Liu, R., . . . Wang, D. (2017). Comparative epidemiology of porcine circovirus type 3 in pigs with different clinical presentations. Virology Journal, 14(1), 222. doi:10.1186/s12985-017-0892-4

Zhang, J., Zheng, Y., Xia, X. Q., Chen, Q., Bade, S. A., Yoon, K. J., . . . Li, G. (2017). High-throughput whole genome sequencing of Porcine reproductive and respiratory syndrome virus from cell culture materials and clinical specimens using next-generation sequencing technology. J Vet Diagn Invest, 29(1), 41-50. doi:10.1177/1040638716673404

Zhang, S., Wang, D., Jiang, Y., Li, Z., Zou, Y., Li, M., . . . Wang, N. (2019). Development and application of a baculovirus-expressed capsid protein-based indirect ELISA for detection of porcine circovirus 3 IgG antibodies. BMC Vet Res, 15(1), 79. doi:10.1186/s12917-019-1810-3

Zhang, Y., Zhang, Z., Wang, Z., Wang, Z., Wang, C., Feng, C., . . . Wu, S. (2019). Development of a droplet digital PCR assay for sensitive detection of porcine circovirus 3. Mol Cell Probes, 43, 50-57. doi:10.1016/j.mcp.2018.11.005

Zhang, Z., Zhang, Y., Lin, X., Chen, Z., & Wu, S. (2019). Development of a novel reverse transcription droplet digital PCR assay for the sensitive detection of Senecavirus A. Transbound Emerg Dis, 66(1), 517-525. doi:10.1111/tbed.13056

Zhao, Y., Liu, F., Li, Q., Wu, M., Lei, L., & Pan, Z. (2019). A multiplex RT-PCR assay for rapid and simultaneous detection of four RNA viruses in swine. J Virol Methods, 269, 38-42. doi:10.1016/j.jviromet.2019.04.001

Zheng, S., Wu, X., Shi, J., Peng, Z., Gao, M., Xin, C., . . . Wang, J. (2018). Rapid specific and visible detection of porcine circovirus type 3 using loop-mediated isothermal amplification (LAMP). Transboundary and Emerging Diseases, 65(3), 597-601. doi:10.1111/tbed.12835

Zhu, N., Zhang, D., Wang, W., Li, X., Yang, B., Song, J., . . . Research, T. (2020). A Novel Coronavirus from Patients with Pneumonia in China, 2019. N Engl J Med, 382(8), 727-733. doi:10.1056/NEJMoa2001017

Zou, Y., Zhang, N., Zhang, J., Zhang, S., Jiang, Y., Wang, D., . . . Wang, N. (2018). Molecular detection and sequence analysis of porcine circovirus type 3 in sow sera from farms with prolonged histories of reproductive problems in Hunan, China. Arch Virol, 163(10), 2841-2847. doi:10.1007/s00705-018-3914-7

Chapter 2 Molecular detection of major porcine viral pathogens

2.1 A multiplex real-time PCR assay for the detection and differentiation of the newly emerged porcine circovirus type 3 and continuously evolving type 2 strains in the United States

Yin Wang, Yuan Feng, Wanglong Zheng, Lance Noll, Elizabeth Porter, Megan Potter, Giselle Cino, Lalitha Peddireddi, Xuming Liu, Gary Anderson, Jianfa Bai

(Journal of Virological Methods, 269 (2019) 7-12)

Abstract: A multiplex quantitative real-time polymerase chain reaction (mqPCR) assay was developed and validated for the detection and differentiation of porcine circovirus type 3 (PCV3) and type 2 (PCV2) strains. The assay coverage was 97.9% (184/188) for PCV3 and 99.1% (1889/1907) for PCV2 sequences that were available from the current GenBank database. The PCR amplification efficiencies were 98–99% for plasmids, and 92–96% for diagnostic samples, with correlation coefficients all greater than 0.99. The limit of detection (LOD) determined as plasmid copies per reaction was 17 for PCV3 and 14 for PCV2. The assay specifically detected the targeted viruses without cross reacting to each other or to other common porcine viruses. Among 336 swine clinical samples collected in 2018, 101 (30.1%) were PCV3 positive, 56 (16.7%) were PCV2 positive and 18 (5.4%) were co-positives. Sixty selected PCV3 positives were confirmed by Sanger sequencing, and 53 of the 56 PCV2 positive samples were tested positive by another validated PCR assay.

2.1.1 Introduction

Different from the non-pathogenic PCV1 strains (Tischer et al., 1974), PCV2 is considered a major swine pathogen causing porcine circovirus-associated diseases (PCVAD) including post-weaning multi- systemic wasting syndrome (PMWS), porcine dermatitis and nephropathy syndrome (PDNS), porcine respiratory disease complex (PRDC), enteritis and reproductive failure (Opriessnig et al., 2007; Tischer et al., 1986). Since its first identification in 1998, PCV2 has been reported worldwide and has caused significant economic losses to the swine industry (Allan et al., 1998).

In 2015, another porcine circovirus, named PCV3, was found in the US that can cause PCVAD-like clinical symptoms similar to those caused by PCV2. The symptoms include PDNS and reproductive failure, and cardiac and multi-organ inflammation (Palinski et al., 2017; Phan et al., 2017). PCV3 has also been detected in several other countries including Brazil, China, Thailand, Sweden, Denmark, Italy, Poland and Spain (Chen et al., 2017; Franzo et al., 2018; Kedkovid et al., 2018; Stadejek et al., 2017; Tochetto et al., 2018; Xu et al., 2018; Ye et al., 2018).

Porcine circoviruses are small non-enveloped viruses with a circular single-stranded DNA genome, belonging to genus Circovirus in the family of *Circoviridae*. In the viral genome, ORF1 codes for the replicase (Rep) protein and ORF2 for the capsid (Cap) protein. The Rep protein is a non-structural protein and functions for the viral replication, while the structural Cap protein dominates immunogenicity (Cheung, 2003; Mankertz et al., 1998a, b; Nawagitgul et al., 2002). As a DNA virus, PCV2 has high evolutionary mutation rate of 1.2×10^{-3} substitutions/ site/year and has been constantly evolving. With the emerging viral strains, PCV2 has been divided into 5

genotypes, namely PCV2a–2e strains, according to the diversity level of the ORF2 nucleotide sequences (Franzo et al., 2016; Segales et al., 2008; Xiao et al., 2016). The continued mutation in the PCV2 genome (Eddicks et al., 2015; Yang et al., 2018) made it more difficult to identify, especially by some older molecular detection methods.

Although the PCV3 genomes are different from PCV2 genomes, they cause similar syndromes and it is difficult to differentiate clinical symptoms caused by the two circoviruses. The objective of this study was to develop a multiplex quantitative real-time PCR (mqPCR) assay to rapidly detect and differentiate the two important circoviruses, with significantly improved diagnostic coverage to current field strains.

2.1.2 Materials and methods

2.1.2.1 Viral isolates

Cell culture isolates of PCV2a, PCV2b and PCV2d, porcine re- productive and respiratory syndrome virus type 2 (PRRSV-2) and Seneca Valley virus 1 (SVV-1) that were previously confirmed by culture and sequencing were used in this study.

2.1.2.2 Multiplex real-time PCR assay design

According to the 188 PCV3 whole genome sequences that were available from the GenBank database, one set each of primers and probes were designed from ORF1 and ORF2. Both PCV3 probes were labeled with 5′-FAM and 3′-BHQ1. Based on 1907 PCV2 whole genome sequences from the GenBank database, two sets of primers and probes were chosen from ORF1 and ORF3 respectively. The PCV2 probes were labeled with 5′-VIC and 3′-BHQ1. A conserved

swine gene, serum beta- 2-microglobulin (*SB2M*) was applied as internal control in the assay, coding for a small membrane protein that may be involved in immune system regulation (Xie et al., 2003). The *SB2M* probe was labeled with 5′-Cy5 and 3′-BHQ2. Information of all primers and probes are given in Table 2.1.1.

2.1.2.3 Viral DNA extraction and standard control constructs preparation

The viral DNA was extracted from 140 μl of clinical samples or cell culture by QIAamp Viral RNA Mini Kit (Qiagen, MD) or ZR Viral DNA/ RNA Kit (Zymo Research, CA) according to the manufacturer's recommendations, and stored at −80 °C until use. To ensure that the obtained PCV3 genome was from a single genome, and not amplified from more than one genome, a full length PCV3 genome was amplified by a single pair of tail-to-tail primers that overlapped at a unique PstI site in the PCV3 genome (illustrated in Figure 2.1.1). The full-genome amplicon of PCV3 was then digested with the PstI restriction enzyme and cloned into pACYC177 cloning vector. The PCV2 fragments containing the assay targets were also amplified, and the PCR product was cloned into the pCR™2.1 vector using the original TA Cloning kit (Invitrogen, CA). The presence of cloned inserts was confirmed by gel electrophoresis and subsequent DNA sequencing. The primers used for cloning are also listed in Table 2.1.1.

2.1.2.4 Multiplex real-time PCR reaction composition and condition

All PCR reactions were performed in a 20 μL reaction composed of 4 μL of DNA samples prepared as described (Shi et al., 2016), 0.4 μM each of forward and reverse PCR primers, 0.2 μM each of probes, and 10 μl of 2X iQ™ Multiplex Powermix (Bio-Rad, CA). The parameters for

thermocycling start with an initial denaturation at 94 °C for 10 min, followed by 45 cycles of 94 °C for 15 s and 60 °C for 45 s. The cycle threshold (Ct) values were generated with CFX96 Touch™ Real-Time PCR Detection System and standard curve results were analyzed with BioRad CFX Manager 3.0.

2.1.2.5 Assay sensitivity and specificity analysis

The analytical sensitivity was determined by generating standard curves with triplicates of 10-fold serial dilutions of control constructs and positive clinical samples, and a cultured PCV2d isolate. To obtain accurate LODs, 2-fold serial dilutions were prepared from the last 10- fold dilution to fine-tune the least concentration that still amplifies. The assay specificity was evaluated with cell cultures (PCV2a, PCV2b, PCV2d, PRRSV-2 and SVV-1) and clinical samples positive to specific pathogens (PCV3, PRRSV-2, groups A, B and C swine rotaviruses, swine influenza virus (SIV), porcine epidemic diarrhea virus (PEDV), porcine delta coronavirus (PDCoV), porcine parvovirus (PPV) and porcine parainfluenza virus type 1 (PPIV-1) (summarized in Table 2.1.3).

2.1.2.6 Comparison of multiplex and singular assays

To compare the performances of the singular PCV2 and PCV3 assays with the multiplex assay, standard curves were also generated for both singular assays and at the multiplexed condition that composed PCV2, PCV3 and the internal control. The performance of multiplex and singular assays was compared using PCV3 and PCV2 standard control constructs and a PCV3 positive sample and a cultured PCV2 isolate. The individual viral DNA was subjected to singular assays while a mixture of equal molarity of PCV2 and PCV3 DNA was used for the multiplex

assay. Standard curves were generated and PCR efficiency analysis between the singular and the multiplex assays was performed.

2.1.2.7 Evaluation with clinical samples

A total of 336 clinical porcine samples collected in 2018 with different sample types including serum, oral fluid, feces and stomached organ tissue homogenates of heart, lung, thymus, tonsil, liver, spleen, kidney, fetus, placenta, lymph nodes and intestine, were collected from Kansas State Veterinary Diagnostic Laboratory (KSVDL). The mqPCR assays were performed on these samples for PCV3 and PCV2 detections, and for potential coinfection identifications.

2.1.3 Results

2.1.3.1 Analysis of assay coverage to GenBank sequence database

Based on 188 PCV3 full genome sequences in the GenBank, two sets of primers and probes, targeting the respective cap gene and rep gene, were designed for PCV3 detection. The cap gene set matched 92.6% (174/188) and the rep gene set matches 89.4% (168/188) of the strains with an overall coverage of 97.9%. The four mismatching strains all had a single nucleotide variation in the primers or probes (data not shown). The PCV2 sets were designed based on 1907 PCV2 whole genome sequences from the GenBank, including five genotypes, PCV2a–2e. To ensure high coverage of divergent PCV2 genomes, two sets of primers and probes were designed in ORF1 and ORF3 genes with coverages of 94.8% (1808/1907) and 90.5% (1726/1907), respectively. The combined coverage of the two PCV2 sets was 99.1% (1889/1907) based on an *in silico* analysis. Information of all primers and probes are shown in Table 2.1.1.

2.1.3.2 Analytical sensitivity of the multiplex real-time PCR assay on cloned positive controls

Analytical sensitivity of the mqPCR assay was analyzed using standard curves generated by three replications of 10-fold serial dilutions of the template and analyzed by plotting their Cts against dilution factors. The results indicated that the PCR amplification efficiencies were 98.9% for PCV3 and 98.5% for PCV2 with correlation coefficient (R^2) both greater than 0.995 (Figure 2.1.2A). For more accurate determination of limit of detection (LOD) of the assay, the cloned standard controls from the last 10-fold dilution were further diluted by 2-fold serial dilutions. The results indicated that LODs were 17 copies per PCR reaction for PCV3 and 14 copies per reaction for PCV2.

2.1.3.3 Analytical sensitivity of the multiplex real-time PCR assay on a viral isolate and the clinical samples

To make sure that the assay sensitivity was not compromised when tested on virus and diagnostic samples, a PCV2d cell culture isolate and PCV3 positive clinical samples (we have not been able to culture PCV3) were also used. The standard curves generated by 10-fold dilutions were plotted with Cts versus dilution factors and showed that the amplification efficiencies were 92.9% for PCV3 and 95.3% for PCV2 with R2 greater than 0.995 for both viruses. The LOD of the PCV2d cell culture isolate was around 1.1×10^{-6} TCID50 per reaction. A more accurate Ct cutoff for detection limit was also determined by 2-fold serial dilutions starting with the last 10-fold dilution that still generated signals. The results indicated that the cutoff for both PCV3 and

PCV2 positive for diagnostic samples was Ct 37. The standard curve of the internal control SB2M showed that there is no inhibition to PCR amplification (Figure 2.1.2).

2.1.3.4 Diagnostic sensitivity of the assay

From mqPCR data, 60 selected PCV3 positive samples with Ct values ranging from 18 to 35 were verified by Sanger sequencing, indicating a 100% diagnostic sensitivity. For PCV2, 53 of 56 positive samples were verified as positives by a previously validated PCV2 qPCR assay that is currently used at KSVDL. Thus, for the 53 positives identified by the current KSVDL assay, the diagnostic sensitivity of the newly developed assay is also 100%. The new assay may have higher diagnostic sensitivity as it detected three more positive samples.

2.1.3.5 Comparison of multiplex and singular assays

As shown in Figure 2.1.2, the mqPCR generated similar correlation coefficients and PCR amplification efficiencies to those generated by singular qPCR reactions. Both multiplex and singular assays had R^2 greater than 0.994 and PCR amplification efficiencies between 92.9% and 96.9%. The Ct values for serial dilutions of clinical positive samples in singular and multiplex reactions were nearly identical (Table 2.1.2) indicating that multiplexing is not reducing the assay's sensitivity.

2.1.3.6 Specificity of multiplex real-time PCR assay

The specificity of primers and probes was evaluated by an *in silico* analysis with NCBI primer design tool, which presented a unique viral target for each set of assay. Assay specificity was further tested experimentally with a PCV3 dominated clinical sample as confirmed by next

generation sequencing, viral isolates (PCV2a, PCV2b, PCV2d, PRRSV-2, and SVV-1), and clinical samples that were previously tested positive to non-target, specific pathogens. The results demonstrated that assay specifically detected PCV2 and PCV3 positive samples without cross detection and no positive targets were detected from samples that were positive to other common porcine viruses that included 16 PEDV positive samples, 16 PRRSV positives, 7 SIV positives, 1 PPIV positive, 1 PDCoV positive, 1 PPV positive, and one positive sample each to group A, group B and group C rotaviruses. Results showed that there was no signal generated on those non-target positive samples indicating a good specificity of the assay (Table 2.1.3).

2.1.3.7 Prevalence of PCV2 and PCV3 on clinical samples collected in 2018

The 336 clinical porcine samples collected in 2018 with different sample types were tested for PCV2 and PCV3 to determine assay performance and viral prevalence in the field. Of the 336 samples, 56 (16.7%) were PCV2 positives, 101 (30.1%) were PCV3 positives. Among the 139 PCV2 and PCV3 positive samples, 18 (5.4% of total number of samples, and 12.9% of positive samples) were positive for both PCV3 and PCV2 viruses (Table 2.1.4). The house keeping gene, SB2M, that was included as an internal control, generated Cts on these diagnostic samples mostly in between 20–30, indicating an efficient nucleic acid extraction and no PCR inhibition observed.

2.1.4 Discussion

PCVAD is a common disease in swine production systems and has caused significant economic losses. PCV2 is a major pathogen involved in PCVAD (Segales et al., 2008). A new porcine circovirus, PCV3, was identified in 2015 and is causing PCVAD-like clinical signs,

including PDNS and reproductive failure, and cardiac and multi-organ inflammation, and thus has attracted researchers' and producers' attention (Chen et al., 2017; Palinski et al., 2017; Phan et al., 2017; Stadejek et al., 2017). Considering the similar clinical symptoms caused by PCV2 and PCV3, and that PCV2 assays built many years ago are no longer covering the majority of field strains, there was a need to develop a mqPCR assay that was based on the most current sequencing data and capable of detecting the two viruses with high diagnostic coverage to field strains.

Although several molecular detection methods were developed for rapid detection of PCV3 and PCV2 (Kim et al., 2017; Li et al., 2018; Zhang et al., 2018), our mqPCR assay showed apparent advantages. With the help of bioinformatics tools, 1907 PCV2 full genome sequences that were currently available in the GenBank were downloaded and analyzed to achieve high coverage in the assay design stage. We believe that the coverage of the primers and probes over available sequences in the designing stage is the best estimation of assay's future diagnostic sensitivity against field strains (Bai et al., 2018). Compared to the three published duplex assays, our assay has much higher coverages: 97.9% (184/188) for PCV3 and 99.1% (1889/1907) for PCV2. All 4 PCV3 strains that our primers or probes mismatch to are all single nucleotide variations, and very often these oligoes that have single nucleotide mismatches will not affect their ability of binding to the templates. Therefore, the actual diagnostic sensitivity for PCV3 can be higher than this estimation. Using two non-overlapping targets for a given virus may not increase the assay's analytical sensitivity, but it will increase field strain coverage, and will help to detect strains with additional mutations, as the chance for a strain to have mutations on both target sites is small. Also,

compared to the LOD of 50 copies per reaction in Kim et al. (2017) and 90 copies per reaction in Zhang et al. (2018), our assay appeared to be more sensitive: 17 copies per reaction of PCV3 and 14 copies per reaction of PCV2. The LOD of PCV2 was also evaluated with cell culture, with an LOD of around 1.1×10^{-6} TCID50 per reaction. In addition, the internal control, swine *SB2M* gene, is included in our assay to monitor nucleic acid extraction efficiencies and potential PCR inhibitions in order to reduce the false-negative rate, which were not used in the previous studies.

In our study, different types of porcine samples were collected and subjected to the mqPCR testing. The viral targets were detected from porcine serum, oral fluid, feces, intestines and tonsil, indicating that our assay can be used for a wide range of sample types that are encountered in routine diagnostic operations. It is interesting to see, with our limited data, that the PCV3 positive rate was 30.1%, which was much higher than the PCV2 positive rate of 16.7%. We currently do not have the data to indicate whether the application of PCV2 vaccines in recent years play a role in reducing PCV2 prevalence. We will keep monitoring the field samples to see if this prevalence data holds true in the future.

In conclusion, the newly developed and validated mqPCR assay enables us to perform rapid, sensitive and specific detection and differentiation of PCV3 and PCV2 strains in clinical samples. *In silico* analysis and clinical sample testing indicated that the assay has high strain coverage for both viruses. Our limited prevalence data indicated that PCV3 strains have been widely distributed and may be more prevalent than PCV2 strains currently in the US.

2.1.5 References

Allan, G.M., McNeilly, F., Kennedy, S., Daft, B., Clarke, E.G., Ellis, J.A., Haines, D.M., Meehan, B.M. and Adair, B.M., 1998. Isolation of porcine circovirus-like viruses from pigs with a wasting disease in the USA and Europe. J Vet Diagn Invest 10, 3-10.

Bai, J., Trinetta, V., Shi, X., Noll, L.W., Magossi, G., Zheng, W., Porter, E.P., Cernicchiaro, N., Renter, D.G. and Nagaraja, T.G., 2018. A multiplex real-time PCR assay, based on invA and pagC genes, for the detection and quantification of Salmonella enterica from cattle lymph nodes. J Microbiol Methods 148, 110-116.

Chen, G.H., Mai, K.J., Zhou, L., Wu, R.T., Tang, X.Y., Wu, J.L., He, L.L., Lan, T., Xie, Q.M., Sun, Y. and Ma, J.Y., 2017. Detection and genome sequencing of porcine circovirus 3 in neonatal pigs with congenital tremors in South China. Transbound Emerg Dis 64, 1650-1654.

Cheung, A.K., 2003. The essential and nonessential transcription units for viral protein synthesis and DNA replication of porcine circovirus type 2. Virology 313, 452-9.

Eddicks, M., Fux, R., Szikora, F., Eddicks, L., Majzoub-Altweck, M., Hermanns, W., Sutter, G., Palzer, A., Banholzer, E. and Ritzmann, M., 2015. Detection of a new cluster of porcine circovirus type 2b strains in domestic pigs in Germany. Vet Microbiol 176, 337-43.

Franzo, G., Legnardi, M., Hjulsager, C.K., Klaumann, F., Larsen, L.E., Segales, J. and Drigo, M., 2018. Full-genome sequencing of porcine circovirus 3 field strains from Denmark, Italy and Spain demonstrates a high within-Europe genetic heterogeneity. Transbound Emerg Dis 65, 602-606.

Franzo, G., Tucciarone, C.M., Cecchinato, M. and Drigo, M., 2016. Porcine circovirus type 2 (PCV2) evolution before and after the vaccination introduction: A large scale epidemiological study. Scientific reports 6, 39458.

Kedkovid, R., Woonwong, Y., Arunorat, J., Sirisereewan, C., Sangpratum, N., Lumyai, M., Kesdangsakonwut, S., Teankum, K., Jittimanee, S. and Thanawongnuwech, R., 2018. Porcine circovirus type 3 (PCV3) infection in grower pigs from a Thai farm suffering from porcine respiratory disease complex (PRDC). Veterinary microbiology 215, 71-76.

Kim, H.R., Park, Y.R., Lim, D.R., Park, M.J., Park, J.Y., Kim, S.H., Lee, K.K., Lyoo, Y.S. and Park, C.K., 2017. Multiplex real-time polymerase chain reaction for the differential detection of porcine circovirus 2 and 3. J Virol Methods 250, 11-16.

Li, X.D., Qiao, M.M., Sun, M. and Tian, K.G., 2018. A Duplex Real-Time PCR Assay for the Simultaneous Detection of Porcine Circovirus 2 and Circovirus 3. Virol Sin 33, 181-186.

Mankertz, A., Mankertz, J., Wolf, K. and Buhk, H.J., 1998a. Identification of a protein essential for replication of porcine circovirus. J Gen Virol 79 (Pt 2), 381-4.

Mankertz, J., Buhk, H.J., Blaess, G. and Mankertz, A., 1998b. Transcription analysis of porcine circovirus (PCV). Virus Genes 16, 267-76.

Nawagitgul, P., Harms, P.A., Morozov, I., Thacker, B.J., Sorden, S.D., Lekcharoensuk, C. and Paul, P.S., 2002. Modified indirect porcine circovirus (PCV) type 2-based and recombinant capsid protein (ORF2)-based enzyme-linked immunosorbent assays for detection of antibodies to PCV. Clin Diagn Lab Immunol 9, 33-40.

Opriessnig, T., Meng, X.J. and Halbur, P.G., 2007. Porcine circovirus type 2 associated disease: update on current terminology, clinical manifestations, pathogenesis, diagnosis, and intervention strategies. J Vet Diagn Invest 19, 591-615.

Palinski, R., Pineyro, P., Shang, P., Yuan, F., Guo, R., Fang, Y., Byers, E. and Hause, B.M., 2017. A Novel Porcine Circovirus Distantly Related to Known Circoviruses Is Associated with Porcine Dermatitis and Nephropathy Syndrome and Reproductive Failure. J Virol 91.

Phan, T.G., Giannitti, F., Rossow, S., Marthaler, D., Knutson, T.P., Li, L., Deng, X., Resende, T., Vannucci, F. and Delwart, E., 2017. Erratum to: Detection of a novel circovirus PCV3 in pigs with cardiac and multi-systemic inflammation. Virol J 14, 87.

Segales, J., Olvera, A., Grau-Roma, L., Charreyre, C., Nauwynck, H., Larsen, L., Dupont, K., McCullough, K., Ellis, J., Krakowka, S., Mankertz, A., Fredholm, M., Fossum, C., Timmusk, S., Stockhofe-Zurwieden, N., Beattie, V., Armstrong, D., Grassland, B., Baekbo, P. and Allan, G., 2008. PCV-2 genotype definition and nomenclature. Vet Rec 162, 867-8.

Shi, X., Liu, X., Wang, Q., Das, A., Ma, G., Xu, L., Sun, Q., Peddireddi, L., Jia, W., Liu, Y., Anderson, G., Bai, J. and Shi, J., 2016. A multiplex real-time PCR panel assay for simultaneous detection and differentiation of 12 common swine viruses. J Virol Methods 236, 258-265.

Stadejek, T., Wozniak, A., Milek, D. and Biernacka, K., 2017. First detection of porcine circovirus type 3 on commercial pig farms in Poland. Transbound Emerg Dis 64, 1350-1353.

Tischer, I., Mields, W., Wolff, D., Vagt, M. and Griem, W., 1986. Studies on epidemiology and pathogenicity of porcine circovirus. Arch Virol 91, 271-6.

Tischer, I., Rasch, R. and Tochtermann, G., 1974. Characterization of papovavirus-and picornavirus-like particles in permanent pig kidney cell lines. Zentralblatt fur Bakteriologie, Parasitenkunde, Infektionskrankheiten und Hygiene. Erste Abteilung Originale. Reihe A: Medizinische Mikrobiologie und Parasitologie 226, 153-67.

Tochetto, C., Lima, D.A., Varela, A.P.M., Loiko, M.R., Paim, W.P., Scheffer, C.M., Herpich, J.I., Cerva, C., Schmitd, C., Cibulski, S.P., Santos, A.C., Mayer, F.Q. and Roehe, P.M., 2018. Full-Genome Sequence of Porcine Circovirus type 3 recovered from serum of sows with stillbirths in Brazil. Transbound Emerg Dis 65, 5-9.

Xiao, C.T., Harmon, K.M., Halbur, P.G. and Opriessnig, T., 2016. PCV2d-2 is the predominant type of PCV2 DNA in pig samples collected in the U.S. during 2014-2016. Veterinary microbiology 197, 72-77.

Xie, J., Wang, Y., Freeman, M.E., 3rd, Barlogie, B. and Yi, Q., 2003. Beta 2-microglobulin as a negative regulator of the immune system: high concentrations of the protein inhibit in vitro generation of functional dendritic cells. Blood 101, 4005-12.

Xu, P.L., Zhang, Y., Zhao, Y., Zheng, H.H., Han, H.Y., Zhang, H.X., Chen, H.Y., Yang, M.F. and Zheng, L.L., 2018. Detection and phylogenetic analysis of porcine circovirus type 3 in central China. Transbound Emerg Dis.

Yang, S., Yin, S., Shang, Y., Liu, B., Yuan, L., Zafar Khan, M.U., Liu, X. and Cai, J., 2018. Phylogenetic and genetic variation analyses of porcine circovirus type 2 isolated from China. Transboundary and emerging diseases 65, e383-e392.

Ye, X., Berg, M., Fossum, C., Wallgren, P. and Blomstrom, A.L., 2018. Detection and genetic characterisation of porcine circovirus 3 from pigs in Sweden. Virus Genes 54, 466-469.

Zhang, L., Luo, Y., Liang, L., Li, J. and Cui, S., 2018. Phylogenetic analysis of porcine circovirus type 3 and porcine circovirus type 2 in China detected by duplex nanoparticle-assisted PCR. Infect Genet Evol 60, 1-6.

Table 2.1.1 Primer and probe information of PCV3 and PCV2 mqPCR assay.

Primer/ Probe	Target Gene	Sequence (5'-3')	Tm(°C)	Amplicon Size (bp)	Coverage	Location on JX535288 (PCV2), KX778720 (PCV3) or AK398890 (SB2M)
		Real-time PCR primers and probes				
PCV3-F1	ORF2	GGTGAAGTAACGGCTGTGTTTT	60.4	86	95.2% (79/83)	1550-1571 nt
PCV3-R1		ACACTTGGCTCCARGACGAC	60.3			1635-1616 nt
PCV3-Pr1		FAM-ATGCGGAAAGTTCCACTCGK-BHQ1	62			1592-1611 nt
PCV3-F2	ORF1	TATAATGGGGAGGGTGCTGT	59.3	76	92.8% (77/83) (100% combined)	820-839 nt
PCV3-R2		CCCCAATTCTCAGCAATTCA	61			895-876 nt
PCV3-Pr2		FAM-TGATTTTTATGGGTGGGTTCCATTT-BHQ1	65.2			849-873 nt
PCV2-F1	ORF1	GARACTAAAGGTGGAACTGTACC	57-58	118	94.8% (1808/1907)	762-784 nt
PCV2-R1		TCCGATARAGAGCTTCTACAGC	59			879-858 nt
PCV2-Pr1		VIC-AGGAGTACCATTCCAACGGGG-BHQ1	62.5			823-843 nt
PCV2-F2	ORF3	CGGGCTGGCTGAACTTTTG	59.5	87	90.5% (1726/1907) (98.9% combined)	494-512 nt
PCV2-R2		CCAGGTGGCCCCACAAT	59			580-564 nt
PCV2-Pr2		VIC-TCACGCTTCTGCATTTTCCCGC-BHQ1	64.5			520-541 nt
SB2M-F	SB2M	TGATGTTACCACAAATGTTGTCTTC	60.2	88		684-708 nt
SB2M-R		CCTCTACATCTACCTGCTCAGACA	60			771-748 nt
SB2M-Pr		Cy5-ATTCTACCTTGGGTGTAGTCTCCATGT-BHQ2	63.4			715-741 nt

		Cloning and sequencing primers			
PCV3-cF	ORF1	GCCTGCAGTATTTATACGCTATGGGC	66.5	2000	618-643 nt
PCV3-cR	ORF1	TACTGCAGGCATCTTCTCCGCAACTTC	71		601-627 nt
PCV2-cF	ORF1	TGGTGACCGTTGCAGAGCAG	65.9	1093	445-464 nt
PCV2-cR	ORF2	TGGGCGGTGGACATGATGAG	67.7		1517-1536 nt

Table 2.1.2 Comparison of multiplex and singular assays for validation of PCV3 and PCV2 mqPCR

		PCV3		PCV2	
		Singular	Multiplex	Singular	Multiplex
Efficiency (E)		94.7%	96.8%	96.9%	92.1%
Correlation coefficient (R^2)		0.994	0.990	0.998	0.993
Mean Cts of 3 replicates of clinical samples at different dilutions	10^{0}	17.14	17.13	17.14	17.07
	10^{-1}	20.69	20.45	21.24	20.62
	10^{-2}	24.37	23.82	24.16	23.86
	10^{-3}	28.54	28.24	27.48	27.17
	10^{-4}	31.73	31.15	30.81	30.64
	10^{-5}	34.92	34.78	34.30	34.79
	10^{-6}	37.1	36.46	37.94	38.28

Table 2.1.3 Viruses or clinical samples used for specificity analysis of PCV3 and PCV2 mqPCR assays.

Pathogen	Source	No. tested	Target gene		
			PCV3 (FAM)	PCV2(VIC)	SB2M(Cy5)
PCV3	Clinical sample*	1	+	-	+
PCV2a	Cell culture	1	-	+	+
PCV2b	Cell culture	1	-	+	+
PCV2d	Cell culture	1	-	+	+
PCV3 + PCV2a	Clinical sample + cell culture	1	+	+	+
PCV3 + PCV2b	Clinical sample + cell culture	1	+	+	+
PCV3 + PCV2d	Clinical sample + cell culture	1	+	+	+
PRRSV-2	Clinical sample/Cell culture	16/2	-	-	+
SVV-1	Cell culture	1	-	-	+
Rotavirus A	Clinical sample	1	-	-	+
Rotavirus B	Clinical sample	1	-	-	+

Rotavirus C	Clinical sample	1	-	-	+
SIV	Clinical sample	7	-	-	+
PEDV	Clinical sample	16	-	-	+
PDCoV	Clinical sample	1	-	-	+
PPV	Clinical sample	1	-	-	+
PPIV	Clinical sample	1	-	-	+

*: Next generation sequencing resulted strong positive to PCV3, and negative to other major swine viruses.

+: Positive; -: Negative

Table 2.1.4 Prevalence of PCV3 and PCV2 in 336 porcine samples used in this study.

PCV3 positive (%)	PCV2 positive (%)	PCV2-PCV3 co-positive (%)
101 (30.1)	56 (16.7)	18 (5.4)

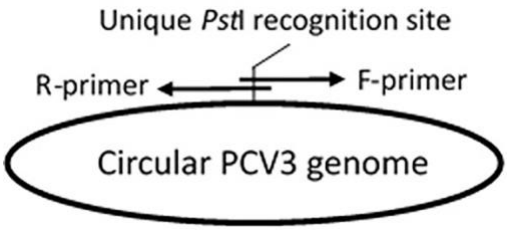

Figure 2.1.1 Sketch of PCV3 genome amplification using tail-to-tail overlapping primers

The primers were designed to have a unique type II restriction endonuclease, *PstI* recognition site in the overlapping region that was later used for full-genome cloning. This is to ensure that the genome amplified is from the same genome, and not from separate genomes.

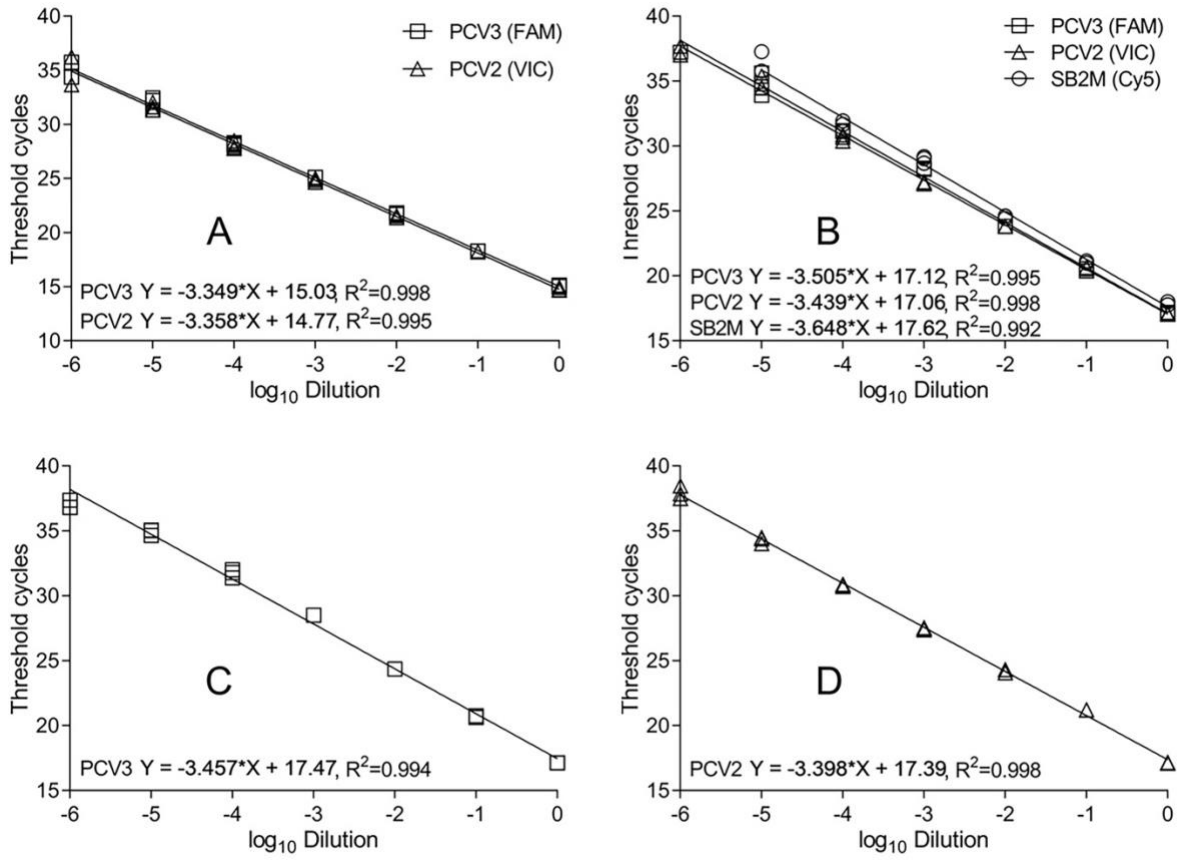

Figure 2.1.2 Standard curves of PCV3 and PCV2 mqPCR assay

(A) PCV3 and PCV2 mqPCR by serial dilutions of cloned control constructs (whole genome of PCV3 and half genome of PCV2); (B) PCV3 and PCV2 mqPCR by serial dilutions of mixture of PCV3 clinical positive samples and PCV2d cell culture; (C) PCV3 singular qPCR by serial dilutions of clinical PCV3 positive sample; (D) PCV2 singular qPCR by serial dilutions of PCV2d cell culture.

2.2 Development of a Multiplex Real-time PCR assay for Porcine Circovirus Type 2 (PCV2) Genotyping of PCV2a, PCV2b and PCV2d

Yin Wang, Lance Noll, Elizabeth Porter, Colin Stoy, Junsheng Dong, Joe Anderson, Jinping Fu, Roman Pogranichniy, Jason Woodworth, Lalitha Peddireddi, and Jianfa Bai

(Journal of Virological Methods, 2020;286:113971)

Abstract: A multiplex quantitative real-time polymerase chain reaction (mqPCR) assay was developed and validated for detection and differentiation of porcine circovirus type 2 (PCV2) genotypes, PCV2a, PCV2b and PCV2d. Single nucleotide polymorphism in primers or probes was deployed for different genotype detections, while conserved sequence in the 3 end of a primer and in the middle of a probe was used for the targeted genotype. *In silico* analysis of 2601 PCV2 ORF2 sequences showed that the predicted strain coverage of the assay was 93.4% (409/438) for PCV2a, 95.1% (1161/1221) for PCV2b and 93.6% (882/942) for PCV2d strains. The PCR amplification efficiencies were 94.5%, 100.2%, and 99.2% for PCV2a, PCV2b and PCV2d, respectively, with correlation coefficients >0.995 for all genotypes. The limits of detection (LOD) were 1.58×10^{-4} TCID50/ml for PCV2a, 5.62×10^{-4} TCID50/ml for PCV2b, and 3.16×10^{-3} TCID50/ml for PCV2d. Sanger sequencing of 74 randomly selected PCV2 positive clinical samples confirmed the genotypes of strains identified by the mqPCR. Validation with clinical samples co-positive for target and non-target pathogens demonstrated that the mqPCR assay specifically detected targeted viruses without cross reacting to each other or to other common porcine viruses.

2.2.1 Introduction

Porcine circovirus type 2 (PCV2) plays a significant role in porcine circovirus associated diseases (PCVAD) and is one of the most economically important porcine viral pathogens (Gillespie et al., 2009). Since it was first isolated as the causative agent of postweaning multisystemic wasting syndrome in 1998 (Ellis et al., 1998), PCV2 has been a highly prevalent disease worldwide, including in Asia, America and Europe (Saporiti et al., 2020; Wang et al., 2019a; Zheng et al., 2020).

With a high substitution rate, 5 major genotypes of PCV2 have been identified based on ORF2 sequences: PCV2a, PCV2b, PCV2c, PCV2d and PCV2e (Davies et al., 2016). Among the five genotypes, PCV2a, PCV2b and PCV2d are the most commonly circulating genotypes in the USA (Wang et al., 2019b; Xiao et al., 2016), in China (Hou et al., 2019; Lv et al., 2020) and in European countries (Saporiti et al., 2020). There are two major genotype shifting events that have occurred globally: PCV2b replaced PCV2a as the dominant genotype around 2003, and PCV2d became the most prevalent genotype beginning in 2012 (Xiao et al., 2016). The first shift is related to increased severity of clinical PCVAD (Beach and Meng, 2012), while the second shift may be related to inappropriate vaccine applications (Karuppannan and Opriessnig, 2017).

ORF2-targeted gene sequencing is widely used as a gold standard for genotyping of PCV2 strains (Wang et al., 2019b). Other methods are developed as well for the differentiation of PCV2a and PCV2b strains, such as real time PCR, loop-mediated isothermal amplification method (LAMP) and restriction fragment length polymorphism (RFLP) (Guo et al., 2010; Qiu et al., 2012; Wozniak et al., 2019; Xiao et al., 2016). However, there's no assay that can simultaneously identify

genotypes PCV2a, PCV2b and PCV2d. Therefore, based on the current PCV2 ORF2 sequences available from GenBank database, we have developed a multiplex quantitative real time PCR for rapid detection and differentiation of the three genotypes with high sensitivity, specificity and strain coverage.

2.2.2 Methods and materials

2.2.2.1 Sequence dataset and phylogenetic analysis

The sequence dataset was established from our previous study (Wang et al., 2019b). Briefly, all available PCV2 ORF2 sequences were downloaded from the GenBank database (https://www.ncbi.nlm.nih.gov/ genbank/). The sequence alignment was performed with MAFFT (Katoh, Misawa, Kuma, & Miyata, 2002). Low quality sequences, as indicated by the presence of premature stop codons, and short sequences were removed from the analysis. The sequence identity matrix calculation was performed using BioEdit 7.2.5 (https://bioedit.software. informer.com/).

The phylogenetic analysis was conducted with MEGA 7.0.26 (Kumar, Stecher, and Tamura, 2016). The best fit model was selected based on Bayesian information criterion (BIC). The maximum likelihood phylogenetic trees were constructed using the best substitution pattern with the lowest BIC scores. The reliability of clusters formed in the tree was evaluated by performing 500 bootstrapping reiterations.

2.2.2.2 Multiplex real-time PCR assay design

Based on the sequences from the dataset, one set of primers and probe was designed for each genotype, PCV2a, PCV2b and PCV2d. The PCV2a probe was labeled with 5′-Texas Red and 3′-BHQ1, PCV2b labeled with 5′-VIC and 3′-BHQ1 and PCV2d with 5′-FAM and 3′-BHQ1. Information of all primers and probes are given in Table 2.2.1.

2.2.2.3 Viral isolates and viral DNA or RNA extraction

Cell culture isolates of PCV2a, PCV2b and PCV2d from the Virology Section of Kansas State Veterinary Diagnostic Laboratory were propagated as previously described (Pogranichniy et al., 2002), which were genotyped by sequencing. The viral DNA was extracted from 140 µl of clinical samples or cell culture by QIAamp Viral RNA Mini Kit (Qiagen, Hilden, Germany) according to the manufacturer's recommendations, and stored at −80 °C until use.

2.2.2.4 Construction of standard plasmid as positive amplification control

For positive assay controls applied in routine testing, PCV2 fragments carrying the target of each genotype were amplified and cloned into the pCR™2.1 vector using the original TA Cloning kit according to the manufacturer's instruction (Invitrogen/ThermoFisher, Waltham, MA). The ligated products were then transformed in Mix & Go competent cells (Zymo Research, Irvine, CA), propagated in LB broth (Teknova Inc, Hollister, CA), and the plasmid construct was then extracted using QIAprep Spin Miniprep Kit (Qiagen). The presence of cloned inserts was confirmed by gel electrophoresis and Sanger sequencing (Genewiz, South Plainfield, NJ). The primers used for cloning are also listed in Table 2.2.1.

2.2.2.5 Multiplex real-time PCR reaction composition and condition

All PCR reactions were performed in a 20 μL total reaction volume composed of 5 μL of DNA samples prepared as described (Wang, Das, et al., 2019), 0.25 μM each of forward and reverse PCR primers, 0.25 μM each of probes, and 10 μl of 2X iQ™ Multiplex Powermix (Bio-Rad, Hercules, CA). Thermocycler running conditions consisted of initial denaturation at 95 °C for 10 min, followed by 45 cycles of 95 °C for 15 s and 60 °C for 45 s. The cycle threshold (Ct) values were generated with CFX96 Touch™ Real-Time PCR Detection System and standard curve results were analyzed with Bio-Rad CFX Manager 3.0 (Bio-Rad) and GraphPad Prism 7 (GraphPad Software, La Jolla, CA).

2.2.2.6 Assay sensitivity and specificity analysis

Standard curves were generated with triplicates of 10-fold serial dilutions of the cell culture isolates of PCV2a, PCV2b and PCV2d to evaluate the analytical sensitivity of the assay. The median tissue culture infectious dose (TCID50) of the highest dilution that still generated positive Ct values was considered the limit of detection (LOD) for cultured viruses.

The specificity of the assay was first evaluated *in silico* with the online NCBI primer designing tool, Primer-Blast (https://www.ncbi.nlm.nih.gov/tools/primer-blast/), followed by confirmation with Sanger sequencing of PCV2 ORF2. The conserved primers flanking the ORF2 were designed and listed in Table 2.2.1. Furthermore, the cell culture isolates and clinical samples that were positive to specific swine pathogens were tested to evaluate the specificity of the assay (Table 2.2.3). Those include PCV2a, PCV2b, PCV2d, porcine circovirus type 3 (PCV3), porcine reproductive and respiratory syndrome virus type 2 (PRRSV-2), swine influenza virus (SIV),

porcine parainfluenza virus (PPIV), rotavirus group A (RVA), rotavirus group B (RVB), rotavirus group C (RVC), porcine epidemic diarrhea virus (PEDV) and transmissible gastroenteritis coronavirus (TGEV).

2.2.3 Results

2.2.3.1 Analysis of assay coverage to sequence dataset

Based on our previous study (Wang et al., 2019b), PCV2 strains were separated into 12 clusters, namely Cluster 1–12, by phylogenetic analysis; Cluster 8, Cluster 3 and Cluster 1 corresponded to genotypes, PCV2a, PCV2b and PCV2d, respectively. The three genotypes were identified as common strains currently circulating in the USA (Wang et al., 2019b; Xiao et al., 2016). An unrooted phylogenetic tree generated with PCV2 ORF2 sequences indicated that the three genotypes grouped into three separate clusters (Figure 2.2.1). The triangle markers in the tree indicated the ORF2 sequences generated in our lab that were used to validate this genotyping real time PCR assay; they share 99.4-100 % identity with the published sequences collected from GenBank database.

More complete analysis with 438 PCV2a strains, 942 PCV2b ORF2 strains and 1221 PCV2d strains has identified one set of primers and probe for each genotype (Illustrated in Figure 2.2.2). *In silico* analysis showed the PCR set can perfectly match 75.3% of PCV2a strains, 86.3% of PCV2b strains, and 78.1% of PCV2d strains. Assuming a single nucleotide mismatch to a primer (excluding the more critical 5 bp in the 3’ end) or a probe (excluding the more critical 5 bp in the middle) in the assay can still amplify and generate signal (Wang et al., 2020b), the strain coverages

would be increased to 93.4%, 95.1% and 93.6% for the three genotypes, respectively. Information of all primers and probes are shown in Table 2.2.1.

2.2.3.2 Analytical sensitivity of the mqPCR assay on cell culture isolates

Analytical sensitivity of the mqPCR assay was analyzed using standard curves generated by three replications of 10-fold serial dilutions of the cell culture isolates. The data was presented by plotting the Ct values against log dilution factors. The PCR amplification efficiencies were 94.5% for PCV2a, 100.2% for PCV2b and 99.2% for PCV2d, with correlation coefficients (R^2) all greater than 0.995 (Figure 2.2.3). The LODs were 1.58×10^{-4} TCID50/ml for PCV2a, 5.62×10^{-4} TCID50/ml for PCV2b, and 3.16×10^{-3} TCID50/ml for PCV2d.

2.2.3.3 Specificity of the mqPCR assay on clinical samples

The specificity of primers and probes was first tested by *in silico* analysis using Primer-Blast, which determined sequences were unique to their respective assay targets. Then, assay specificity was evaluated by comparison with Sanger sequencing results. Seventy-four PCV2 positive samples were tested by the genotyping real-time PCR; results showed 8 PCV2a, 6 PCV2b and 60 PCV2d strains. Genotypes of all 74 samples were confirmed by Sanger sequencing (Table 2.2.2). Specificity was also tested with clinical samples that previously tested positive to non-target pathogens. The results demonstrated that the assay specifically detected positive samples and identified PCV2a, PCV2b or PCV2d genotypes without cross-detecting each other. Furthermore, no positive signals were generated from clinical samples that were positive to PCV3 (n=3),

PRRSV-2 (n=6), SIV (n=2), PPIV (n=5), RVA (n=2), RVB (n=1), RVC (n=1), PEDV (n=16), and TGEV (n=2), indicating a good specificity of the assay (Table 2.2.3).

2.2.4 Discussion

PCV2 is a small DNA virus with a circular genome of 1767-1768 nucleotides. The ORF2 gene (702 nucleotides) encodes the Capsid protein, which dominates immunogenicity (Nawagitgul et al., 2002).Extensive investigations have been done on genetic variations caused by point-mutations and recombinations (Firth et al., 2009; Franzo et al., 2016a), association of genotypes and disease severity (An et al., 2007; Opriessnig et al., 2006; Opriessnig et al., 2008), and viral evolution under the selection pressure of vaccination (Franzo et al., 2016b; Karuppannan and Opriessnig, 2017; Xiao et al., 2016). Apparently genotyping of PCV2 is an important diagnostic tool for the study of viral pathogenesis and epidemiology of the disease, which will provide key information towards formulating strategies for disease management and vaccine development and applications.

By analyzing whole genome sequences, sequence variations among different genotypes were found mostly in the capsid gene, ORF2, which is consistent with previous studies (Cheung et al., 2007; Olvera, Cortey, and Segales, 2007; Wang et al., 2019b). In this study, all PCV2 ORF2 sequences were downloaded from the current GenBank database and included in the genetic analysis to ensure high strain coverage. Due to the high rate of nucleotide substitution in the genome, PCV2 displays substantial genetic variations (Firth et al., 2009). In our previous study, the inter-cluster and intra-cluster identities were as low as 83.6% and 87.9%, respectively. (Wang

et al., 2019b). Because of this high sequence variation within each genotype and relatively high genome homology between genotypes, the development of a molecular genotyping assay with high strain coverage can be challenging. In our design, the three sets of primers and probes can match 75.3-86.3% strains of each genotype. In general, an assay with single nucleotide mismatches occurring in the middle, especially in the 5′ end of a primer, or in the two ends of a probe may still amplify and generate a signal (Wang et al., 2020a). Therefore, when single nucleotide mismatch in such situations is considered in the design of the primers and probes, strain coverage can potentially increase to 93.4%-95.1%. With that said, this genotyping assay should not replace general detection assays that may have higher strain coverage (Wang et al., 2019a).

Although some PCV2 genotyping assays have been published, these assays only differentiate between PCV2a and PCV2b strains (Wozniak et al., 2019; Xiao et al., 2016). For that reason, Sanger sequencing of the ORF2 gene, which is a labor intensive and time-consuming process (Lv et al., 2020; Zheng et al., 2020), is still widely used for PCV2 genotyping. We have developed this genotyping mqPCR assay that can use a single PCR reaction to differentiate the three major PCV genotypes, (PCV2a, PCV2b and PCV2d) circulating in the US. This simplified method is a low-cost and faster turnaround protocol and should facilitate the genotyping process for field PCV2 strains. We have already developed a PCV2 general assay using the conserved ORF1 gene as the target (Wang et al., 2019a), which enabled us to have a much higher strain coverage (99.1%) for PCV2 detections. By utilizing that generic test for general detection and

surveillance, followed by the genotyping PCR reported here, we should be able to detect and differentiate the majority of field PCV2 strains.

In conclusion, the newly developed and validated mqPCR assay allows for rapid, sensitive and specific detection and differentiation of the most common PCV2 genotypes, (PCV2a, PCV2b and PCV2d) in clinical samples. *In silico* analysis and clinical sample testing indicated that the assay has relatively high strain coverage. It can be used as an alternative method for PCV2 genotyping.

2.2.5 Reference

An, D.J., Roh, I.S., Song, D.S., Park, C.K. and Park, B.K., 2007. Phylogenetic characterization of porcine circovirus type 2 in PMWS and PDNS Korean pigs between 1999 and 2006. Virus Research 129, 115-122.

Beach, N.M. and Meng, X.J., 2012. Efficacy and future prospects of commercially available and experimental vaccines against porcine circovirus type 2 (PCV2). Virus Res 164, 33-42.

Cheung, A.K., Lager, K.M., Kohutyuk, O.I., Vincent, A.L., Henry, S.C., Baker, R.B., Rowland, R.R. and Dunham, A.G., 2007. Detection of two porcine circovirus type 2 genotypic groups in United States swine herds. Arch Virol 152, 1035-44.

Davies, B., Wang, X., Dvorak, C.M., Marthaler, D. and Murtaugh, M.P., 2016. Diagnostic phylogenetics reveals a new Porcine circovirus 2 cluster. Virus Res 217, 32-7.

Ellis, J., Hassard, L., Clark, E., Harding, J., Allan, G., Willson, P., Strokappe, J., Martin, K., McNeilly, F., Meehan, B., Todd, D. and Haines, D., 1998. Isolation of circovirus from lesions of pigs with postweaning multisystemic wasting syndrome. Can Vet J 39, 44-51.

Firth, C., Charleston, M.A., Duffy, S., Shapiro, B. and Holmes, E.C., 2009. Insights into the Evolutionary History of an Emerging Livestock Pathogen: Porcine Circovirus 2. J Virol 83, 12813-12821.

Franzo, G., Cortey, M., Segales, J., Hughes, J. and Drigo, M., 2016a. Phylodynamic analysis of porcine circovirus type 2 reveals global waves of emerging genotypes and the circulation of recombinant forms. Mol Phylogenet Evol 100, 269-280.

Franzo, G., Tucciarone, C.M., Cecchinato, M. and Drigo, M., 2016b. Porcine circovirus type 2 (PCV2) evolution before and after the vaccination introduction: A large scale epidemiological study. Sci Rep-Uk 6.

Gillespie, J., Opriessnig, T., Meng, X.J., Pelzer, K. and Buechner-Maxwell, V., 2009. Porcine circovirus type 2 and porcine circovirus-associated disease. J Vet Intern Med 23, 1151-63.

Guo, L.J., Lu, Y.H., Wei, Y.W., Huang, L.P. and Liu, C.M., 2010. Porcine circovirus type 2 (PCV2): genetic variation and newly emerging genotypes in China. Virol J 7, 273.

Hou, Z., Wang, H., Feng, Y., Song, M., Li, Q. and Li, J., 2019. Genetic variation and phylogenetic analysis of Porcine circovirus type 2 in China from 2016 to 2018. Acta Virol 63, 459-468.

Karuppannan, A.K. and Opriessnig, T., 2017. Porcine Circovirus Type 2 (PCV2) Vaccines in the Context of Current Molecular Epidemiology. Viruses 9.

Kumar, S., Stecher, G. and Tamura, K., 2016. MEGA7: Molecular Evolutionary Genetics Analysis Version 7.0 for Bigger Datasets. Mol Biol Evol 33, 1870-1874.

Lv, N., Zhu, L., Li, W., Li, Z., Qian, Q., Zhang, T., Liu, L., Hong, J., Zheng, X., Wang, Y., Zhang, Y. and Chai, J., 2020. Molecular epidemiology and genetic variation analyses of porcine circovirus type 2 isolated from Yunnan Province in China from 2016-2019. Bmc Vet Res 16, 96.

Nawagitgul, P., Harms, P.A., Morozov, I., Thacker, B.J., Sorden, S.D., Lekcharoensuk, C. and Paul, P.S., 2002. Modified indirect porcine circovirus (PCV) type 2-based and recombinant capsid protein (ORF2)-based enzyme-linked immunosorbent assays for detection of antibodies to PCV. Clin Diagn Lab Immunol 9, 33-40.

Olvera, A., Cortey, M. and Segales, J., 2007. Molecular evolution of porcine circovirus type 2 genomes: phylogeny and clonality. Virology 357, 175-85.

Opriessnig, T., McKeown, N.E., Zhou, E.M., Meng, X.J. and Halbur, P.G., 2006. Genetic and experimental comparison of porcine circovirus type 2 (PCV2) isolates from cases with and without PCV2-associated lesions provides evidence for differences in virulence. J Gen Virol 87, 2923-2932.

Opriessnig, T., Ramamoorthy, S., Madson, D.M., Patterson, A.R., Pal, N., Carman, S., Meng, X.J. and Halbur, P.G., 2008. Differences in virulence among porcine circovirus type 2 isolates are unrelated to cluster type 2a or 2b and prior infection provides heterologous protection. J Gen Virol 89, 2482-2491.

Pogranichniy, R.M., Yoon, K.J., Harms, P.A., Sorden, S.D. and Daniels, M., 2002. Case-control study on the association of porcine circovirus type 2 and other swine viral pathogens with postweaning multisystemic wasting syndrome. J Vet Diagn Invest 14, 449-456.

Qiu, X., Li, T., Zhang, G., Cao, J., Jin, Y., Xing, G., Liao, M. and Zhou, J., 2012. Development of a loop-mediated isothermal amplification method to rapidly detect porcine circovirus genotypes 2a and 2b. Virol J 9, 318.

Saporiti, V., Huerta, E., Correa-Fiz, F., Grosse Liesner, B., Duran, O., Segales, J. and Sibila, M., 2020. Detection and genotyping of Porcine circovirus 2 (PCV-2) and detection of Porcine circovirus 3 (PCV-3) in sera from fattening pigs of different European countries. Transbound Emerg Dis.

Wang, Y., Das, A., Zheng, W., Porter, E., Xu, L., Noll, L., Liu, X., Dodd, K., Jia, W. and Bai, J., 2020a. Development and evaluation of multiplex real-time RT-PCR assays for the detection and differentiation of foot-and-mouth disease virus and Seneca Valley virus 1. Transbound Emerg Dis 67, 604-616.

Wang, Y., Feng, Y., Zheng, W., Noll, L., Porter, E., Potter, M., Cino, G., Peddireddi, L., Liu, X., Anderson, G. and Bai, J., 2019a. A multiplex real-time PCR assay for the detection and differentiation of the newly emerged porcine circovirus type 3 and continuously evolving type 2 strains in the United States. J Virol Methods 269, 7-12.

Wang, Y., Noll, L., Lu, N., Porter, E., Stoy, C., Zheng, W., Liu, X., Peddireddi, L., Niederwerder, M. and Bai, J., 2019b. Genetic diversity and prevalence of porcine circovirus type 3 (PCV3) and type 2 (PCV2) in the Midwest of the USA during 2016-2018. Transbound Emerg Dis.

Wang, Y., Xu, L., Noll, L., Stoy, C., Porter, E., Fu, J., Feng, Y., Peddireddi, L., Liu, X., Dodd, K.A., Jia, W. and Bai, J., 2020b. Development of a real-time PCR assay for detection of African swine fever virus with an endogenous internal control. Transboundary and emerging diseases.

Wozniak, A., Milek, D., Matyba, P. and Stadejek, T., 2019. Real-Time PCR Detection Patterns of Porcine Circovirus Type 2 (PCV2) in Polish Farms with Different Statuses of Vaccination against PCV2. Viruses 11.

Xiao, C.T., Harmon, K.M., Halbur, P.G. and Opriessnig, T., 2016. PCV2d-2 is the predominant type of PCV2 DNA in pig samples collected in the US during 2014-2016. Vet Microbiol 197, 72-77.

Zheng, G.M., Lu, Q.X., Wang, F.Y., Xing, G.X., Feng, H., Jin, Q.Y., Guo, Z.H., Teng, M., Hao, H.F., Li, D.L., Wei, X., Zhang, Y.H., Deng, R.G. and Zhang, G.P., 2020. Phylogenetic analysis of porcine circovirus type 2 (PCV2) between 2015 and 2018 in Henan Province, China. Bmc Vet Res 16.

Table 2.2.1 Primers and probes used in PCV2 genotyping real-time PCR assays and construction of positive standards

Primer/Probe	ORF location	Sequence (5'-3')	Tm (°C)	Amplicon size (bp)	% Coverage (matched/ total[a])	References
Real-time PCR primers and probes						
PCV2a-F1	ORF2	CGGTGGACATGMTGAGATTTA	58.4-61.0	118	75.3~93.4[b] (330/438~ 409/438)	This study
PCV2a-R1	ORF2	GGCCAGAATTCAACCTTAACYT	58.7-60.7			
PCV2a-Pr1	ORF2	Texas Red-CAAAGGGTATAGAGATTTTGTTGGTCCC-BHQ2	65.7			
PCV2b-F1	ORF2	TTCTCCTACCACTCCCGCTA	59.8	78	86.3~95.1[b] (1054/1221~ 1161/1221)	This study
PCV2b-R1	ORF2	TTTGTTGTTTGGTTGGAAGTAATC	59.3			
PCV2b-Pr1	ORF2	VIC-CTGTCCTAGATTCCACTAT-MGBNFQ	66			
PCV2d-F1	ORF2	AGCCCTTCTCCTACCACTCM	58.9-59.7	88	78.0~93.6[b] (736/942~ 882/942)	This study
PCV2d-R1	ORF2	TTTCTTTTGTTATTGGGTTGGAA	59.8			
PCV2d-Pr1	ORF2	FAM-TGATRGGACAATCGATTAC-MGBNFQ	66			
Cloning primers						
PCV2-cF	ORF1	TGGTGACCGTTGCAGAGCAG	65.9	1093		Wang et al, 2019
PCV2-cR	ORF2	TGGGCGGTGGACATGATGAG	67.7			

Sanger sequencing primers					
PCV2-sF	ORF1	CCCATGCCCTGAATTTCCATATG	66.4	862	This study
PCV2-sR	Untranslated Region	CATGTTGCTGCTGAGGTGCT	62.6		

a: Indicates number of matched sequences over total sequences used in the analysis.

b: The lower boundary of the range of percentage match is generated from perfect matches in a primer pair and its corresponding probe against total sequences analyzed; the higher boundary of the range is generated by allowing presence of single nucleotide variation in each primer (but keep the 5bp conserved in the 3 end), or in the probe (but keep the 5pb conserved in the middle).

Table 2.2.2 Threshold cycle (Ct) distribution and specificity of the PCV2 genotyping real-time PCR compared with the Sanger sequencing results

Sample #	Ct value of Real-time PCR			Genotype by PCR	Genotype by Sanger sequencing
	PCV2a	PCV2b	PCV2d		
1	0	0	22.2	d	d
2	11.2	0	0	a	a
3	23	0	0	a	a
4	0	27.2	0	b	b
5	0	0	15.7	d	d
6	10.6	0	0	a	a
7	0	20	0	b	b
8	0	0	27.4	d	d
9	0	0	26.7	d	d
10	0	0	17.1	d	d
11	0	0	15.1	d	d
12	0	0	15.7	d	d
13	0	0	19.5	d	d
14	0	0	11	d	d
15	0	0	31.6	d	d
16	0	0	27.8	d	d
17	34	0	0	a	a
18	0	0	25	d	d
19	0	21.3	0	b	b
20	0	0	23.3	d	d
21	0	0	30.6	d	d
22	0	0	30.9	d	d

23	0	0	19.8	d	d
24	0	0	34.3	d	d
25	0	0	31.3	d	d
26	0	0	10.7	d	d
27	0	0	32.9	d	d
28	0	0	15	d	d
29	0	0	28.7	d	d
30	0	0	9.9	d	d
31	0	30.1	0	b	b
32	0	0	5.1	d	d
33	0	38.2	5.1	d	d
34	0	0	8.2	d	d
35	0	0	5.5	d	d
36	0	38.9	5.7	d	d
37	0	38.8	6.8	d	d
38	0	0	6.5	d	d
39	0	0	7.7	d	d
40	0	0	4.7	d	d
41	0	0	5.8	d	d
42	0	0	7.5	d	d
43	0	0	6.1	d	d
44	0	6	0	b	b
45	0	7	0	b	b
46	0	0	5.9	d	d
47	0	0	5.1	d	d
48	0	0	6.2	d	d
49	0	38.8	6	d	d

50	0	36.4	29.7	d	d
51	0	0	30.8	d	d
52	0	0	27.8	d	d
53	22.6	0	0	a	a
54	0	0	25.5	d	d
55	0	0	27.9	d	d
56	0	0	28.6	d	d
57	0	0	6.9	d	d
58	0	0	30.6	d	d
59	0	0	5.7	d	d
60	0	0	10.7	d	d
61	0	0	28.1	d	d
62	0	0	28.5	d	d
63	0	0	31.4	d	d
64	27.2	0	0	a	a
65	25.1	0	0	a	a
66	0	0	31.8	d	d
67	0	0	31.2	d	d
68	0	0	29.1	d	d
69	0	0	29.1	d	d
70	23.4	0	0	a	a
71	0	0	10.3	d	d
72	0	0	21.1	d	d
73	0	0	22.1	d	d
74	0	0	28.1	d	d

Table 2.2.3 Assay specificity tested on PCV2 cell cultures and positive samples, and diagnostic samples positive to other common swine pathogens

Pathogen	Source	No. tested	Target gene		
			PCV2a	PCV2b	PCV2d
PCV2a	Clinical sample	8	+	-	-
	Cell culture	1	+	-	-
PCV2b	Clinical sample	6	-	+	-
	Cell culture	1	-	+	-
PCV2d	Clinical sample	60	-	-	+
	Cell culture	1	-	-	+
PCV3	Clinical sample	3	-	-	-
PRRSV-2	Clinical sample	6	-	-	-
SIV	Clinical sample	2	-	-	-
PPIV	Clinical sample	5	-	-	-
Rotavirus A	Clinical sample	2	-	-	-
Rotavirus B	Clinical sample	1	-	-	-
Rotavirus C	Clinical sample	1	-	-	-
PEDV	Clinical sample	16	-	-	-
TGEV	Clinical sample	2	-	-	-

+: Positive; -: Negative

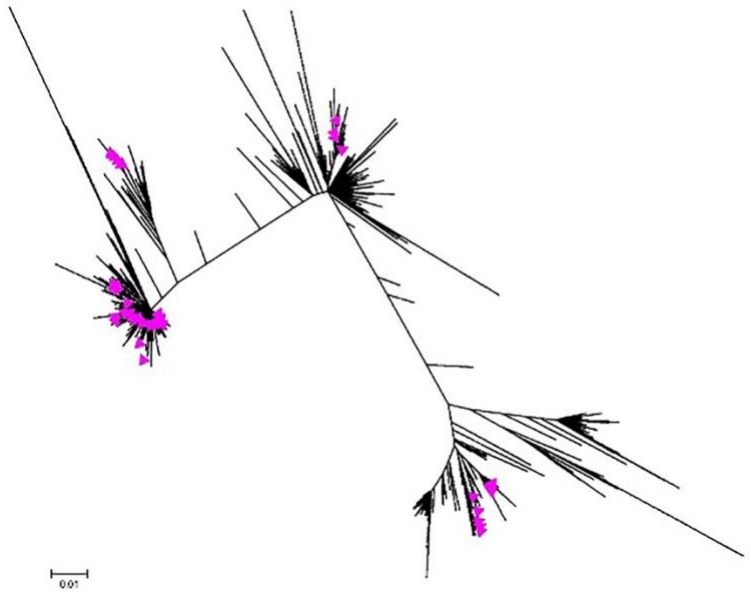

Figure 2.2.1Phylogenetic tree of PCV2a, PCV2b and PCV2d.

The triangle markers indicate ORF2 gene sequences used for PCV2 genotyping by sequencing and validation of genotyping results by real time PCR.

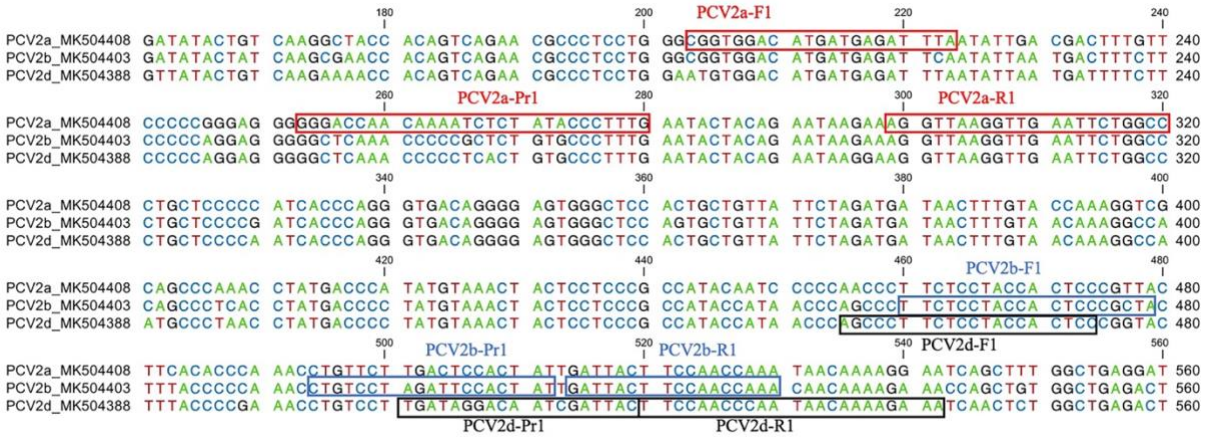

Figure 2.2.2 Primer and probe locations of the PCV2 genotyping real-time PCR assay

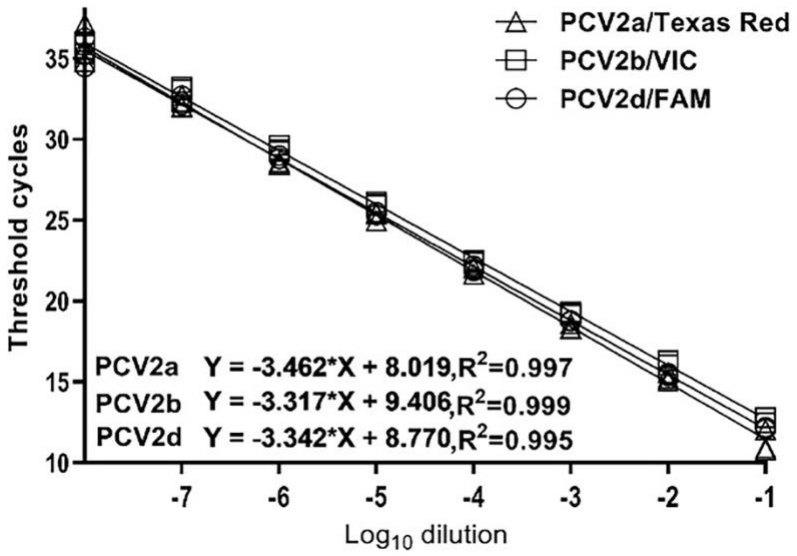

Figure 2.2.3 standard curves of PCV2a, PCV2b and PCV2d by serial dilutions of the cell culture isolates.

2.3 Development and evaluation of multiplex real-time RT-PCR assays for the detection and differentiation of foot-and-mouth disease virus and Seneca Valley virus 1

Yin Wang, Amaresh Das, Wanglong Zheng, Elizabeth Porter, Lizhe Xu, Lance Noll, Xuming Liu, Kimberly Dodd, Wei Jia, Jianfa Bai

(Transboundary and Emerging Disease. 2019; 67:604-616)

Abstract: Foot-and-mouth disease virus (FMDV) causes a highly contagious and economically important vesicular disease in cloven-hoofed animals that is clinically indistinguishable from symptoms caused by Seneca Valley virus 1 (SVV-1). To differentiate SVV-1 from FMDV infections, we developed an SVV-1 real-time RT-PCR (RT-qPCR) assay and multiplexed with published FMDV assays. Two published FMDV assays (Journal of the American Veterinary Medical Association, 220, 2002, 1636; Journal of Virological Methods, 236, 2016, 258) targeting the 3D polymerase (3D) region were selected and multiplexed with the SVV-1 assay that has two targets, one in the 5′ untranslated region (5′ UTR, this study) and the other in the 3D region (Journal of Virological Methods, 239, 2017, 34). In silico analysis showed that the primers and probes of SVV-1 assay matched 98.3% of the strain sequences (113/115). The primer and probe sequences of the Shi FMDV assay matched 85.4% (806/944), and that of the Callahan FMDV assay matched 62.7% (592/944) of the sequences. The limit of detection (LOD) for the two multiplex RT-qPCR assays for SVV-1 was both 9 copies per reaction by cloned positive plasmids and 0.16 TCID50 per reaction by cell culture. The LOD for FMDV by both multiplex assays was 11 copies per reaction using cloned positive plasmids. With cell cultures of the seven serotypes of FMDV, the

Shi assay (Journal of Virological Methods, 236, 2016, 258) had LODs between 0.04 and 0.18 TCID50 per reaction that were either the same or lower than the Callahan assay. Interestingly, multiplexing with SVV-1 increased the amplification efficiencies of the Callahan assay (Journal of the American Veterinary Medical Association, 220, 2002, 1636) from 51.5%–66.7% to 89.5%–96.6%. Both assays specifically detected the target viruses without cross-reacting to SVV-1 or to other common porcine viruses. An 18S rRNA housekeeping gene that was amplified from multiple cloven-hoofed animal species was used as an internal control. The prevalence study did not detect any FMDV, but SVV-1 was detected from multiple types of swine samples with an overall positive rate of 10.5% for non-serum samples.

2.3.1 Introduction

Foot-and-mouth disease (FMD) is a highly contagious disease of cloven-hoofed animals including pigs, cattle, sheep and goats. Although the United States eradicated FMD and has not seen the disease since 1929, the disease is still a major concern and listed as one of the Tier-1 select agents by the US Department of Agriculture (USDA), because it can spread very quickly and impose significant economic impact. Globally, FMD is considered endemic in about two-thirds of the continents, including Europe, Africa, Asia and South America (Arzt et al., 2019; Poonsuk, Gimenez- Lirola, & Zimmerman, 2018). Therefore, accurate detection of the disease is a very important measure for the surveillance of FMD in the United States. FMD is caused by the FMD virus (FMDV), a single-stranded positive-sense RNA virus, which belongs to the genus *Aphthovirus* of family *Picornaviridae*. Lack of proofreading mechanisms has resulted in a high

mutation rate during FMDV replication, in both the capsid-coding P1 region and the nonstructural protein-coding regions. Combined with the recombination events that can occur in the protein-coding regions, the high level of FMDV genetic diversity has been observed and that can create challenges for accurate detection (Garcia-Arriaza, Ojosnegros, Davila, Domingo, & Escarmis, 2006). Laboratory-based diagnostic tests are the definitive way to identify the virus. The most used and validated tests for the detection of FMDV are those quantitative (q) real-time reverse transcription (RT) polymerase chain reaction (RT-qPCR) assays (Ferris, King, Reid, Shaw, & Hutchings, 2006; Shaw et al., 2007). Several standardized assays are applied following the recommendation from the World Organization for Animal Health (OIE) and USDA. One of the recommended assays targets the 3D region and shares a high degree of nucleotide identity among different FMDV isolates and serotypes (Callahan et al., 2002; Carrillo et al., 2005). Previously, we developed a FMDV RT-qPCR assay at Kansas State Veterinary Diagnostic Laboratory (KSVDL), Kansas State University (KSU), targeting the 3D region (Shi et al., 2016).

The SVV-1 is a single-stranded positive-sense RNA virus, belonging to the genus *Senecavirus* in the family *Picornaviridae*. Since its discovery in 1998, SVV-1 has been reported in swine population globally, including the United States, Canada, Brazil, Colombia, Thailand and China (Armson et al., 2018; Fowler et al., 2017; Leme et al., 2015; Pasma, Davidson, & Shaw, 2008; Saengchuto et al., 2018; Sun, Vannucci, Knutson, Corzo, & Marthaler, 2017; Wu et al., 2016). The SVV-1 causes vesicular disease in pigs, which is clinically indistinguishable from FMD and characterized by vesicles on the snouts and coronary bands, lameness, anorexia, lethargy, fever

and diarrhoea (Hause et al., 2016; Segalés et al., 2017). Hence, molecular diagnostic techniques are essential for the differentiation and rule out of FMD. Like most single-stranded RNA viruses, SVV-1 has high nucleotide substitution rate by the phylogenetic analyses (Guo et al., 2016; Saengchuto et al., 2018; Xu et al., 2017). It requires reliable and sensitive diagnostics to detect the SVV-1 strain with variable mutations. Besides the 'gold standard' virus isolation (Hales et al., 2008), several molecular methods have been established to identify SVV-1, including conventional PCR assays, RT-qPCR assays, reverse transcription loop- mediated isothermal amplification (RT-LAMP) assays and reverse transcription droplet digital PCR assay. In these assays, the 3D region, VP1 coding region and 5' UTR are the selected detection targets (Dall Agnol, Otonel, Leme, Alfieri, & Alfieri, 2017; Bracht, O'Hearn, Fabian, Barrette, & Sayed, 2016; Feronato et al., 2018; Fowler et al., 2017; Gimenez-Lirola et al., 2016; Zhang, Zhang, Xiangmei, Chen, & Shaoqiang, 2018).

In this study, we developed a new RT-qPCR assay for SVV-1 detection with higher strain coverage compared to the assay we developed earlier (Fowler et al., 2017). The SVV-1 assays were multiplexed separately with two published FMDV assays (Callahan et al., 2002; Shi et al., 2016). The two quantitative multiplex RT-PCR (RT-mqPCR) assays were compared for the detection and differentiation of FMDV and SVV-1.

2.3.2 Methods and Materials

2.3.2.1 Virus strains

Seven serotypes of FMDV isolates, A, O, Asia1, SAT1, SAT2, SAT3 and C, 21 additional FMDV isolates and 21 SVV-1 isolates were supplied by the biological repository of the Reagents and Vaccine Services Section of the USDA Foreign Animal Disease Diagnostic Laboratory, located at the Plum Island Animal Disease Center, Orient Point, New York, USA. An SVV-1 cell culture isolate was pro- vided by Dr. Ying Fang in the Department of Diagnostic Medicine/ Pathobiology, KSU. Cell culture isolates of vesicular stomatitis virus (VSV), including New Jersey (VSV-NJ) and Indiana (VSV-IND) serotypes, genotypes 1–7 of porcine teschovirus, a strain of sapelovirus A (formerly porcine sapelovirus), porcine reproductive and respiratory syndrome virus type 2 (PRRSV-2), and swine influenza A virus (SIV), were provided by the Diagnostic Virology Laboratory at KSVDL, KSU. All work using FMDV isolates were done at FADDL, NVSL, DD and USDA. Initial analytical analysis was done at KSVDL using a synthesized FMDV 3D segment as template.

2.3.2.2 Viral RNA extraction

The viral RNA was extracted from 140 µl of cell culture or clinical samples using RNeasy Mini Kit (FADDL) or QIAamp Viral RNA Mini Kit (KSVDL) according to the manufacturer's instructions (Qiagen). To avoid template degradation, eluted RNA was appropriately diluted, aliquoted into smaller volumes for one time use only and stored in −70°C freezer.

2.3.2.3 The SVV-1 primers and probes

Based on the 115 whole-genome sequences of SVV-1 isolates from the current GenBank database, the SVV-1 assay we developed earlier (Fowler et al., 2017) has dropped the strain

coverage from 100% (designed with only 17 available sequences) to 88.7% (102/115), and thus, a new assay was designed in this study. All available SVV-1 whole-genome sequences were extracted from the GenBank database, aligned and analyzed with the Qiagen CLC Main Workbench 7. One set of primers and probe was designed, targeting the conserved 5′ UTR region that is a different region from the Fowler et al. assay design (Fowler et al., 2017). To achieve the maximum coverage, the published Fowler assay that targeted the 3D region was multiplexed with the newly designed SVV-1 assay (this study), and both SVV-1 probes were labelled with 5′- VIC and 3′-BHQ1 to better cover the potential variations in the future (Bai et al., 2018).

2.3.2.4 The multiplex assays of FMDV and SVV-1

Two FMDV assays were selected to multiplex with SVV-1 assays for the detection and differentiation of the two viruses. One is the USDA-approved and OIE-recommended Callahan assay (Callahan et al., 2002), which was designed on the conserved 3D region, and the other targeting the same region and was recently developed by Shi et al., 2016). The FMDV probes were labelled with 5′-FAM and 3′-BHQ1. The 18S rRNA housekeeping gene that is conserved and amplified from multiple animal species including cattle, pigs, sheep and goats was used as the internal control, and labelled with 5′-Cy5 and 3′-BHQ2 (Bai et al., 2018). Sequences and genome positions of all primers and probes are listed in Table 2.3.1.

2.3.2.5 Real-time RT-PCR composition and condition

Polymerase chain reaction tests for diagnosis were performed as described (Fowler et al., 2017; Shi et al., 2016). Briefly, a master mix of a 20 µl reaction is composed of 5 µl of template

RNA, 0.4 µM each of species-specific forward and reverse PCR primers, 0.2 µM each of probes, and 10 µl reaction buffer and 2 µl of enzyme mix from Path-ID™ Multiplex One-Step RT-PCR Kit (ThermoFisher Scientific). The parameters for thermocycling start with a reverse transcription step at 48°C for 10 min, a denaturation step at 95°C for 10 min, followed by 45 cycles of denaturation at 95°C for 15s and annealing/extension at 60°C for 50 s. The cycle threshold values (Cts) of the FMDV cell culture samples were generated with Applied Biosystems ABI 7500 Fast Real-Time PCR System (ThermoFisher Scientific), while other assays were performed with CFX96 Touch Real-Time PCR Detection System and the results were analyzed with CFX Manager 3.0 (Bio-Rad) and GraphPad Prism 7 (GraphPad Software).

2.3.2.6 Construction of positive standard plasmids

The SVV-1 5′ UTR-positive control plasmids were constructed by RT- PCR amplification of a genomic piece flanking the qPCR regio and cloned into pCR™ 2.1 vector using the TA Cloning kit (Invitrogen/ThermoFisher). The presence of cloned inserts was confirmed by gel electrophoresis and Sanger sequencing. The positive standards for the 3D-based SVV-1 assay and the FMDV assay in the Shi et al. assay were either amplified (SVV-1) or synthesized (FMDV) and cloned in the previous studies (Fowler et al., 2017; Shi et al., 2016). As both the Shi assay and the Callahan assay are using a similar region for primer designs, the positive amplification control works for both assays. Sequences of the cloning primers are listed in Table 2.3.1.

2.3.2.7 RNA synthesis by in vitro transcription

To study the analytical sensitivity of FMDV in BSL-2 facility at KSVDL, RNA fragments of the targeted 3D gene were synthesized from the cloned plasmid with MEGAscript T7 Transcription Kit according to the manufacturer's protocols (ThermoFisher Scientific). Following DNase treatment and purification by lithium chloride precipitation, the concentration of the resuspended RNA was measured with a NanoDrop 8000 spectrophotometer (ThermoFisher Scientific).

2.3.2.8 Assay sensitivity and specificity analysis

The analytical sensitivity was determined by standard curves generated with triplicates of 10-fold serial dilutions of positive standards and the RNA extracted from SVV-1 cell culture and in vitro-transcribed FMDV RNA, respectively. To obtain accurate LODs, twofold serial dilutions were applied at the last positive 10-fold dilution to fine-tune the least concentration that still amplifies. In addition, the FMDV sensitivity was studied with cell cultures of the 7 serotypes (A, O, Asia1, SAT1, SAT2, SAT3 and C). The specificity analysis was first performed in silico with Primer-Blast, the NCBI primer design tool (https://www.ncbi.nlm.nih.gov/tools/primer-blast/). The specificity then was experimentally evaluated using cell cultures, including the 7 serotypes of FMDV, 21 additional FMDV strains isolated from diagnostic samples, 21 SVV-1 strains, genotypes 1–7 of porcine teschovirus, a strain each of sapelovirus A, VSV New Jersey (VSV-NJ) and Indiana (VSV-IND) serotypes, PRRSV-2, SIV and clinical samples that were positive to specific pathogens including SVV-1, SIV, PRRSV-2, porcine epidemic diarrhoea virus (PEDV), porcine circovirus type 2 (PCV2) and porcine circovirus type 3 (PCV3) as shown in Table 2.3.2.

2.3.2.9 Comparison of multiplex and singular assays

Standard curves for FMDV and SVV-1 singular assays were generated with in vitro-transcribed RNA of FMDV-positive control plasmid or viral RNA of SVV-1 cell culture. To compare the sensitivity and amplification efficiency of the singular assays with the multiplex assays, standard curves were also generated with FMDV, SVV-1 and the internal control in the multiplex reactions. The single viral RNA was subjected to singular assays, while a mixture of equal amount of FMDV and SVV-1 templates was used for the multiplex assays. Standard curves were generated and compared between the singular and the multiplex assays.

To compare the two published FMDV assays, standard curves were generated with representative strains of all 7 FMDV serotypes. To study the performance of the assays at multiplex conditions, standard curves were also generated at the multiplexed conditions that composed of FMDV, SVV-1 and the 18S rRNA gene internal control. The performance of the two assays was compared in terms of LODs, amplification efficiencies and correlation coefficients of the linear regression curves.

2.3.2.10 Prevalence of FMDV and SVV-1 with the new RT-mqPCR

All samples used in this study were animal diagnostic samples submitted by our clients, and there was no animal handling involved. For the prevalence study, a total of 444 clinical porcine samples, including 225 serum samples, 73 faecal, 53 tissue, 19 nasal swabs, 68 oral fluid samples and 6 vesicular lesion swab samples, were collected from KSVDL between April 2017 and September 2017 and tested for the prevalence of the viruses. The RT-mqPCR assays were

performed on these samples for FMDV and SVV-1 detections and for potential co-infection identifications.

2.3.3 Results

2.3.3.1 Primer and probe design and strain coverage analysis for SVV-1

Based on the 115 whole-genome sequences of SVV-1 from GenBank database, a new SVV-1 assay targeting the conserved 5′ UTR region was designed. The primers and probe matched 107 strains. Combined with the previously designed SVV-1 assay targeting the 3D region (Fowler et al., 2017), the overall coverage was 98.3% (113/115). For the two mismatching strains, there was only one nucleotide mismatch at the 5′ side of the forward primer in one strain (MG765565) and single nucleotide mismatch in the 3′ side of the probe in the other strain (MF967574), which may not affect the detection. In that case, the strain coverage would be 100% (Table 2.3.1).

2.3.3.2 Strain coverage analysis for the two published FMDV assays

Two published FMDV RT-qPCR assays, Callahan et al., (2002) and Shi et al., (2016) (Callahan et al., 2002; Shi et al., 2016), were selected for evaluations. In total, 944 FMDV 3D genes from GenBank database representing all 7 serotypes were applied for the *in silico* strain coverage analysis. The primers and probe from Callahan et al., (2002) assay has 62.7% (592/944) match to the strain sequences, while the Shi et al., (2016) assay has 85.4% (806/944) of match to the sequences. Assuming a single nucleotide mismatch to a primer (exclude the more critical 6 bp in the 3′ end) or a probe (exclude the 6 bp in the middle) in the assay can still amplify and generate

signal, the strain coverage of Callahan et al., (2002) assay would be increased to 86.8% (819/944), and Shi et al., (2016) assay would be 95.4% (901/944, Table 2.3.1).

2.3.3.3 Analytical sensitivity of the multiplex real-time PCR assay on positive standard plasmids

The SVV-1 assay designed and validated in this study was multiplexed with either the Callahan et al., (2002) FMDV assay or the Shi et al., (2016) FMDV assay. Analytical sensitivity of the RT-mqPCR assay was analyzed using standard curves generated by three replicates of 10-fold serial dilutions of the template and analyzed by plotting their Cts against log dilution factors. The PCR amplification efficiencies for the SVV-1 assay multiplexed with Callahan et al., (2002) FMDV assay were 97.7% for FMDV and 95.1% for SVV-1, both had high correlations coefficient (R^2) that were greater than 0.994. When the Shi et al., (2016) assay was multiplexed with our SVV-1 assay, the PCR amplification efficiencies were 97.3% for FMDV and 91.4% for SVV with R^2 that were both greater than 0.995. To get more accurate LODs of the assay, the cloned standard controls at the last 10-fold dilution were further diluted by twofold serial dilutions. The results indicated identical LODs of the two multiplex assays, which were both 11 copies per PCR reaction for FMDV and nine copies per reaction for SVV-1.

2.3.3.4 Analytical sensitivity of the RT-mqPCR assay on viral isolates and in vitro-transcribed RNA

To make sure that the assay sensitivity is not compromised when testing on viral RNA, the SVV-1 cell culture and in vitro-transcribed FMDV RNA were also used as templates. The standard

curves generated by 10-fold dilutions were plotted with Cts against log dilution factors. The amplification efficiencies of the SVV-1 assay multiplexed with the Callahan assay were 84% for FMDV and 93.4% for SVV-1 with R2 greater than 0.991, while with the Shi assay, amplification efficiencies were higher, 92.1% for FMDV and 94.8% for SVV-1 with R2 greater than 0.995 (Table 2.3.3). The LODs of SVV-1 in the two multiplex assays were similar and were around 0.16 TCID50 per reaction. The standard curve on the internal control 18S rRNA gene showed that there is no inhibition to PCR amplification (Figure 2.3.1).

2.3.3.5 Comparison of multiplex and singular assays on viral isolates and in vitro-transcribed RNA

As shown in Table 2.3.3, the amplification efficiency of FMDV assay from the Callahan assay was 65%. Interestingly, when multiplexed with SVV-1, the PCR amplification efficiency for FMDV increased to 84%. Both the multiplex and singular assays had R^2 greater than 0.991. Using FMDV viral isolates as templates had generated similar results. In the multiplex assay of SVV-1 with the Shi et al. assay, the amplification efficiencies of both SVV-1 and FMDV were greater than 90%. Both of the multiplex and singular assays had R^2 greater than 0.991. Comparing the multiplex with the singular assays, Ct values for the serial dilutions of the viral RNA were nearly identical, indicating that multiplexing was not reducing the sensitivity of the assays (Table 2.3.3).

2.3.3.6 Comparison of the two RT-mqPCR assays on FMDV cell culture isolates

Seven serotypes of FMDV were subjected to the standard curve analyses by 10-fold serial dilutions to compare the performance of the two published FMDV assays, Callahan et al., (2002) and Shi et al., (2016), in singular and multiplex conditions. Consistent with results of positive standards and in vitro-transcribed RNA, the efficiencies of the Callahan assay were between 51.1% and 66.5%. The Ct values at the last dilutions were between 39.6 and 42.2. However, when multiplexed with SVV-1 and the 18S rRNA gene internal control, the amplification efficiencies increased dramatically. The multiplex assay with the Callahan FMDV assay on 6 of the 7 serotypes had amplification efficiencies above 90%, and up to 96.6%, with the exception for serotype C that had 89.5% efficiency. The Ct values at the last dilutions were lower than 38 except for SAT3, which had a higher Ct value (39.3). The LODs of the singular assays were between 0.04 and 8.83 TCID50 per reaction, while the multiplex reactions had LODs between 0.04 and 0.88 TCID50 per reaction.

In the multiplex reactions with the Shi FMDV assay, the assay efficiencies on the seven serotypes were between 88.6% and 97.8%, in which only SAT1 had efficiency below 90%. The multiplex assays had similar end Ct values to that in singular assays. The LODs of the seven serotypes had LODs between 0.03 and 0.18 TCID50 per reaction.

Comparing the two multiplex assays, the amplification efficiencies were similar: only one serotype virus was lower than 90%, but close to 90% for both assays. The LODs of the multiplex assay with the Shi et al. assay were the same or one log TCID50 lower than the multiplex assay with the Callahan et al. assay. The R^2 values of both assays were all above 0.991 (Table 2.3.4).

2.3.3.7 Analytical specificity of the RT-mqPCR assays

The specificity of primers and probes was tested by an *in silico* analysis with Primer-Blast, which presented unique viral target for each set of assay. Assay specificity was also experimentally tested and confirmed with viral isolates that included 7 serotypes of FMDV, 21 additional FMDV strains isolated from diagnostic samples, 21 SVV-1 strains, genotypes 1–7 of porcine teschovirus, a strain each of sapelovirus A, VSV New Jersey (VSV-NJ) and Indiana (VSV-IND) serotypes, PRRSV-2 and SIV. Specificity was also tested with clinical samples that were previously tested positive to non-target specific pathogens. The results demonstrated that the assay specifically detected FMDV and SVV-1-positive samples without cross-detecting each other and no positive targets were detected from above-mentioned non-target viral strains, and clinical samples that were positive to PRRSV-2 (n=8), SIV (n=4), PEDV (n=4), PCV2 (n=27) and PCV3(n=2). Results showed that there is no signal generated on those non- target positive samples indicating a good specificity of the assays (Table 2.3.2).

2.3.3.8 Prevalence of SVV-1 in diagnostic samples

The 444 clinical porcine samples collected from KSVDL between April 2017 and September 2017, including 225 serum samples, 73 faecal samples, 53 tissue samples, 19 nasal swabs, 68 oral fluid samples and 6 lesion swab samples, were tested for the prevalence study. The overall SVV-1 positive rate was 5.4%, which is lower than previous studies (Hause et al., 2016). Our results indicated that the SVV-1 virus does not commonly present in serum samples.

Therefore, the positive rate is increased to 10.5% if the 225 serum samples are excluded from the calculation (Table 2.3.5).

2.3.4 Discussion

Foot-and-mouth disease virus is a highly contagious livestock disease, and an outbreak in the United States would have catastrophic impact on the nation's economy. Since the United States is currently free of FMDV, preventative measures are essential and accurate detection is an important integrated component. Although transmission and pathogenesis of SVV-1 are not fully understood, SVV-1 is identified from vesicular lesions, and it has spread to different countries and regions worldwide. The indistinguishable clinical signs produced by SVV-1 and FMDV require laboratory diagnostics including molecular testing to differentiate between the two diseases. Recently, several FMDV RT-qPCR assays have been applied following the recommendation of OIE and one of the most commonly used assays is the Callahan et al. assay (Callahan et al., 2002) that targets the conserved 3D region. Previous studies have already demonstrated the strengths of the method including good assay sensitivity, specificity, repeatability and reproducibility (Vandenbussche, Lefebvre, De Leeuw, Van Borm, & De Clercq, 2017). The results from this study indicated a low amplification efficiency in singular assays with both in vitro-transcribed RNA and viral isolates. Interestingly, when multiplexed with SVV-1, the amplification efficiency of the Callahan FMDV assay was noticeably increased. When in vitro-transcribed RNA was used, the amplification efficiency was improved from 65% to 84%, and the corresponding Ct value of the last dilution decreased from 41.5 to 36.2. The results were consistent with those with FMDV viral

isolates. In most PCRs when Ct value is greater than 36, the higher the Ct value, the lower the repeatability. Reducing the LOD from Ct 41.5 to 36.2 may increase detection accuracy especially when viral concentration is low. The potential reason for the increased amplification efficiency under multiplexed conditions may be due to the denaturation and stabilization of the secondary structure of the primer–viral RNA complex as indicated in the previous study (Vandenbussche et al., 2017). Our sequence analysis also indicated that the target region in the Callahan assay has a stem-loop structure. Such phenomena have scarcely been reported, and we are still searching for other potential explanations. Shi et al., (2016) developed another RT-qPCR assay targeting the same region of 3D. The above assay had high amplification efficiency of 99.4% in singular assay and 92.1% in multiplex ones (Figure 2.3.1 & Table 2.3.3), both are within the standard acceptable range of 90%–110%. Comparing their primers and probes, the reverse primers in Shi et al. (2016) assay shifted 8–10 nucleotides towards the 3′ end of the primer. Secondary structure predicted with CLC workbench 7.6 indicated that this shifted primer location has avoided the stem-loop structure that was used in the Callahan et al. (2002) design.

In PCR assays, the mismatches may negatively impact amplification (Stadhouders et al., 2010). FMDV and SVV-1 are variable RNA viruses with high substitution rates. It brings challenges for designing assays with high coverage to field strains. In this study, the most current data sets were analyzed with bioinformatic tools that support the design of primers and probes with high coverage across strains. Based on the 115 whole-genome sequences of SVV-1 isolates that are currently available in the GenBank database, SVV-1 assay targeting the conserved 5′ UTR

region was designed and added into the previously designed PCR set targeting the 3D region to overcome the high mutation rate. The SVV-1 assays could match 98.3% (113/115) of the strains. The two mismatched strains only have a single nucleotide mismatch at the 5′ side of the forward primer in one strain (MG765565) and single nucleotide mismatch in the 3′ side of the probe in the other strain (MF967574), therefore are most likely amplified by the assay. If that is the case, the SVV-1 assay coverage would be 100%. Merging the two SSV-1 assays that are targeted on two separate regions on the genome will help to overcome future variations on the genome (Bai et al., 2018). When lacking the coverage analysis or using incomplete data sets for assay design, the established molecular methods may lose the power to detect pathogens especially those with a divergent genome (Dall Agnol et al., 2017; Armson et al., 2018; Bai et al., 2018; Zeng et al., 2018). Strain coverage of the two published FMDV assays was also analyzed with the most current data sets. From the 944 of FMDV 3D sequences achieved from GenBank database, Shi et al., (2016) assay has perfect match to 85.4% (806/944) of the sequences, while the Callahan assay that was designed in 2002, only 62.7% of strains (592/944) had perfect matches. In general, an assay with a single nucleotide mismatch occurred in the middle especially in the 5′ end of a primer, or in the two ends of a probe will still amplify and generate signal. When single nucleotide mismatches in such situations allowed for the primers and probes, the strain coverage could be increased to 95.4% for the Shi et al. (2016) assay and 86.8% for the Callahan et al. (2002) assay. From this in silico analysis, Shi et al. (2016) assay is expected to detect more FMDV strains in the field.

Sensitivity of the two RT-mqPCR assays to detect the SVV-1 is better than or comparable to other RT-qPCR assays or RT-LAMP assays (Dall Agnol et al., 2017; Armson et al., 2018; Fowler et al., 2017; Zeng et al., 2018); LAMP assays require multiple primer sets that appear to be difficult to have high strain coverage for viruses with divergent genomes. Although sensitivity for our SVV-1 assay is lower than the droplet digital PCR assay (Zhang et al., 2018), the sophisticated and expensive equipment limits the applicability of digital PCR in veterinary diagnostic practices. The sensitivity level (nine copies/ reaction) of our SVV-1 RT-qPCR meets the requirements as a routine diagnostic tool. For FMDV detection, the multiplex RT-qPCR we developed here did not affect the sensitivity of the assay as compared to singular assays published previously.

From the 444 samples collected from KSVDL during April 2017 and September 2017, there was no FMDV-positive observed, and 23 (5.2%) SVV-1-positive samples were identified. The SVV-1-positive results were from different sample types, including serum, faeces, tissue, nasal swab, oral fluid and lesion swab samples, indicating potential variable ways to spread the disease. In the SVV-1 positives, only one (0.4%) positive sample was found from the 225 serum samples. Therefore, the positive rate is increased to 10.1% for non-serum samples.

In conclusion, we developed and evaluated two RT-mqPCR assays for the detection and differentiation of FMDV and SVV-1. Our results showed that multiplexing improved the amplification efficiency of FMDV assay from Callahan et al., (2002) assay but did not affect the FMDV assay from Shi et al., (2016) assay. *In silico* analysis and clinical sample testing indicated

that the SVV-1 assays had high strain coverage and FMDV assay from the more recent Shi et al., (2016) assay had higher strain coverage than the Callahan assay that was developed in 2002. Our prevalence data indicated that SVV-1 strains have been widely distributed in the United States.

2.3.5 References

Armson, B., Walsh, C., Morant, N., Fowler, V. L., Knowles, N. J., & Clark, D. (2018). The development of two field-ready reverse transcription loop-mediated isothermal amplification assays for the rapid detec- tion of Seneca Valley virus 1. Transboundary and Emerging Diseases. 66(1), 497–504. https://doi.org/10.1111/tbed.13051

Arzt, J., Fish, I., Pauszek, S. J., Johnson, S. L., Chain, P. S., Rai, D. K., … Stenfeldt, C. (2019). The evolution of a super-swarm of foot-and- mouth disease virus in cattle. PLoS ONE, 14, e0210847. https://doi. org/10.1371/journal.pone.0210847

Bai, J., Trinetta, V., Shi, X., Noll, L.W., Magossi, G., Zheng, W., … Nagaraja, T. G. (2018). A multiplex real-time PCR assay, based on invA and pagC genes, for the detection and quantification of Salmonella enterica from cattle lymph nodes. Journal of Microbiological Methods, 148, 110–116. https://doi.org/10.1016/j. mimet.2018.03.019

Bracht, A. J., O'Hearn, E. S., Fabian, A. W., Barrette, R. W., & Sayed, A. (2016). Real-time reverse transcription PCR assay for detection of senecavirus A in swine vesicular diagnostic specimens. PLoS ONE, 11, e0146211. https://doi.org/10.1371/journal.pone.0146211

Callahan, J. D., Brown, F., Osorio, F. A., Sur, J. H., Kramer, E., Long, G. W., … Nelson, W. M. (2002). Use of a portable real-time reverse transcriptase-polymerase chain reaction assay for rapid detection of foot-and-mouth disease virus. Journal of the American Veterinary Medical Association, 220, 1636–1642. https://doi.org/10.2460/ javma.2002.220.1636

Carrillo, C., Tulman, E. R., Delhon, G., Lu, Z., Carreno, A., Vagnozzi, A., … Rock, D. L. (2005). Comparative genomics of foot-and-mouth disease virus. Journal of Virology., 79, 6487–6504. https://doi.org/10.1128/JVI.79.10.6487-6504.2005

Dall Agnol, A. M., Otonel, R. A. A., Leme, R. A., Alfieri, A. A., & Alfieri, A. F. (2017). A TaqMan-based qRT-PCR assay for Senecavirus A detection in tissue samples of neonatal piglets. Molecular and Cellular Probes, 33, 28-31.https://doi.org/10.1016/j.mcp.2017.03.002

Feronato, C., Leme, R. A., Diniz, J. A., Agnol, A. M. D., Alfieri, A. F., & Alfieri, A. A. (2018). Development and evaluation of a nested-PCR assay for Senecavirus A diagnosis. Tropical Animal Health and Production, 50, 337–344. https://doi.org/10.1007/s11250-017-1436-z

Ferris, N. P., King, D. P., Reid, S. M., Shaw, A. E., & Hutchings, G. H. (2006). Comparisons of original laboratory results and retrospective analysis by real-time reverse transcriptase-PCR of virological samples collected from confirmed cases of foot-and-mouth disease in the UK in 2001. Veterinary Record, 159, 373–378. https://doi.org/10.1136/vr.159.12.373

Fowler, V. L., Ransburgh, R. H., Poulsen, E. G., Wadsworth, J., King, D. P., Mioulet, V., … Bai, J. (2017). Development of a novel real-time RT- PCR assay to detect Seneca Valley virus-1 associated with emerging cases of vesicular disease in pigs. Journal of Virological Methods, 239, 34–37. https://doi.org/10.1016/j.jviromet.2016.10.012

Garcia-Arriaza, J., Ojosnegros, S., Davila, M., Domingo, E., & Escarmis, C. (2006). Dynamics of mutation and recombination in a replicating population of complementing, defective viral genomes. Journal of Molecular Biology, 360, 558–572. https://doi.org/10.1016/j.jmb.2006. 05.027

Gimenez-Lirola, L. G., Rademacher, C., Linhares, D., Harmon, K., Rotolo, M., Sun, Y., … Pineyro, P. (2016). Serological and molec- ular detection of senecavirus A associated with an outbreak of swine idiopathic vesicular disease and neonatal mortality. Journal of Clinical Microbiology, 54, 2082–2089. https://doi.org/10.1128/ JCM.00710-16

Guo, B., Pineyro, P. E., Rademacher, C. J., Zheng, Y., Li, G., Yuan, J., … Yoon, K. J. (2016). Novel senecavirus A in swine with vesicular dis- ease, United States, July 2015. Emerging Infectious Diseases., 22, 1325–1327. https://doi.org/10.3201/eid2207.151758

Hales, L. M., Knowles, N. J., Reddy, P. S., Xu, L., Hay, C., & Hallenbeck, P. L. (2008). Complete genome sequence analysis of Seneca Valley virus-001, a novel oncolytic picornavirus. The Journal of General Virology., 89, 1265–1275. https://doi.org/10.1099/ vir.0.83570-0

Hause, B. M., Myers, O., Duff, J., & Hesse, R. A. (2016). Senecavirus A in Pigs, United States, 2015. Emerging Infectious Diseases, 22, 1323– 1325. https://doi.org/10.3201/eid2207.151591

Leme, R. A., Zotti, E., Alcantara, B. K., Oliveira, M. V., Freitas, L. A., Alfieri, A. F., & Alfieri, A. A. (2015). Senecavirus A: An emerging vesicular infection in brazilian pig herds. Transboundary and Emerging Diseases, 62, 603–611.

Pasma, T., Davidson, S., & Shaw, S. L. (2008). Idiopathic vesicular disease in swine in Manitoba. The Canadian Veterinary Journal, 49, 84–85.

Poonsuk, K., Gimenez-Lirola, L., & Zimmerman, J. J. (2018). A review of foot-and-mouth disease virus (FMDV) testing in livestock with an emphasis on the use of alternative diagnostic specimens. Animal Health Research Reviews, 19(2), 100–112. https://doi.org/10.1017/S1466 252318000063

Saengchuto, K., Stott, C. J., Wegner, M., Kaewprommal, P., Piriyapongsa, J., & Nilubol, D. (2018). The full-length genome characterization, genetic diversity and evolutionary analyses of Senecavirus A isolated in Thailand in 2016. Infection Genetics and Evolution, 64, 32–45. https:// doi.org/10.1016/j.meegid.2018.06.011

Segalés, J., Barcellos, D., Alfieri, A., Burrough, E., & Marthaler, D. (2017). Senecavirus A: An emerging pathogen causing vesicular disease and mortality in pigs? Veterinary Pathology, 54, 11–21. https://doi.org/10.1177/0300985816653990

Shaw, A. E., Reid, S. M., Ebert, K., Hutchings, G. H., Ferris, N. P., & King, D. P. (2007). Implementation of a one-step real-time RT-PCR protocol for diagnosis of foot-and-mouth

disease. Journal of Virological Methods, 143, 81–85. https://doi.org/10.1016/j.jviromet.2007.02.009

Shi, X., Liu, X., Wang, Q., Das, A., Ma, G., Xu, L., … Shi, J. (2016). A multiplex real-time PCR panel assay for simultaneous detection and differentiation of 12 common swine viruses. Journal of Virological Methods, 236, 258–265. https://doi.org/10.1016/j.jviromet.2016.08.005

Stadhouders, R., Pas, S. D., Anber, J., Voermans, J., Mes, T. H. M., & Schutten, M. (2010). The effect of primer-template mismatches on the detection and quantification of nucleic acids using the 5 ' nucle- ase assay. Journal of Molecular Diagnostics, 12, 109–117. https://doi.org/ 10.2353/jmoldx.2010.090035

Sun, D., Vannucci, F., Knutson, T. P., Corzo, C., & Marthaler, D. G. (2017). Emergence and whole-genome sequence of Senecavirus A in Colombia. Transboundary and Emerging Diseases, 64, 1346–1349. https://doi.org/10.1111/tbed.12669

Vandenbussche, F., Lefebvre, D. J., De Leeuw, I., Van Borm, S., & De Clercq, K. (2017). Laboratory validation of two real-time RT-PCR methods with 5'-tailed primers for an enhanced detection of foot- and-mouth disease virus. Journal of Virological Methods, 246, 90–94. https://doi.org/10.1016/j.jviromet.2017.04.014

Wu, Q., Zhao, X., Chen, Y., He, X., Zhang, G., & Ma, J. (2016) Complete genome sequence of seneca valley virus CH-01-2015 identified in China. Genome Announcements, 4. https://doi.org/10.1128/genomeA.01509-15

Xu, W., Hole, K., Goolia, M., Pickering, B., Salo, T., Lung, O., & Nfon, C. (2017). Genome wide analysis of the evolution of Senecavirus A from swine clinical material and assembly yard environmental samples. PLoS ONE, 12, e0176964. https://doi.org/10.1371/journal.pone.0176964

Zeng, F., Cong, F., Liu, X., Lian, Y., Wu, M., Xiao, L., … Luo, M. (2018). Development of a real time loop-mediated isothermal am- plification method for detection of Senecavirus A. Journal of Virological Method, 261, 98–103. https://doi.org/10.1016/j.jviromet.2018.08.005

Zhang, Z., Zhang, Y., Xiangmei, L., Chen, Z., & Shaoqiang, W. (2018). Development of a novel reverse transcription droplet digital PCR assay for the sensitive detection of Senecavirus A. Transboundary and Emerging Diseases. 66(1), 517–525. https://doi.org/10.1111/tbed.13056

Table 2.3.1 Primers and Probes of FMDV and SVV-1 assays

PCR set	Target	Sequence (5'-3')	Tm (°C)	Amplicon (bp)	Coverage (%)		Ref.
SVV-11	3D	F1: AGAATTTGGAAGCCATGCTCT	60.2	78	88.7 (102/115)	98.3~100 (113/115~115/115* combined)	Fowler, 2017
		R1: GAGCCAACATAGARACAGATTGC	60.2				
		Pr1: VIC-TTCAAACCAGGAACACTACTCGAGA-BHQ1	63.4				
SVV-12	5'-UTR	F2: TGGAGCTCGACCCTCCTT	60.9	62	93.0 (107/115)		This study
		R2: CTGTGTCGGAGCTTGTTGC	60.6				
		Pr2: VIC-TAAGGGAACCGAGAGGCCTTC-BHQ1	63.9				
FMDV-Callahan	3D	F: ACTGGGTTTTACAAACCTGTGA	58.5	107	62.8~86.9 (592/943~819/943)		Callahan et al., 2002
		R: GCGAGTCCTGCCACGGA	64.8				
		Pr: FAM-TCCTTTGCACGCCGTGGGAC-BHQ1	70.9				
FMDV-Shi	3D	F1: ACTGGGTTTTACAAACCTGTGATG	59.0	99	89.8~95.7 (847/943~902/943)		Shi et al., 2016
		F2: CTGGGTTTTATAAACCTGTGATGGC	60.4				
		R1: CCACGGAGATCAACTTCTCCT	59.2				
		R2: TGCCACAGAGATCAACTTCTCC	60.0				
		R3: CCACGGAAATCAACTTCTCCTG	59.3				
		Pr: FAM-TCTCCTTTGCACGCCGTGG-BHQ1	64.1				
18S rRNA	rRNA	F: GGAGTATGGTTGCAAAGCTGA	60.2	100	98.9~100 (88/89~88/89)		Bai et al., 2018
		R: GGTGAGGTTTCCCGTGTTG	61.4				
		Pr: Cy5-AAGGAATTGACGGAAGGGCA-BHQ2	64.0				
SVV-1 clone 1	3D	cF1: AGAATTTGGAAGCCATGCTCT	60.2	494			Fowler, 2017
		cR1: GAGCCAACATAGARACAGATTGC	60.1				
SVV-1 clone 2	5'-UTR	cF2: CGGAAAGCGCTGTAACCA	61.0	308			This study
		cR2: GCCCTATCAGGCAGTATCCA	60.1				
FMDV clone	3D	cF: ACTGGGTTTTACAAACCTGTGA	58.5	500			Shi et al., 2016
		cR: GCGAGTCCTGCCACGGA	64.8				

*The lower boundary of the range of percentage match is generated from perfect matches in a primer pair and its corresponding probe against sequences analyzed; the higher boundary of the

range is generated by allowing the present of a single nucleotide variation in each primer in a primer pair and in its corresponding probe.

Table 2.3.2 Specificity of the SVV-1 RT-mqPCR assays multiplexed with either the Callahan FMDV assay or the Shi FMDV assay

Pathogen	Source	No. tested	Target gene		
			FMDV (FAM)	SVV-1(VIC)	18S(Cy5)
FMDV	Cell culture	7	+	-	+
SVV-1	Cell culture	1	-	+	+
	Clinical sample	21	-	+	+
VSV-NJ	Cell culture	1	-	-	+
VSV-IND	Cell culture	1	-	-	+
PRRSV-2	Cell culture	1	-	-	+
	Clinical sample	8	-	-	+
SIV	Cell culture	1	-	-	+
	Clinical sample	4	-	-	+
PEDV	Clinical sample	4	-	-	+
PCV2	Clinical sample	27	-	-	+
PCV3	Clinical sample	2	-	-	+

Table 2.3.3 PCR amplification efficiencies and correlation coefficients of the Callahan FMDV assay and the Shi FMDV assay as singular assays and as multiplex assays with the SVV-1 assay using *in vitro* transcribed RNA

Assay		SVV-1 singular	SVV-1 multiplex-Callahan	SVV-1 multiplex-Shi	FMDV singular-Callahan	FMDV multiplex-Callahan	FMDV singular-Shi	FMDV multiplex-Shi
Efficiency (E)		95.5%	93.4%	94.8%	65.0%	84.0%	99.4%	92.1%
Correlation coefficient (R^2)		0.998	0.998	0.997	0.995	0.991	0.991	0.995
Mean Cts of viral RNA with different dilutions	10^{-1}	13.15	14.32	13.62	13.38	13.35	13.99	14.02
	10^{-2}	17.34	18.00	16.98	18.37	17.16	17.74	17.51
	10^{-3}	20.39	22.09	20.68	23.78	20.37	21.25	21.48
	10^{-4}	23.34	25.13	24.31	28.04	24.11	25.00	24.78
	10^{-5}	27.14	28.61	28.07	32.78	27.64	28.23	28.73
	10^{-6}	30.96	31.98	31.62	35.99	31.23	31.19	31.88
	10^{-7}	33.89	35.10	34.05	41.56	36.18	34.78	35.72

Table 2.3.4 PCR amplification efficiencies and correlation coefficients of the Callahan FMDV assay and the Shi FMDV assay as singular assays and as multiplex assays with the SVV-1 assay using viral strains representing the seven FMDV serotypes

FMDV assay	Serotype	Assay	Slope	Efficiency (%)	Correlation coefficient (R^2)	LOD (Ct/TCID50)
Callahan et al., 2002	A	Singular	-5.287	54.6	0.989	42.2/0.04
		Multiplex	-3.556	91.1	0.999	35.6/0.04
	O	Singular	-4.964	59.0	0.986	41.1/0.18
		Multiplex	-3.506	92.9	0.995	35.9/0.18
	Asia1	Singular	-4.954	59.2	0.992	41.1/0.35
		Multiplex	-3.582	90.2	0.999	35.7/0.35
	SAT1	Singular	-4.508	66.7	0.993	41.0/0.07
		Multiplex	-3.406	96.6	0.994	36.2/0.07
	SAT2	Singular	-4.61	64.8	0.991	40.8/0.88
		Multiplex	-3.537	91.8	0.999	36.2/0.88
	SAT3	Singular	-4.515	66.5	0.984	39.6/8.83
		Multiplex	-3.466	94.3	0.991	39.3/0.88
	C	Singular	-5.54	51.5	0.991	40.9/1.76
		Multiplex	-3.603	89.5	0.998	37.5/0.18
Shi et al., 2016	A	Singular	-3.729	85.4	0.997	36.4/0.04
		Multiplex	-3.476	94.0	0.998	36.4/0.04
	O	Singular	-3.42	96.1	0.985	36.5/0.18
		Multiplex	-3.469	94.2	0.999	37.8/0.18
	Asia1	Singular	-3.519	92.4	0.995	39.4/0.04
		Multiplex	-3.392	97.2	0.991	38.9/0.04
	SAT1	Singular	-3.56	90.9	0.988	40.3/0.07
		Multiplex	-3.63	88.6	0.999	40.0/0.07
	SAT2	Singular	-3.882	81.0	0.999	40.8/0.09
		Multiplex	-3.488	93.5	0.999	38.0/0.09
	SAT3	Singular	-3.806	83.1	0.999	38.3/0.88
		Multiplex	-3.375	97.8	0.997	39.0/0.09

	C	Singular	-3.356	98.6	0.987	35.0/0.18
		Multiplex	-3.587	90.0	0.999	37.1/0.18

Table 2.3.5 Prevalence of SVV-1 in swine diagnostic samples

	Serum	Feces	Tissue	Nasal Swab	Oral Fluid	Lesion Swab	Total
# Clinical Sample (# positive)	225 (1)	73 (3)	53 (5)	19 (1)	68 (8)	6 (6)	444 (21)

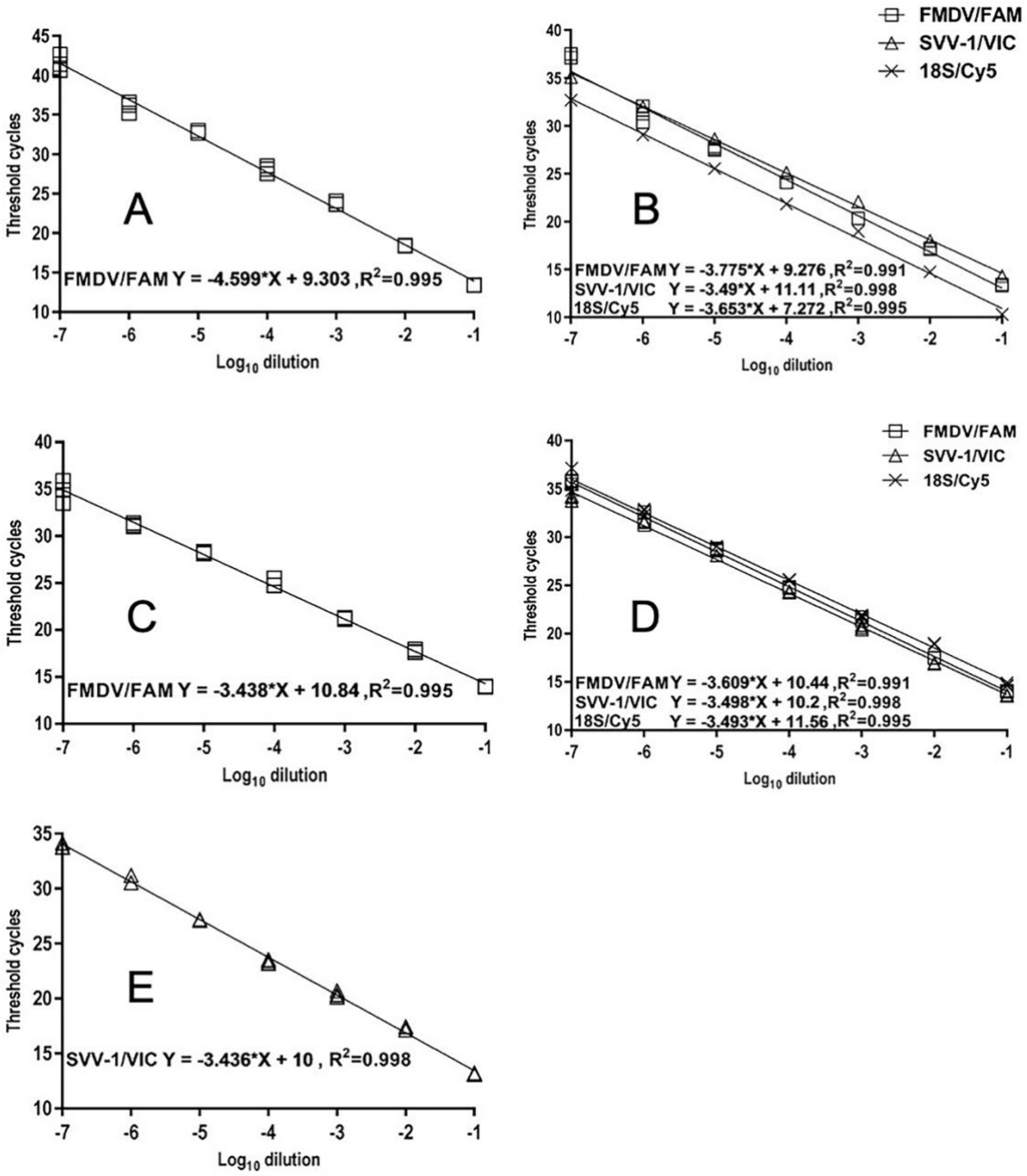

Figure 2.3.1 Standard curves of FMDV and SVV-1 assays

(A) FMDV assay from Callahan et al., 2002 by serial dilutions of FMDV *in vitro* transcribed RNA; (B) FMDV assay from Callahan et al., 2002 multiplexed with SVV-1 assay by serial dilutions of mixture of FMDV *in vitro* transcribed RNA and SVV-1 cell culture; (C) FMDV assay from Shi et al., 2016 by serial dilutions of FMDV *in vitro* transcribed RNA; (D) FMDV assay from Shi et al., 2016 multiplexed with SVV-1 assay by serial dilutions of mixture of FMDV *in vitro* transcribed RNA and SVV-1 cell culture; (E) SVV-1 assay by serial dilutions of SVV-1 cell culture.

2.4 Development of a real-time PCR assay for detection of African swine fever virus with an endogenous internal control

Yin Wang, Lizhe Xu, Lance Noll, Colin Stoy, Elizabeth Porter, Jinping Fu, Yuan Feng, Lalitha Peddireddi, Xuming Liu, Kimberly A. Dodd, Wei Jia, Jianfa Bai

(Transboundary and Emerging Disease. 2020; 00:1–9)

Abstract: Real-time PCR assays are highly sensitive, specific and rapid techniques for the identification of ASF virus (ASFV) (Section 3.8, OIE Terrestrial Manual, 2019). Although an ASFV p72 gene-based real-time PCR assay (a.k.a. the Zsak assay) (Journal of Clinical Microbiology, 2005, 43, 112) has been widely used for ASFV detection, several more ASFV whole genome sequences have become available in the 15 years since the design of the Zsak assay. In this study, we developed a new ASFV p72 gene-based real-time PCR after analysis of all currently available sequences of the p72 gene and multiplexed the new assay with a modified Zsak assay aiming to have a broader coverage of ASFV strain/isolates. To reduce false-negative detections, porcine house-keeping gene, beta actin (*ACTB*), was applied as an internal control. Eight ACTB sequences from the GenBank and 61 partial ACTB sequences generated in this study, and 1,012 p72 sequences from the GenBank and 23 p72 sequences generated at FADDL, were used for ACTB and ASFV primer and probe designs, respectively, to ensure broader host and ASFV coverage. Multiplexing ACTB in the reaction did not affect ASFV amplification. The multiplex assay was evaluated for strain/isolate coverage, sensitivity and specificity. The *in silico* analysis showed high ASFV strain/isolate coverage: 98.4% (978/994) of all p72 sequences

currently available. The limit of detection (LOD) was 6 plasmid copies or 0.1–1 TCID50/ml of ASFV isolates per reaction. Only targeted ASFV isolates and the viruses in the positive clinical samples were detected, indicating that the assay is highly specific (100% specificity). The test results of 26 ASFV isolates with different country origins showed that this newly developed multiplex assay performed better than the Zsak assay that has been widely accepted and used worldwide, indicating that it may be used as an alternative assay for ASFV detection.

2.4.1 Introduction

African swine fever (ASF), a highly contagious swine viral disease, characterized by a wide range of clinical signs from subclinical signs to sudden death that often occurs within 7 − 10 days but can be as early as 4 days after infection (Bellini, Rutili, & Guberti, 2016). It has attracted worldwide attention since its spread through Western Europe and Asia in 2017, and particularly to China, the largest pork producer in the world (Ge et al., 2018). The outbreak has caused severe economic losses in the global swine industry. Currently, the new and ongoing outbreaks are reported in 24 countries in three continents: 11 in Europe, 9 in Asia and 4 in Africa (Dixon, Sun, & Roberts, 2019; Lu et al., 2015). Previous studies demonstrated that the worldwide epidemic situation may dramatically increase the risk of introduction to ASF-free countries, such as the USA and Japan (Ito, Jurado, Sanchez-Vizcaino, & Isoda, 2019; Jurado et al., 2019).

African swine fever virus (ASFV) is the causative agent of ASF, the only member of the family *Asfarviridae* (Alonso et al., 2018). It's a large double-stranded DNA virus, with a linear genome of 173–193 kb long, encoding 151–167 open reading frames (ORFs) (Salas & Andres,

2013). Currently there's no specific treatment or effective vaccine available to fight the disease. Therefore, ASF control mainly relies on classic measures, including early detection, movement control, and depopulation of the infected animals. Real-time PCR assays are highly sensitive, specific and rapid techniques, and are widely used for ASFV detection around the world including the USA (OIE, 2019; SPS, 2017; Zsak et al., 2005).

Compared to other molecular diagnostic methods, such as loop-mediated isothermal amplification (LAMP), recombinase polymerase amplification (RPA), bead-based multiplex PCR and whole genome sequencing, the real-time PCR assay is considered more reliable, sensitive and cost effective (O'Donnell et al., 2019; Wang, Yu, et al., 2019; Wang, Wang, Geng, & Yuan, 2017; Xiao et al., 2018). Although several ASFV real-time PCR assays were developed recently (Fernandez-Pinero et al., 2013; Haines, Hofmann, King, Drew, & Crooke, 2013; McKillen et al., 2010; Wang, Jia, et al., 2019), their strain coverage and detection sensitivity can be further improved, and an internal control should be included to ensure detection accuracy.

The major capsid protein gene, p72, is used in most ASFV PCR assays including the widely accepted Zsak assay (Zsak et al., 2005) that has been used for ASF surveillance around the world. Yet, sequence analysis revealed that each primer used in the Zsak assay has one mismatching base against most of the 77 p72 gene sequences currently available in the GenBank, and the 23 p72 sequences generated at FADDL. Additionally, the two primers have very different annealing temperatures. In this study, we have redesigned the primers of the Zsak assay, added a new set of primers and probes to cover the region upstream of that used by the Zsak assay based on the

analysis of all currently available sequences of the *p72* gene, and formed a multiplex assay to increase the strain coverage and diagnostic sensitivity of the assay.

2.4.2 Methods and materials

2.4.2.1 Virus strains

The 26 ASFV strains, 9 classical swine fever virus (CSFV) strains, and 7 serotype strains of food and mouth disease virus (FMDV), including A, O, Asia1, C, Sat1, Sat2 and Sat3, were supplied by the United States Department of Agriculture (USDA) Foreign Animal Disease Diagnostic Laboratory (FADDL), located at the Plum Island Animal Disease Center, Orient Point, New York, US. All work involving the use of live ASFV, CSFV and FMDV (Table 2.4.3) strains were conducted at FADDL, National Veterinary Services Laboratories (NVSL), USDA.

Vesicular stomatitis virus (VSV) serotypes New Jersey (VSV-NJ) and Indiana (VSV-IN), Seneca Valley virus -1 (SVV-1), porcine reproductive and respiratory syndrome virus type 2 (PRRSV-2), swine influenza virus (SIV) and porcine circovirus type 2 (PCV2) strains were provided by the Virology Section at KSVDL. The analytical analysis using the positive plasmids and the viral isolates other than ASFV, CSFV and FMDV was done at the Molecular Research and Development Section (Molecular R&D) at KSVDL.

2.4.2.2 Viral DNA/RNA extraction

The viral DNA or RNA was extracted using MagMAX™ Pathogen RNA/DNA Kit (ThermoFisher Scientific) or MagMAX™ CORE Nucleic Acid Purification Kit (ThermoFisher) from the cell cultures or clinical samples according to the manufacturer's instructions. To avoid

template degradation, eluted nucleic acid was appropriately diluted, aliquoted into smaller volumes, and stored in a −70°C freezer.

2.4.2.3 The ASFV primers and probes

Twenty-three full or partial ASFV p72 sequences were generated at FADDL. Other complete or partial p72 sequences were extracted from the GenBank database. All of these p72 sequences were aligned and analyzed with the Qiagen CLC Main Workbench 7 (Qiagen) for assay primer and probe designs. The Zsak assay (Zsak et al., 2005) was designed in a region that currently has 77 sequences available from the GenBank. The probe of the Zsak assay has perfect match to all 77 sequences, thus is used in this study without any change; however, each primer contains a mismatched base against all or 75 of the 77 p72 gene sequences. Primers in the Zsak assay also have a melting temperature (Tm) of 68.3 and 53.7°C (Table 2.4.1), respectively, which may not be optimized for amplification. A new pair of primers was designed to match 76 of the 77 sequences, and to bring Tms to close to 60°C (modified Zsak assay). Upstream of the Zsak design, there is a region that has 956 sequences available in the GenBank, and these sequences were used for the new target design, in hope to increase the assay's strain coverage and its diagnostic sensitivity (Bai et al., 2018). For the maximum strain coverage and better detection of future mutations, the newly designed assay and the modified Zsak assay were multiplexed, and both probes were labelled with 5′-FAM and 3′- BHQ1. The details of primers and probes are listed in Table 2.4.1.

2.4.2.4 The internal control primers and probe

The porcine house-keeping gene, beta actin (ACTB), was applied as an endogenous internal control to avoid false-negative results. However, limited porcine ACTB sequences were found in the NCBI GenBank database. To ensure the amplification from the majority of the pig populations, 61 porcine samples selected from the recent 5 years, 2015–2019, were used for ACTB gene sequencing and assay design. The ACTB gene fragments were amplified from the extracted DNA and proceed with Sanger sequencing (Genewiz, NJ). The resulting raw sequences were trimmed, assembled and aligned with the Qiagen CLC Main Workbench 7 (Qiagen). The primers and probe were designed based on the conserved region and labelled with 5′-Cy5 and 3′- BHQ2. Details of the primers and probe are listed in Table 2.4.1.

2.4.2.5 Real-time PCR composition and condition

The real-time PCR tests for diagnosis were performed as described (Wang, Das, et al., 2019; Wang, Feng, et al., 2019). Briefly, a master mix of a 20 µl reaction is composed of 5 µl of template DNA, 0.25 µM of each primer, 0.25 µM of each probe and 10 µl of 2X iQ™ Multiplex Powermix (Bio-Rad). The parameters for thermocycling starts with a denaturation step at 95°C for 10 min, followed by 45 cycles of denaturation at 95°C for 15 s and annealing/extension at 65°C for 45 s. The cycle threshold value (Ct) of different cell culture isolates of ASFV, CSFV and FMDV were generated with Applied Biosystems ABI 7500 Fast Real-Time PCR System (ThermoFisher Scientific) while assays of cloned ASFV DNA fragments, and cell culture isolates and clinical samples other than ASFV, CSFV and FMDV were performed with Bio-Rad CFX96

Touch Real-Time PCR Detection System. The results were analyzed with CFX Manager 3.0 (Bio-Rad) and GraphPad Prism 7 (GraphPad Software).

2.4.2.6 Construction of standard plasmid as positive amplification control

To develop the ASFV assay in our BSL-2 laboratory, ASFV p72 fragments were synthesized (Genewiz), which include targeted regions of primers and probes in all assays: the Zsak assay, the modified Zsak assay, and the newly designed assay. The positive standard plasmid was constructed by ligation of synthesized fragment into the pCR™ 2.1 vector using the TA Cloning kit according to the manufacturer's instruction (Invitrogen/ThermoFisher). Then, it was transformed in Mix & Go competent cells (Zymo), propagated in LB broth (Teknova Inc), and the plasmid construct was extracted using QIAprep Spin Miniprep Kit (Qiagen). The presence of cloned insert was confirmed by gel electrophoresis and Sanger sequencing (Genewiz).

2.4.2.7 Assay sensitivity analysis

The analytical sensitivity was firstly studied by standard curves generated with triplicates of 10-fold serial dilutions of the standard plasmid. To mimic a clinical testing condition, the standard plasmid was serially diluted in the nucleic acid extraction from porcine tissue homogenates to supply with naturally occurring internal control template of the *ACTB* gene. The DNA copy number of the last dilution that still amplifies was calculated as the limit of detection (LOD). Similarly, ASFV cell culture isolates were also used to generate standard curves with 10-fold serial dilutions in triplicate for further sensitivity analysis. The median tissue culture

infectious dose (TCID50) of the last dilution with positive Ct values was calculated as the LOD for cultured viruses.

2.4.2.8 Assay specificity analysis

The specificity was evaluated in silico with the online NCBI primer designing tool, Primer-Blast (https://www.ncbi.nlm.nih.gov/tools/primer-blast/), followed with the experimental evaluation using cell culture isolates or challenged pig blood samples of common swine disease pathogens, including ASFV, CSFV, FMDV, VSV-NJ, VSV-IN, SVV-1, PRRSV-2, SIV and PCV2, and clinical samples that were positive to specific pathogens including bovine viral diarrhoea virus (BVDV), SVV-1, PRRSV-2, SIV, porcine parainfluenza virus type 1 (PPIV-1), PCV2, porcine circovirus type 3 (PCV3), rotavirus group A (RVA), rotavirus group B (RVB), rotavirus group C (RVC), porcine epidemic diarrhoea virus (PEDV), porcine delta coronavirus (PDCoV) and transmissible gastroenteritis coronavirus (TGEV).

2.4.2.9 Comparison of the performance of the singular assay with the multiplex assay

The multiplex assay of the modified Zsak assay and the new assay was compared to three singleplex assays, the original Zsak assay (Zsak et al., 2005), the modified Zsak assay and the newly designed assay, using standard curves generated by both the standard control plasmid and two ASFV cell culture isolates. The performance of the assays was compared in terms of LOD, amplification efficiency and correlation coefficient generated from the linear regression curves. To ensure that swine blood is not interfering with the assay performance, standard curves using the control plasmid were spiked with nucleic acid extracted from pig blood (Figure 2.4.1).

2.4.3 Results

2.4.3.1 Primer and probe design and coverage analysis of ASFV strains *in silico*

In total, 1,012 ASFV complete or partial p72 genes were downloaded from the GenBank database by searching keywords, 'ASFV p72'. In addition, 23 ASFV *p72* gene sequences were generated at FADDL. Among these sequences, 100 sequences included the target region used in the Zsak assay (Zsak et al., 2005) design. The forward primer has a single nucleotide mismatch in all 100 sequences; the reverse primer has a single nucleotide mismatch in 98 of the 100 sequences. Although both mismatches are located close to the 5′ end of the primers, and may still amplify, they have a Tm of 68.3 and 53.7°C (assessed in Primer3), respectively, thus may not be optimized for amplifications. The modified primers (Table 2.4.1) have perfect matches to 99 of the 100 sequences (99.0%), and the modified Zsak assay still uses the probe designed in the Zsak assay. To cover the most published strain sequences in the GenBank, the region upstream of the Zsak assay, and close to the 3′ end of ASFV p72 gene was selected for the new assay design, from which 979 of the 1,035 sequences covered this region. In silico analysis indicated the new assay has perfect match to 960 of the 979 (98.1%) sequences. To get the maximum coverage and include more diverse strains during the evolution, the modified Zsak assay and the new assay were multiplexed. Analyzed with the 994 sequences containing at least one of the targeted regions, the overall coverage of the multiplex assay is 98.4% (978/994) (Table 2.4.1).

Among 23 ASFV sequenced at FADDL, the sequences of 15 isolates were submitted to NCBI GenBank and the accession numbers are from MN886925 to MN886939. The other eight

isolates do not meet the submission requirement as their sequences were not fully covered with reads from both strands by Sanger sequencing.

2.4.3.2 Pig beta actin gene (ACTB) gene sequencing and primer and probe design

Sixty-one partial pig ACTB genes were sequenced from porcine di- agnostic samples of different cases collected during 2015–2019 in KSVDL, of which 5 tonsils were collected in 2015; 3 tonsils and 1 pooled tissue in 2016; 6 pooled tissues, 3 lungs and 1 intestine in 2017; 14 tonsils, 4 pooled tissues, 2 intestines and 1 lung in 2018 and 9 pooled tissues, 5 intestines, 4 lungs, 2 foetuses and 1 blood sample in 2019 (data not shown). Combined with 8 available pig ACTB sequences in GenBank database, one set of primers and probe was designed targeting the conserved region. In silico analysis indicated the coverage was 100% (69/69) (Table 2.4.1).

2.4.3.3 Analytical sensitivity of the multiplex real-time PCR assay on positive standard plasmids and ASFV cell culture isolates

The multiplex assay was comprised of the newly designed assay and the modified Zsak assay targeting ASFV *p72* gene and the porcine *ACTB* gene as the endogenous internal control. Analytical sensitivity was firstly conducted using standard curves generated with the standard plasmid and analyzed by plotting the Cts against log dilution factors. The results indicated that the PCR amplification efficiencies were 102.8% with correlation coefficient (R^2) >.999 (Figure 2.4.1a). The LOD calculated was 6 copies per PCR reaction. The standard curve showed that the internal control *ACTB* gene had no interference to target gene amplification (Figure 2.4.1a).

To make sure that the assay sensitivity is not compromised when testing on viral DNA, two ASFV cell culture isolates, the Georgia strain and the Uganda strain, were then applied as templates for the assay's sensitivity analysis. The standard curves generated by 10-fold dilutions were plotted with Cts against log dilution factors. The amplification efficiencies were 94.7% for the Georgia strain and 99.8% for the Uganda strain with $R^2 > .998$ (Figure 2.4.2a). The LODs were around 1.25 TCID50 per reaction for the Georgia strain and around 0.14 TCID50 per reaction for the Uganda strain. The standard curves showed the internal control *ACTB* gene had no interference to target gene amplification (Figure 2.4.2a).

2.4.3.4 Comparison of multiplex and singular assays on positive standard plasmid and ASFV isolates

In comparison with the multiplex assay (Figures 2.4.1a and 2.4.2a), the standard curves of three singular assays, the newly designed assay, the modified Zsak assay and the original Zsak assay (Zsak et al., 2005), were performed with both the standard plasmid and ASFV cell culture isolates. As shown in Figure 2.4.1b–2.4.1d, amplification efficiencies of the three assays using the standard plasmid were between 90%– 100% and the R^2 values were greater than .992, comparative to the multiplex assay. However, the LODs of the Zsak assay and the modified Zsak assay were one log lower than the new designed assay and the multiplex assay. For ASFV cell culture isolates, the results indicated similar performance of the singular and multiplex assays in terms of amplification efficiencies (90%–100%), R^2 values (>.991) and LODs. However, the Zsak assay had Ct values around 40 at the final dilution, about 3 Ct value higher than the multiplex assay and

the other two singular assays (modified Zsak assay and the newly designed assay) for the same dilutions of the viruses (Figure 2.4.2).

Additionally, 24 more ASFV strains isolated from different countries or regions were applied for the comparison among the multiplex assay, and the three singular assays. Except the Kitali strain, the multiplex assay has the lowest Ct values while the Zsak assay has the highest. Interestingly, the Kitali strain had Ct value 8–10 Ct higher in the newly designed assay than the Zsak assay and the modified Zsak assay, which targeted different region in ASFV *p72* gene (Table 2.4.2). Sequenced and compared the targeted region, one nucleotide mismatch at the middle of the reverse primer weakened the amplification. However, the multiplex assay has the similar result as the modified Zsak assay, which had the lowest Ct value (Table 2.4.2).

2.4.3.5 Analytical specificity of the multiplex real-time PCR assay

The specificity of primers and probes in the study was firstly analyzed in silico with Primer-Blast, which presented unique viral target for each set of the assay. Then, it was experimentally verified with viral isolates, challenged pig blood samples and the clinical samples positive of target or non-target pathogens. The results demonstrated good specificity of the assay, which could specifically detect ASFV positive samples without detection of non-target pathogens, including CSFV, FMDV, VSV-NJ, VSV-IN, SVV-1, PRRSV-2, SIV, BVDV, PPIV-1, PCV2, PCV3, RVA, RVB, RVC, PEDV, PDCoV and TGEV (Table 2.4.3).

2.4.4 Discussion

The recent spread of ASFV in Asia, especially in the biggest pork production and consumption country, China, has triggered global concerns. Tremendous ecological losses would occur if it emerged in the United States (Jurado et al., 2019). Without ASF specific treatment and an effective vaccine to use, rapid and accurate laboratory diagnosis for ASFV identification is a critical integrated component of ASF management.

In this study, we developed and evaluated a multiplex real-time PCR assay for ASFV detection. The assay we developed was a new design multiplexed with the modified Zsak assay (Zsak et al., 2005), which has increased strain coverage and detection sensitivity. The Zsak assay has been used for ASFV diagnostics in the USA (SPS, 2017), which targets the middle region of ASFV p72 gene. However, this p72 gene region only has 77 sequences available in the GenBank. From the analysis of the 1,012 available p72 sequences, we identified another region in the 5′ end of the gene, and upstream of the Zsak assay region, which included 956 sequences. In general, the more sequences used in the assay design, the better diagnostic sensitivity will be (Bai et al., 2018).

Primer mismatches can often affect primer binding to the template, and thus affect detection sensitivity. In the Zsak assay, the forward primer has a mismatch in 98 of the 100 sequences, and the reverse primer has a mismatch to all 100 sequences. Both mis- matches are located close to the less critical 5′ end of the primers, thus may still amplify. However, the Tm for the forward and reverse primers is at 68.3°C and 53.7°C, respectively, that is a Tm difference of 14.6°C. Together with the mismatches in the primers, PCR amplification with the Zsak primers may not be optimized and was also discussed in the previous study (Stadhouders et al., 2010). Our

data also showed a lower analytical sensitivity for the Zsak assay as compared with the newly designed assays in this study (Table 2.4.3). Location of a mismatching base can be critical to amplification. The reverse primer in the newly designed assay has a mismatching base towards the 3′ end, and that single base mismatch has caused 8–10 Ct shift on the Kitali strain compared to the Zsak and modified Zsak assays. Because the multiplex assay has both the new target and the modified Zsak design, the detection of this Kitali strain was not affected and would be significantly affected if the new design was used as a single-plex assay. Therefore, using two molecular targets can have obvious benefits in detecting strains with divergent genomes, including new genotypes that may merge in the future. The reason is that for a given strain, the chance to have simultaneous mutations on two molecular targets is much lower than what may occur at a single locus (Bai et al., 2018).

Another advantage of the ASFV multiplex assay we developed is that it is more sensitive as compared to the single-plex Zsak assay (Zsak et al., 2005). Based on the analysis of standard plasmid, the ASFV multiplex assay showed higher sensitivity (6 copies per reaction) compared to other ASFV real-time PCR assays (Fernandez- Pinero et al., 2013; Haines et al., 2013; McKillen et al., 2010; Wang, Jia, et al., 2019; Zsak et al., 2005), LAMP assays (James et al., 2010; Wang, Yu, et al., 2019), RPA assays (Wang et al., 2017) or regular PCR assays (Gonzague, Plin, Bakkali-Kassimi, Boutrouille, & Cruciere, 2002; Luo et al., 2017; Xiao et al., 2018). Although LODs of the ASFV multiplex assay and Zsak assay are the same using cell culture isolates, our new assay is 3-Ct lower than the Zsak assay, indicating it is analytically a more sensitive and reliable assay.

Internal controls are commonly used to monitor extraction efficiencies and potential PCR inhibitions. To ensure the accuracy of the test results, and to minimize false-negative detection rate, we also included the pig *ACTB* gene as an endogenous internal control. Others reported the use of exogenous internal controls, including competitive (Gonzague et al., 2002) and non-competitive (Haines et al., 2013) controls to monitor nucleic acid extraction efficiency and PCR inhibitions contained in the samples. However, using exogenous internal control requires the preparation of control DNA or RNA, and the inoculation of the internal control into each sample prior to extraction. We chose to use a pig house-keeping gene as an endogenous internal control that is embedded in most types of samples already and does not require extra steps for internal control preparation or spike-in inoculation. Due to the lack of the *ACTB* sequences in the GenBank (n = 8), we sequenced 61 partial *ACTB* genes from clinical samples of different diagnostic cases submitted to KSVDL during the recent 5 years in order to detect different pig breeds. The performance of the internal control was evaluated by analytical analysis, which showed no interaction with the ASFV targets. The internal control was detected in all pig samples we have tested so far indicating a good diagnostic performance. Addition of nucleic acid extracted from swine blood did not affect the performance of the assay.

In conclusion, to improve the diagnostic sensitivity of the Zsak assay, we developed and evaluated an ASFV multiplex assay, which covers the 5′ end region of *p72* and incorporated with pig *ACTB* gene as the endogenous internal control. In silico analysis showed 98.5% (955/970) of strains were covered; LOD was 6 copies of positive standard plasmids per reaction or about 0.1–1

TCID50 of ASFV isolates per reaction; and only ASFV strains were detected rather than non-targeted common swine viruses tested in this study. Furthermore, the detection of 26 ASFV isolates with different country origins by the multiplex assay performed better than the Zsak assay. Our newly developed multiplex ASFV assay detects a broader range of strains and is more sensitive than the Zsak assay.

2.4.5 Reference

Alonso, C., Borca, M., Dixon, L., Revilla, Y., Rodriguez, F., & Escribano, J. M., & Ictv Report Consortium (2018). ICTV virus taxonomy profile: Asfarviridae. Journal of General Virology, 99, 613–614. https://doi. org/10.1099/jgv.0.001049

Bai, J., Trinetta, V., Shi, X., Noll, L. W., Magossi, G., Zheng, W., … Nagaraja, T. G. (2018). A multiplex real-time PCR assay, based on invA and pagC genes, for the detection and quantification of Salmonella enterica from cattle lymph nodes. Journal of Microbiological Methods, 148, 110–116. https://doi.org/10.1016/j.mimet.2018.03.019

Bellini, S., Rutili, D., & Guberti, V. (2016). Preventive measures aimed at minimizing the risk of African swine fever virus spread in pig farm- ing systems. Acta Veterinaria Scandinavica, 58(1), 82. https://doi. org/10.1186/s13028-016-0264-x

Dixon, L. K., Sun, H., & Roberts, H. (2019). African swine fever. Antiviral Research, 165, 34–41. https://doi.org/10.1016/j.antiv iral.2019.02.018

Fernandez-Pinero, J., Gallardo, C., Elizalde, M., Robles, A., Gomez, C., Bishop, R., … Arias, M. (2013). Molecular diagnosis of African swine fever by a new real-time PCR using universal probe library. Transboundary and Emerging Diseases, 60, 48–58. https://doi.org/10.1111/ j.1865-1682. 2012.01317.x

Ge, S., Li, J., Fan, X., Liu, F., Li, L., Wang, Q., … Wang, Z. (2018). Molecular characterization of African swine fever virus, China, 2018. Emerging Infectious Diseases, 24, 2131–2133. https://doi.org/10.3201/eid2411.181274

Gonzague, M., Plin, C., Bakkali-Kassimi, L., Boutrouille, A., & Cruciere, C. (2002). Development of an internal control for the detection of the African swine fever virus by PCR. Molecular and Cellular Probes, 16, 237–242. https://doi.org/10.1006/mcpr.2002.0416

Haines, F. J., Hofmann, M. A., King, D. P., Drew, T. W., & Crooke, H. R. (2013). Development and validation of a multiplex, real-time RT PCR assay for the simultaneous detection of classical and African swine fever viruses. PLoS ONE, 8, e71019. https://doi.org/10.1371/journal.pone. 0071019

Ito, S., Jurado, C., Sanchez-Vizcaino, J. M., & Isoda, N. (2019). Quantitative risk assessment of African swine fever virus introduction to Japan via pork products brought in air passengers'

luggage. Transboundary and Emerging Diseases, 67, 894–905. https://doi.org/10.1111/tbed.13414

James, H. E., Ebert, K., McGonigle, R., Reid, S. M., Boonham, N., Tomlinson, J. A., … King, D. P. (2010). Detection of African swine fever virus by loop-mediated isothermal amplification. Journal of Virological Methods, 164, 68–74. https://doi.org/10.1016/j.jviromet.2009.11.034

Jurado, C., Mur, L., Aguirreburualde, M. S. P., Cadenas-Fernandez, E., Martinez-Lopez, B., Sanchez-Vizcaino, J. M., & Perez, A. (2019). Risk of African swine fever virus introduction into the United States through smuggling of pork in air passenger luggage. Scientific Reports, 9, 14423. https://doi.org/10.1038/s41598-019-50403-w

Lu, W. H., Tun, H. M., Sun, B. L., Mo, J., Zhou, Q. F., Deng, Y. X., … Ma, J. Y. (2015). Re-emerging of porcine respiratory and reproductive syn- drome virus (lineage 3) and increased pathogenicity after genomic recombination with vaccine variant. Veterinary Microbiology, 175, 332–340. https://doi.org/10.1016/j.vetmic.2014.11.016

Luo, Y. Z., Atim, S. A., Shao, L. N., Ayebazibwe, C., Sun, Y., Liu, Y., … Qiu, H. J. (2017). Development of an updated PCR assay for detection of African swine fever virus. Archives of Virology, 162, 191–199. https:// doi.org/10.1007/s00705-016-3069-3

McKillen, J., McMenamy, M., Hjertner, B., McNeilly, F., Uttenthal, A., Gallardo, C., … Allan, G. (2010). Sensitive detection of African swine fever virus using real-time PCR with a 5' conjugated minor groove binder probe. Journal of Virological Methods, 168, 141–146. https:// doi.org/10.1016/j.jviromet.2010.05.005

O'Donnell, V. K., Grau, F. R., Mayr, G. A., Sturgill Samayoa, T. L., Dodd, K. A., & Barrette, R. W. (2019). Rapid sequence-based characterization of African swine fever virus using the Oxford Nanopore min- ion sequence sensing device and a companion analysis software tool. Journal of Clinical Microbiology, 58(1), e01104-19. https://doi.org/10.1128/JCM.01104-19

OIE (2019). Manual of diagnostic tests and vaccines for terrestrial animals [online]. Paris, France: OIE. African swine fever. Retrieved from https://www.oie.int/fileadmin/Home/eng/Health_standards/tahm/3.08.01_ASF.pdf

Salas, M. L., & Andres, G. (2013). African swine fever virus morpho- genesis. Virus Research, 173, 29–41. https://doi.org/10.1016/j.virusres.2012.09.016

SPS (2017). Surveillance Guidance to Support the SPS Continuity of Business Plan during an FMD, CSF, or ASF Outbreak.

Stadhouders, R., Pas, S. D., Anber, J., Voermans, J., Mes, T. H. M., & Schutten, M. (2010). The effect of primer-template mismatches on the detection and quantification of nucleic acids using the 5′ Nuclease Assay. Journal of Molecular Diagnostics, 12, 109–117. https://doi.org/10.2353/jmoldx.2010.090035

Wang, A., Jia, R., Liu, Y., Zhou, J., Qi, Y., Chen, Y., … Zhang, G. (2019). Development of a novel quantitative real-time PCR assay with lyophilized powder reagent to detect African

swine fever virus in blood samples of domestic pigs in China. Transboundary and Emerging Diseases, 67(1), 284–297. https://doi.org/10.1111/tbed.13350

Wang, D., Yu, J., Wang, Y., Zhang, M., Li, P., Liu, M., & Liu, Y. (2019). Development of a real-time loop-mediated isothermal amplification (LAMP) assay and visual LAMP assay for detection of African swine fever virus (ASFV). Journal of Virological Methods, 276, 113775. https://doi.org/10.1016/j.jviromet.2019.113775

Wang, J., Wang, J., Geng, Y., & Yuan, W. (2017). A recombinase polymerase amplification-based assay for rapid detection of African swine fever virus. Canadian Journal of Veterinary Research, 81, 308–312.

Wang, Y., Das, A., Zheng, W., Porter, E., Xu, L., Noll, L., … Bai, J. (2019). Development and evaluation of multiplex real-time RT-PCR assays for the detection and differentiation of foot-and-mouth disease virus and Seneca Valley virus 1. Transboundary and Emerging Diseases, 67(2), 604–616. https://doi.org/10.1111/tbed.13373

Wang, Y., Feng, Y., Zheng, W. L., Noll, L., Porter, E., Potter, M., … Bai, J. F. (2019). A multiplex real-time PCR assay for the detection and differentiation of the newly emerged porcine circovirus type 3 and continuously evolving type 2 strains in the United States. Journal of Virological Methods, 269, 7–12. https://doi.org/10.1016/j.jviro met.2019.03.011

Xiao, L., Wang, Y., Kang, R., Wu, X., Lin, H., Ye, Y., … Li, X. (2018). Development and application of a novel Bio-Plex suspension array system for high-throughput multiplexed nucleic acid detection of seven respiratory and reproductive pathogens in swine. Journal of Virological Methods, 261, 104–111. https://doi.org/10.1016/j.jviro met.2018.08.017

Zsak, L., Borca, M. V., Risatti, G. R., Zsak, A., French, R. A., Lu, Z., … Rock, D. L. (2005). Preclinical diagnosis of African swine fever in contact-ex- posed swine by a real-time PCR assay. Journal of Clinical Microbiology, 43, 112–119. https://doi.org/10.1128/JCM.43.1.112-119.2005

Table 2.4.1 Primers and Probes from the reference ASFV assay and the ASFV assays designed in this study

PCR set	Target	Sequence (5'-3')	Tm (°C)	Amplicon (bp)	% Coverage (matched/total[a])		Ref.
Reference	p72	F: CCTCGGCGAGCGCTTTATCAC	68.3	78	0.0% (100.0% with 1 bp mismatch to each primer)		Zsak et al, 2005
		R: AACTCATTCACCAAATCCTT	53.7				
		Pr: FAM-CGATGCAAGCTTTAT-MGBNFQ	67				
Modified reference	p72	F: GGAAAYTCATTCACCAAATCCT	59.2	62	99.0% (99/100)		This study
		R: TTCGGCGAGCGCTTTAT	60.6				
		Pr: FAM-CGATGCAAGCTTTAT-MGBNFQ	67				Zsak et al, 2005
New design	p72	Fa: CCTCCRTAGTGGAAGGGTATGT	59.2 - 61.5[b]	75	98.1% (960/979)	98.4% (978/994) Combined	This study
		Fb: CCTCCGTAGTGAAAGGGTATGT	59.4				
		Fc: CCTCCGTAGTGGAAAGGTATGT	59.4				
		Ra: TGCTCATGGTATCAATCTTATCG	59.1				
		Rb: TGCTCATGGCATCAATCTTATC	60.1				
		Rc: GCTCACGGTATCAATCTTATCG	58.7				
		Pr: FAM-TTTCCMTCAAAGTTCTGCAGCTC-BHQ1	62.9 - 64.2[b]				
ACTB (PCR)	ACTB	F: GACCTGACCGACTACCTCATG	59.6	94	100.0% (69/69)		This Study
		R: TCTCCTTGATGTCCCGCAC	62.2				
		Pr: Cy5-CTACAGCTTCACCACCACGGC-BHQ2	65.3				
ACTB (sequencing)	ACTB	F: CATGTACGTGGCCATCCAGG	64.6	700			This study
		R: CTCGTCGTACTCCTGCTTGC	61.1				

a: Indicates number of matched sequences over total sequences used in the analysis; b: Tm range of degenerate primers. MGBNFQ: minor grove binder nonfluorescent quencher

Table 2.4.2 ASFV real time PCR assay results of 26 ASFV isolates tested with singular and multiplex assays

Strain Name	Ct values from different assays			
	Reference	Modified Reference	New design	Multiplex[a]
Georgia	29.4	27.1	27.7	27.1
Uganda	29.2	26.9	26.9	26.8
Africa 64 LEE	30.3	28.2	28.1	27.4
Bartlett II	29.9	27.8	27.5	27.0
Brazil	30.7	28.1	27.8	27.4
Brescia 68	30.8	28.7	28.8	27.9
Caserta 68	29.1	27.1	26.9	26.2
Davis	31.9	29.8	29.4	28.9
Diouroup II	30.5	28.4	28.0	27.6
Dominican Republic	30.7	28.5	28.8	28.0
French 86, Souche	34.0	31.0	31.0	26.5
Gasson	31.1	29.0	28.7	28.1
Haiti, ACC 871-78	31.6	29.4	29.1	28.8
Killean III	31.1	28.8	28.5	27.9
Kimaxia	29.3	27.2	27.1	24.9
Kitali, Sow I	21.2	19.0	29.4	20.0
LaGrantia	32.1	30.1	30.1	29.4
Lisbon 60	31.0	28.8	28.8	28.1
Malta	29.9	27.7	27.7	27.0
Nanuyuki	32.2	30.2	29.7	29.2
Paracambi II	29.6	27.6	27.4	26.7
Rhodesia Non-Had	28.2	27.4	27.2	26.7
Salamanca 2851	29.0	26.9	26.8	26.1
Spencer ACC 121-2	30.8	28.5	28.9	28.0
Trench I	31.4	29.4	29.2	28.6
Zaire II	27.0	24.8	24.6	24.1

a: Multiplexed with the modified reference design and the new design.

Table 2.4.3 Specificity of the ASFV multiplex real time PCR assay

Pathogen	Source	No. tested	Target gene	
			ASFV	ACTB
ASFV	Cell culture	26	+	+
CSFV-Paderborn (2.1)	Cell culture	1	-	+
CSFV-Parma 98 (Italy 98) (2.2)	Cell culture	1	-	+
CSFV-Vi 2(3)837/38/Germany 99 (2.3)	Cell culture	1	-	+
CSFV-Trem. Cong. 10/19/01 (GB 64) (3.1)	Cell culture	1	-	+
CSFV-Kanagawa (Japan 74) (3.4)	Cell culture	1	-	+
CSFV-Alfort 10/19/01 (France 68) (1.1)	Cell culture	1	-	+
CSFV-PAV 250 Vaccine	Cell culture	1	-	+
CSFV-Brescia (Italy NA) (1.3)	Cell culture	1	-	+
CSFV-Haiti-96	Blood	1	-	+
BVDV	Clinical sample	3	-	-[a]
FMDV-A	Cell culture	1	-	+
FMDV-O	Cell culture	1	-	+
FMDV-Asia1	Cell culture	1	-	+
FMDV-C	Cell culture	1	-	+
FMDV-Sat1	Cell culture	1	-	+
FMDV-Sat2	Cell culture	1	-	+
FMDV-Sat3	Cell culture	1	-	+
VSV-NJ	Cell culture	1	-	-[b]
VSV-IN	Cell culture	1	-	-[b]
SVV-1	Cell culture	1	-	-[b]
	Clinical sample	1	-	+
PRRSV-2	Cell culture	1	-	+
	Clinical sample	2	-	+
SIV	Cell culture	1	-	-[b]
	Clinical sample	2	-	+
PPIV-1	Clinical sample	2	-	+
PCV2	Cell culture	3	-	+
	Clinical sample	2	-	+
PCV3	Clinical sample	3	-	+
RVA	Clinical sample	5	-	+
RVB	Clinical sample	2	-	+

RVC	Clinical sample	5	-	+
PEDV	Clinical sample	2	-	+
PDCoV	Clinical sample	1	-	+
TGEV	Clinical sample	2	-	+

a: Pig beta actin genes weren't detected from the bovine samples; b: Pig beta actin genes weren't detected from the non-swine culture cells.

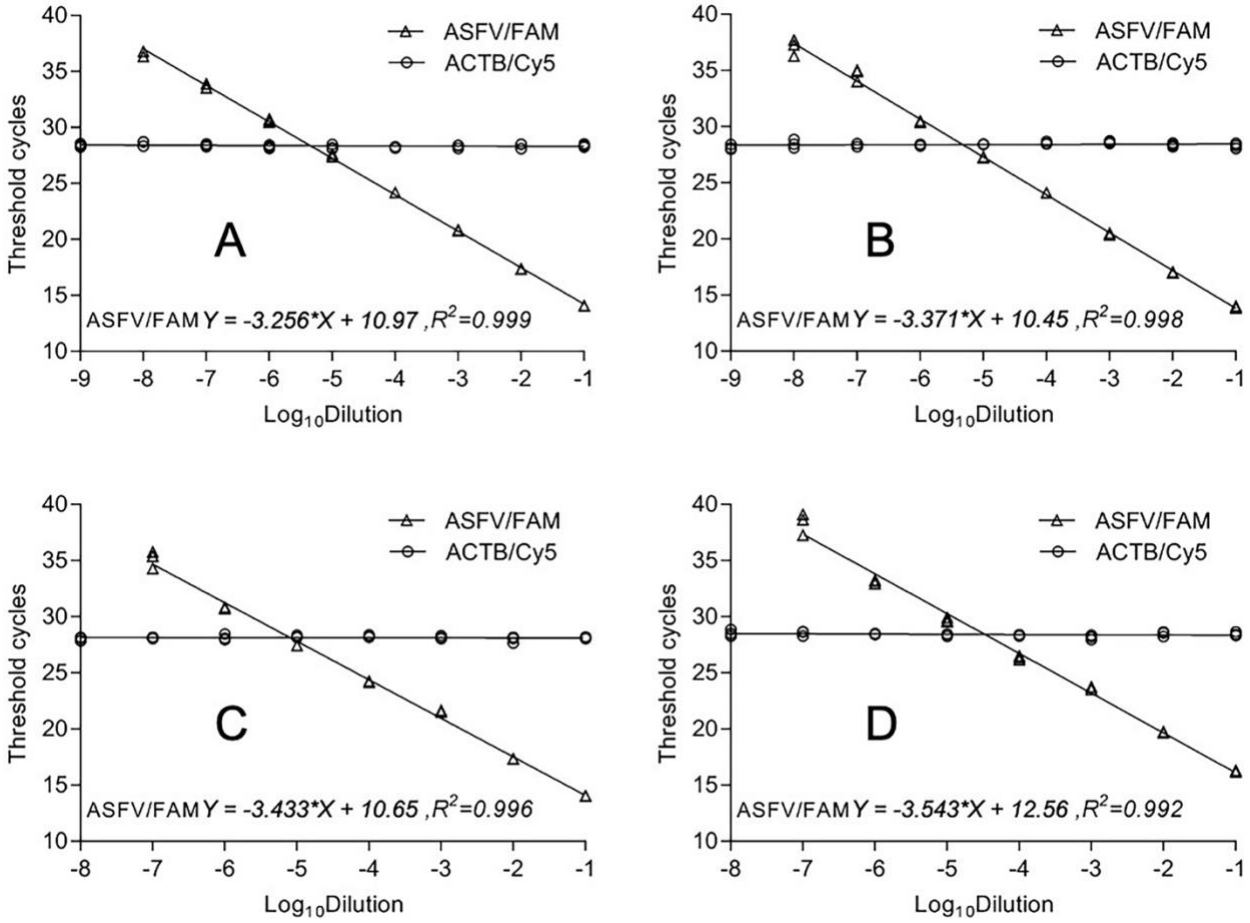

Figure 2.4.1 Standard curves of the ASFV assays with positive standard plasmids (A) multiplex assays; (B) new designed assays; (C) modified reference assays; and (D) the reference assay (Zsak et al., 2005) by serial dilutions of positive standard plasmids with the inclusion of the intrinsic internal control, *ACTB*.

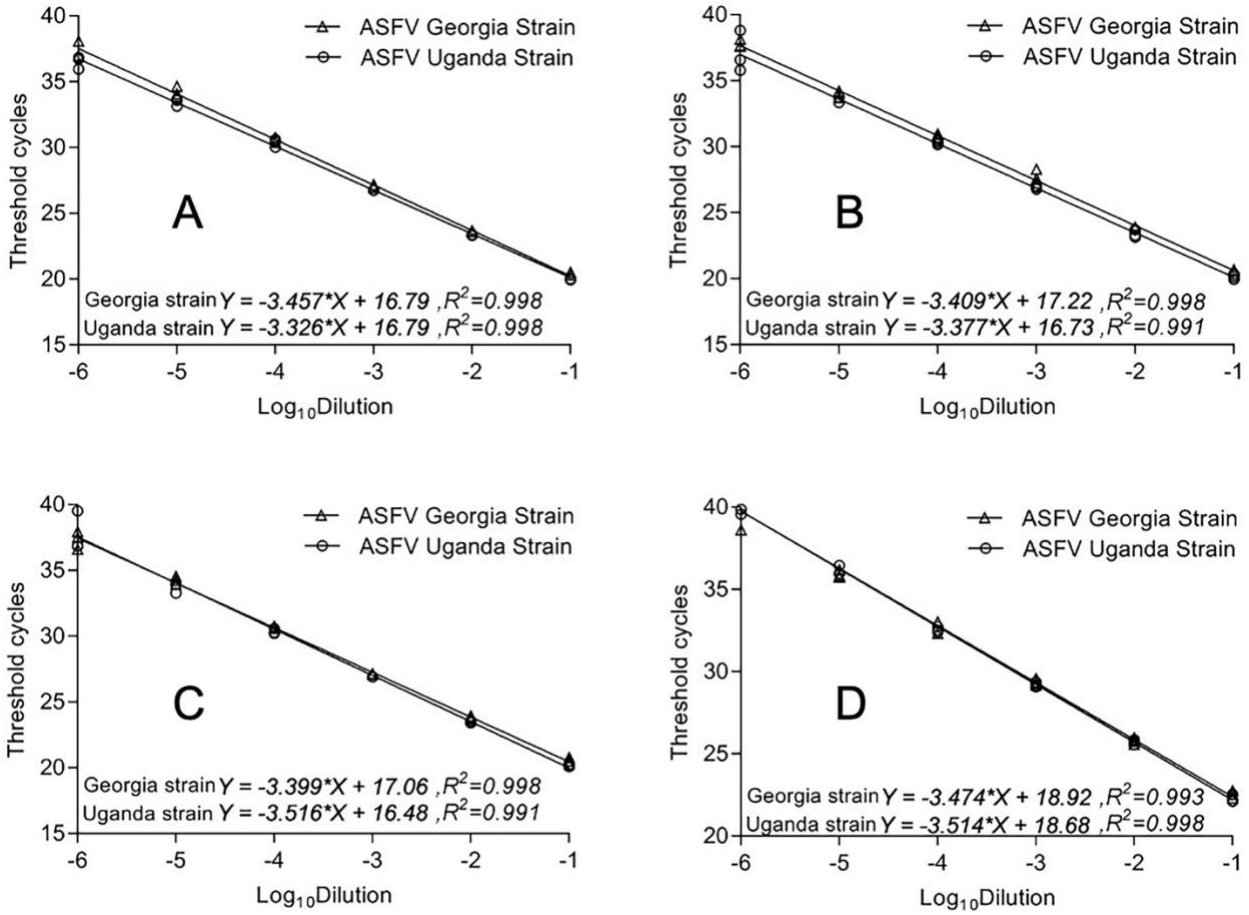

Figure 2.4.2 Standard curves of the ASFV assays with cell isolates

(A) multiplex assays; (B) new designed assays; (C) modified reference assays; and (D) the reference assay (Zsak et al., 2005) by serial dilutions of ASFV isolates, the Georgia strain and Uganda strain.

2.5 Development of a Luminex xTAG® assay for detection and differentiation of field strains and vaccine strains of type 2 porcine reproductive and respiratory syndrome virus (PRRSV-2) in the USA

Yin Wang, Wannarat Yim-im, Elizabeth Porter, Nanyan Lu, Joe Anderson, Lance Noll, Ying Fang, Jianqiang Zhang, Jianfa Bai

(Transboundary and Emerging Disease. 2010; 00:1-10)

Abstract: Porcine reproductive and respiratory syndrome (PRRS) remains as the most economically devastating disease in swine population in the USA. Due to high mutation rate of PRRS virus (PRRSV) genome, it's difficult to develop an accurate diagnostic assay. Four vaccines have been used in the US, namely Ingelvac PRRS® MLV, Ingelvac® ATP, Fostera® PRRS and Prime Pac® PRRS. For limited channels for target detection and diversity of the virus strains, real-time PCR is no longer a powerful tool to detect and differentiate the field strains from the vaccine strains. Luminex xTAG technology allows us to detect more molecular targets in a single reaction with the cost similar to real-time PCR. By analyzing all available 678 type 2 PRRSV (PRRSV-2) complete genome sequences, two pairs of primers were designed targeting the conserved regions of ORF4-ORF7, with high coverage of 98.8% (670/678) based on in silico analysis. The strains shared above 98% similarity of the complete genome with four vaccine strains were defined as the group of vaccine strains. One pair of primers for each group of vaccine strains was designed targeting on nsp2. *In silico* analysis showed the assay matched 94.7% (54/57) of Ingelvac PRRS® MLV strains and 100% of the other three groups of vaccine strains. Analytical sensitivity of the

Luminex assay was one to two logs lower than that of the reverse transcription real-time PCR assay. Evaluated with 417 PRRSV-2 positive clinical samples, 95% (396/417) samples can be detected by the Luminex assay. Compared to ORF5 sequencing results, the Luminex assay detected 92.4% (73/79) of MLV strains, 78.3% (18/23) of Fostera strains and 50% (2/4) of ATP strains. None of Prime Pac strain was detected either in ORF5 sequence alignment nor in the Luminex assay.

2.5.1 Introduction

Porcine reproductive and respiratory syndrome (PRRS) is one of the most economically significant infectious disease to the pork production in the USA. It was estimated that PRRS could result in $664 million losses in the national breeding and growing-pig herds annually. (Holtkamp et al., 2013) PRRS virus (PRRSV), a single stranded positive-sense RNA virus, is the etiological agent of the disease. Due to clear divergence, PRRSV was divided into two different species, PRRSV-1 and PRRSV-2 by the International Committee on Taxonomy of Viruses (ICTV) in 2016. (Kappes & Faaberg, 2015; Kuhn et al., 2016) Although some PRRSV-1 strains circulated have been reported (A. Wang et al., 2019), PRRSV-2 is the main species affecting the swine industry in the USA (Shi et al., 2013).

PRRSV-2 has the genome of about 15.5 kb in length, which contains more than10 open reading frames (ORFs). From 5’ UTR to 3’ UTR, ORF1a and ORF1b encode non-structural proteins (nsps), nsp1α, nsp1β, nsp2-nsp6, nsp7α, nsp7β and nsp8-nsp12, and ORF2-ORF7 encode structural proteins, GP2, E, GP3, GP4, GP5a, GP5, M and N, respectively. (Kappes & Faaberg,

2015) In which, nsp2 gene is well known as the most variable region with mutations and deletions (Allende et al., 2000; Tian et al., 2007). ORF5 encoded the major envelope protein is highly variable (N. H. Chen, Trible, Kerrigan, Tian, & Rowland, 2016; Meng, Paul, Halbur, & Morozov, 1995). Therefore, nsp2 and ORF5 have been used as the important targets for molecular epidemiology study and diagnostics to differentiate strains in studies. It is challenging to get accurate detection resulted from their high variation. (Murtaugh, Elam, & Kakach, 1995; Wang et al., 2017; Yu et al., 2017; M. X. Zhang et al., 2016) Furthermore, the use of modified live vaccine strains makes the virus detection more complicated, like shedding of the live vaccine strains or the vaccine-like strains (A. P. Wang et al., 2019). The commercial vaccines include four vaccines that have been used in the US, Ingelvac PRRS® MLV, Ingelvac® ATP, Fostera® PRRS and Prime Pac® PRRS (Kim, Kim, Cha, & Yoon, 2008; Kwon, Ansari, Pattnaik, & Osorio, 2008; Opriessnig et al., 2002; A. P. Wang et al., 2019). For virus control, it's necessary to differentiate the field strains from the vaccine strains.

Till now, several technologies have been applied for PRRSV detection and differentiation. Currently, the conventional multiplex reverse transcription PCR (RT-PCR) is still the most popular method to use (Hu et al., 2016; Li et al., 2017; Wu et al., 2017; K. Yang et al., 2017; Y. Zhao et al., 2019). Simultaneous detection of PRRSV by Real time PCR is becoming more frequently applied for high efficiency (N. Chen et al., 2019; Park et al., 2019). Lots of other technologies are also applied for its study, including restriction fragment length polymorphism (RFLP) (Ramirez et al., 2019), loop-mediated isothermal amplification (LAMP) (Park et al., 2016), melting curve

analysis (Sun et al., 2018), microarray (Erickson et al., 2018), Luminex xTAG (Xiao et al., 2018), droplet digital PCR (Q. Yang et al., 2017) and next generation sequencing (NGS) (J. Q. Zhang et al., 2017).

Luminex technology, the bead-based detection platform, has become an advanced system for multiplexed biological assays, including both protein and nucleic acid detection due to its powerful capability of multiplexing and the low cost comparable to real time PCR. (Clavijo, Hole, Li, & Collignon, 2006; Navidad, Griswold, Gradus, & Bhattacharyya, 2013). In this study, a Luminex assay was firstly developed to detect and differentiate the PRRSV field strains from the vaccine strains in the USA.

2.5.2 Methods and materials

2.5.2.1 Virus strains, viral RNA extraction and viral RNA of clinical samples

Prototype strains of Ingelvac PRRS® MLV, Ingelvac® ATP and Fostera® PRRS were kindly provided by Virology section in KSVDL. The viral RNA was extracted from 140 µl of cell culture by QIAamp Viral RNA Mini Kit (Qiagen, MD) according to the manufacturer's recommendations, and stored at −80 °C until use. Viral RNA extracted from 472 PRRSV positive clinical samples were kindly provided by Iowa State University Veterinary Diagnostic Laboratory (ISUVDL) to evaluate the performance of the Luminex assay.

2.5.2.2 Construction of positive standards of the PRRSV vaccine strains

Four fragments containing detection region and differentiation region of each vaccine strain were artificially synthesized (IDT, San Diego, CA) and cloned into the pCR™2.1 vector

using the original TA Cloning kit according to the manufacturer's instruction (Invitrogen, CA). The ligation products were then transformed into Mix & Go competent cells (Zymo), propagated in LB broth (Teknova Inc), and the plasmid constructs were extracted using QIAprep Spin Miniprep Kit (Qiagen). The presence of cloned inserts was confirmed by gel electrophoresis and Sanger sequencing (Genewiz). The primers used for cloning are also listed in Table 2.5.1.

2.5.2.3 Primer and probe designing

In total, 678 PRRSV-2 complete genome sequences available from GenBank database and in-house dataset were aligned with Qiagen CLC Genomic Workbench 7. Two pairs of primers targeting the PRRSV genes were designed at the conserved regions to detect all of the PRRSV-2 strains. To differentiate, one group of vaccine strains was defined as those shared 98% similarity of the vaccine strain at complete genome level (Key et al., 2003). One pair of primers targeting PRRSV-2 vaccine characterized region was designed to differentiate each vaccine or vaccine-like strains. The TAG sequences, reverse complementary to the anti-TAG sequences of Magplex TAG microspheres, were added at 5' end of the forward primers. To facilitate signal reporting, the 18-atom hexa-ethylene glycol spacer internal spacer (iSp18) was added between the TAG and target specific sequences to position the coupled sequences off the bead surface. The reverse primers were synthesized with biotin at the 5' end for virus positive signal reporting. (Figure 2.5.1 and Table 2.5.1)

In reverse transcription real-time PCR assay (RT-qPCR), one set of primers and probe was designed for each group of vaccine strains, Ingelvac PRRS® MLV (MLV), Ingelvac® ATP (ATP),

Fostera® PRRS (Fostera) and Prime Pac® (Prime Pac). All of the probes were labeled with 5′-FAM and 3′-BHQ1. Information of all primers and probes are listed in Table 2.5.1.

2.5.2.4 Luminex assay

Standard laboratory procedure was applied according to Chapter 5.3.3 in Luminex xMAP Cookbook (3rd edition), "Target-Specific PCR Sequence Detection with MagPlex-TAG Microspheres". Briefly, 20 pmol of each primer was used in the multiplex RT-PCR amplification with Qiagen One-step RT-PCR Kit (Qiagen, Valencia, CA) following the manufacturer's instructions. 2-5µl of PCR products was transferred into the 96-well plates containing 33 µl of tetramethylammonium chloride (TMAC) hybridization solution (3 M TMAC, Sigma, St. Louis, MO; 1% N-Lauroylsarcosine sodium salt solution, Sigma, St. Louis, MO; 50 mM Tris-HCl, Sigma, St. Louis, MO; 4 mM EDTA, Thermo Fisher Scientific, Waltham, MA) and the bead mixture comprised of 2,500 MagPlex-TAG Microsphere beads of each TAG set. Nuclease free water was added to total volume of 50 µl. After fast vortex, the mixture was denatured at 95°C for 2 min and hybridized at 50°C for 30 min. Shaking for 5 min, the beads were washed three times by plate magnet in 75 uL of TMAC Buffer and resuspended in 50uL 3 µg/mL of streptavidin-R-phycoerythrin (SAPE, MossBio, Pasadena, MD) for 15min at 52°C. Subsequently, the beads were washed three times with 50 uL of TMAC buffer. Beads were analyzed for internal bead color and SAPE reporter fluorescence on Bio-Plex 200 analyzer (Bio-Rad, Hercules, CA). The median fluorescence intensity (MFI) of at least 50 beads was computed for each TAG set.

2.5.2.5 RT-qPCR assay

The RT-qPCR reactions were performed as described (Wang, Das, et al., 2019). Briefly, a master mix of a 20 µl reaction is composed of equal amount of template RNA or DNA used in the Luminex assay, 0.5 µM of each primer, 0.25 µM of each probe, 10 µl reaction buffer and 2 µl of enzyme mix from Path-ID™ Multiplex One-Step RT-PCR Kit (Thermo Fisher Scientific). The thermocycling started with a reverse transcription step at 48°C for 10 min, a denaturation step at 95°C for 10 min, followed by 45 cycles of denaturation at 95°C for 15 s and annealing/extension at 60°C for 50 s. The cycle threshold values (Cts) were generated with CFX96 Touch Real-Time PCR Detection System. The results were analyzed with CFX Manager 3.0 (Bio-Rad) and GraphPad Prism 7 (GraphPad Software).

2.5.2.6 Comparison of Luminex assay and ORF5 sequencing

The ratio of MFI signal of sample-to-non-template control (S/N) was used to describe the results of Luminex assays. The cutoff of S/N was determined with PRRSV positive and negative samples. The ORF5 sequences of the clinical samples were sequenced by ISUVDL. They were aligned with vaccine strains by MAFFT (Katoh, Misawa, Kuma, & Miyata, 2002) and then the identity matrix was calculated with BioEdit7.2.5 (https://bioedit.software. informer.com/).

2.5.3 Results

2.5.3.1 Analysis of assay coverage to sequence dataset

Based on 678 PRRSV-2 complete genome sequences in the dataset described above, two sets of primers, targeting the conserved regions of ORF4, ORF5, ORF6 and ORF7, were designed for PRRSV-2 detection. *In silico* analysis showed the first set, named Detect1, matched 91.9%

(623/678) of strains and the second set, named Detect2, matched 83.3% (565/678) of the strains. The overall coverage for PRRSV-2 detection was 98.8%.

To differentiate, one group of vaccine strains was defined as those shared 98% similarity of complete genome with the vaccine strains (Key et al., 2003). The vaccine sequences were available in GenBank, AF066183 for MLV group, DQ988080 for ATP, AF494042 for Fostera and DQ779791 for Prime Pac. One pair of primers was designed for each group of the vaccine strains. Except the MLV set matched 94.7% (54/57) of strains, other sets matched 100% of the vaccine strains.

To evaluate performance of the Luminex assay, four RT-qPCR assays were developed. The primers and probes were designed based on the four vaccine strains. Information of all primers and probes are shown in Table 2.5.1.

2.5.3.2 Analytical sensitivity of the Luminex assay compared to the RT-qPCR assay on positive standard plasmids

The analytical sensitivity was firstly determined by standard curves generated with triplicates of 10-fold serial dilutions of positive standard plasmids. The real time PCR assay was analyzed by plotting their Ct values against log dilution factors. As shown in Figure 2.5.2, the PCR amplification efficiencies ranged from 92.1-97.4% with high correlations coefficient (R^2) all greater than 0.998. Corresponding to the RT-qPCR assays, the LODs of the Luminex assays were one log lower, Ct 34 for MLV, Ct 36 for ATP, Ct 37 for Fostera, and Ct 36 for Prime Pac. (Figure 2.5.2 and Table 2.5.2)

2.5.3.3 Analytical sensitivity of the Luminex assay compared to the RT-qPCR assay on cell culture isolates

The analytical sensitivity was then determined by standard curves generated with triplicates of 10-fold serial dilutions of cell culture isolates of the vaccine strains. The RT-qPCR assay was analyzed by plotting their Ct values against log dilution factors. As shown in Figure 2.5.3, the PCR amplification efficiency was 100.5% for MLV, 102.0% for ATP and 96.3% for Fostera. The R^2 ranged from 0.956 to 0.99. Corresponding to the RT-qPCR assays, the LODs of the Luminex assays showed two logs lower for MLV detection, one log lower for ATP detection and one log lower for Fostera detection. (Figure 2.5.3 and Table 2.5.2)

2.5.3.4 Comparison of the Luminex assay and ORF5 sequencing on clinical samples

The 472 PRRSV-2 samples from ISUVDL were tested by the Luminex assays, in which only 396 (83.9%) were PRRSV positive. To verify, 35 randomly selected negative samples were tested by the highly sensitive PRRSV real-time PCR assay in KSVDL. The results showed only 21 of the 76 samples were positive. It indicated that 55 of the remaining samples were PRRSV-negative. After adjusting the data based on this number, the Luminex assay would detect 95% (396/417) of the PRRSV-2-positive samples.

For vaccine differentiation, the ORF5 sequences were aligned and the identity matrix was calculated. The strains shared 99% similarity with the vaccine strain were grouped into the vaccine strains (Key et al., 2003). Compared to ORF5 sequence alignment results, the Luminex assay detected 92.4% (73/79) of MLV strains, 78.3% (18/23) of Fostera strains and 50% (2/4) of ATP

strains. None of Prime Pac strain was detected either in ORF5 sequence alignment nor in the Luminex assay. (Table 2.5.3)

2.5.4 Discussion

A multiplex Luminex assay was developed for PRRSV detection and differentiation of the filed strains from the four vaccine strains used in the USA. In silico analysis showed the assay could detect at least 98.8% of PRRSV-2 strains, but the clinical sample detection results showed the coverage was 95%. The gap may result from degradation of the viral RNA during long time storage or continued evolution of the current circulating strains.

The PRRSV vaccine-like strains have been reported (Balka et al., 2008; Eclercy et al., 2020; Opriessnig et al., 2002). In another study, the PRRSV strains sharing 98% similarity of complete genome with the four vaccine strains were categorized into respective vaccine groups (Key et al., 2003). Our sequence analysis of 678 complete genomes indicated nsp2 is the suitable region to differentiate the vaccine strains from field strains. However, sequencing the ORF5 region is the most frequently used method for PRRSV genotyping and for investigation of genetic relationship in clinical strains (Kim et al., 2013; Martin-Valls et al., 2014). Thus, the clinical samples in our study only included the information of ORF5 sequences. A cut-off of 99% identity of the ORF5 sequences to the vaccine strains was used to form the vaccine groups (Key et al., 2003). The non-ideal consistency (50%–92.4%) between the Luminex assay (targeting nsp2 region) and ORF5 sequencing for vaccine differentiation can come from defining the vaccine group based on two different levels of sequence analysis, a complete genome versus ORF5.

Evaluation on more clinical samples may be needed to illustrate the need of generating complete genome sequences against the use of ORF5 in defining the diversity and potential recombination of PRRSV field strains and their differentiation from the vaccine strains.

Similar to other Luminex assays (Gadsby, Hardie, Claas, & Templeton, 2010), sensitivity of our assay was compared with the real time PCR as the gold standard. The analytical sensitivity data showed promising results, only one log lower detection than the highly sensitive RT-qPCR assay on positive standard plasmids and one or two logs lower on cell culture isolates. 32 But the Luminex technology has its obvious advantages. Highly multiplexing capability is a major feature that real-time PCR-based technology cannot compete with (Bai et al., 2015; Glushakova et al., 2015); Luminex assays can also achieve higher strain coverage due to the fact that only two oligos may be required in the detection system (Wu et al., 2018). Most real-time PCR assays involve 3 oligos (2 primers and a probe), which can be difficult sometimes to have high strain coverage, especially for those that have more divergent genomes.

In conclusion, a Luminex assay was developed to rapidly detect and differentiate the PRRSV field strains and vaccine strains. Both in silico analysis and clinical sample testing showed high coverage of the assay, 98.8% and 95% respectively. Compared to the results of the RT-qPCR gold standard, the sensitivity of the Luminex assay was 1-2 log less. Its performance of differentiation was compared with ORF5 sequencing, which indicated 50-92.4% of consistency for the four vaccine strains. It needs to be clarified with further investigation.

2.5.5 Reference

Allende, R., Kutish, G. F., Laegreid, W., Lu, Z., Lewis, T. L., Rock, D. L., . . . Osorio, F. A. (2000). Mutations in the genome of porcine reproductive and respiratory syndrome virus responsible for the attenuation phenotype. Arch Virol, 145(6), 1149-1161. doi:10.1007/s007050070115

Bai, X., Liu, Z., Ji, S., Gottschalk, M., Zheng, H., & Xu, J. (2015). Simultaneous detection of 33 Streptococcus suis serotypes using the luminex xTAG® assay™. Journal of Microbiol Methods, 117, 95–99. https://doi.org/10.1016/j.mimet.2015.07.018

Balka, G., Hornyák, A., Bálint, A., Kiss, I., Kecskeméti, S., Bakonyi, T., & Rusvai, M. (2008). Genetic diversity of porcine reproductive and respiratory syndrome virus strains circulating in Hungarian swine herds. Veterinary Microbiology, 127(1–2), 128–135. https://doi. org/10.1016/j.vetmic.2007.08.001

Chen, N., Ye, M., Xiao, Y., Li, S., Huang, Y., Li, X., . . . Zhu, J. (2019). Development of universal and quadruplex real-time RT-PCR assays for simultaneous detection and differentiation of porcine reproductive and respiratory syndrome viruses. Transbound Emerg Dis, 66(6), 2271-2278. doi:10.1111/tbed.13276

Chen, N. H., Trible, B. R., Kerrigan, M. A., Tian, K. G., & Rowland, R. R. R. (2016). ORF5 of porcine reproductive and respiratory syndrome virus (PRRSV) is a target of diversifying selection as infection progresses from acute infection to virus rebound. Infection Genetics and Evolution, 40, 167-175. doi:10.1016/j.meegid.2016.03.002

Clavijo, A., Hole, K., Li, M., & Collignon, B. (2006). Simultaneous detection of antibodies to foot-and-mouth disease non-structural proteins 3ABC, 3D, 3A and 3B by a multiplexed Luminex assay to differentiate infected from vaccinated cattle. Vaccine, 24(10), 1693-1704. doi:10.1016/j.vaccine.2005.09.057

Erickson, A., Fisher, M., Furukawa-Stoffer, T., Ambagala, A., Hodko, D., Pasick, J., . . . Lung, O. (2018). A multiplex reverse transcription PCR and automated electronic microarray assay for detection and differentiation of seven viruses affecting swine. Transbound Emerg Dis, 65(2), e272-e283. doi:10.1111/tbed.12749

Gadsby, N. J., Hardie, A., Claas, E. C., & Templeton, K. E. (2010). Comparison of the Luminex Respiratory Virus Panel fast assay with in-house real-time PCR for respiratory viral infection diagnosis. J Clin Microbiol, 48(6), 2213-2216. doi:10.1128/JCM.02446-09

Glushakova, L. G., Bradley, A., Bradley, K. M., Alto, B. W., Hoshika, S., Hutter, D., … Benner, S. A. (2015). High-throughput multiplexed xMAP Luminex array panel for detection of twenty two medically important mosquito-borne arboviruses based on innovations in synthetic biology. Journal of Virological Methods, 214, 60–74. https://doi.org/10.1016/j.jviromet.2015.01.003

Holtkamp, D. J., Kliebenstein, J. B., Neumann, E. J., Zimmerman, J. J., Rotto, H. F., Yoder, T. K., . . . Haley, C. A. (2013). Assessment of the economic impact of porcine reproductive and respiratory syndrome virus on United States pork producers. Journal of Swine Health and Production, 21(2), 72-84.

Hu, L., Lin, X. Y., Nie, F. P., Yang, Z. X., Yao, X. P., Li, G. L., . . . Wang, Y. (2016). Simultaneous typing of seven porcine pathogens by multiplex PCR with a GeXP analyser. Journal of Virological Methods, 232, 21-28. doi:10.1016/j.jviromet.2015.12.004

Kappes, M. A., & Faaberg, K. S. (2015). PRRSV structure, replication and recombination: Origin of phenotype and genotype diversity. Virology, 479-480, 475-486. doi:10.1016/j.virol.2015.02.012

Katoh, K., Misawa, K., Kuma, K., & Miyata, T. (2002). MAFFT: A novel method for rapid multiple sequence alignment based on fast Fourier transform. Nucleic Acids Research, 30, 3059–3066

Key, K. F., Guenette, D. K., Yoon, K. J., Halbur, P. G., Toth, T. E., & Meng, X. J. (2003). Development of a heteroduplex mobility assay to identify field isolates of porcine reproductive and respiratory syndrome virus with nucleotide sequences closely related to those of modified live-attenuated vaccines. Journal of Clinical Microbiology, 41(6), 2433-2439. doi:10.1128/Jcm.41.6.2433-2439.2003

Kim, W. I., Kim, J. J., Cha, S. H., Wu, W. H., Cooper, V., Evans, R., . . . Yoon, K. J. (2013). Significance of genetic variation of PRRSV ORF5 in virus neutralization and molecular determinants corresponding to cross neutralization among PRRS viruses. Veterinary Microbiology, 162(1), 10-22. doi:10.1016/j.vetmic.2012.08.005

Kim, W. I., Kim, J. J., Cha, S. H., & Yoon, K. J. (2008). Different biological characteristics of wild-type porcine reproductive and respiratory syndrome viruses and vaccine viruses and identification of the corresponding genetic determinants. J Clin Microbiol, 46(5), 1758-1768. doi:10.1128/JCM.01927-07

Kuhn, J. H., Lauck, M., Bailey, A. L., Shchetinin, A. M., Vishnevskaya, T. V., Bao, Y., . . . Goldberg, T. L. (2016). Reorganization and expansion of the nidoviral family Arteriviridae. Arch Virol, 161(3), 755-768. doi:10.1007/s00705-015-2672-z

Kwon, B., Ansari, I. H., Pattnaik, A. K., & Osorio, F. A. (2008). Identification of virulence determinants of porcine reproductive and respiratory syndrome virus through construction of chimeric clones. Virology, 380(2), 371-378. doi:10.1016/j.virol.2008.07.030

Li, Y., Ji, G., Xu, X., Wang, J., Li, Y., Tan, F., & Li, X. (2017). Development and Application of an RT-PCR to Differentiate the Prevalent NA-PRRSV Strains in China. Open Virol J, 11, 66-72. doi:10.2174/1874357901711010066

Martin-Valls, G. E., Kvisgaard, L. K., Tello, M., Darwich, L., Cortey, M., Burgara-Estrella, A. J., . . . Mateu, E. (2014). Analysis of ORF5 and full-length genome sequences of porcine reproductive and respiratory syndrome virus isolates of genotypes 1 and 2 retrieved worldwide provides evidence that recombination is a common phenomenon and may produce mosaic isolates. J Virol, 88(6), 3170-3181. doi:10.1128/JVI.02858-13

Meng, X. J., Paul, P. S., Halbur, P. G., & Morozov, I. (1995). Sequence comparison of open reading frames 2 to 5 of low and high virulence United States isolates of porcine reproductive and respiratory syndrome virus. J Gen Virol, 76 (Pt 12), 3181-3188. doi:10.1099/0022-1317-76-12-3181

Murtaugh, M. P., Elam, M. R., & Kakach, L. T. (1995). Comparison of the structural protein coding sequences of the VR-2332 and Lelystad virus strains of the PRRS virus. Arch Virol, 140(8), 1451-1460. doi:10.1007/BF01322671

Navidad, J. F., Griswold, D. J., Gradus, M. S., & Bhattacharyya, S. (2013). Evaluation of Luminex xTAG gastrointestinal pathogen analyte-specific reagents for high-throughput, simultaneous detection of bacteria, viruses, and parasites of clinical and public health importance. J Clin Microbiol, 51(9), 3018-3024. doi:10.1128/JCM.00896-13

Opriessnig, T., Halbur, P. G., Yoon, K. J., Pogranichniy, R. M., Harmon, K. M., Evans, R., . . . Meng, X. J. (2002). Comparison of molecular and biological characteristics of a modified live porcine reproductive and respiratory syndrome virus (PRRSV) vaccine (ingelvac PRRS MLV), the parent strain of the vaccine (ATCC VR2332), ATCC VR2385, and two recent field isolates of PRRSV. J Virol, 76(23), 11837-11844. doi:10.1128/jvi.76.23.11837-11844.2002

Park, J. Y., Kim, S. H., Lee, K. K., Kim, Y. H., Moon, B. Y., So, B., & Park, C. K. (2019). Differential detection of porcine reproductive and respiratory syndrome virus genotypes by a fluorescence melting curve analysis using peptide nucleic acid probe-mediated one-step real-time RT-PCR. Journal of Virological Methods, 267, 29-34. doi:10.1016/j.jviromet.2019.02.008

Park, J. Y., Park, S., Park, Y. R., Kang, D. Y., Kim, E. M., Jeon, H. S., . . . Park, C. K. (2016). Reverse-transcription loop-mediated isothermal amplification (RT-LAMP) assay for the visual detection of European and North American porcine reproductive and respiratory syndrome viruses. J Virol Methods, 237, 10-13. doi:10.1016/j.jviromet.2016.08.008

Ramirez, M., Bauermann, F. V., Navarro, D., Rojas, M., Manchego, A., Nelson, E. A., . . . Rivera, H. (2019). Detection of porcine reproductive and respiratory syndrome virus (PRRSV) 1-7-4-type strains in Peru. Transbound Emerg Dis, 66(3), 1107-1113. doi:10.1111/tbed.13134

Shi, M., Lemey, P., Singh Brar, M., Suchard, M. A., Murtaugh, M. P., Carman, S., . . . Chi-Ching Leung, F. (2013). The spread of type 2 Porcine Reproductive and Respiratory Syndrome Virus (PRRSV) in North America: a phylogeographic approach. Virology, 447(1-2), 146-154. doi:10.1016/j.virol.2013.08.028

Sun, J., Bingga, G., Liu, Z., Zhang, C., Shen, H., Guo, P., & Zhang, J. (2018). A novel HRM assay for differentiating classical strains and highly pathogenic strains of type 2 porcine reproductive and respiratory syndrome virus. Mol Cell Probes, 39, 25-32. doi:10.1016/j.mcp.2018.03.004

Tian, K., Yu, X., Zhao, T., Feng, Y., Cao, Z., Wang, C., . . . Gao, G. F. (2007). Emergence of fatal PRRSV variants: unparalleled outbreaks of atypical PRRS in China and molecular dissection of the unique hallmark. PLoS One, 2(6), e526. doi:10.1371/journal.pone.0000526

Wang, A., Zhang, J., Shen, H., Zheng, Y., Feng, Q., Yim-Im, W., . . . Li, G. (2019). Genetic diversity of porcine reproductive and respiratory syndrome virus 1 in the United States of

America from 2010 to 2018. Vet Microbiol, 239, 108486. doi:10.1016/j.vetmic.2019.108486

Wang, A. P., Chen, Q., Wang, L. Y., Madson, D., Harmon, K., Gauger, P., . . . Li, G. W. (2019). Recombination between Vaccine and Field Strains of Porcine Reproductive and Respiratory Syndrome Virus. Emerging Infectious Diseases, 25(12), 2335-2337. doi:10.3201/eid2512.191111

Wang, Y., Das, A., Zheng, W., Porter, E., Xu, L., Noll, L., … Bai, J. (2019). Development and evaluation of multiplex real-time RT-PCR assays for the detection and differentiation of foot-and-mouth disease virus and Seneca Valley virus 1. Transboundary and Emerging Diseases, 67(2), 604–616. https://doi.org/10.1111/tbed.13373

Wang, P. P., Dong, J. G., Zhang, L. Y., Liang, P. S., Liu, Y. L., Wang, L., . . . Song, C. X. (2017). Sequence and Phylogenetic Analyses of the Nsp2 and ORF5 Genes of Porcine Reproductive and Respiratory Syndrome Virus in Boars from South China in 2015. Transboundary and Emerging Diseases, 64(6), 1953-1964. doi:10.1111/tbed.12594

Wu, X. L., Xiao, L., Lin, H., Yang, M., Chen, S. J., An, W., . . . Tang, Z. Z. (2017). A Novel Capillary Electrophoresis-Based High-Throughput Multiplex Polymerase Chain Reaction System for the Simultaneous Detection of Nine Pathogens in Swine. Biomed Res Int, 2017, 7243909. doi:10.1155/2017/7243909

Xiao, L., Wang, Y., Kang, R., Wu, X., Lin, H., Ye, Y., . . . Li, X. (2018). Development and application of a novel Bio-Plex suspension array system for high-throughput multiplexed nucleic acid detection of seven respiratory and reproductive pathogens in swine. J Virol Methods, 261, 104-111. doi:10.1016/j.jviromet.2018.08.017

Yang, Q., Xi, J., Chen, X., Hu, S., Chen, N., Qiao, S., . . . Bao, D. (2017). The development of a sensitive droplet digital PCR for quantitative detection of porcine reproductive and respiratory syndrome virus. Int J Biol Macromol, 104(Pt A), 1223-1228. doi:10.1016/j.ijbiomac.2017.06.115

Yu, L., Zhao, P., Dong, J., Liu, Y., Zhang, L., Liang, P., . . . Song, C. (2017). Genetic characterization of 11 porcine reproductive and respiratory syndrome virus isolates in South China from 2014 to 2015. Virol J, 14(1), 139. doi:10.1186/s12985-017-0807-4

Zhang, J. Q., Zheng, Y., Xia, X. Q., Chen, Q., Bade, S. A., Yoon, K. J., . . . Li, G. W. (2017). High-throughput whole genome sequencing of Porcine reproductive and respiratory syndrome virus from cell culture materials and clinical specimens using next-generation sequencing technology. Journal of Veterinary Diagnostic Investigation, 29(1), 41-50. doi:10.1177/1040638716673404

Zhang, M. X., Li, X. N., Cai, X. N., Qu, Y. J., Hu, D. F., Lv, L., . . . Xiao, Y. H. (2016). Evaluation of infection status in Chinese swinewith porcine reproductive and respiratory syndrome virus by nested RT-PCR targeting nsp2 gene. Infection Genetics and Evolution, 44, 55-60. doi:10.1016/j.meegid.2016.06.020

Zhao, H., Han, Q., Zhang, L., Zhang, Z., Wu, Y., Shen, H., & Jiang, P. (2017). Emergence of mosaic recombinant strains potentially associated with vaccine JXA1-R and predominant

circulating strains of porcine reproductive and respiratory syndrome virus in different provinces of China. Virol J, 14(1), 67. doi:10.1186/s12985-017-0735-3

Zhao, Y., Liu, F., Li, Q., Wu, M., Lei, L., & Pan, Z. (2019). A multiplex RT-PCR assay for rapid and simultaneous detection of four RNA viruses in swine. J Virol Methods, 269, 38-42. doi:10.1016/j.jviromet.2019.04.001

Table 2.5.1 Primers and probes used in PRRSV-2 Luminex assays and real time PCR assays

Primers	Target Gene	Sequence (5'-3')	T_m[a]	Amplicon (bp)	Coverage (matched/total)	
Primers used in Luminex assays						
Detect1-F	ORF6	ACTTACAATAACTACTAATACTCT/iSp18/CCTCGTGTTGGGTGGCAG	63.8	122	623/678 (91.9%)	670/678
Detct1-R	ORF7	Biotin-CAGCTGATTGACTGGCTGG	60.6			
Detect2-F	ORF4	CATAATCAATTTCAACTTTCTACT/iSp18/GCRACYGTTTTAGCCTGTCT	61.7	120	565/678 (83.3%)	(98.8%)
Detect2-R	ORF5	Biotin-GGCACGATACACCACAAARAARGC	65.7			
MLV-F	nsp2	TAACTTACACTTAACTATCATCTT/iSp18/ACATCAGCTCCGTCCGCA	64.1	116	54/57 (94.7%)	
MLV-R	nsp2	Biotin-TCAGCTTTTCTTTTTACCGTCCGA	65.2			
ATP-F	nsp2	ACATCAAATTCTTTCAATATCTTC/iSp18/GCTCTGGTATGACCACCACAG	60.6	107	17/17 (100%)	
ATP-R	nsp2	Biotin-CCTGAGATGCACAGCCTTATCA	62.6			
Fostera-F	nsp2	AATTTCTTCTCTTTCTTTCACAAT/iSp18/ATTATGGCAGCCCGATTTTGA	63.7	140	1/1 (100%)	
Fostera-R	nsp2	Biotin-CACTGGCCTGGAAATAAGTACA	59.2			
PrimePac-F	nsp2	TACAACATCTCATTAACATATACA/iSp18/GCCCTGGAGTGAGAGAAGTG	60.0	141	3/3 (100%)	
PrimePac-R	nsp2	Biotin-CGCCCGCATCTATACCGC	64.8			
Primers and probes used in RT-qPCR assays						
MLV-qF	nsp2	TGGCGCCGGCTCTTTT	64	89	AF066183 (vaccine strain)	
MLV-qR	nsp2	CAGCTTTTCTTTTTACCGTCCGAAAC	65.9			
MLV-qPr	nsp2	FAM-ACCGATTTGCCGCCTTCAGATG-BHQ1	69.5			
ATP-qF	nsp2	CCACCACAGTCGCTCAC	56.9	95	DQ988080 (vaccine strain)	
ATP-qR	nsp2	CCTGAGATGCACAGCCTTATCA	62.6			
ATP-qPr	nsp2	FAM-TCGTGAAATCCAGCAAGCCAA-BHQ1	66.1			
Fostera-qF	nsp2	ATGGCAGCCCGATTTTGATG	65.3	110	AF494042 (vaccine strain)	
Fostera-qR	nsp2	ACTCAGAGGTGTCATCGGC	58.8			
Fostera-qPr	nsp2	FAM-ACGGTTGGGAAGATTCGACTGTT-BHQ1	65.2			
PrimePac-qF	nsp2	TTCGGGCCCTGGAGTGAG	64.7	150	DQ779791 (vaccine strain)	
PrimePac-qR	nsp2	CTCCCGCCCGCATCTATAC	62.8			
PrimePac-qPr	nsp2	FAM-AGTGGATTCATGTGAGGCGAGC-BHQ1	66.0			

a: Melting temperature (Tm) of the target sequence. The tag sequence at the 5'end and inter spacer are not included for the forward primers in the Luminex assays.

Table 2.5.2 Limits of detection of PRRSV-2 Luminex assay corresponding to the RT-qPCR assays

Vaccine	MLV		ATP		Fostera		PrimePac
target type	Cloned DNA	Viral isolate	Cloned DNA	Viral isolate	Cloned DNA	Viral isolate	Cloned DNA
Real time PCR Ct value	34	31	36	32	37	32	36

Table 2.5.3 Comparison of PRRSV-2 Luminex assay and ORF5 sequencing on vaccine identification of clinical samples

Vaccine	MLV	Fostera	ATP	PrimePac
ORF5 sequencing	79	23	4	0
Luminex assay	73	18	2	0
Percentage of co-detection	92.4%	78.2%	50%	N/A

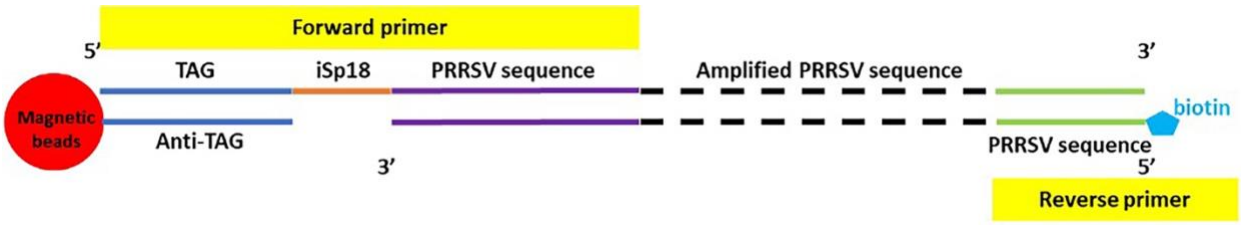

Figure 2.5.1 Illustration of primer design of the Luminex assay

Each Luminex bead is coupled with a TAG oligo. The forward primer includes a TAG sequence, complementary to anti-TAG oligo, an inter spacer and the PRRSV specific sequence from 5' to 3' end. The reverse primer of PRRSV sequence is labeled with biotin at 5' end. Adapted from Figure 23 in Luminex xMAP Cookbook (3rd edition).

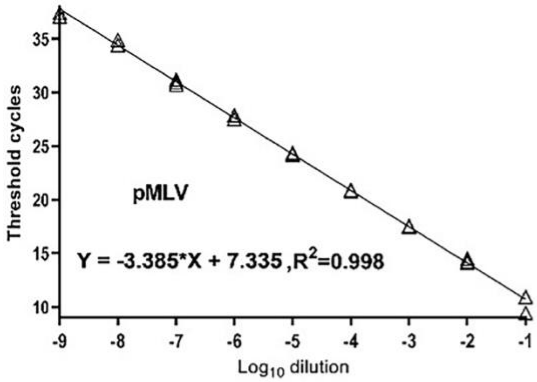

Sample	Detect1	Detect2	MLV	ATP	Fostera	Prime Pac
NTC	845	314	303.5	285	332	1235.5
10^-6	6131.5	245	8102	170.5	160.5	269
10^-7	4867	147.5	6238	104	153	296
10^-8	3476	165	3364.5	158	156.5	248

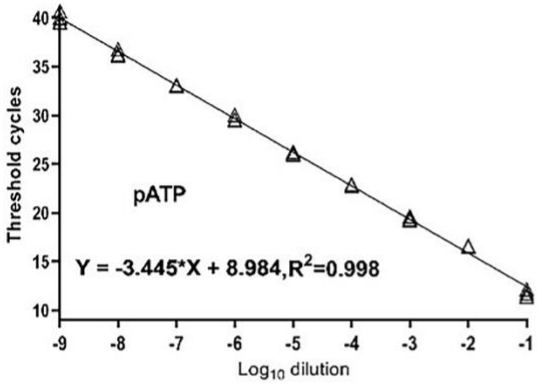

Sample	Detect1	Detect2	MLV	ATP	Fostera	Prime Pac
NTC	518.5	297	420.5	323	358	519
10^-6	5515	235	114	4787	127.5	167
10^-7	5414	208	218	3948.5	260.5	315.5
10^-8	5209	454.5	511	3125	424	757

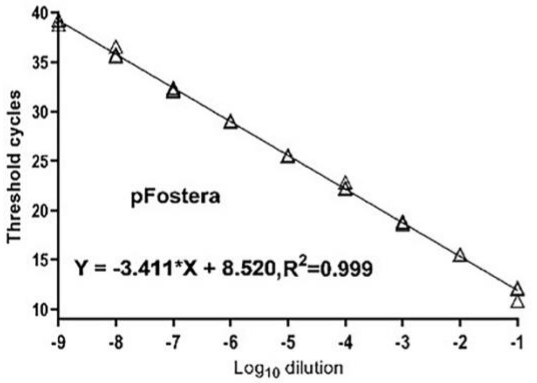

Sample	Detect1	Detect2	MLV	ATP	Fostera	Prime Pac
NTC	282.5	211.5	326	194	301	318
10^-6	7094	351.5	182	181	4341	390
10^-7	7979	383	338	351	3977	621.5
10^-8	6275.5	634	743	659	2309	1258

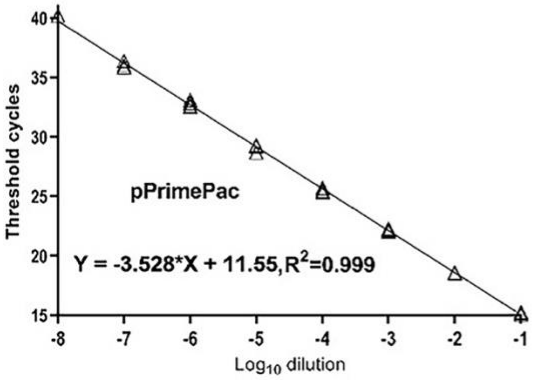

Sample	Detect1	Detect2	MLV	ATP	Fostera	Prime Pac
NTC	680	708	547	405.5	602	884
10^-5	7095	398	380.5	270	339	5221
10^-6	8973	762.5	822	502	620.5	6123.5
10^-7	4875.5	512	775	491	693	4090

Figure 2.5.2 Analytic sensitivity analysis of PRRSV-2 Luminex assays with positive standard plasmids

The assays were performed with ten-fold serial dilutions of positive standards containing target sequences of the four PRRSV vaccine strains: PRRSV MLV, PRRSV ATP, PRRSV Fostera, and PRRSV Prime Pac, by the RT-qPCR assays (left) and Luminex assays (right). The RT-qPCR assays demonstrated as Ct values while the Luminex assays presented as the median fluorescent intensity (MFI) of the bead signals for each channel. NTC: non-template control.

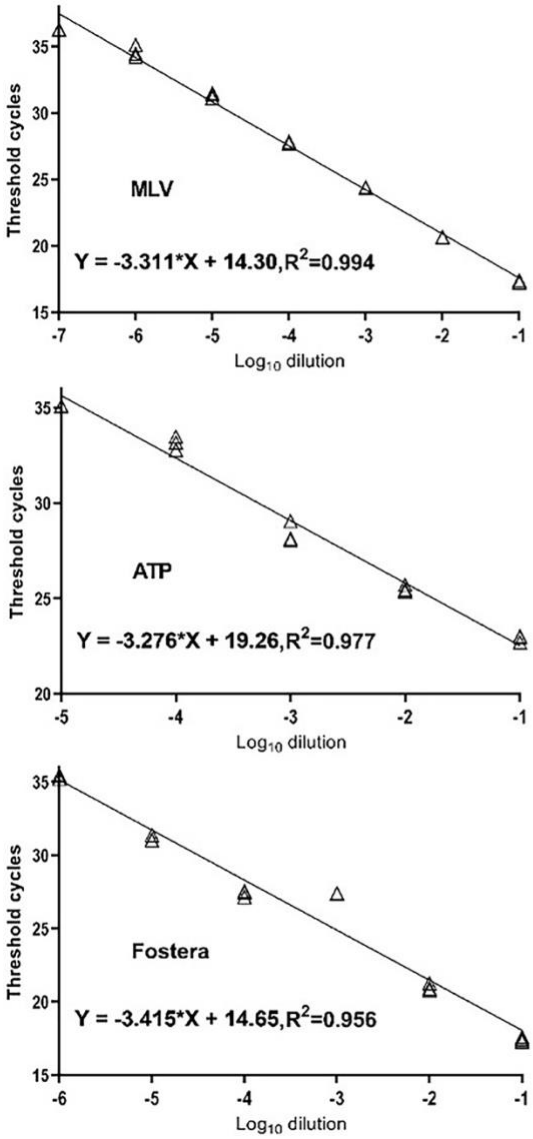

Sample	Detect1	Detect2	MLV	ATP	Fostera	Prime Pac
NTC	942	475	542.5	452	1361.5	705.5
10^-1	14772.5	9003	16983	581	606	952.5
10^-2	13199.5	4750	16367.5	565	628.5	1165
10^-3	11564	2652.5	14208	629	658.5	1286.5
10^-4	6675	749	9604	470	767	1723.5
10^-5	2279	506.5	4891.5	496	557	2721

Sample	Detect1	Detect2	MLV	ATP	Fostera	Prime Pac
NTC	1342	577	484.5	406	542.5	2259
10^-1	13464	4093	552.5	14457	535	870
10^-2	13187	1484.5	1278	12512.5	542	1138
10^-3	12638	1068	979	8343	681	1373.5
10^-4	7839	693	1467	2480.5	750.5	1719

Sample	Detect1	Detect2	MLV	ATP	Fostera	Prime Pac
NTC	720	347.5	545	417	415	2324
10^-1	10502.5	5944	499	523.5	8367	679
10^-2	12266.5	4964	791.5	749.5	10479	874
10^-3	12596.5	2234.5	810.5	791	10300.5	1950
10^-4	10035	918	1075	661	8373	2044
10^-5	6681.5	1046.5	813.5	769	5227	1837

Figure 2.5.3 Analytic sensitivity analysis of PRRSV-2 luminex assays with cell isolates

The assays were performed with ten-fold serial dilutions of cell culture isolates of the three PRRSV vaccine strains: PRRSV MLV, PRRSV ATP, and PRRSV Fostera, by the RT-qPCR assays (left) and Luminex assays (right). The RT-qPCR assays demonstrated as Ct values while

the Luminex assays presented as the median fluorescent intensity (MFI) of the bead signals for each channel. NTC: non-template control.

Chapter 3 Genetic diversity and prevalence of major porcine viral pathogens

3.1 Genetic diversity and prevalence of porcine circovirus type 3 (PCV3) and type 2 (PCV2) in the Midwest of the USA during 2016–2018

Yin Wang, Lance Noll, Nanyan Lu, Elizabeth Porter, Colin Stoy, Wanglong Zheng, Xuming Liu, Lalitha Peddireddi, Megan Niederwerder, Jianfa Bai

(Transboundary and Emerging Disease. 2020; 67:1284–1294)

Abstract: In recent years, reports indicated that PCV3 may be involved in porcine dermatitis and nephropathy syndrome (PDNS)-like disease similar to that linked to PCV2. A total of 2,125 porcine samples from 910 cases were collected during 2016–2018 and tested for presence of PCV3 and PCV2 by real-time PCR assays. Results showed high prevalence of PCV3 and PCV2: 28.4% samples from 41.2% cases were PCV3 positive and 16.4% samples from 16.7% cases were PCV2 positive. The overall coinfection rate was 5.4% and 8.4% at the sample and case level, respectively. Temporal analysis indicated that PCV3 positive case rate increased from 31.6% in 2016, 40.9% in 2017, to 55.6% in 2018. Although its prevalence was lower, PCV2-positive case rate in 2018 (28.8%) doubled that in 2017 (14.4%). The coinfection case rate also increased from 3.4% in 2016, 8.0% in 2017 to 16.1% in 2018. The high positive rate of PCV3 (56.9%) and PCV2 (33.8%) in oral fluids, PCV3 in foetuses (57.1%) and PCV2 in tonsils (54.8%) implied viral transmission route and tissue tropism. In phylogenetic analysis, two small PCV3 clusters (1 and 2) were separated but others were clustered with low bootstrapping values indicating overall low genetic

diversity. Genotypes, PCV2a-h, were confirmed by analyzing 2,944 strains, with a new genotype proposed as PCV2i. In this study, 61 PCV3 unique whole genomes were sequenced; 12 belonged to a separate cluster that were characterized by five consistent amino acid changes in the capsid protein (24V, 27K, 56D, 98R and 168K) and may be associated with potential differences in immunogenicity. Among the 43 unique PCV2 whole genomes sequenced, 31 belonged to PCV2d, 7 to PCV2a and 5 to PCV2b. Thus, our study demonstrates that PCV2d is the predominant genotype and PCV3 is widely circulating in the Midwest of the USA.

3.1.1 Introduction

Porcine circoviruses are small, circular, single-strand DNA viruses, belonging to family *Circoviridae*, genus *Circovirus*. Porcine circovirus type 1 (PCV1) was first discovered in the PK-15 porcine kidney cell line and then subsequently reported as non-pathogenic to swine (Allan et al., 1995; Tischer, Mields, Wolff, Vagt, & Griem, 1986). Different from PCV1, PCV2 is the causative agent of porcine circovirus associated disease (PCVAD), including post-weaning multi-systemic wasting syndrome (PMWS), porcine dermatitis and nephropathy syndrome (PDNS), reproductive disorders and respiratory disease (Darwich, Segales, & Mateu, 2004; Kim, Chung, & Chae, 2003; Rosell et al., 2000; West et al., 1999). In 2015, PCV3 was identified by next-generation sequencing analysis as the pathogen that may be associated with PDNS-like disease and reproductive failure in the USA (Palinski et al., 2017). Although the pathogenesis of PCV3 has not been fully studied, Jiang et al. have recently reported that PDNS-like disease can be reproduced in pigs infected with a cloned PCV3 virus (Jiang et al., 2019).

PCV2 swine infection has been reported worldwide, and the virus has undergone significant genome changes. The virus has been classified into five major genotypes (PCV2a, 2b, 2c, 2d and 2e) based on the ORF2 sequences encoding the capsid protein (Davies, Wang, Dvorak, Marthaler, & Murtaugh, 2016). In the past 20 years, two major shifts in the predominant genotype were ob- served globally: PCV2a towards PCV2b around 2003 and PCV2b towards PCV2d around 2012. Although the genotype shift in 2003 was associated with increased pathogenic virulence, the PCV2a-based vaccines were still effective against the emerged PCV2b strains (Afolabi, Iweriebor, Obi, & Okoh, 2019; Beach & Meng, 2012). The genotype shift to the PCV2d strains appears to be associated with both the increased pathogen virulence and vaccine failure (Beach & Meng, 2012; Guo et al., 2012; Xiao, Halbur, & Opriessnig, 2015). Although PCV2d has been reported as the predominant genotype circulating within the USA during 2014–2016 (Xiao, Harmon, Halbur, & Opriessnig, 2016), neither the PCV2 prevalence level nor the coinfection rate of PCV3 and PCV2 in the USA has been studied extensively after the new circovirus was identified.

Since the discovery of PCV3 in the USA, the virus has been reported in South Korea, China, Thailand, Brazil, Italy, Spain, Sweden, Germany and Poland (Faccini et al., 2017; Fux et al., 2018; Kim et al., 2018; Klaumann et al., 2018; Qi et al., 2019; Stadejek, Wozniak, Milek, & Biernacka, 2017; Sukmak et al., 2019; Tochetto et al., 2018; Ye, Berg, Fossum, Wallgren, & Blomstrom, 2018). Based on limited PCV3 sequences, two major genotypes, PCV3a and PCV3b, have been suggested by phylogenetic analysis in a previous study (Li et al., 2018). The PCV3

evolutionary rate was estimated as fast as PCV2, but a recent study indicated a far slower rate, approximately 10^{-5} substitution/site/year (Franzo et al., 2019). Nevertheless, genetic diversity and prevalence of PCV3 strains circulating in the US swine population has not been well studied.

The objectives of this study were to investigate the prevalence of PCV3 and PCV2 from 2,125 randomly selected porcine samples in 910 clinical cases submitted to KSVDL during 2016–2018 using a fully validated multiplex real-time PCR assay (Wang et al., 2019). The coinfection rate of PCV3 and PCV2 was also studied. Whole genome sequences of PCV2 and PCV3 strains were generated from selected samples and com- pared to published sequences in GenBank to study genetic diversity of the viruses currently circulating in the Midwest of the USA during 2016–2018.

3.1.2 Material and methods

3.1.2.1 Sample collection and processing

A total of 2,125 samples were randomly collected from 910 routine porcine diagnostic cases submitted to KSVDL during January 2016 and December 2018. Number of samples for each case varied from 1 to 30, with a range of 1–6 for 96.0% of the cases. Different sample types including serum, oral fluid, faeces, tonsil, nasal swab, lung, foetus, intestine, uterus, thorax, colostrum, semen, urine, placenta and pooled tissue as stomached organ tissue homogenates were collected. Animal age varied from young piglets to finishing pigs. 78.7% (1,673/2,125) of the samples were submitted for diagnostics, and the other 21.3% (452/2,125) were collected from healthy animals and tested for surveillance monitoring. Among diagnostic samples, 85.7% were submitted for respiratory syndrome pathogen identifications, and 14.3% were for enteric diarrhoea

pathogen diagnostics. Samples were processed following standard operating procedures at KSVDL.

3.1.2.2 Ethics statement

The study did not involve any human samples, and all samples used were porcine samples and were from diagnostic samples submitted by our clients. Thus, the study did not have any ethical issues. All samples were handled in our biosafety level 2 facility under protocol IBC-1322 that is approved by the Institutional Biosafety Committee of Kansas State University.

3.1.2.3 Viral DNA extraction

Viral DNA was extracted from 60 µl of clinical samples using the MagMAX 96 Viral RNA Isolation Kit (Thermo Fisher Scientific) on the automated extraction platform (KingFisher Flex; Thermo Fisher Scientific Inc.) according to the manufacturer's instructions. Each extraction included a positive sample stored in KSVDL as positive control and Dulbecco's Modified Eagle's medium (DMEM, Corning) as negative control. The extracted DNA was stored at −80°C until use.

3.1.2.4 PCV3 and PCV2 detection with a multiplex real-time PCR assay

To detect PCV3 and PCV2 in clinical samples, the fully validated multiplex real-time PCR assay was performed as previously described (Wang et al., 2019). In brief, the PCR reactions were performed in a 20 µl total reaction consisting of 4 µl of extracted sample DNA, 0.4 µM each of forward and reverse primers, 0.2 µM each of probes and 10 µl of 2X iQ™ Multiplex Powermix (Bio-Rad). The amplification was performed using CFX96 Touch Real-Time PCR Detection

System (Bio-Rad) with an initial denaturation at 94°C for 10 min, followed by 45 cycles of 94°C for 15 s and 60°C for 45 s. The results were analyzed with Bio-Rad CFX Manager 3.0.

3.1.2.5 Whole genome sequencing of PCV3 and PCV2

Positive samples with a Ct < 32 were selected for whole genome sequencing. To study the evolution rate and genetic diversity of the viruses, samples submitted for sequencing were selected at different time points and from different regions if possible. The PCV3 whole genomes were amplified using two pairs of primers: PCV3-sF1 (5′-TCGTGGAAAGTTGGAGGC-3′), PCV3-sR1 (5′-AGTCCTTATCTTCAGGACACTCG-3′) and PCV3-sF2 (5′-CGGATCCACGGAGGTCT-3′), PCV3-sR2 (5′-GTGCGGGCACAGGTAAAC-3′). Similarly, the PCV2 whole genomes were amplified by two pairs of primers: PCV2-sF1 (5′-TGGTGACCGTTGCAGAGCAG-3′), PCV2-sR1 (5′-TGGGCGGTGGACATGATGAG-3′) and PCV2-sF2 (5′-KGTATGGCGGGAGGAGTAG-3′), PCV2-sR2 (5′-AGGTGGTTTCCAGTATGTGG-3′). The overlapping amplicons for each virus were sequenced at an outsourced sequencing facility (Genewiz).

3.1.2.6 Sequence analysis

The general analysis, including trimming and assembling of raw sequencing data, conversion into reverse complement sequences and conceptual translation into protein sequences, was performed using CLC Main Workbench 7 (Qiagen). All available PCV3 whole genomes, PCV2 whole genomes and PCV2 ORF2 sequences were downloaded from the GenBank as reference sequences for the analysis. The alignment was performed using MAFFT (Katoh, Misawa, Kuma, & Miyata, 2002). The sequences with premature stop codons were removed from

the analysis. The sequence identity matrix calculation and the amino acid diversity analysis were performed using BioEdit7.2.5 (https://bioedit.software.informer.com/). The phylogenetic analysis was conducted with MEGA7.0.26 (Kumar, Stecher, & Tamura, 2016). The best fit model was selected based on Bayesian information criterion (BIC). The maximum likelihood phylogenetic trees were constructed using the best substitution pattern with the lowest BIC scores. The reliability of the cluster separated in the tree was evaluated by performing the bootstrap replicates of 500.

3.1.2.7 Prevalence data analysis

The prevalence data analysis was performed with Excel 2010. One-way analysis of variance (ANOVA) was used to compare the prevalence of PCV3 with PCV2 during 2016–2018. The chi-square test was applied for the data analysis, including infection rates by year, the rates in different sample types, and infection rates in enteric-disease-causing virus infection cases and respiratory-disease-causing virus infection cases. The enteric-disease-causing cases included samples that were positive to rotavirus A (RVA), RVB and RVC, porcine epidemic diarrhoea virus (PEDV) or porcine delta-coronavirus (PDCoV); and the respiratory-disease-causing cases included those that were positive to porcine reproductive and respiratory syndrome virus (PRRSV) or swine influenza virus (SIV). Number of samples in each case varied from 1–30, with majority in the range of 1–6. For cases with multiple samples submitted, a positive case was defined as one or more samples in the case tested positive.

3.1.3 Results

3.1.3.1 Prevalence of PCV3 and PCV2 in porcine samples collected from KSVDL during 2016-2018

3.1.3.1.1 Overall prevalence of PCV3 and PCV2

Among the 2,125 porcine clinical samples submitted to KSVDL in 2016–2018 and tested by real-time PCR (Wang et al., 2019), PCV3 and PCV2 were identified in 28.4% (604/2,125) and 16.4% (348/2,125) of samples, respectively. The PCV2 and PCV3 coinfection rate was 5.4% (115/2,125). However, the positive rates were dramatically affected by the unbalanced number of samples submitted for each case. Cases containing more samples weighed more in the overall result and vice versa. Therefore, the prevalence was further analyzed at case level to minimize the bias. The percentage of PCV3 and PCV2 positive cases were 41.2% (375/910) and 16.7% (152/910), respectively. There were 8.4% (76/910) of cases positive for both PCV3 and PCV2 (Table 3.1.1).

When the data were analyzed by year, prevalence of PCV3 at sample level was 24.6% (105/426) in 2016, 29.5% (260/880) in 2017 and 29.2% (239/819) in 2018, which were significantly higher ($p < .01$) for each corresponding year compared to those observed for PCV2: 14.6% (62/426) in 2016, 15.7% (138/880) in 2017 and 18.1% (148/819) in 2018. At case level, the prevalence of PCV3 increased continuously during 2016–2018 resulting in positive rates of 31.6% (93/294) in 2016, 40.9% (168/411) in 2017 and 55.6% (114/205) in 2018. It was significantly higher ($p < .05$) than the prevalence of PCV2 in each corresponding year: 11.6% (34/294) in 2016, 14.4% (59/411) in 2017 and 28.8% (59/205) in 2018. Interestingly, the prevalence of PCV2 in

2018 doubled from that observed in 2017. The coinfection rate of PCV3 and PCV2 at case level also increased rapidly, from 3.4% (10/294) in 2016, to 8.0% (33/411) in 2017, then to 16.1% (33/205) in 2018 (Table 3.1.1).

3.1.3.1.2 Prevalence of PCV3 and PCV2 in different sample types

Among the 15 different sample types that were tested for PCV3 and PCV2 in this study, 60.0% (1,276/2,125) were porcine serum, of which 25.0% (319/1,276) were PCV3 positive and 12.3% (157/1,276) were PCV2 positive; 14.1% (299/2,125) of samples were oral fluids, of which 56.9% (170/299) were PCV3 positive and 33.8% (101/299) were PCV2 positive; 9.4% (199/2,125) were faecal samples, of which 17.1% (34/199) were PCV3 positive and 6.0% (12/199) were PCV2 positive. Thus, in the three most common diagnostic sample types, which composed 83.5% of total samples, the prevalence of PCV3 was significantly higher ($p < .01$) than that of PCV2. However, prevalence of both PCV3 and PCV2 was high in oral fluids. In Table 3.1.2, it illustrates that in the tissue samples, 23.7% (31/131) of pooled tissues were PCV3 positive and 22.1% (29/131) were PCV2 positive; 21.0% (13/62) of tonsils were PCV3 positive while 54.8% (34/62) were PCV2 positive; 20.0% (10/50) of lungs were PCV3 positive and 18.0% (9/50) were PCV2 positive; 57.1% (8/14) of foetuses were PCV3 positive while none were PCV2 positive; 13.2% (5/38) of intestines were PCV3 positive and 10.5% (4/38) were PCV2 positive. Except tonsils and foetuses, PCV3 and PCV2 were prevalent at a similar level in the tissues. Interestingly, PCV3 was prevalent in foetuses while PCV2 was more frequently observed in tonsils. The coinfection rates in oral fluid and tonsils were significantly higher than those in other sample types ($p < .01$).

3.1.3.1.3 Geographic distribution of PCV3 and PCV2

The clinical samples were collected from 17 states during 2016–2018. PCV3 was identified from samples of 12 states, and PCV2 was identified from samples of 10 states. A majority of the samples collected were from 5 of the 17 states, Kansas (KS), Nebraska (NE), Illinois (IL), Minnesota (MN) and Iowa (IA). They comprise 94.6% of total cases (Table 3.1.3). For seasonality analysis of the viral infection in the region, positive rates of PCV3 and PCV2 in each season were analyzed, and no seasonal infection patterns were observed (Data was not shown).

3.1.3.1.4 Coinfection with other porcine viruses

Besides the coinfection of PCV3 and PCV2 described above, we investigated the coinfection rates of the PCVs and the other viruses commonly infecting pigs. In the 70 enteric-disease-causing virus infection cases, 24.3% (17/70) were PCV3 positive and 11.4% (8/70) were PCV2 positive. In the 79 respiratory-disease-causing virus infection cases, 38.0% (30/79) were PCV3 positive and 24.1% (19/79) were PCV2 positive. Compared to the overall positive rates, the PCV3 positive rate in enteric-disease-causing virus infection cases was significantly different at $p < .05$, but not at $p < .01$. There was no statistical difference in respiratory-disease-causing virus infection cases compared to the overall positive rate. These results indicated that the PCV2 positive rate in respiratory-disease-causing virus infection cases was significantly higher ($p < .05$), but no statistical difference in enteric-disease-causing virus infection cases compared to the overall positive rate. Comparison of positive rates between the two viruses, the PCV3 positive rate in

enteric-disease-causing virus infection cases is significantly higher than that of PCV2 ($p < .05$; Table 3.1.4).

3.1.3.2 Sequence analysis of PCV3 and PCV2 circulating in the Midwest of the USA during 2016-2018

3.1.3.2.1 Submission of nucleotide sequences to the NCBI GenBank

From this study, 61 PCV3 and 43 PCV2 whole genome sequences were generated and deposited in the NCBI GenBank under the following accession numbers: MH603533-MH603563 (PCV3), MH603565 (PCV3), MK496269-MK496297 (PCV3), and MK504381-MK504423 (PCV2).

3.1.3.2.2 PCV3 strains circulating in the Midwest of the USA during 2016–2018

There were 77 PCV3 whole genomes sequenced from the porcine samples collected during 2016–2018, including 32 sera, 15 oral fluids, 15 pooled tissues, five lungs, three nasal swabs, three tonsils, two intestines, one foetus and one faecal sample. Among which 61 were unique sequences, and 44 were from KS, five from IA, three from MN, three from NE, two from IL and one each from Missouri (MO), North Carolina (NC), Wisconsin (WI) and Quebec (QC), Canada. The 61 PCV3 whole genomes were subjected to further sequence analysis and phylogenetic studies.

Sequence analysis indicated that the 61 strains shared 98.2%– 99.9% identity of their whole genomes, 96.7%–100% identity of ORF2 and 98.6%–100% identity of ORF1. Compared to the 243 unique PCV3 whole genomes available in GenBank database (accessed Mar 9, 2019), the 61 strains in the study shared 97.5%–100% identity of their whole genomes, 95.9%–100% identity of

ORF2 and 96.9%–100% identity of ORF1. The nucleotide mutations in the 61 unique PCV3 sequences resulted in 20 unique conceptually translated capsid (Cap) proteins and 11 unique replicase (Rep) proteins. At amino acid level, the 20 Cap proteins shared 95.8%–99.5% similarity to each other and 94.4%–100% similarity with the 243 published genomes. Similarly, the 11 Rep proteins shared higher similarity with each other (97.9%–99.5%) and lower similarity with the 243 published sequences (95.1%–100%). The diversity of PCV3 ORF2 and ORF1 encoded amino acid sequences from this study are shown in Figure 1. In total, mutations were found in 20 amino acid positions in the Cap protein and in 10 positions in the Rep protein (Figure 3.1.1).

The 304 PCV3 full-genome nucleotide sequences shared 97%–100% whole genome identity, 95.8%–100% of ORF2 identity and 96.2%–100% of ORF1 identity. The whole genomes were subjected to phylogenetic analysis (Figure 3.1.2). The phylogenetic tree showed that the strains from different continents clustered together randomly, including those from North America, South America, Asia and Europe. However, there were two small clusters with strong bootstrap support ($n > 70$). Cluster 1, comprised of 12 US strains sequenced in this study and four Chinese strains, shared 98.3%–99.9% whole genome identity, 96.5%–100% ORF2 identity and 98.7%–100% ORF1 identity. Compared to other strains, Cluster 1 strains shared 97.2%–99.1% whole genome identity, 95.8%–99.3% ORF2 identity and 96.5%–99.5% ORF1 identity. Among Cluster 1 strains, the 12 US strains sequenced in the study and 2 Chinese strains had five characterized amino acids in the Cap protein: 24V, 27K, 56D, 98R and 168K. Two of the mutations, 24V and 27K, were in the epitope that is recognized by the antibody from the PCV3 immunized pigs with

an ELISA assay (unpublished data). Three of the mutations, 24V, 56D and 98R were in the predicted B-cell epitopes (Li et al., 2018; Figure 3.1.1).

Cluster 2 was comprised of only 4 strains, 3 of which were from China and one from Germany. The four strains shared 98.4%–99.8% whole genome identity, 97.9%–100% ORF2 identity and 98.2%–100% ORF1 identity. Compared to other strains, Cluster 2 strains shared 97%–98.6% of whole genome identity, 96.5%–99.0% of ORF2 identity and 96.2%–98.9% of ORF1 identity (Figure 3.1.2).

3.1.3.2.3 PCV2 strains circulating in the Midwest of the USA during 2016 and 2018

In this study, 53 PCV2 whole genomes were sequenced from different porcine samples, including 18 serum samples, 14 oral fluids, 9 pooled tissues, 5 tonsils, 4 lungs, 1 intestine and 1 colostrum. Among them, 43 were unique sequences, of which 25 were from KS, 6 from IA, 3 from IL, 2 from MN, 2 from NC and one each from MO, MT (Montana), NE, Indiana (IN) and MI (Michigan). All strains were subjected to sequence analysis and phylogenetic studies.

Sequence analysis indicated that the 43 strains shared 94.5%–99.9% whole genome nucleotide identity, 89.5%–100% ORF2 identity and 96.8%–100% ORF1 identity. Compared to 1,812 unique PCV2 whole genomes available in the GenBank database (accessed March 9, 2019), the 43 strains shared 90.0% –100% whole genome identity, 79.7% –100% ORF2 identity and 91.8% – 100% ORF1 identity. The nucleotide mutations in the 43 PCV2 sequences resulted in 14 unique Cap proteins and 22 unique Rep proteins. The 14 Cap proteins shared 89.7% – 99.5% similarity to each other and 76.8% – 100% similarity to the 1,812 published PCV2 genomes.

Similarly, the 22 Rep proteins shared high similarity with each other (98.0%–99.6%), but low similarity with some of the 1,812 published genomes (79.5%–100%). Mutations were observed at 30 amino acid positions of the Cap protein and at 15 positions of the Rep protein.

When all 1,855 PCV2 sequences, including 1,812 from the GenBank and 43 we generated, were analyzed, they shared 87.8%–100% whole genome identity, 77.5%–100% ORF2 identity and 89.9%-100% ORF1 identity. Compared to ORF1, ORF2 had greater mutation rate than ORF1. Additionally, PCV2 Cap protein encoded by ORF2 was the major immunogenic protein, capable of inducing protective immunity. Therefore, ORF2 sequences were subjected to phylogenetic analysis. For a more thorough analysis of the genotypes, 2,941 unique PCV2 ORF2 sequences were downloaded from the GenBank (accessed March 30, 2019) for the construction of a phylogenetic tree.

The phylogenetic analysis indicated there were 12 separate clusters, namely Cluster 1–12. Consistent with the previous study (Franzo & Segales, 2018), the 8 clusters, 1, 3, 4 and 8–12, corresponding to genotypes PCV2a-2h. Cluster 7 appeared unique compared to both adjacent clusters. Strains within Cluster 7 shared 91.2%–99.8% identity. Compared to the adjacent Cluster 8, representing PCV2a genotype, they shared 88.5%–95.8% identity. Also, three intermediate clusters, 2, 5 and 6, were observed. Nucleotide identity between Cluster 7 and the adjacent intermediate Cluster 6 was 88.1%–96.6%, which is similar to that with Cluster 8. Cluster information, including intra-cluster and inter-cluster identity matrix data, and the number of sequences and their genotypes, is summarized in Table 3.1.5. A majority of the strains, 72.10%

(31/43) sequenced in this study, belonged to PCV2d in Cluster 1, while 16.28% (7/43) of strains belonged to PCV2a in Cluster 8, and 11.63% (5/43) of strains to PCV2b in Cluster 3. No strains were identified from samples in this study corresponding to other genotypes (Figure 3.1.3 and Table 3.1.5).

3.1.4 Discussion

Due to significant economic loss caused by PCVAD, the emergence of PCV3 has attracted the attention in the swine industry. A few studies have reported high prevalence of PCV3 in regions of China and South Korea (Kwon, Yoo, Park, & Lyoo, 2017; Qi et al., 2019). Similarly, our study found a high prevalence of PCV3 and PCV2 in the Midwest of the United States. In total, 2,125 porcine samples from 910 randomly selected clinical cases submitted to KSVDL during 2016–2018 were tested. PCV3 had a higher prevalence at both sample level (28.4%) and at case level (41.2%), compared to PCV2 (16.4%, 16.7%, respectively). The low PCV2 prevalence may partially be attributed to routine PCV2 vaccination of swine in the USA since 2006 (Dvorak, Yang, Haley, Sharma, & Murtaugh, 2016). In the last 3 years, the positive case rates of both PCV3 and PCV2 have steadily increased. Interestingly, at case level, the PCV2 prevalence increased dramatically from 14.4% in 2017 to 28.8% in 2018. Further investigation into the association between the increased infection rates and the reduced efficacy of PCV2a-based vaccines is warranted, especially since it has been shown that the current predominant genotype, PCV2d, is distantly related to the PCV2a strains (Figure 3.1.3 and Table 3.1.5).

The overall coinfection rates at both the sample (5.4%) and case level (8.4%) were low, which may indicate that PCV2 and PCV3 viruses act as individual pathogens during a majority of infections. One study (Jiang et al., 2019) reproduced PDNS-like clinical disease in piglets by PCV3 challenge alone, which may be further evidence supporting this hypothesis. The coinfection rate at case level doubled from 2016 (3.40%) to 2017 (8.03%), and again from 2017 to 2018 (16.10%). Coincidently, positive cases for individual PCV2 and PCV3 infections both increased from 2016 to 2018 (Table. 3.1.1). The role of PCV3 in swine disease remains controversial. Higher infection rates for PCV3 have been reported when other viruses are also present, including porcine parvovirus (PPV) and PRRSV (Ha et al., 2018; Sukmak et al., 2019). Also, higher PCV3 infection rates have been reported in animals with digestive and respiratory diseases (Qi et al., 2019). However, not all studies support the putative role of PCV3 as a major threat to swine health (Franzo et al., 2018; Kim et al., 2018; Saporiti et al., 2019). Prevalence data presented here do not support the positive association of PCV3 infection with enteric-disease-causing or respiratory-disease-causing viral infections. Better-controlled experiments including the use of healthy age-matched animals may be needed to demonstrate the association between the prevalence of viruses, and viral pathogenesis and related clinical signs in the field.

Recent reports (Jiang et al., 2019; Kwon et al., 2017) indicate that PCV3 can be detected from various tissues and body fluids. Our own data showed that eight of the 14 foetuses were positive for PCV3 while all were negative for PCV2. However, a majority of tonsils (54.8%; 34/62) were positive for PCV2 while only 21.0% (13/62) were positive for PCV3 (Table 3.1.2). These

findings are consistent with studies showing that PCV3 was associated with reproductive failure and that PCV2 showed tropism towards lymphoid tissues (Palinski et al., 2017; Segales & Mateu, 2006). Among body fluid samples, PCV3 and PCV2 positive rates were both the highest in oral fluids, indicating oral exposure as the possible active route of transmission. Therefore, oral fluid should serve as an important sample type for PCV prevalence and epidemiology studies.

In previous studies, PCV3 was grouped into two genotypes, PCV3a and PCV3b, based on phylogenetic analysis of whole genomes (Fux et al., 2018; Li et al., 2018). However, the classification of some strains was not consistent in different studies when different numbers of sequences were used. In this study, all currently available PCV3 whole genomes, 304 in total, were included in the phylogenetic analysis. Majority of the strains clustered randomly into different clusters with the exception of two small clusters separated by strong bootstrap support (Figure 3.1.2). The analysis of the current PCV3 whole genomes, as well as the ORF2 gene that codes for the Cap protein, does not support the classification of PCV3 into different genotypes. However, the two separated clusters share as low as 95.8% ORF2 identity with other strains, which may indicate that the continuous viral evolution and potential for more distinct genotypes to emerge in the future.

Interestingly, in Cluster 1 of Figure 2, the 12 US strains sequenced in this study, together with two Chinese strains, shared an identical capsid protein characterized by five amino acids (24V, 27K, 56D, 98R and 168K) that appeared conserved among stains in this group and distinct from other strains. Four mutations were at the antibody recognition epitope; 24V and 27K were in

the epitope mapped and used in an antibody ELISA test (unpublished data); 24V, 56D and 98R were in the predicted B-cell epitopes by in silico analysis (Li et al., 2018), which may indicate that this cluster of strains could have different immunogenicity conferred by the Cap protein (Figure 3.1.2).

Instead of genetic distance cut-off, phylogenetic analysis is the most widely accepted classification method for identifying PCV2 genotypes. Over the last three decades, PCV2 has evolved fast and been classified into five main genotypes based on ORF2, PCV2a-2e, in which PCV2a, PCV2b and PCV2d are globally distributed. Although PCV2b still plays a major role in PCVAD in some countries, including South Africa, England and Wales (Afolabi et al., 2019; Grierson, Werling, Bidewell, & Williamson, 2018), PCV2d has become the predominant genotype in major pork-producing countries, including China, the USA and South Korea (Xiao et al., 2016; Yang et al., 2018). In this study, 43 unique PCV2 whole genomes were sequenced. Consistent with previous reports, PCV2d was the predominant genotype circulating in the Midwest of the USA, with a majority of strains sequenced (72.10%; 31/43) belonging to this genotype. However, PCV2a and PCV2b were also detected in this study population, representing 11.63% (5/43) and 16.28% (7/43), respectively, of the PCV2 positive samples.

Phylogenetic genotyping analysis may have been influenced by using selected strains representing different genotypes. To avoid potential bias in selecting representative strains, all 2,941 PCV2 ORF2 sequences in our PCV2 phylogenetic analysis were included in the analysis. Low quality sequences containing stop codons or frame shifts in known ORFs were removed.

Eight distinct clusters were identified corresponding to the eight known genotypes, PCV2a-2h, proposed by Franzo and Segales (Franzo & Segales, 2018). In comparison to the eight clusters and few intermediate small clusters, a new cluster, Cluster 7, appeared unique. Cluster 7 strains shared 91.2%–99.8% identity within the cluster and 88.5%–95.8% identity with the adjacent PCV2a cluster, Cluster 8. This identity range is nearly identical to that between Cluster 8 and 9, which represent genotypes 2a and 2h; therefore, Cluster 7 may be considered a new PCV2 genotype, for example PCV2i. Although the sequences fell within well-defined clusters, some clusters lacked bootstrapping support, which may be due to limited differences in the short ORF2 sequences among these strains. Genotyping of the strains should have epidemiological and pathogenesis implications. Whether PCV2i should be considered a new genotype warrants further epidemiological and pathogenesis studies, including the use of more sequences in the analysis.

In conclusion, we investigated the prevalence of PCV3 and PCV2 in the Midwest of the USA during 2016–2018. PCV3 was detected in 28.4% (604/2,125) of samples from 41.2% (375/910) of cases while PCV2 was detected in 16.4% (348/2,125) of samples from 16.7% (152/910) of cases. PCV2d was the predominant genotype identified in this study population. However, PCV2a and PCV2b are still circulating at reduced prevalence. The increasing prevalence of PCV3 and PCV2 and the growing coinfection rate may indicate high risk of porcine circovirus disease in swine production systems in the Midwest USA. Excluding the PCV3 strains sequenced in this study that clustered with other sequences generated from different continents, the 12 strains of this study and the two Chinese strains are clustered separately with strong bootstrap support,

and shared identical capsid proteins different from other strains. These 14 strains were also characterized by five distinct amino acids (24V, 27K, 56D, 98R and 168K), which may indicate potential differences in immunogenicity. PCV2 is a major swine pathogen with a relatively high mutation rate. Genotyping of the PCV2 strains will likely remain an important and ongoing task that may re- quire support from more epidemiological and pathogenesis studies.

3.1.5 Reference

Afolabi, K. O., Iweriebor, B. C., Obi, C. L., & Okoh, A. I. (2019). Genetic characterization and diversity of porcine circovirus type 2 in non-vaccinated South African swine herds. Transboundary and Emerging Diseases, 66, 412–421.

Allan, G. M., Mcneilly, F., Cassidy, J. P., Reilly, G. A. C., Adair, B., Ellis, W. A., & Mcnulty, M. S. (1995). Pathogenesis of porcine circovirus-experimental infections of colostrum deprived piglets and examination of pig fetal material. Veterinary Microbiology, 44, 49–64.

Beach, N. M., & Meng, X. J. (2012). Efficacy and future prospects of commercially available and experimental vaccines against porcine circovirus type 2 (PCV2). Virus Research, 164, 33–42.

Darwich, L., Segales, J., & Mateu, E. (2004). Pathogenesis of postweaning multisystemic wasting syndrome caused by porcine circovirus 2: An immune riddle. Archives of Virology, 149, 857–874.

Davies, B., Wang, X., Dvorak, C. M. T., Marthaler, D., & Murtaugh, M. P. (2016). Diagnostic phylogenetics reveals a new porcine circovirus 2 cluster. Virus Research, 217, 32–37.

Dvorak, C. M. T., Yang, Y., Haley, C., Sharma, N., & Murtaugh, M. P. (2016). National reduction in porcine circovirus type 2 prevalence following introduction of vaccination. Veterinary Microbiology, 189, 86–90.

Faccini, S., Barbieri, I., Gilioli, A., Sala, G., Gibelli, L. R., Moreno, A., … Nigrelli, A. (2017). Detection and genetic characterization of porcine circovirus type 3 in Italy. Transboundary and Emerging Diseases, 64, 1661–1664.

Franzo, G., He, W. T., Correa-Fiz, F., Li, G. R., Legnardi, M., Su, S., & Segales, J. (2019). A shift in porcine circovirus 3 (PCV-3) history paradigm: Phylodynamic analyses reveal an ancient origin and prolonged undetected circulation in the worldwide swine population. Advanced Sciences, 6, 1901001.

Franzo, G., Legnardi, M., Tucciarone, C. M., Drigo, M., Klaumann, F., Sohrmann, M., & Segales, J. (2018). Porcine circovirus type 3: A threat to the pig industry? The Veterinary Record, 182, 83.

Franzo, G., & Segales, J. (2018). Porcine circovirus 2 (PCV-2) genotype update and proposal of a new genotyping methodology. PLoS ONE, 13(12), e0208585.

Fux, R., Sockler, C., Link, E. K., Renken, C., Krejci, R., Sutter, G., … Eddicks, M. (2018). Full genome characterization of porcine circovirus type 3 isolates reveals the existence of two distinct groups of virus strains. Virology Journal, 15, 25.

Grierson, S. S., Werling, D., Bidewell, C., & Williamson, S. (2018). Characterisation of porcine circovirus type 2 in porcine circovirus disease cases in England and Wales. The Veterinary Record, 182(1), 22.

Guo, L. J., Fu, Y. J., Wang, Y. P., Lu, Y. H., Wei, Y. W., Tang, Q. H., … Liu, C. M. (2012). A porcine circovirus type 2 (PCV2) mutant with 234 amino acids in capsid protein showed more virulence in vivo, compared with classical PCV2a/b strain. PLoS ONE, 7(7), e41463.

Ha, Z., Xie, C. Z., Li, J. F., Wen, S. B., Zhang, K. L., Nan, F. L., … Jin, N. Y. (2018). Molecular detection and genomic characterization of porcine circovirus 3 in pigs from Northeast China. BMC Veterinary Research, 14(1), 321.

Jiang, H. J., Wang, D., Wang, J., Zhu, S. S., She, R. P., Ren, X. X., … Liu, J. (2019). Induction of porcine dermatitis and nephropathy syndrome in piglets by infection with porcine circovirus type 3. Journal of Virology, 93(4), e02045.

Katoh, K., Misawa, K., Kuma, K., & Miyata, T. (2002). MAFFT: A novel method for rapid multiple sequence alignment based on fast Fourier transform. Nucleic Acids Research, 30, 3059–3066.

Kim, J., Chung, H. K., & Chae, C. (2003). Association of porcine circovirus 2 with porcine respiratory disease complex. The Veterinary Journal, 166, 251–256.

Kim, S. C., Nazki, S., Kwon, S., Juhng, J. H., Mun, K. H., Jeon, D. Y., … Kim, W. I. (2018). The prevalence and genetic characteristics of porcine circovirus type 2 and 3 in Korea. BMC Veterinary Research, 14, 294.

Klaumann, F., Franzo, G., Sohrmann, M., Correa-Fiz, F., Drigo, M., Nunez, J. I., … Segales, J. (2018). Retrospective detection of porcine circovirus 3 (PCV-3) in pig serum samples from Spain. Transboundary and Emerging Diseases, 65, 1290–1296.

Kumar, S., Stecher, G., & Tamura, K. (2016). MEGA7: Molecular evolutionary genetics analysis version 7.0 for bigger datasets. Molecular Biology and Evolution, 33, 1870–1874.

Kwon, T., Yoo, S. J., Park, C. K., & Lyoo, Y. S. (2017). Prevalence of novel porcine circovirus 3 in Korean pig populations. Veterinary Microbiology, 207, 178–180.

Li, G. R., He, W. T., Zhu, H. A., Bi, Y. H., Wang, R. Y., Xing, G., … Su, S. (2018). Origin, genetic diversity, and evolutionary dynamics of novel porcine circovirus 3. Advanced Science, 5(9), 1800275.

Palinski, R., Pineyro, P., Shang, P. C., Yuan, F. F., Guo, R., Fang, Y., … Hause, B. M. (2017). A novel porcine circovirus distantly related to known circoviruses is associated with porcine dermatitis and nephropathy syndrome and reproductive failure. Journal of Virology, 91(1), e01879.

Qi, S. S., Su, M. J., Guo, D. H., Li, C. Q., Wei, S., Feng, L., & Sun, D. B. (2019). Molecular detection and phylogenetic analysis of porcine circovirus type 3 in 21 provinces of China during 2015–2017. Transboundary and Emerging Diseases, 66, 1004–1015.

Rosell, C., Segales, J., Ramos-Vara, J. A., Folch, J. M., Rodriguez-Arrioja, G. M., Duran, C. O., … Domingo, M. (2000). Identification of porcine circovirus in tissues of pigs with porcine dermatitis and nephropathy syndrome. The Veterinary Record, 146, 40–43.

Saporiti, V., Cruz, T. F., Correa-Fiz, F., Nunez, J. I., Sibila, M., & Segales, J. (2019). Similar frequency of porcine circovirus 3 (PCV-3) detection in serum samples of pigs affected by digestive or respiratory disorders and age-matched clinically healthy pigs. Transboundary and Emerging Diseases.

Segales, J., & Mateu, E. (2006). Immunosuppression as a feature of post-weaning multisystemic wasting syndrome. The Veterinary Journal, 171, 396–397.

Stadejek, T., Wozniak, A., Milek, D., & Biernacka, K. (2017). First detection of porcine circovirus type 3 on commercial pig farms in Poland. Transboundary and Emerging Diseases, 64, 1350–1353.

Sukmak, M., Thanantong, N., Poolperm, P., Boonsoongnern, A., Ratanavanichrojn, N., Jirawattanapong, P., … Wajjwalku, W. (2019). The retrospective identification and molecular epidemiology of por- cine circovirus type 3 (PCV3) in swine in Thailand from 2006 to 2017. Transboundary and Emerging Diseases, 66, 611–616.

Tischer, I., Mields, W., Wolff, D., Vagt, M., & Griem, W. (1986). Studies on epidemiology and pathogenicity of porcine circovirus. Archives of Virology, 91, 271–276.

Tochetto, C., Lima, D. A., Varela, A. P. M., Loiko, M. R., Paim, W. P., Scheffer, C. M., … Roehe, P. M. (2018). Full-Genome sequence of por- cine circovirus type 3 recovered from serum of sows with stillbirths in Brazil. Transboundary and Emerging Diseases, 65, 5–9.

Wang, Y., Feng, Y., Zheng, W., Noll, L., Porter, E., Potter, M., … Bai, J. (2019). A multiplex real-time PCR assay for the detection and differentiation of the newly emerged porcine circovirus type 3 and continuously evolving type 2 strains in the United States. Journal of Virological Methods, 269, 7–12.

West, K. H., Bystrom, J. M., Wojnarowicz, C., Shantz, N., Jacobson, M., Allan, G. M., … Ellis, J. A. (1999). Myocarditis and abortion associated with intrauterine infection of sows with porcine circovirus 2. Journal of Veterinary Diagnostic Investigation, 11, 530–532.

Xiao, C. T., Halbur, P. G., & Opriessnig, T. (2015). Global molecular genetic analysis of porcine circovirus type 2 (PCV2) sequences confirms the presence of four main PCV2 genotypes and reveals a rapid increase of PCV2d. Journal of General Virology, 96, 1830–1841.

Xiao, C. T., Harmon, K. M., Halbur, P. G., & Opriessnig, T. (2016). PCV2d-2 is the predominant type of PCV2 DNA in pig samples collected in the US during 2014–2016. Veterinary Microbiology, 197, 72–77.

Yang, S., Yin, S., Shang, Y., Liu, B., Yuan, L., Khan, M. U. Z., … Cai, J. (2018). Phylogenetic and genetic variation analyses of porcine circovirus type 2 isolated from China. Transboundary and Emerging Diseases, 65, e383–e392.

Ye, X. Y., Berg, M., Fossum, C., Wallgren, P., & Blomstrom, A. L. (2018). Detection and genetic characterization of porcine circovirus 3 from pigs in Sweden. Virus Genes, 54, 466–469.

Table 3.1.1 Temporal prevalence rates of PCV3 and PCV2 at sample level and case level from swine specimens collected in the Midwest of the US during 2016-2018.

Year	Prevalence at sample level			Prevalence at case level		
	PCV3 Positive /Total (%)	PCV2 Positive /Total (%)	Coinfection Positive/Total (%)	PCV3 Positive /Total (%)	PCV2 Positive /Total (%)	Coinfection Positive/Total (%)
2016	105/426 (24.6%)	62/426 (14.6%)	11/426 (2.6%)	93/294 (31.6%)	34/294 (11.6%)	10/294 (3.4%)
2017	260/880 (29.5%)	138/880 (15.7%)	51/880 (5.8%)	168/411 (40.9%)	59/411 (14.4%)	33/411 (8.0%)
2018	239/819 (29.2%)	148/819 (18.1%)	53/819 (6.5%)	114/205 (55.6%)	59/205 (28.8%)	33/205 (16.1%)
Total	604/2125 (28.4%)	348/2125 (16.4%)	115/2125 (5.4%)	375/910 (41.2%)	152/910 (16.7%)	76/910 (8.4%)

Table 3.1.2 Prevalence rates of PCV3 and PCV2 of swine sample types submitted to KSVDL during 2016-2018.

Sample Type	PCV3 Positive Rate Positive/Total (%)	PCV2 Positive Rate Positive/Total (%)	Coinfection Rate Positive/Total (%)
Serum	319/1276 (25.0%)	157/1276 (12.3%)	37/1276 (2.9%)
OF	170/299 (56.9%)	101/299 (33.8%)	57/299 (19.1%)
Feces	34/199 (17.1%)	12/199 (6.0%)	1/199 (0.5%)
T-pool	31/131 (23.7%)	29/131 (22.1%)	10/131 (7.6%)
Tonsil	13/62 (21.0%)	34/62 (54.8%)	8/62 (12.9%)
NS	11/35 (31.4%)	1/35 (2.9%)	0/35
Lung	10/50 (20.0%)	9/50 (18.0%)	1/50 (2.0%)
Fetus	8/14 (57.1%)	0/14	0/14
Intestine	5/38 (13.2%)	4/38 (10.5%)	1/38 (2.6%)
Unknown	1/3 (33.3%)	0/3	0/3
Uterus	1/2 (50.0%)	0/2	0/2
Thorax	1/1 (100%)	0/1	0/1
Colostrum	0/11	1/11 (9.1%)	0/11
Semen	0/2	0/2	0/2
Urine	0/1	0/1	0/1
Placenta	0/1	0/1	0/1
Total	604/2125 (28.4%)	348/2125 (16.4%)	115/2125 (5.4%)

OF: oral fluid; NS: nasal swab; T-pool: pooled tissue.

Table 3.1.3 State level prevalence rates of PCV3 and PCV2 cases submitted to KSVDL during 2016-2018.

State	PCV3 Positive Case Rate (%)			PCV2 Positive Case Rate (%)		
	2016	2017	2018	2016	2017	2018
KS	72/223 (32.3%)	146/358 (40.8%)	87/144 (60.4%)	21/223 (9.4%)	44/358 (12.3%)	38/144 (26.4%)
NE	3/19 (15.8%)	2/9 (22.2%)	9/18 (50.0%)	5/19 (26.3%)	4/9 (44.4%)	2/18 (11.1%)
IL	4/13 (30.8%)	3/7 (42.9%)	7/9 (77.8%)	0/13	2/7 (28.6%)	3/9 (33.3%)
MN	7/11 (63.6%)	5/12 (41.7%)	0/2	3/11 (27.3%)	2/12 (16.7%)	0/2
IA	2/4 (50.0%)	5/9 (55.6%)	9/23 (39.1%)	0/4	6/9 (66.7%)	13/23 (56.5%)
IN	2/4	--	1/2	0/4	--	1/2
NC	1/3	5/7	--	3/3	0/7	--
MT	1/3	0/2	--	1/3	1/2	--
MO	1/2	--	0/2	1/2	--	1/2
HI	0/3	0/1	0/2	0/3	0/1	1/2
VA	--	1/3	0/1	--	0/3	0/1
TX	0/1	1/1	--	0/1	0/1	--
WI	--	--	1/1	--	--	0/1

CO	0/4	--	0/1	0/4	--	0/1
KY	0/3	0/1	--	0/3	0/1	--
ID	0/1	--	--	0/1	--	--
OK	--	0/1	--	--	0/1	--

KS: Kansas, NE: Nebraska, IL: Illinois, MN: Minnesota, IA: Iowa, IN: Indiana, NC: North Carolina, MT: Montana, MO: Missouri, HI: Hawaii, VA: Virginia, TX: Texas, WI: Wisconsin, CO: Colorado, KY: Kentucky, ID: Idaho, OK: Oklahoma

Table 3.1.4 PCV2 and PCV3 positive rates in other viral infection cases submitted to KSVDL during 2016-2018.

Year	RVA, RVB, RVC, PEDV and/or PDCoV Positive Cases Positive/total (%)		PRRSV and/or SIV Positive Cases Positive/total (%)	
	PCV3	PCV2	PCV3	PCV2
2016	4/20 (20.0%)	4/20 (20.0%)	3/19 (15.8%)	4/19 (21.1%)
2017	8/27 (29.6%)	3/27 (11.1%)	7/24 (29.2%)	6/24 (25.0%)
2018	5/23 (21.7%)	1/23 (4.3%)	20/36 (55.6%)	9/36 (25.0%)
Total	17/70 (24.3%)	8/70 (11.4%)	30/79 (38.0%)	19/79 (24.1%)

RVA: rotavirus A; RVB: rotavirus B; RVC: rotavirus C; PEDV: porcine epidemic diarrhea virus; PDCoV: porcine deltacoronavirus; PRRSV: porcine reproductive and respiratory syndrome virus; SIV: swine influenza virus.

Table 3.1.5 Nucleotide identities of PCV2 ORF2 within each cluster and between adjacent clusters from major clusters (n>10) generated in Figure 3.1.3.

Cluster	Intra-cluster identity matrix (%)	Inter-cluster identity matrix (%)	Genotype	No. Sequence ¶	No. Sequence from this study
Cluster 1	87.9-100[£]		PCV2d	942	31
		89.9-98			
Cluster 2	95.8-99.8		PCV2-IM	15	0
		90.6-97.8			
Cluster 3	89.9-99.8[£]		PCV2b	1221	5
		86.4-98			
Cluster 4	91.6-99.8		PCV2g[#]	39	0
		90.0-97.4			
Cluster 5	94.4-99.8		PCV2-IM	13	0
		92.2-97.1			
Cluster 6	90.7-99.0		PCV2-IM	16	0
		88.1-96.6			
Cluster 7	91.2-99.8		PCV2i*	141	0
		88.5-95.8			
Cluster 8	90.2-100		PCV2a	438	7
		88.8-95.1			
Cluster 9	91.9-99.8		PCV2h[#]	63	0
		90.3-94.3			

Cluster 10	93.4-99.8	88.9-91.0	PCV2f[#]	25	0
Cluster 11	99.0-99.4	83.6-84.5	PCV2c	4	0
Cluster 12	99.1-99.8		PCV2e	6	0

PCV2-IM: intermediate strains; *: the new genotype suggested in this study; [#]: the new genotypes were suggested in (Franzo and Segales, 2018); [¶]: the sequences include the unique sequences available in GenBank and those sequenced in the study; £: only two strains shared lower 90% of identity with other strains in the cluster.

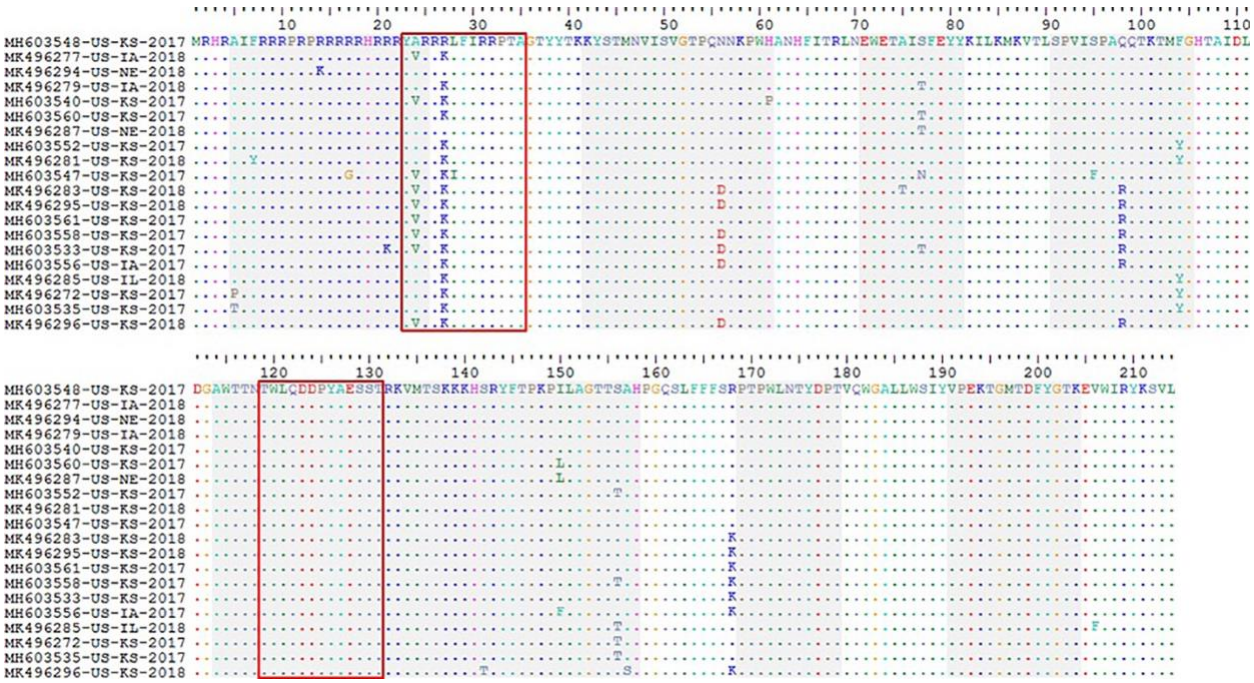

Figure 3.1.1 The unique amino acid sequences encoded by ORF2s of the PCV3 strains

The red open box shows the antibody recognition domains (unpublished data). The grey areas represent in silico predicted B-cell epitopes (Li et al., 2018)

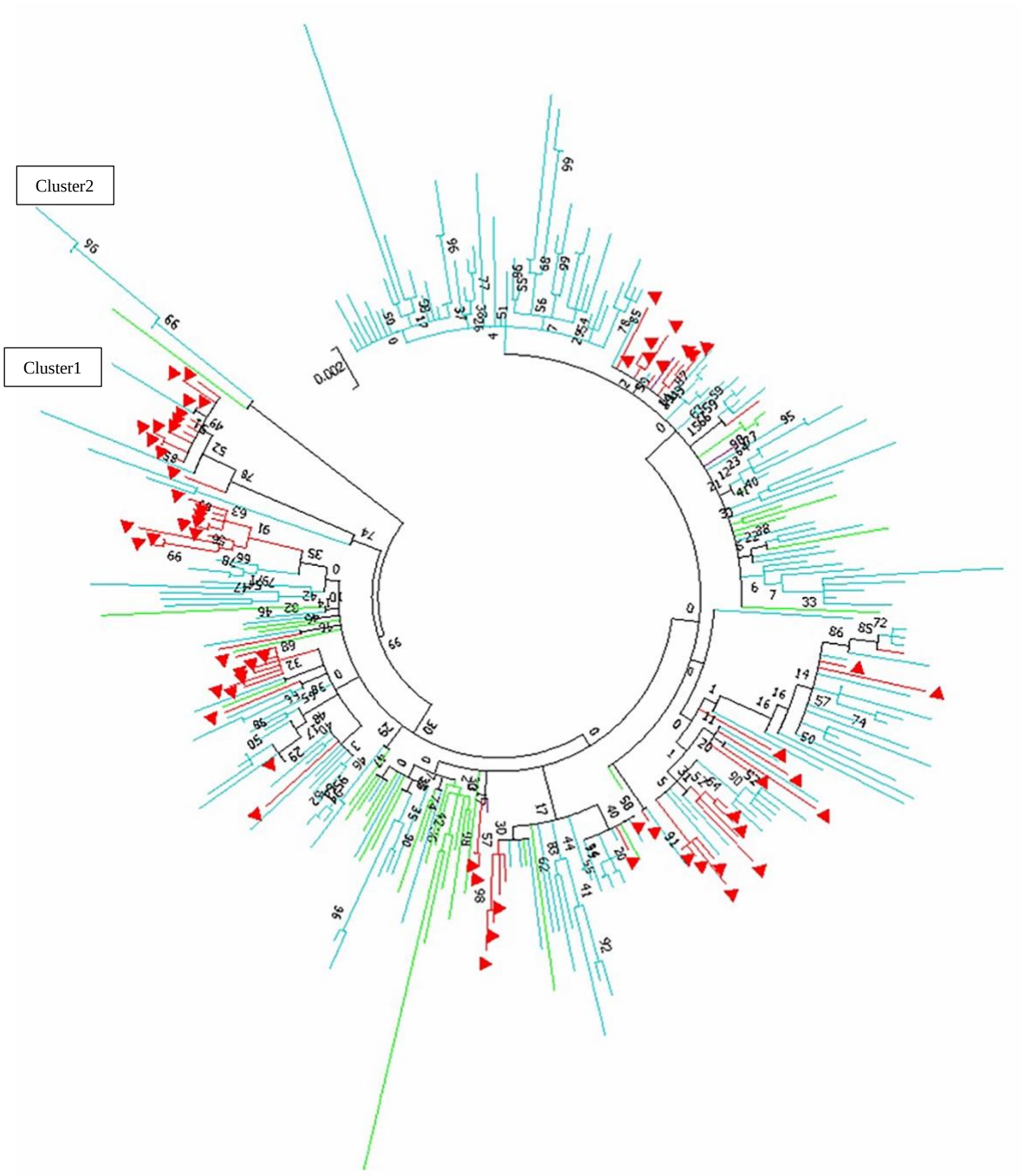
Cluster2
Cluster1
0.002

Figure 3.1.2 Phylogenetic analysis of PCV3 strains circulating in the Midwest of the USA during 2016 – 2018

The phylogenetic tree was constructed by maximum likelihood analysis using the general time-reversible model with gamma distribution with tree topology evaluated with 500 bootstrap replicates. The sequences generated in this study were labelled with ▲. The 243 PCV3 whole genomes published in GenBank were included for the phylogenetic analysis. North American strains from the United States and Canada are in red; Asian strains from China, Japan, South Korea and Thailand are in blue; South American strains from Brazil and Colombia are in purple; European strains from Denmark, Germany, Hungary, Italy, Spain, Swede and Russia are in green.

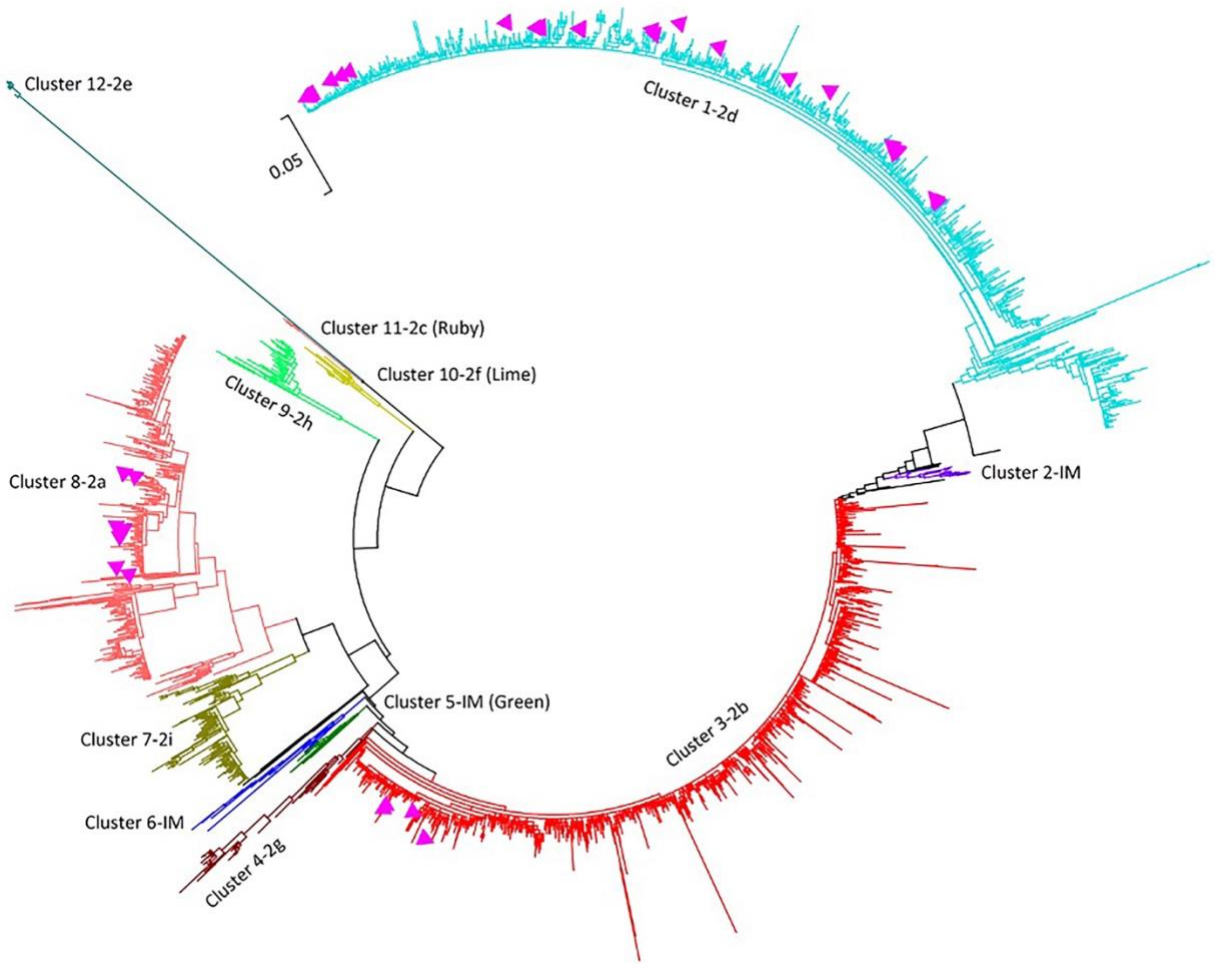

Figure 3.1.3 Phylogenetic analysis of PCV2 strains circulating in the Midwest of the USA during 2016 – 2018

The maximum likelihood phylogenetic tree was constructed by using the general time-reversible model with gamma distribution with tree topology. The sequences generated in this study were labelled with ▲. The 2,941 unique PCV2 ORF2 genes published in GenBank were included in the phylogenetic analysis.

3.2 Whole genome classification and diversity analysis of Rotavirus C strains

Yin Wang, Elizabeth Porter, Nanyan Lu, Cong Zhu, Lance Noll, Susan Brown, Jianfa Bai

The manuscript is in preparation to publish

Abstract: Rotavirus C (RVC) is associated with acute diarrhea in both children and young animals and because of more frequent presence, additional sequences have recently been generated. In this study, we sequenced 31 complete genomes from porcine diarrhea samples and analyzed them together with all available reference sequences collected from GenBank. Based on phylogenetic analysis and genetic distance calculation, the number of each segment identified as 31G, 26P, 13I, 5R, 5C, 5M, 12A, 10N, 9T, 8E and 4H, were identified for VP7, VP4, VP6, VP1, VP2, VP3 and NSP1, NSP2, NSP3, NSP4 and NSP5, respectively. From the analysis, genotypes G118-G31, P[22]-P[26], R5, A9-A12, N9-N10, T7-T9 and E6-E8, were defined as newly identified genotypes and genotypes C6 and M6 were combined to C5 and M1, respectively, due to their closely related nature. Estimated with identity frequency ratio between inter-genotype and intragenotype, the nucleotide identity cutoff values were determined as 85%, 85%, 86%, 84%, 83%, 84%, 82%, 87%, 84%, 81% and 79% for VP7, VP4, VP6, VP1, VP2, VP3 and NSP1, NSP2, NSP3, NSP4 and NSP5. Genotyping of the 31 complete genomes indicated potential segment reassortment in the 7 segments VP7, VP4, VP6, VP2, NSP1, NSP2 and NSP3 among the strains. Our study updated the genotypes of RVC strains and provided more evidence of RVC strain diversity that may be relevant to better understand RVC strain diversity and evolution.

3.2.1 Introduction

Rotavirus C has a global distribution including North America (Chepngeno, Diaz, Paim, Saif, & Vlasova, 2019), South America (Costa, Flores, Amorim, Mendes, & Santos, 2020), Asia (Joshi, Walimbe, Dilpak, Cherian, & Gopalkrishna, 2019) and Europe (Theuns et al., 2016). A few studies have illustrated its association with diarrheal disease in both humans and animals (Martella et al., 2007; Marthaler et al., 2013). Its more frequent presence correlates with increased economic losses from the acute infectious disease (Campanha et al., 2020; Chepngeno et al., 2019).

RVC is a non-enveloped double-stranded segmented RNA virus, belonging to the family Reoviridae, genus Rotavirus. Its genome consists of 11 segments, which coded for six structural proteins, VP1, VP2, VP3, VP4, VP6 and VP7, and five non-structural proteins, NSP1, NSP2, NSP3, NSP4 and NSP5 (Sadiq, Bostan, Yinda, Naseem, & Sattar, 2018). Due to high mutation rates and frequent reassortment in segmented RNA viruses (Donker & Kirkwood, 2012; McDonald, Nelson, Turner, & Patton, 2016), RVC genomes are reported to be highly diverse (Trovao et al., 2019). Rather than the dual gene classification system of VP7 and VP4, complete genome is applied to identify the strains. To date, 11 segments of the RVC strains have been identified into 18G, 21P, 13I, 4R, 6C, 6M, 9A, 8N, 6T, 5E and 4H for genes VP7, VP4, VP6, VP1, VP2, VP3, NSP1, NSP2, NSP3, NSP4 and NSP5, respectively (Suzuki & Hasebe, 2017).

In this study, RVC complete genomes from 31 porcine samples were sequenced and analyzed together with all available RVC sequence data from GenBank. With the database, genotypes of the 11 segments were identified based on the cutoff values and phylogenetic analyses and the genetic diversity of RVC was further defined.

3.2.2 Materials and methods

3.2.2.1 RNA extraction

The 31 porcine clinical samples comprising feces and intestinal samples, tested positive by multiplex rotavirus real time PCR conducted in Kansas State Veterinary Diagnostic laboratory (KSVDL), were selected for Trizol extraction. Briefly, 250 µl of samples weas added into 750 µl of Trizol reagent (Ambion, Carlsbad, CA, USA) and homogenized by low-speed vortex. Then, the aqueous phase was achieved after adding 200 µl of chloroform (Fisher scientific, Fair Lawn, NJ, USA). Linear acrylamide was added for better performance of extraction. Equal volume of isopropanol was added and centrifuged. The pellets were washed with 75% ethanol, dried up and eluted with nuclease-free water. Finally, the RNA was cleaned with RNeasy MinElute Cleanup Kit (Qiagen, Hilden, Germany). The purified RNA product was quantified with Nanodrop (Thermo scientific, Waltham, MA, USA) and stored at -80°C until further use.

3.2.2.2 Full-length cDNA preparation and next-generation sequencing

Full-length cDNA was produced by the single primer amplification technique (SPAT) as described previously (Lambden, Cooke, Caul, & Clarke, 1992; Maan et al., 2007). Briefly, the universal DNA primers were ligated onto the 3′ ends of each double-stranded RNA segment. The reverse complement counterparts were applied for reverse transcript step and PCR. Then, the amplicons were used for the library preparation with NexTera XT library preparation kit (Illumina, San Diego, CA, USA) followed with sequencing by Miseq (Illumina) NGS platform with the 2 × 150 bp run option. Finally, the raw demultiplexed sequencing reads were trimmed and the de novo

assembly was done with the CLC Genomics Workbench (Qiagen Bioinformatics/CLC Bio, Redwood City, CA, USA). The complete coding region (CDS) were obtained from each segment.

3.2.2.3 Sequence and phylogenetic analysis

All of RVC sequences available from the GenBank were downloaded and analyzed together with the complete genomes sequenced in the study. Strains with less than 95% of the open reading frame were excluded from analysis. Sequence alignment was performed with Muscle alignment in Geneious Prime software (Kearse et al., 2012). To classify the genotypes, phylogenetic analyses and genetic distances were conducted with Mega7.0.26 (Kumar, Stecher, & Tamura, 2016). The phylogenetic analyses were based on the maximum-likelihood method with the general time reversible nucleotide substitution model and 500 bootstrap replicates. The genetic distances were calculated using the Kimura two-parameter correction at the nucleotide level. The cutoff values were defined as the percentage separating the intergenotype and the intragenotype identities or the percentage at the ratio of the intergenotype identity to the intragenotype identity dropped below 1. (Matthijnssens et al., 2008)

3.2.3 Results

3.2.3.1 Sequence submission information

The complete genomes from the 31 porcine samples collected from Minnesota, South Dakota, Nebraska, Kansas and Illinois during 2011 to 2013 were sequenced by NGS technology and submitted to GenBank (NCBI). The sequences are under the following accession numbers: VP7 genes (MT771589-MT771624), VP4 genes (MT771516-MT771551), VP6 genes (MT771552

- MT771588), VP1 genes (MT771420-MT771452), VP2 genes (MT771453-MT771483), VP3 genes (MT771484-MT771515), NSP1 genes (MT761701-MT761735), NSP2 genes (MT761736-MT761767), NSP3 genes (MT761768-MT761799), NSP4 genes (MT771353-MT771388) and NSP5 genes (MT771389-MT771419).

3.2.3.2 Phylogenetic analyses and genotype identification

Analyzed on the 772 RVC VP7 gene sequences, genetic distances were calculated and the phylogenetic tree was generated. As shown in Figure 3.2.1B, the sequence identities were between 0.59 and 1. According to the ratio of inter-genotype to intra-genotype identity frequencies, the cutoff value was 85%. In the study, 31 VP7 genotypes, G1-G31, were recognized, in which, genotypes G1-G17 were named following the previous study (Suzuki & Hasebe, 2017), while G18-G31 were determined herein. (Figure 3.2.1A) Except the human cluster of G4, bovine cluster of G2 and canine cluster of G11, other genotypes only included porcine strains. Results indicated the strains sequenced in the study were clustered with other porcine strains, belonged to genotypes, G1, G3, G5, G6, G9 and G21 (Figure 3.2.1C).

The VP4 gene analysis showed the genetic distances of the 225 sequences were between 0.58 and 1. The cutoff value was 85% to separate the genotypes (Figure 3.2.2B). There were 26 genotypes identified, P[1]- P[26]. Of which, P[22]-P[26] were determined in the study. The human strains belonged to P[2], bovine strains to P[3], canine strain to P[11] and porcine strains to other genotypes, P[1], P[4]-P[10] and P[12]-P[26] (Figure 3.2.2A). The strains sequenced in the study

were together with other porcine strains, belonging to genotypes, P[4], P[5] and P[23] (Figure 3.2.2C).

Similarly, the analyses were performed on other gene segments. Compared to VP7 and VP4, the other 4 gene segments encoding structural proteins were more conserved with identities above 70% (Table 3.2.2). The cutoff values were 86%, 84%, 83% and 84% for VP6, VP1, VP2 and VP3 respectively. For genotype identification, no new genotypes were defined for VP6. Genotypes of I4-I7 and I10-I13 were porcine, I3 was bovine, I8 was canine and I9 was ferret. However, genotype I2 included both human and porcine strains, and I1 included both porcine and bovine. Our porcine strains belonged to I1, I5, I6 and I13 (Figure 3.2.3A). For VP1, a new genotype R5 was defined. Genotypes R1 and R5 were porcine, R2 was human, R3 was bovine and R4 was canine. All of our sequenced strains belonged to R1 (Figure 3.2.3B). VP2 had 5 genotypes, C1-C5. The strains sequenced in the study belonged to two porcine genotypes, C1 and C5. Genotypes C2-C4 were human, bovine and canine, respectively (Figure 3.2.3C). VP3 also had 5 genotypes identified, M1-M5. M1 was porcine, M2 was human, M4 was bovine and M5 was canine while M3 included both human and porcine strains. All of our sequenced strains belonged to M1 (Figure 3.2.3D).

In the NSP genes, NSP1 and NSP4 were highly diverse with identities as low as 47% and 33% respectively (Table 3.2.2). Based on cutoff value of 82%, 12 NSP1 genotypes A1-A12 were identified, in which, A9-A12 were determined herein. The strains sequenced in the study clustered together with other porcine strains, belonging to genotypes A5, A7, A8 and A11. The porcine

strains had the most genotypes, A1 and A5-A12 while human strains belonged to A2, bovine strains to A3 and canine strains to A4 only (Figure 3.2.4A). For NSP4, the 8 genotypes, E1-E8, were separated with cutoff value of 81%. E6, E7 and E8 were newly defined here. Therefore, there were four genotypes of E1, E5, E7 and E8 from swine, two genotypes of E2 and E6 from human, genotype E3 from bovine and genotype E4 from canine. All of our porcine strains belonged to E1 (Figure 3.2.4D).

The other three NSP genes, NSP2, NSP3 and NSP5, were more conserved with the lowest identities of 71%, 66% and 65% respectively (Table 3.2.2). For NSP2, two genotypes N9 and N10 were newly defined and 8 genotypes, N1-N8, were confirmed based on the cutoff of 87%. The porcine strains had 7 genotypes N1, N5-N10 while only one genotype for human (N2), bovine (N3) and canine strains (N4). The porcine strains sequenced in the study belonged to N1, N9 and N10 (Figure 3.2.4B). For NSP3, three genotypes T7-T9 were determined and T1-T6 were confirmed here. With cutoff value of 84%, genotype T2 was human, T3 was bovine, T4 was canine and others were porcine, T1 and T5-T9. The strains sequenced in the study belonged to T1, T5 and T6 (Figure 3.2.4C). Without new genotype definition, NSP5 had only 4 genotypes, H1-H4. H1 was porcine, H2 was human, H3 was bovine and H4 was canine. Our sequenced strains were clustered with other porcine strains in H1 (Figure 3.2.4E). The complete genome constellations of the 31 RVC strains sequenced in the study were listed in Table 3.2.1. The information of sequence number included in the analyses, identity range and nucleotide cutoff values of each gene segment, and genotypes in each host species proposed in this study were summarized in Table 3.2.2.

3.2.4 Discussion

In the prevalence studies, VP7, VP4 and VP6 were generally applied to classify the RVC strains (Abid, Guix, Aouni, Pinto, & Bosch, 2007; Possatti, Lorenzetti, Alfieri, & Alfieri, 2016). To better classify the virus of segmented genes, complete genomes were sequenced by Sanger sequencing (Suzuki & Hasebe, 2017) or next-generation sequencing technology (Trovao et al., 2019). In the study, 31 complete genomes were sequenced and analyzed with all available reference sequences from GenBank. Based on the database, we re-genotyped the 11 segments.

From the phylogenetic analysis, new genotypes were defined. Except E6 of human strains, other genotypes were porcine, including G118-G31, P[22]-P[26], R5, A9-A12, N9-N10, T7-T9 and E7-E8. It indicated very high diversity of porcine RVC strains and the ongoing evolution of human NSP4 genes. Compared to porcine, other host strains had conserved RVC genotypes, G4-P[2]-I2-R2-C2-M2/M3-A2-N2-T2-E2/E6-H2 for human, G2-P[3]-I1/I3-R3-C3-M4-A3-N3-T3-E3-H3 for bovine and G11-P[11]-I8-R4-C4-M5-A4-N4-T4-E4-H4 for canine. The result was consistent with previous study that the RVC was mainly evolving within host-defined lineages (Trovao et al., 2019). However, reassortment of VP3 and VP6 segments between porcine and human or bovine implied possibility cross host-species transmission (Chang, Nielsen, Ward, & Saif, 1999; Suzuki & Hasebe, 2017). All of the genomes sequenced in the study were genotyped in the porcine clusters except I1 of VP6 clustered with bovine RVC.

The genetic distance calculation showed VP7, VP4, NSP1 and NSP4 had very large identity ranges as low as 59%, 58%, 47% and 33%, respectively. It was consistent with their fast

evolution rates described previously (Trovao et al., 2019; Zeller et al., 2012). Although other gene segments showed higher identities, VP3 and VP6 had inter-species reassortment. Therefore, the complete genome sequences are required to classify the highly diverse virus.

In conclusion, we applied the recent RVC sequence database to genotype the virus strains. New genotypes were defined for VP7, VP4, VP1, NSP1, NSP2, NSP3 and NSP4. 31 RVC complete genomes were sequenced and genotyped with the new genotyping system.

3.2.5 References

Abid, I., Guix, S., Aouni, M., Pinto, R., & Bosch, A. (2007). Detection and characterization of human group C rotavirus in the pediatric population of Barcelona, Spain. J Clin Virol, 38(1), 78-82. doi:10.1016/j.jcv.2006.09.012

Campanha, J. E. T., Possatti, F., Lorenzetti, E., de Almeida Moraes, D., Alfieri, A. F., & Alfieri, A. A. (2020). Longitudinal study of rotavirus C VP6 genotype I6 in diarrheic piglets up to 1 week old. Braz J Microbiol. doi:10.1007/s42770-020-00234-z

Chang, K. O., Nielsen, P. R., Ward, L. A., & Saif, L. J. (1999). Dual infection of gnotobiotic calves with bovine strains of group A and porcine-like group C rotaviruses influences pathogenesis of the group C rotavirus. J Virol, 73(11), 9284-9293. doi:10.1128/JVI.73.11.9284-9293.1999

Chepngeno, J., Diaz, A., Paim, F. C., Saif, L. J., & Vlasova, A. N. (2019). Rotavirus C: prevalence in suckling piglets and development of virus-like particles to assess the influence of maternal immunity on the disease development. Veterinary Research, 50(1).

Costa, F. B., Flores, P. S., Amorim, A. R., Mendes, G. D. S., & Santos, N. (2020). Porcine rotavirus C strains carrying human-like NSP4 and NSP5. Zoonoses Public Health. doi:10.1111/zph.12713

Donker, N. C., & Kirkwood, C. D. (2012). Selection and evolutionary analysis in the nonstructural protein NSP2 of rotavirus A. Infect Genet Evol, 12(7), 1355-1361. doi:10.1016/j.meegid.2012.05.002

Joshi, M. S., Walimbe, A. M., Dilpak, S. P., Cherian, S. S., & Gopalkrishna, V. (2019). Whole-genome-based characterization of three human Rotavirus C strains isolated from gastroenteritis outbreaks in Western India and a provisional intra-genotypic lineage classification system. J Gen Virol, 100(7), 1055-1072. doi:10.1099/jgv.0.001284

Kearse, M., Moir, R., Wilson, A., Stones-Havas, S., Cheung, M., Sturrock, S., . . . Drummond, A. (2012). Geneious Basic: an integrated and extendable desktop software platform for the

organization and analysis of sequence data. Bioinformatics, 28(12), 1647-1649. doi:10.1093/bioinformatics/bts199

Kumar, S., Stecher, G., & Tamura, K. (2016). MEGA7: Molecular Evolutionary Genetics Analysis Version 7.0 for Bigger Datasets. Mol Biol Evol, 33(7), 1870-1874. doi:10.1093/molbev/msw054

Lambden, P. R., Cooke, S. J., Caul, E. O., & Clarke, I. N. (1992). Cloning of noncultivatable human rotavirus by single primer amplification. J Virol, 66(3), 1817-1822.

Maan, S., Rao, S., Maan, N. S., Anthony, S. J., Attoui, H., Samuel, A. R., & Mertens, P. P. (2007). Rapid cDNA synthesis and sequencing techniques for the genetic study of bluetongue and other dsRNA viruses. J Virol Methods, 143(2), 132-139. doi:10.1016/j.jviromet.2007.02.016

Martella, V., Banyai, K., Lorusso, E., Bellacicco, A. L., Decaro, N., Camero, M., . . . Buonavoglia, C. (2007). Prevalence of group C rotaviruses in weaning and post-weaning pigs with enteritis. Vet Microbiol, 123(1-3), 26-33. doi:10.1016/j.vetmic.2007.03.003

Marthaler, D., Rossow, K., Culhane, M., Collins, J., Goyal, S., Ciarlet, M., & Matthijnssens, J. (2013). Identification, phylogenetic analysis and classification of porcine group C rotavirus VP7 sequences from the United States and Canada. Virology, 446(1-2), 189-198. doi:10.1016/j.virol.2013.08.001

Matthijnssens, J., Ciarlet, M., Heiman, E., Arijs, I., Delbeke, T., McDonald, S. M., . . . Van Ranst, M. (2008). Full genome-based classification of rotaviruses reveals a common origin between human Wa-Like and porcine rotavirus strains and human DS-1-like and bovine rotavirus strains. J Virol, 82(7), 3204-3219. doi:10.1128/JVI.02257-07

McDonald, S. M., Nelson, M. I., Turner, P. E., & Patton, J. T. (2016). Reassortment in segmented RNA viruses: mechanisms and outcomes. Nat Rev Microbiol, 14(7), 448-460. doi:10.1038/nrmicro.2016.46

Possatti, F., Lorenzetti, E., Alfieri, A. F., & Alfieri, A. A. (2016). Genetic heterogeneity of the VP6 gene and predominance of G6P[5] genotypes of Brazilian porcine rotavirus C field strains. Arch Virol, 161(4), 1061-1067. doi:10.1007/s00705-016-2750-x

Sadiq, A., Bostan, N., Yinda, K. C., Naseem, S., & Sattar, S. (2018). Rotavirus: Genetics, pathogenesis and vaccine advances. Rev Med Virol, 28(6), e2003. doi:10.1002/rmv.2003

Suzuki, T., & Hasebe, A. (2017). A provisional complete genome-based genotyping system for rotavirus species C from terrestrial mammals. J Gen Virol, 98(11), 2647-2662. doi:10.1099/jgv.0.000953

Theuns, S., Conceicao-Neto, N., Zeller, M., Heylen, E., Roukaerts, I. D., Desmarets, L. M., . . . Matthijnssens, J. (2016). Characterization of a genetically heterogeneous porcine rotavirus C, and other viruses present in the fecal virome of a non-diarrheic Belgian piglet. Infect Genet Evol, 43, 135-145. doi:10.1016/j.meegid.2016.05.018

Trovao, N. S., Shepherd, F. K., Herzberg, K., Jarvis, M. C., Lam, H. C., Rovira, A., . . . Marthaler, D. G. (2019). Evolution of rotavirus C in humans and several domestic animal species. Zoonoses Public Health, 66(5), 546-557. doi:10.1111/zph.12575

Zeller, M., Patton, J. T., Heylen, E., De Coster, S., Ciarlet, M., Van Ranst, M., & Matthijnssens, J. (2012). Genetic analyses reveal differences in the VP7 and VP4 antigenic epitopes between human rotaviruses circulating in Belgium and rotaviruses in Rotarix and RotaTeq. J Clin Microbiol, 50(3), 966-976. doi:10.1128/JCM.05590-11

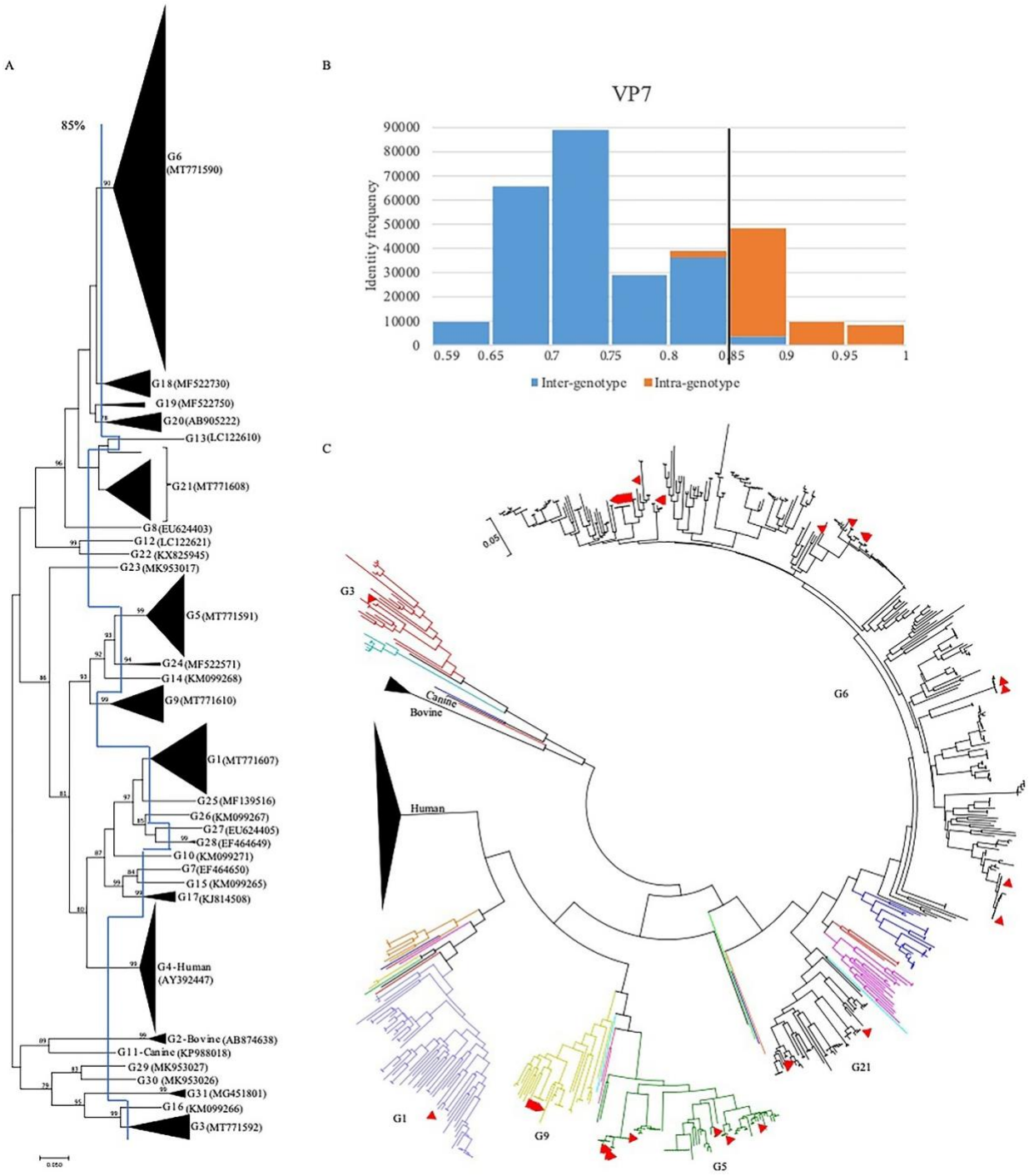
A
85%
G6 (MT771590)
G18 (MF522730)
G19 (MF522750)
G20 (AB905222)
G13 (LC122610)
G21 (MT771608)
G8 (EU624403)
G12 (LC122621)
G22 (KX825945)
G23 (MK953017)
G5 (MT771591)
G24 (MF522571)
G14 (KM099268)
G9 (MT771610)
G1 (MT771607)
G25 (MF139516)
G26 (KM099267)
G27 (EU624405)
G28 (EF464649)
G10 (KM099271)
G7 (EF464650)
G15 (KM099265)
G17 (KJ814508)
G4-Human (AY392447)
G2-Bovine (AB874638)
G11-Canine (KP988018)
G29 (MK953027)
G30 (MK953026)
G31 (MG451801)
G16 (KM099266)
G3 (MT771592)
0.050
B
VP7
Identity frequency
90000
80000
70000
60000
50000
40000
30000
20000
10000
0
0.59
0.65
0.7
0.75
0.8
0.85
0.9
0.95
1
Inter-genotype
Intra-genotype
C
0.05
G3
Canine
Bovine
Human
G6
G21
G1
G9
G5

Figure 3.2.1 Phylogenetic analysis based on RVC VP7 gene sequences.

(A) Phylogenetic tree with compressed clusters labeled as triangles. The representatives were added following the genotypes. The lines indicated the division into different genotypes. (B) The identity frequencies of inter- and intra-genotypes. The line showed the cutoff value for genotyping. (C) Phylogenetic tree in circle with colored genotypes. The strains sequenced in this study were labeled with ▲ and their genotypes were written beside. One strain was selected as the representative for each genotype in the brackets.

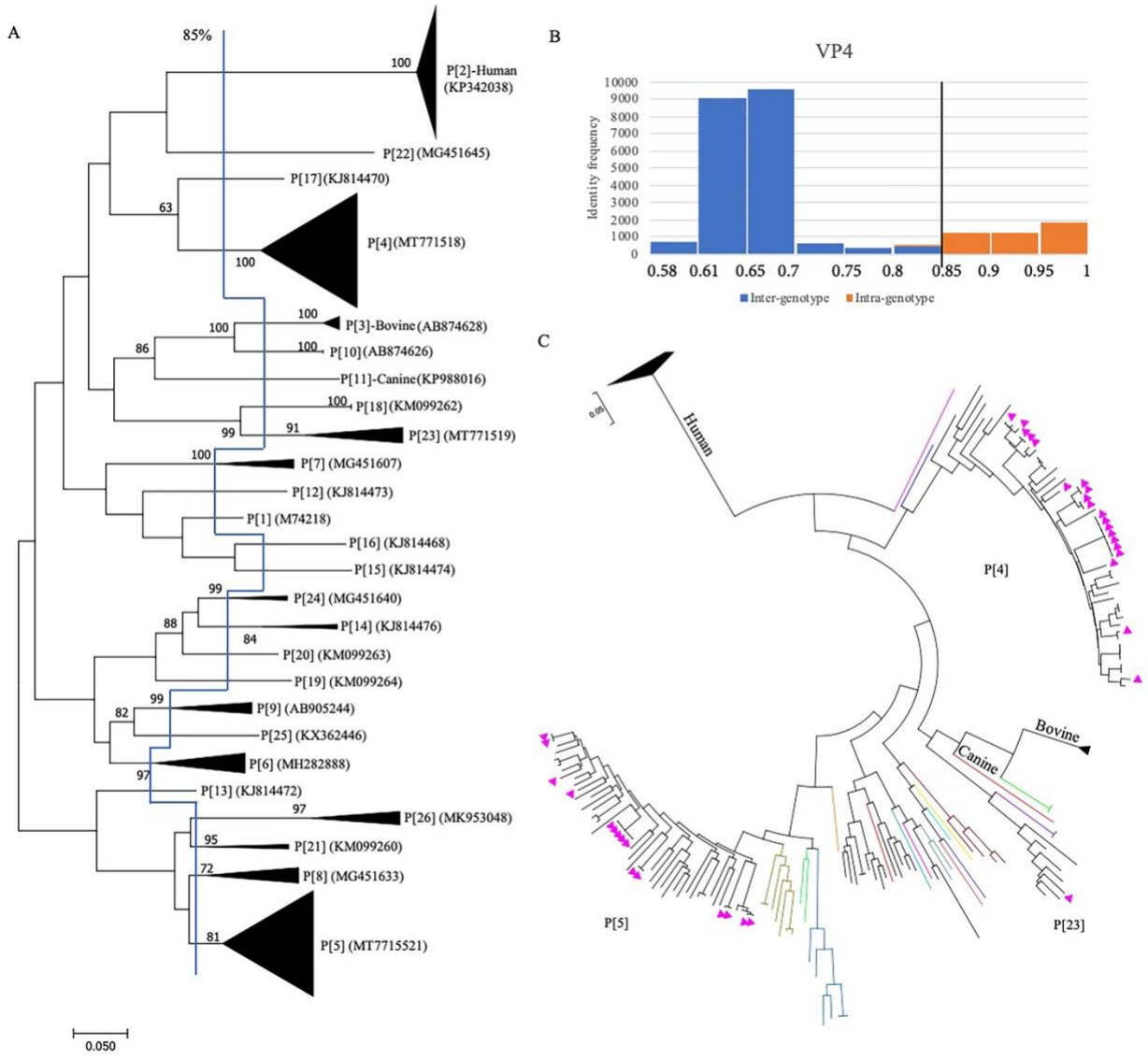

Figure 3.2.2 Phylogenetic analysis based on RVC VP4 gene sequences

(A) Phylogenetic tree with compressed clusters labeled as triangles. The representatives were added following the genotypes. The lines indicated the division into different genotypes. (B) The identity frequencies of inter- and intra-genotypes. The line showed the cutoff value for genotyping.

(C) Phylogenetic tree in circle with colored genotypes. The strains sequenced in this study were labeled with ▲ and their genotypes were written beside. One strain was selected as the representative for each genotype in the brackets.

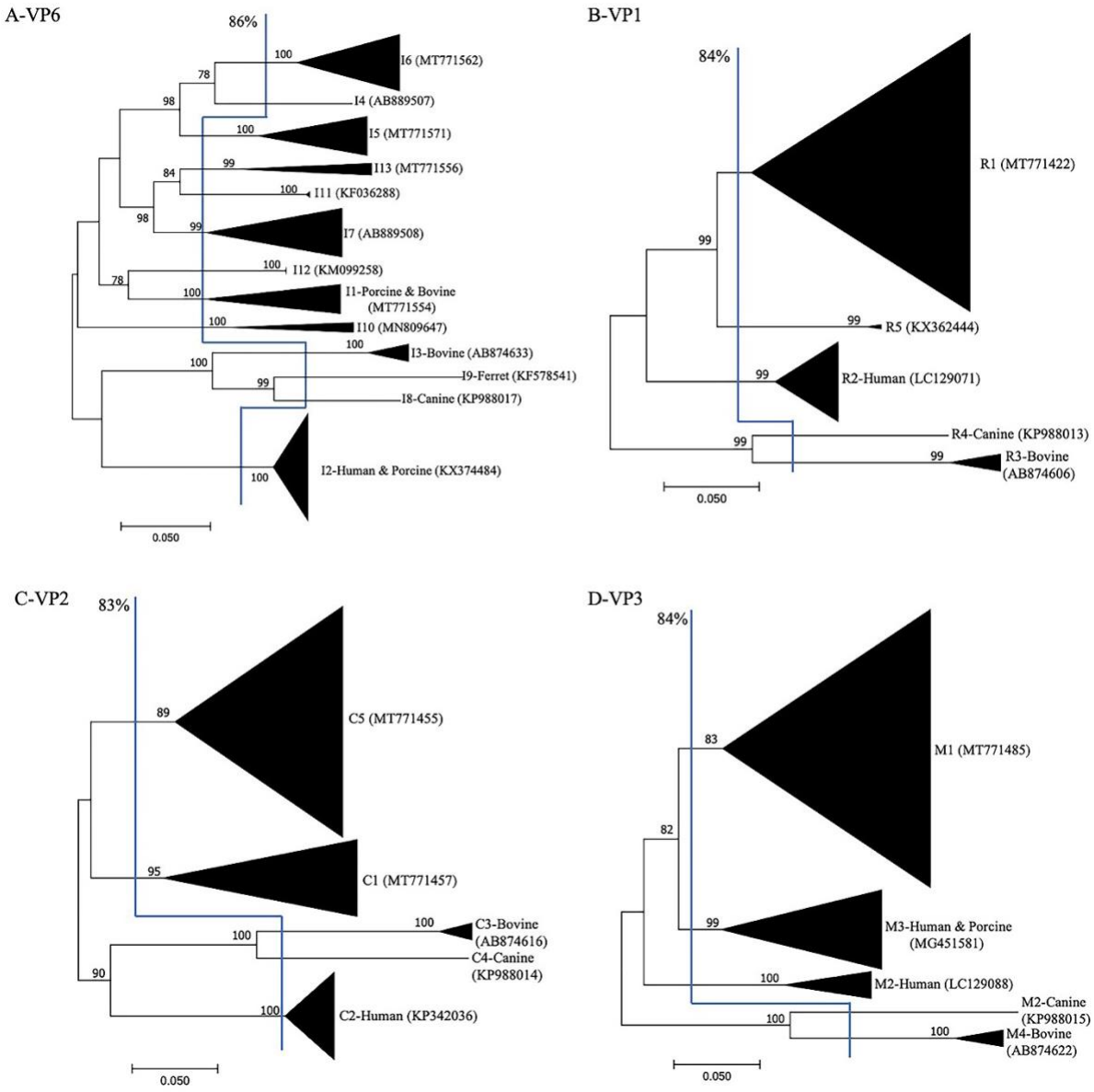

Figure 3.2.3 Phylogenetic analysis of RVC genes of VP6, VP1, VP2 and VP3 proteins (A)VP6, (B) VP1, (C) VP2 and (D) VP3 genes. Phylogenetic trees with compressed clusters were labeled as triangles. The representatives were added following the genotypes. The lines indicated

the division into different genotypes. One strain was selected as the representative for each genotype in the brackets.

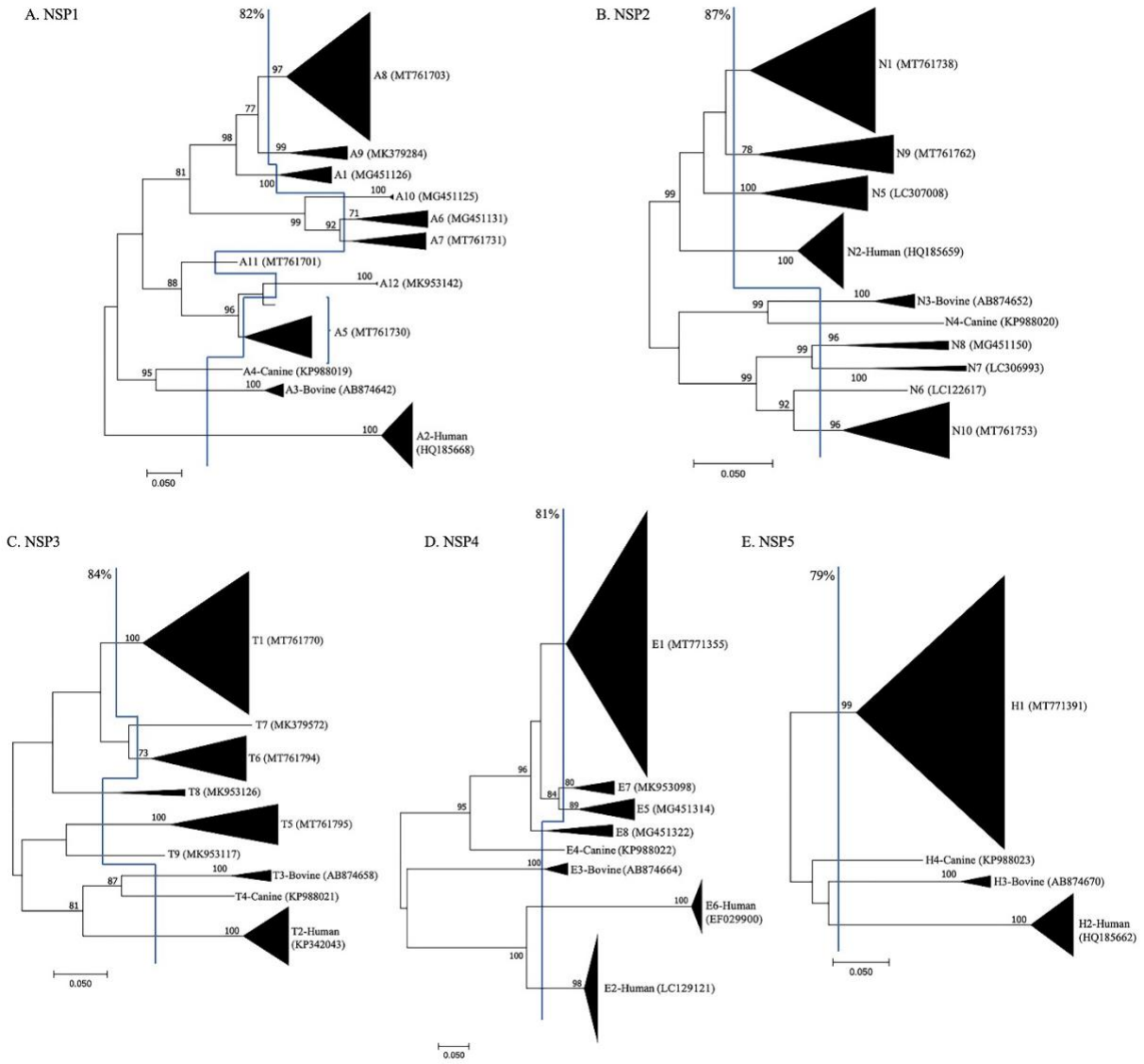

Figure 3.2.4 Phylogenetic analysis of RVC NSP1-NSP5 genes

(A) NSP1, (B) NSP2, (C) NSP3, (D) NSP4 and (E) NSP5. Phylogenetic tree with compressed clusters were labeled as triangles. The representatives were added following the genotypes. The lines indicated the division into different genotypes. One strain was selected as the representative for each genotype in the brackets.

Table 3.2.1 Complete genome constellations for the 31 RVC strains sequenced in this study

#	Strain	VP7	VP4	VP6	VP1	VP2	VP3	NSP1	NSP2	NSP3	NSP4	NSP5
1	SD_6031/2011	G5	P4	I6	R1	C5	M1	A11	N1	T6	E1	H1
2	KS_1319/2011	G6	P4	I5	R1	C5	M1	A8	N10	T1	E1	H1
3	KS_7894/2012	G5	P4	I1	R1	C5	M1	A8	N1	T1	E1	H1
4	NE_5735/2013	G3	P23	I1	R1	C5	M1	A8	N10	T6	E1	H1
5	IL_6269_1/2013	G5	P4	I13	R1	C1	M1	A8	N1	T1	E1	H1
6	IL_6269_3/2013	G6	P5	I5	R1	C5	M1	A8	N1	T1	E1	H1
7	IL_6269_6/2013	G6	P5	I5	R1	C5	M1	A8	N1	T1	E1	H1
8	IL_626971/2013	G5	P4	I13	R1	C1	M1	A8	N1	T1	E1	H1
9	IL_7787/2013	G6	P5	I5	R1	C5	M1	A8	N1	T1	E1	H1
10	IL_8390/2013	G6	P5	I5	R1	C5	M1	A8	N1	T1	E1	H1
11	IL_8901_2/2013	G5	P4	I6	R1	C5	M1	A8	N1	T1	E1	H1
12	IL_8901_3/2013	G5	P4	I6	R1	C5	M1	A8	N1	T1	E1	H1
13	MN_1246/2012	G6	P5	I6	R1	C5	M1	A8	N1	T1	E1	H1
14	MN_1837_6/2012	G6	P4/P5	I6	R1	C5	M1	A8	N1	T1	E1	H1
15	MN_1837_7/2012	G6	P4/P5	I6/I5	R1	C5	M1	A8	N1	T1	E1	H1
16	MN_1837_8/2012	G6/G9	P4/P5	I6/I5	R1	C5	M1	A8	N1	T1	E1	H1
17	MN_2974/2012	G21	P4	I6	R1	C5	M1	A8	N10	T1	E1	H1
18	MN_3659/2012	G1	P4	I5	R1	C5	M1	A8	N10	T1	E1	H1
19	MN_4188/2012	G21	P4	I5	R1	C5	M1	A8	N1	T1	E1	H1
20	MN_4333/2012	G21	P4	I6	R1	C5	M1	A8	N10	T1	E1	H1
21	MN_4887_2/2012	G6/G9	P4	I6/I5	R1	C5	M1	A8	N1	T1	E1	H1
22	MN_4887_4/2012	G6/G9	P4/P5	I6	R1	C5	M1	A8	N1	T1	E1	H1
23	MN_4887_5/2012	G6/G9	P4/P5	I6/I5	R1	C5	M1	A8	N1	T1	E1	H1
24	MN_4887_6/2012	G6/G9	P4	I6/I5	R1	C5	M1	A8	N1	T1	E1	H1

25	MN_0339/2013	G5	P4	I6	R1	C5	M1	A5	N1	T1	E1	H1
26	MN_1233/2013	G6	P5	I5	R1	C5	M1	A5	N1	T6	E1	H1
27	MN_1239/2013	G6	P5	I6	R1	C5	M1	A7	N9	T5	E1	H1
28	MN_1834/2013	G5	P4	I6	R1	C5	M1	A8	N10	T1	E1	H1
29	MN_2369/2013	G6	P5	I5	R1	C5	M1	A8	N1	T1	E1	H1
30	MN_2413/2013	G6	P5	I5	R1	C5	M1	A8	N1	T1	E1	H1
31	MN_2708/2013	G6	P5	I6	R1	C5	M1	A7	N1/N9	T5	E1	H1

Table 3.2.2 Summary of sequence number included in the analysis, identity range and nucleotide cutoff values of each gene segment, and genotypes in each host species proposed in this study.

Gene segment	Sequence #	Identity range	Nucleotide cutoff (%)	Genotypes in each host species				
				Porcine	Human	Bovine	Canine	Ferret
VP7	772	0.59-1	85	G1, G3, G5-10, G12-31	G4	G2	G11	NA
VP4	225	0.58-1	85	P[1], P[4]-[10], P[12]-[26]	P[2]	P[3]	P[11]	NA
VP6	173	0.75-1	86	I1, I2, I4-7, I10-113	I2	I1, I3	I8	I9
VP1	177	0.75-1	84	R1, R5	R2	R3	R4	NA
VP2	194	0.72-1	83	C1, C5	C2	C3	C4	NA
VP3	193	0.7-1	84	M1, M3	M2, M3	M4	M5	NA
NSP1	194	0.47-1	82	A1, A5-12	A2	A3	A4	NA
NSP2	206	0.71-1	87	N1, A5-10	N2	N3	N4	NA
NSP3	191	0.66-1	84	T1, T5-9	T2	T3	T4	NA
NSP4	319	0.33-1	81	E1, E5, E7, E8	E2, E6	E3	E4	NA
NSP5	206	0.65-1	79	H1	H2	H3	H4	NA

Chapter 4 Conclusion

Molecular diagnostics has been developed and used extensively for rapid and accurate detection of infectious agents in animal disease. Compared to conventional methods, nucleic acid detection has several advantages, such as high sensitivity, high specificity, high throughput and short turnaround time.

In Chapter 2, we developed and validated four real time PCR assays and one Luminex assay to detect major porcine viral pathogens. We built the most recent viral sequence databases to design the assays to get high strain coverages. Then, the analytical analyses of sensitivity and specificity were conducted with the positive plasmids, viral isolates or clinical positive samples. Finally, clinical samples of different sample types were applied to evaluate the diagnostic performances. In the assays, the internal controls were added to monitor extraction and amplification efficiencies and to avoid false negative results. In Chapter 2.1, a mqPCR assay was developed to provide rapid, sensitive and specific detection and differentiation of PCV2 and PCV3 strains, which cause diseases of similar symptoms. In Chapter 2.2, a mqPCR assay was developed and validated for the rapid detection and differentiation of three PCV2 genotypes, PCV2a, PCV2b and PCV2d, the most frequently circulating genotypes in the US. In Chapter 2.3, a RT-qPCR assay for SVV-1 was developed and multiplexed with the published FMDV assays to differentiate the two viruses caused similar swine vesicular diseases. In Chapter 2.4, a real-time PCR assay was developed for rapid detection of ASFV with new swine internal control gene designed. In Chapter 2.5, a Luminex xTAG assay was developed to detect and differentiate the PRRSV-2 field strains

from the vaccine strains. All of the assays developed have high strain coverage, high sensitivity and high specificity.

In Chapter 3.1, we studied prevalence and genetic diversity of PCV3 and PCV2 with the developed mqPCR assay and Sanger sequencing. It showed high prevalence of PCV3 and PCV2 in the swine herds in the Midwest of the US during 2016-2018. PCV3 was detected in 28.4% (604/2,125) of samples from 41.2% (375/910) of cases while PCV2 was detected in 16.4% (348/2,125) of samples from 16.7 (152/910) of cases. The increasing prevalence of PCV3 and PCV2 and the growing coinfection rate may indicate high risk of porcine circovirus disease in swine production systems in the Midwest of the USA. The phylogenetic analysis indicated low genetic diversity of PCV3. However, 12 PCV3 strains sequenced in the study and two Chinese strains were clustered separately from other strains with strong bootstrap support. They were characterized by five distinct amino acids (24V, 27K, 56D, 98R and 168K) in the capsid protein, inferred differences in immunogenicity. PCV2 is a major swine pathogen with high mutation rate. In the study, PCV2d was the predominant genotype identified. However, PCV2a and PCV2b were still circulating at reduced prevalence. A new genotype, PCV2i, was proposed in this study.

In Chapter 3.2, we classified RVC strains with complete genomes and investigated their genetic diversity by NGS technology. In the study, complete genomes of 31 strains were sequenced and analyzed with all available reference sequences from GenBank database. Based on the phylogenetic analysis, several new genotypes were defined here, G18-G31 for VP7, P[22]-P[26] for VP4, R5 for VP1, A9-A12 for NSP1, N9-N10 for NSP2, T7-T9 for NSP3 and E6-E8 for NSP4.

Genotyping of the 31 complete genomes indicated potential reassortment may exist in 7 segments, VP7, VP4, VP6, VP2, NSP1, NSP2 and NSP3. The study updated the knowledge of RVC strains and provided more evidence of RVC strain diversity.